



COMSATS IIT, Lahore

# 2016

## RESEARCH PRODUCTIVITY Abstract Book



Library Information Services, CIIT Lahore

Defence Road, Off Riawind Road, Lahore  
+92 42 111 001 007, [library@ciitlahore.edu.pk](mailto:library@ciitlahore.edu.pk)



**Table of Contents**

✚ Preface: -----	02
✚ Summary/ Table: -----	03
✚ Department of Management Sciences: -----	04
✚ Department of Chemical Engineering: -----	39
✚ Department of Mathematics: -----	64
✚ Department of Electrical Engineering: -----	108
✚ Department of Computer Sciences: -----	126
✚ Department of IRCBM:-----	146
✚ Department of Statistics: -----	196
✚ Department of Physics: -----	202
✚ Department of Humanities: -----	266
✚ Author Index: -----	281

**Preface:**

CIIT is not only providing quality education, but also producing the valued research publications. Due to this research work, the CIIT got its better ranking in Pakistan and Higher Education Commission declared CIIT at top ranking among Pakistani Universities. The credit goes to the researchers of CIIT, who, as usual, produced lots of papers in the year 2016. For this accomplishment, the contribution of researchers of CIIT Lahore is also extraordinary. They produced 434 journal papers during the year 2016. The compilation in your hands consists of the papers which published during the year 2016 and at CIIT platform. We only included journal papers for this anthology. The purpose of this compilation is to record the research work of our faculty members and also to facilitate the users to get all the research papers of all departments in one binding. Apart from the record, I am also sure that this compilation will provide the guidelines to new researchers of CIIT and to the researchers of other institutes, as well. I am very much thankful to worthy Director CIIT-Lahore Dr. Qaiser Abbas and Dr. Robbina Farooq, Convener Library Affairs Committee, they not only provided the guidelines, but also encourage us to prepare this compilation in appropriate form. I am also very much thankful to ORIC, which provided the data to compile this report. Without this help, it was very difficult to prepare this collection of research articles. I am also indebted to Ms. Nasira Munir, Assistant Librarian for his technical support and coordination. She did a very good job to compile this publication.

With Regards

**Dr. Muhammad Tariq**

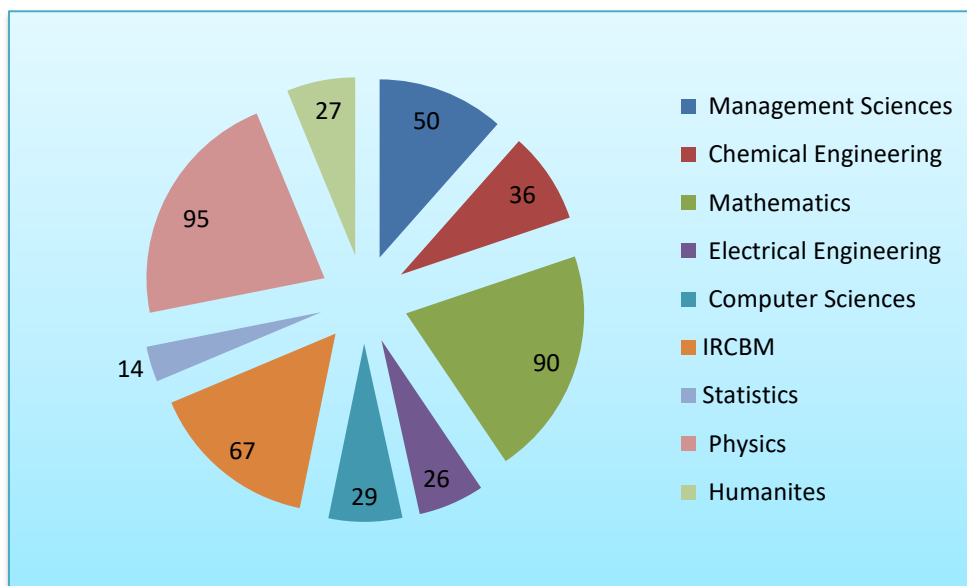
Incharge, Library Information Services

CIIT Lahore

October, 2017

# SUMMARY

Departments	Journal Papers
Department of Management Sciences	50
Department of Chemical Engineering	36
Department of Mathematics	90
Department of Electrical Engineering	26
Department of Computer Sciences	29
IRCBM	67
Department of Statistics	14
Department of Physics	95
Department of Humanites	27
<b>Total</b>	<b>434</b>



# DEPARTMENT OF MANAGEMENT SCIENCES

## Journal Papers

1. Hussain, G., Ismail, W. K. B. W., Rashid, M. A., & Nisar, F. (2016). Substitutes for leadership among the faculty of institutions of higher education and their moderating effects on leadership styles and individual outcomes. *International Journal of Management in Education*, 10(3), 250-277.

**ABSTRACT:**

We test (a) the direct effects of leadership styles and substitutes for leadership on followers' outcomes and (b) the moderating effects of substitutes for leadership on the relationship between leadership styles and followers' outcomes. We use a random sampling technique to define a sample of 416 PhD faculty members of institutions of higher education who are on the list of Higher Education Commission (HEC)-approved PhD supervisors. Using structural equation modelling, we find that leadership styles and substitutes for leadership have significant effects on followers' outcomes and that some of the substitutes for leadership also significantly moderate the relationship between leadership styles and followers' outcomes in a manner consistent with the substitutes for leadership proposition. Discussion, implications, and limitations of the study are offered.

**Web URL:** <http://www.inderscienceonline.com/doi/pdf/10.1504/IJMIE.2016.077507>

2. Ahmad, S., Nisar, Q. A., & Naqvi, S. M. (2016). EFFECT OF PSYCHOLOGICAL CONTRACT FULFILLMENT AND ORGANIZATIONAL JUSTICE ON EMPLOYEE REACTIONS UNDER MODERATION BY ORGANIZATIONAL TRUST: A STUDY ON THE LADY HEALTH WORKERS IN PAKISTAN. *Science International*, 28(1).

**ABSTRACT:**

Different factors contribute to shape employee reactions (ERs). Organization justice (OJ) and psychological contract fulfillment (PCF) have mammoth importance for ERs. Lady health workers (LHW) in Pakistan remained in protests and strikes complaining about these variables. Therefore, this study investigated the effects of OJ and PCF on ERs under the moderation of organizational trust (OT) among 340 LHWs selected through simple random sampling from district Gujranwala, Punjab, Pakistan. Our findings revealed that OJ and PCF had positive and significant relationships with ERs. Further, OT antagonistically moderated their relationships. Such findings were novel and different from exiting literature, but still congruent with only few. The significance, rationale, limitations and future directions were delineated for policy makers managing LHWs.

**Web URL:** <http://www.ciitlahore.edu.pk/Papers/Abstracts/538-8587410582872432058.pdf>

**3. Tang, C. F., Tiwari, A. K., & Shahbaz, M. (2016). Dynamic Inter-relationships among tourism, economic growth and energy consumption in India. *Geosystem Engineering*, 19(4), 158-169.**

**ABSTRACT:**

This study attempts to explore the dynamic causal and inter-relationships among tourism, economic growth and energy consumption in India. This study covers the annual data from 1971 to 2012. This study applies the cointegration and generalised variance decomposition methods to verify the relationship. The bounds testing approach to cointegration and the Gregory-Hansen test for cointegration with structural break consistently reveal that energy consumption, tourism and economic growth in India are cointegrated. We find that tourism and economic growth strongly affects energy consumption in the long-run. Additionally, we also find that tourism and economic growth in India are inter-related, but the causal effect of tourism on economic growth is stronger than the other way around in both the short- and long-run. Therefore, this study concludes that the tourism-led growth hypothesis is valid but the energy-led growth hypothesis is invalid in India. With such findings, we can confirm that tourism is an important catalyst of growth to the Indian economy. Therefore, policymakers should promote and expand tourism industry in order to sustain the process of economic growth and development in India.

**Web URL:** [https://mpa.ub.uni-muenchen.de/69848/1/MPRA\\_paper\\_69848.pdf](https://mpa.ub.uni-muenchen.de/69848/1/MPRA_paper_69848.pdf)

4. Raza, S. A., Shahbaz, M., & Paramati, S. R. (2016). Dynamics of military expenditure and income inequality in Pakistan. *Social Indicators Research*, 1-21.

**ABSTRACT:**

This study investigates the impact of military expenditures on income inequality in Pakistan using data over the period of 1972–2012. For this purpose, we applied the ARDL bounds testing cointegration approach which confirmed the presence of long-run equilibrium relationship between military expenditure and income inequality. Furthermore, empirical analysis indicates that military spending has a positive impact on income inequality. The analysis of Granger causality, Toda–Yamamoto Modified Wald test and variance decomposition approaches confirm the presence of unidirectional causality running from military expenditure to income inequality. The findings of our study suggest that higher military expenditure leads to higher income inequality in Pakistan. Therefore, we advise the policy makers to focus more on the policies which can increase the economic activities in the country and eventually reduce income inequality.

**Web URL:**

[https://www.researchgate.net/profile/Syed\\_Raza23/publication/296031957\\_Dynamics\\_of\\_Military\\_Expenditures\\_and\\_Income\\_Inequality\\_in\\_Pakistan/links/56ded68f08aed4e2a99dbdcd.pdf](https://www.researchgate.net/profile/Syed_Raza23/publication/296031957_Dynamics_of_Military_Expenditures_and_Income_Inequality_in_Pakistan/links/56ded68f08aed4e2a99dbdcd.pdf)

5. Leitão, N. C., & Shahbaz, M. (2016). Economic Growth, Tourism Arrivals and Climate Change. *Bulletin of Energy Economics*, 4(1), 35-43.

**ABSTRACT:**

This paper investigates the link between economic growth, tourism arrivals and climate change. In this research, we formulate three equations. The first equation evaluates the correlation between economic growth and tourism arrivals. The second model considers carbon dioxide emissions and tourism arrivals. Finally, we consider the determinants of tourism arrivals. We selected the period 1990-2009 for European economy using the panel data. The equation that evaluates economic growth demonstrates that tourist arrivals, energy consumption, carbon

dioxide emissions and openness trade are positively correlated with economic growth. A large number of studies consider that there is a positive correlation between tourism and climate change. However, some studies show that there is an alternative hypothesis i.e. a negative association between tourist arrivals and climate change. Our results are in this direction. When we apply the fixed effects and GMM-system, the results show that income per capita, and energy consumption present a positive impact on CO<sub>2</sub> emissions. The econometric results also demonstrate that tourism arrivals and squared income per capita are negatively correlated with CO<sub>2</sub> emissions. The equation that analyses the determinants of tourism arrivals demonstrates that income per capita, openness trade and energy consumption present a positive effect on tourism arrivals.

**Web URL:** [http://www.tesdo.org/shared/upload/pdf/papers/BEE,%204\\_1\\_%2035-43%20.pdf](http://www.tesdo.org/shared/upload/pdf/papers/BEE,%204_1_%2035-43%20.pdf)

**6. Shahbaz, M., Solarin, S. A., & Ozturk, I. (2016). Environmental Kuznets Curve hypothesis and the role of globalization in selected African countries. *Ecological Indicators*, 67, 623-636.**

**ABSTRACT:**

The present study incorporates globalization and energy intensity into the CO<sub>2</sub> emissions function and investigates the presence of Environmental Kuznets Curve (EKC) in 19 African countries for the time period of 1971–2012. We have applied the ARDL bounds testing approach for cointegration to examine the long run relationship in the variables. Our results confirmed the presence of cointegration between the series in Africa, Algeria, Angola, Cameroon, Congo Republic, Ghana, Kenya, Libya, Morocco, Nigeria, South Africa, Sudan, Tanzania, Togo, Tunisia, Zambia and Zimbabwe. The results indicated the positive effect of energy intensity on CO<sub>2</sub> emissions in Africa, Algeria, Angola, Cameroon, Congo Republic, Ghana, Kenya, Libya, Morocco, Nigeria, South Africa, Sudan, Togo, and Tunisia while energy intensity declines CO<sub>2</sub> emissions in the case of Zambia and Zimbabwe. Globalization decreases CO<sub>2</sub> emissions in Africa, Angola, Cameroon, Congo Republic, Egypt, Kenya, Libya, Tunisia and Zambia but increases CO<sub>2</sub> emissions in Ghana, Morocco, South Africa, Sudan and Tanzania. The EKC exists in Africa, Algeria, Cameroon, Congo Republic, Morocco, Tunisia and Zambia but U-

shaped relationship is found between economic growth and CO<sub>2</sub> emissions in Sudan and Tanzania.

**Web URL:** <http://www.sciencedirect.com/science/article/pii/S1470160X16301285>

**7. Azam, M., Shahbaz, M., Kyophilavong, P., & Abbas, Q. (2016). External sources and economic growth-the role of foreign remittances: Evidence from Europe and Central Asia. *The Journal of Developing Areas*, 50(2), 367-387.**

**ABSTRACT:**

Achieving higher level of economic growth in order to enhance social welfare is one of the primary motives of every country. However, developing countries have yet not achieved the desirable level of economic growth due to several socioeconomic and political factors prevailing domestically as well as globally. Therefore, the main purpose of this study is to empirically examine the effects of various external sources namely foreign remittances, foreign direct investment (FDI) and some other notable variables exports and investment on economic growth measured by real GDP per capita in 12 countries from Europe and Central Asia (ECA). This study utilizes annual panel data over the period of 1993–2013 for empirical investigation. After checking stationary properties of the data, Panel Ordinary Least Squares, Fully Modified OLS and Dynamic OLS methods have been employed as analytical techniques for parameters estimation. Empirical result reveals that foreign remittances and FDI inflows have significant positive effects on economic growth in ECA during the period under the study. In addition, the empirical results show that exports and investment also accelerate economic growth. The results of Dumitrescu and Hurlin causality test demonstrate that foreign remittances cause economic growth and economic growth causes FDI inflows. The feedback effect exists between external debt and economic growth. Economic growth leads exports validating growth-led exports hypothesis. Incoming FDI causes exports and exports cause FDI in Granger sense. Furthermore, the feedback hypothesis is valid for foreign aid and external debt, exports and external debt, exports and investment. The main points emerging from this study purport that both foreign remittances and FDI inflows are vital sources of economic growth in ECA. The findings are expected to guide the management authorities with reference to the effects of

foreign remittances and incoming FDI on ECA economic growth and development. Moreover, ensuring macroeconomic stability in the recipient countries can help to create environment conducive to investment, thus, encourage immigrants and foreign investors to transfer remittances and make investments with higher degree of confidence. Consequently, it would have a positive multiplier effect on the entire macroeconomic performance of ECA economies.

**Web URL:** <https://muse.jhu.edu/article/621351>

**8. Amir-ud-Din, R., & Malik, S. (2016). Protecting the Vulnerable: The Case of IDPs in Pakistan. *European Online Journal of Natural and Social Sciences*, 5(1), 82.**

**ABSTRACT:**

Vulnerability as a measure of human deprivations is a more comprehensive and value-laden term than poverty. While the poverty analysis provides a profile of the characteristics of the poor people, vulnerability analysis explains, among other factors, the role of risk in creating the dynamics that contribute to the observed poverty level. Social protection is an important concept in the policy dialogue on the vulnerabilities of the people and is aimed at finding ways to help the vulnerable people in managing the risks and becoming less susceptible to the welfare losses. Vulnerability takes a number of forms and requires different types of social protection mechanisms. This paper analyses the vulnerabilities of internally displaced persons (IDPs) in Pakistan and identifies the social protection delivered by various government and non-government stakeholders. The paper also reviews the literature on the vulnerabilities of the IDPs in different parts of the world to explore the best practices in providing social protection to IDPs.

**Web URL:** <http://search.proquest.com/openview/fe4fb3cdb3b499ca83b203ea5630f88f/1?pq-origsite=gscholar&cbl=2029677>

**9. Malik, S., Zameer, A., Khaliq, I. H., & Uzair, L. (2016). Determinants of Consumer Satisfaction at Supermarkets: An Empirical Study from Pakistan.**

**ABSTRACT:**

Pakistan is an emerging economy. It provides great opportunity for organized corporate driven retailing. There have been few global retailers who have already tasted some success with their cash-n-carry and supermarket formats. Some home grown retailers have also made forays into this market. There is a lot of need to understand the consumer behavior towards modern retail practices in Pakistan. This research study is conducted with an objective to find out how various factors influence shoppers' behavior towards supermarkets with 300 respondents consisting of 150 males and 150 females by using shop intercept method in the cities of Lahore and Faisalabad in Pakistan. The outcomes of this study provide the insights to understand the influence of several factors like promotion and special offers, easy access to supermarket, geographically convenience and locality, customer services, exploration, pricing factor, socio-economic effects, cleanliness, aesthetics and escape from routine work on the consumer's perception.

**Web URL:** [https://papers.ssrn.com/sol3/papers.cfm?abstract\\_id=2783460](https://papers.ssrn.com/sol3/papers.cfm?abstract_id=2783460)

**10. Ali, S. A., & Hussin, H. M. R. Risk Management Practices and Company Performance: An Empirical Evidence from cement sector of Pakistan. *CORPORATE OWNERSHIP & CONTROL*, 438.**

**ABSTRACT:**

The study investigates the impact of risk management on the company performance. Degree of financial leverage (DFL), degree of operating leverage (DOL) and the working capital ratio (WCR) are taken as independent variables which are the representative of risk and the earning price per share (EPS), return on assets (ROA), return on equity (ROE), Sales and Net profits are taken as the representative of performance. Last 10 years (2004-2013) of Cement sector of Pakistan data is chosen as sample for analyze their relations by multiple regression technique. Results reveal that WCR impact adequately on the company performance because if company has enough liquidity than it perform its operations smoothly and enhance its performance very well. DFL should be control moderately because enough DFL leads performance of company downward. On the other hand, the DOL should be less because it causes the less profitability for the company from its operations.

**Web URL:**

[http://www.virtusinterpress.org/IMG/pdf/COC\\_Volume\\_13\\_Issue\\_2\\_Winter\\_2016\\_Continued\\_2\\_.pdf#page=28](http://www.virtusinterpress.org/IMG/pdf/COC_Volume_13_Issue_2_Winter_2016_Continued_2_.pdf#page=28)

**11. Umair, T., Javaid, M. F., Amir, H., & Luqman, M. K. (2016). Effect of Perceived Appraisal Fairness on Job Satisfaction. *J. Appl. Environ. Biol. Sci*, 6(2), 12-20.**

**ABSTRACT:**

This study investigates the employees' perception of fairness in the performance appraisal system and its effect on job satisfaction of an employee. The perceived fairness in appraisal system is discussed with the help of organizational justice theory which was principally derived from Adam's equity theory and used by many researchers in organizational research. The perception of fairness in performance appraisal system consists of three main factors: Distributive justice, procedural justice, interactional justice and are used as independent variables and job satisfaction of an employee as dependent variable. The survey method by using random sampling technique was used to collect the data from garment firms of Pakistan which are registered under PRGMEA (Pakistan Readymade Garment and Manufacturer and Exporter Association). Data analysis were conducted by using Bivariate correlation and multiple regression analysis. The findings of the result explored that distributive, procedural and interactional fairness in the appraisal system are the three significant variables that enhances the job satisfaction of an employee in the garment sector of Pakistan. This is the first empirical study in order to evaluate the perception of employees about performance appraisal system in the Garment sector of Pakistan and this study provides significant result to understand the importance of perceived fairness and satisfaction among employees in the performance evaluation process.

**Web URL:**

[https://www.researchgate.net/profile/Kashif\\_Luqman/publication/294693464\\_Effect\\_of\\_Perceived\\_Appraisal\\_Fairness\\_on\\_Job\\_Satisfaction/links/579dad2808ae6a2882f35f43/Effect-of-Perceived-Appraisal-Fairness-on-Job-Satisfaction.pdf](https://www.researchgate.net/profile/Kashif_Luqman/publication/294693464_Effect_of_Perceived_Appraisal_Fairness_on_Job_Satisfaction/links/579dad2808ae6a2882f35f43/Effect-of-Perceived-Appraisal-Fairness-on-Job-Satisfaction.pdf)

12. Hussain, G., Hussain, G., Wan Ismail, W. K., Wan Ismail, W. K., Rashid, M. A., Rashid, M. A., ... & Nisar, F. (2016). Substitutes for leadership: alternative perspectives. *Management Research Review*, 39(5), 546-568.

**ABSTRACT:**

Purpose – The purpose of this study is to explore alternative models of substitutes for leadership. These alternative models are a leadership-only model, substitutes for the leadership-only model and substitutes for the leadership-mediated-effects model. Design/methodology/approach – Four occupational groups were targeted, namely, PhD faculty of institutions of higher education, medical doctors who work in district headquarters' hospitals, licensed pharmacists and certified engineers. Also, a self-administered questionnaire was used to collect data, and 523 usable responses were received. Findings – Partial least square path modeling was used for data analysis, and the results of structural models revealed that: the dimensions of transformational leadership significantly affected the followers' outcomes; a few substitutes for leadership also significantly affected the followers' outcomes; and, in some cases, substitutes for leadership significantly mediated the relationship between dimensions of transformational leadership and followers' outcomes. Practical implications – Findings of the study provide useful implications to improve the managerial practices of organizational leaders, work design strategies in organizations and overall organizational policies for effective functioning. Other developing countries with similar socio-economic status may use these findings to improve organizational functioning. Originality/value – This study makes important contributions to the leadership literature. It tests three alternative models in the domain of substitutes for the leadership theory and tests the separate effects of dimensions of transformational leadership and substitutes for leadership on followers' work outcomes. Further, it specifies the mediating effects of substitutes for leadership on the dimensions of transformational leadership and followers' work outcomes. Most important, this study for the first time tests transformational leadership and substitutes for leadership concepts in Pakistani work settings and advances the theoretical and empirical literature in this local context.

**Web URL:** <http://www.emeraldinsight.com/doi/pdfplus/10.1108/MRR-03-2015-0044>

**13. Javed, M., Rashid, M. A., & Hussain, G. (2016). When does it pay to be good—A contingency perspective on corporate social and financial performance: would it work?. *Journal of Cleaner Production*, 133, 1062-1073.**

**ABSTRACT:**

The findings on corporate social and financial performance research has exposed the universal approach as tenuous and questionable, so the current approach of corporate social and financial performance research has been subject to severe criticism. Instead of exploring a universal corporate social and financial performance link, scholars have called for a contingency perspective in order to determine the conditions and context that catalyzes positive connections between the constructs. This study systematically reviews the literature on the moderators exploited in corporate social and financial performance research and finds, by and large, that a positive corporate social and financial performance association dominates, although the relationship is stronger in advanced economies and institutionalized contexts. Although research on the contingency perspective has progressed, theoretical support for this relationship is thin, and the lack of appropriate research design and stereotyped constructs thwart its positive implications. A review of the literature shows that although organizational factors seem to moderating the corporate social and financial performance relationship strongly yet industry and country factors also tend to affect this association. Important consistencies included that a dynamic business environment reinforces the corporate social and financial performance relationship. Differentiation in social responsibility practices moderates the responsibility-performance link, but not often positively. The effect of R&D intensity is equivocal, and advertising intensity did not strengthen this relationship across the level. Avenues for future research conclude our discussion.

**Web URL:**

[http://s3.amazonaws.com/academia.edu.documents/46643066/Final\\_Version.pdf?AWSAccessKeyId=AKIAIWOWYYGZ2Y53UL3A&Expires=1496132349&Signature=B%2FzQHt9vsKDH7Z0JsfC5](http://s3.amazonaws.com/academia.edu.documents/46643066/Final_Version.pdf?AWSAccessKeyId=AKIAIWOWYYGZ2Y53UL3A&Expires=1496132349&Signature=B%2FzQHt9vsKDH7Z0JsfC5)

[TPqLXXQ%3D&response-content-disposition=inline%3B%20filename%3DWhen+does+it+pay+to+be+good+e+A+continge.pdf](#)

**14. Alam, M. S., Raza, S. A., Shahbaz, M., & Abbas, Q. (2016). Accounting for contribution of trade openness and foreign direct investment in life expectancy: The long-run and short-run analysis in Pakistan. *Social Indicators Research*, 129(3), 1155-1170.**

**ABSTRACT:**

This paper examines the impact of trade openness and foreign direct investment (FDI) on life expectancy using time series data over the period of 1972–2013. We have applied structural break unit root as well as cointegration tests to examine integrating properties of the variables and cointegration among the variables. The causal linkage between the variables has been tested by applying the VECM Granger causality. The empirical evidence confirms the presence of cointegration amid the variables. Moreover, trade openness and FDI increase population health measured by life expectancy in the long-run. Furthermore, the analysis suggests that trade openness and FDI cause life expectancy in the short-run. These findings have several policy implications to improve life expectancy for the people of Pakistan in particular and other developing countries in general.

**Web URL:**

[https://www.researchgate.net/profile/Syed\\_Raza23/publication/283512576\\_Accounting\\_for\\_Contribution\\_of\\_Trade\\_Openness\\_and\\_Foreign\\_Direct\\_Investment\\_in\\_Life\\_Expectancy\\_The\\_Long-Run\\_and\\_Short-Run\\_Analysis\\_in\\_Pakistan/links/5673e5d808aedbbb3fa19fd3.pdf](https://www.researchgate.net/profile/Syed_Raza23/publication/283512576_Accounting_for_Contribution_of_Trade_Openness_and_Foreign_Direct_Investment_in_Life_Expectancy_The_Long-Run_and_Short-Run_Analysis_in_Pakistan/links/5673e5d808aedbbb3fa19fd3.pdf)

**15. Afza, T., Ahmed, K., & Shahbaz, M. (2016). Does Harberger–Laursen–Metzler (HLM) Exist in Pakistan? Cointegration, Causality and Forecast Error Variance Decomposition Tests. *Global Business Review*, 17(4), 759-778.**

**ABSTRACT:**

This article investigates the validation of Harberger–Laursen–Metzler hypothesis using Pakistani data over the period of 1978Q1–2012Q4. We have used Gregory–Hansen cointegration approach accommodating structural break in the series. The results confirm the presence of

cointegration between the variables. The impact of terms of trade is positive on Pakistan's trade balance. Domestic income improves local trade balance. Foreign income has a positive impact on Pakistan's trade balance. The causality analysis indicates the presence of feedback effect between terms of trade and trade balance. Domestic income Granger causes trade balance. The unidirectional causality is running from foreign income to Pakistan's trade balance. This study opens up new directions for policymakers for improvements in terms of trade to sustain trade balance in Pakistan.

**Web URL:**

[https://www.researchgate.net/profile/Khalid\\_Ahmed15/publication/303738266\\_Does\\_Harberger-Laursen-Metzler\\_HLM\\_Exist\\_in\\_Pakistan\\_Cointegration\\_Causality\\_and\\_Forecast\\_Error\\_Variance\\_Decomposition\\_Tests\\_Talat\\_Afza1\\_Khalid\\_Ahmed2\\_Muhammad\\_Shahbaz3/links/575f18fd08ae414b8e548a47.pdf](https://www.researchgate.net/profile/Khalid_Ahmed15/publication/303738266_Does_Harberger-Laursen-Metzler_HLM_Exist_in_Pakistan_Cointegration_Causality_and_Forecast_Error_Variance_Decomposition_Tests_Talat_Afza1_Khalid_Ahmed2_Muhammad_Shahbaz3/links/575f18fd08ae414b8e548a47.pdf)

**16. Shahbaz, M., Nasreen, S., & Ozturk, I. (2016). FDI, Growth and CO2 Emissions Relationship: Evidence from High, Middle and Low Income Countries. *Bulletin of Energy Economics (BEE)*, 4(1), 54-69.**

**ABSTRACT:**

The present study aims to investigate the causal relationship between foreign direct investments, economic growth and CO2 emissions using data of 117 countries over the period of 1985-2010. Our results showed that relationship between these variables change from country to country. In regional analysis, feedback effect exists between foreign direct investment and CO2 emissions and, the same is true for economic growth and CO2 emissions. The results are different on a country and regional level. These dissimilarities may due to the level of development, energy per capita use, amount of FDI, types energy sources used, population growth and etc.

**Web URL:** [http://tesdo.org/shared/upload/pdf/papers/BEE,%204\\_1,%2054-69%20.pdf](http://tesdo.org/shared/upload/pdf/papers/BEE,%204_1,%2054-69%20.pdf)

**17. Shahbaz, M., Loganathan, N., Muzaffar, A. T., Ahmed, K., & Jabran, M. A. (2016). How urbanization affects CO<sub>2</sub> emissions in Malaysia? The application of STIRPAT model. *Renewable and Sustainable Energy Reviews*, 57, 83-93.**

**ABSTRACT:**

We investigate the impact of urbanisation on CO<sub>2</sub> emissions by applying the Stochastic Impacts by Regression on Population, Affluence and Technology (STIRPAT) in the case of Malaysia over the period of 1970Q1-2011Q4. Empirically, after testing the integrating properties of the variables using unit root test, we applied the Bayer-Hanck combined cointegration approach to examine the cointegration relationship between the variables. Further, we tested the robustness of long-run relationship in the presence of structural breaks using ARDL bounds testing approach. The causal relationship between the variables is investigated by applying the VECM Granger causality test. Our results validate the existence of cointegration in the presence of structural breaks. The empirical results exposed that economic growth is a major contributor to CO<sub>2</sub> emissions. Besides, energy consumption raises emissions intensity and capital stock boosts energy consumption. Trade openness leads affluence and hence increases CO<sub>2</sub> emissions. More importantly, we find that the relationship between urbanisation and CO<sub>2</sub> emissions is U-shaped i.e. urbanisation initially reduces CO<sub>2</sub> emissions, but after a threshold level, it increases CO<sub>2</sub> emissions. The causality analysis suggests that the urbanization Granger causes CO<sub>2</sub> emissions.

**Web URL:** [https://mpra.ub.uni-muenchen.de/68422/1/MPRA\\_paper\\_68422.pdf](https://mpra.ub.uni-muenchen.de/68422/1/MPRA_paper_68422.pdf)

**18. Mujahid, N., Shabbir, M. S., & Shahbaz, M. (2016). Labour Market Conditions–Female Labour Supply Nexus: The Role of Globalization in Pakistan. *Global Business Review*, 17(1), 68-87.**

**ABSTRACT:**

This study examines the impact of female wages, unemployment, foreign remittances and globalization on female labor supply over the period from 1980 to 2010. We have applied the ARDL bounds testing to test whether cointegration exists between variables. Our results show that variables are integrated for long run relationship. Moreover, female wages attract female

labor supply. Foreign remittances and globalization raises female labor supply but unemployment declines it. The relation between female wages and female labor supply is Ushaped. The causality analysis reveals that female wage, foreign remittances, globalization and unemployment Granger cause female labor supply.

**Web URL:** [https://mpra.ub.uni-muenchen.de/57179/1/MPRA\\_paper\\_57179.pdf](https://mpra.ub.uni-muenchen.de/57179/1/MPRA_paper_57179.pdf)

**19. Abosedra, S., Shahbaz, M., & Nawaz, K. (2016). Modeling causality between financial deepening and poverty reduction in Egypt. *Social Indicators Research*, 126(3), 955-969.**

**ABSTRACT:**

This study deals with the linkages between financial development and poverty reduction in Egypt using data for the period of 1975Q1-2011Q4. The stationarity properties of the variables are tested by applying Zivot-Andrews structural break unit root test. The structural break autoregressive distributed lag-bounds testing approach to cointegration is used to examine long run relationship between the variables. Our results show evidence of cointegration which confirms the presence of long run relationship between financial deepening, economic growth and poverty reduction. The VECM Granger causality results are somewhat interesting. The findings indicate that financial development reduces poverty when domestic credit to private sector is used as proxy for financial development. The direct channel that financial sector development can lead to enabling the poor to access or broaden their access to financial services, such as credit and insurance-risk services, is therefore confirmed in case of Egypt. Furthermore, the indirect channel where financial sector development contributes to poverty reduction through economic growth is also confirmed for Egypt. This is only found when M2 is used as a proxy for financial development and infant mortality per capita as proxy for poverty. We find that the causal relationship between financial development and poverty reduction is sensitive to the proxy used to measure the level of financial development and the level of poverty. When the domestic credit to the private sector is used as a proxy for financial development, causality is found to prevail between financial development and poverty reduction in short run. However, when the broad money supply is used as a proxy, we find that financial development causes growth which in turn causes poverty reduction. These results

show that the poverty-reduction programs are desirable not only because they reduce poverty but also because they possibly lead to further development of financial sector in long run. Furthermore, our results show that appropriate reforms aimed at developing a financial sector in Egypt that is wellorganized and spread throughout the country can help reduce poverty by availing more domestic credit to the poor

**Web URL:** [https://mpa.ub.uni-muenchen.de/67166/1/MPRA\\_paper\\_67166.pdf](https://mpa.ub.uni-muenchen.de/67166/1/MPRA_paper_67166.pdf)

**20. Shahbaz, M., Jam, F. A., Bibi, S., & Loganathan, N. (2016). Multivariate granger causality between CO2 emissions, energy intensity and economic growth in Portugal: evidence from cointegration and causality analysis. *Technological and Economic Development of Economy*, 22(1), 47-74.**

**ABSTRACT:**

The present study aims to investigate the relationship between economic growth, energy intensity and CO2 emissions by incorporating financial development in CO2 emissions function using Portuguese annual data over the period of 1971–2011. The unit root analysis of variables is examined by applying Zivot-Andrews unit root test and the ARDL bounds testing approach is for long run relationship. The direction of causal relationship between the series is examined by the VECM Granger causality approach and robustness of causality analysis is tested by innovative accounting approach (IAA). Our empirical evidence confirmed that the variables are cointegrated for long run relationship. The results exposed that economic growth and energy intensity increase CO2 emissions, while financial development condenses it. The VECM Granger causality analysis showed the feedback effect between energy intensity and CO2 emissions, while economic growth and financial development Granger causes CO2 emissions. The study suggests that environment degradation can be controlled by using energy efficient technologies. Financial development can also play its role in improving the environmental quality by encouraging investment in energy efficient technology to enhance domestic production and save the environment from degradation.

**Web URL:**

[https://www.researchgate.net/profile/Nanthakumar\\_Loganathan/publication/279923861\\_Mul](https://www.researchgate.net/profile/Nanthakumar_Loganathan/publication/279923861_Mul)

[tivariate Granger causality between CO2 emissions energy intensity and economic growth in Portugal evidence from cointegration and causality analysis/links/56752ea808ae0ad265bedf38.pdf](https://www.researchgate.net/publication/310512111/tivariate-Granger-causality-between-CO2-emissions-energy-intensity-and-economic-growth-in-Portugal-evidence-from-cointegration-and-causality-analysis/links/56752ea808ae0ad265bedf38.pdf)

**21. Shahbaz, M., Kumar, R. R., Ivanov, S., & Loganathan, N. (2015). Nexus between Tourism demand and output per capita with relative importance of trade and financial development: A study of Malaysia.**

**ABSTRACT:**

This paper revisits the tourism-growth nexus in Malaysia using time series quarter frequency data over the period of 1975-2013. We examine the impact of tourism using two separate indicators – tourism receipts per capita and visitor arrival per capita. Using the augmented Solow (1956) production function and the ARDL bounds procedure, we also incorporate trade openness and financial development, and account for structural break in series. Our results show the evidence of cointegration between the variables. Assessing the long-run results using both indicators of tourism demand, it is noted that the elasticity coefficient of tourism is 0.13 and 0.10 when considering visitor arrival and tourism receipts (in per capita terms) respectively. Notably, the impact of tourism demand is marginally higher with visitor arrival. The elasticity for trade openness is 0.19, financial development is 0.09, and capital share is 0.15. In the short-run, the coefficient of tourism is marginally negative, and for financial development and trade openness, it is 0.01 and 0.18, respectively. The Granger causality tests show bi-directional causation between tourism and output per capita; financial development and tourism; and trade openness and tourism demand, duly indicating the feedback or mutually reinforcing impact between the variables, and the evidence that tourism is central to enhancing the key sectors and the overall income level.

**Web URL:** [https://mpra.ub.uni-muenchen.de/67226/1/MPRA\\_paper\\_67226.pdf](https://mpra.ub.uni-muenchen.de/67226/1/MPRA_paper_67226.pdf)

**22. Ahmed, K., Shahbaz, M., & Kyophilavong, P. (2016). Revisiting the emissions-energy-trade nexus: evidence from the newly industrializing countries. *Environmental Science and Pollution Research*, 23(8), 7676-7691.**

**ABSTRACT:**

This paper applies Pedroni's panel cointegration approach to explore the causal relationship between trade openness, carbon dioxide emissions, energy consumption, and economic growth for the panel of newly industrialized economies (i.e., Brazil, India, China, and South Africa) over the period of 1970–2013. Our panel cointegration estimation results found majority of the variables cointegrated and confirm the long-run association among the variables. The Granger causality test indicates bidirectional causality between carbon dioxide emissions and energy consumption. A unidirectional causality is found running from trade openness to carbon dioxide emission and energy consumption and economic growth to carbon dioxide emissions. The results of causality analysis suggest that the trade liberalization in newly industrialized economies induces higher energy consumption and carbon dioxide emissions. Furthermore, the causality results are checked using an innovative accounting approach which includes forecast-error variance decomposition test and impulse response function. The long-run coefficients are estimated using fully modified ordinary least square (FMOLS) method, and results conclude that the trade openness and economic growth reduce carbon dioxide emissions in the long run. The results of FMOLS test sound the existence of environmental Kuznets curve hypothesis. It means that trade liberalization induces carbon dioxide emission with increased national output, but it offsets that impact in the long run with reduced level of carbon dioxide emissions.

**Web URL:** <https://link.springer.com/article/10.1007/s11356-015-6018-x>

**23. Ling, C. H., Ahmed, K., Muhamad, R., Shahbaz, M., & Loganathan, N. Testing the Social Cost of Rapid Economic Development in Malaysia: The Effect of Trade on Life Expectancy. *Social Indicators Research*, 1-19.**

**ABSTRACT:**

The sheer size of industrializing economies' echo rising health challenges, are we ignoring the darker side of economic development? Thus, this paper explores the impact of trade openness on life expectancy in Malaysia using time series data over the period of 1960–2014. We have applied structural break unit root and as well as cointegration tests to examine integrating properties of the variables and cointegration between the variables. The causal linkage between the variables is tested by applying the VECM Granger causality. The empirical evidence confirms the presence of cointegration amid the variables. Furthermore, economic growth

increases life expectancy. Exports and imports have positive impact on life expectancy. The feedback effect exists between economic growth and life expectancy. Exports and imports cause life expectancy in Granger sense.

**Web URL:**

[https://www.researchgate.net/profile/Khalid\\_Ahmed15/publication/288823913\\_Testing\\_the\\_Social\\_Cost\\_of\\_Rapid\\_Economic\\_Development\\_in\\_Malaysia\\_The\\_Effect\\_of\\_Trade\\_on\\_Life\\_Expectancy/links/5684011e08ae1975839375f6.pdf](https://www.researchgate.net/profile/Khalid_Ahmed15/publication/288823913_Testing_the_Social_Cost_of_Rapid_Economic_Development_in_Malaysia_The_Effect_of_Trade_on_Life_Expectancy/links/5684011e08ae1975839375f6.pdf)

**24. Kyophilavong, P., Uddin, G. S., & Shahbaz, M. (2016). The Nexus between Financial Development and Economic Growth in Lao PDR. *Global Business Review*, 17(2), 303-317.**

**ABSTRACT:**

The relationship between financial development and economic growth is not conclusive in existing economics literature. The aim of this paper is to test two hypotheses: 'supply-leading' hypothesis and 'demand-following' hypothesis, using Laos time series data. The ARDL bounds testing approach to cointegration is used to carry out this task. Our results confirm the presence of feedback effect between both variables. Financial development promotes economic growth and in resulting, economic growth leads financial development.

**Web URL:** [https://mpa.ub.uni-muenchen.de/57308/1/MPRA\\_paper\\_57308.pdf](https://mpa.ub.uni-muenchen.de/57308/1/MPRA_paper_57308.pdf)

**25. Shahbaz, M., Mallick, H., Mahalik, M. K., & Sadorsky, P. (2016). The role of globalization on the recent evolution of energy demand in India: Implications for sustainable development. *Energy Economics*, 55, 52-68.**

**ABSTRACT:**

Using annual data for the period 1971-2012, this study explores the relationship between globalization and energy consumption for India by endogenizing economic growth, financial development and urbanization. The cointegration test proposed by Bayer-Hanck (2013) is applied to estimate the long-run and short-run relationships among the variables. After confirming the existence of cointegration, the overall results from the estimation of an ARDL energy demand function reveal that in the long run, the acceleration of globalization (measured in three dimensions - economic, social and overall globalization) leads to a decline in energy

demand in India. Furthermore, while financial development is negatively related to energy consumption, economic growth and urbanization are the key factors leading to increased energy demand in the long run. These results have policy implications for the sustainable development of India. In particular, globalization and financial development provide a win-win situation for India to increase its economic growth in the long run and become more environmentally sustainable.

**Web URL:** [https://mpra.ub.uni-muenchen.de/69127/1/MPRA\\_paper\\_69127.pdf](https://mpra.ub.uni-muenchen.de/69127/1/MPRA_paper_69127.pdf)

**26. Zaman, K., Shahbaz, M., Loganathan, N., & Raza, S. A. (2016). Tourism development, energy consumption and Environmental Kuznets Curve: Trivariate analysis in the panel of developed and developing countries. *Tourism Management*, 54, 275-283.**

**ABSTRACT:**

The study investigates the relationship between economic growth, carbon dioxide emissions, tourism development, energy demand, domestic investment and health expenditures with an aim to test the validity of the Environmental Kuznets Curve (EKC) hypothesis in the panel of three diversified World's region including East Asia & Pacific, European Union and High income OECD and Non-OECD countries. The study covers the period of last nine years i.e. 2005e2013. The study used the principal component analysis (PCA) to construct tourism development index which is the amalgamation of number of tourists' arrivals, tourism receipts and international tourism expenditures. The results validate the inverted Ushaped relationship between carbon emissions and per capita income in the region. The results further substantiate the following causal relationships i.e. i) tourism-induced carbon emissions, ii) energyinduced emissions, iii) investment e induced emissions, iv) growth led tourism, v) investment led tourism and vi) health led tourism development in the region.

**Web URL:**

[https://www.researchgate.net/profile/Muhammad\\_Shahbaz29/publication/287841443\\_Tourism\\_development\\_energy\\_consumption\\_and\\_Environmental\\_Kuznets\\_Curve\\_Trivariate\\_analysis\\_in\\_the\\_panel\\_of\\_developed\\_and\\_developing\\_countries/links/56dd1bb908aebabdb415a7ae.pdf](https://www.researchgate.net/profile/Muhammad_Shahbaz29/publication/287841443_Tourism_development_energy_consumption_and_Environmental_Kuznets_Curve_Trivariate_analysis_in_the_panel_of_developed_and_developing_countries/links/56dd1bb908aebabdb415a7ae.pdf)

**27. Exchange Rate Volatility and Pakistan's Exports to Major Markets: A Sectoral Analysis ",****Not found****ABSTRACT:****Web URL:**

**28. Shahbaz, M., Islam, F., & Butt, M. S. (2016). Finance–Growth–Energy Nexus and the Role of Agriculture and Modern Sectors: Evidence from ARDL Bounds Test Approach to Cointegration in Pakistan. *Global Business Review*, 17(5), 1037-1059.**

**ABSTRACT:**

This paper explores the relationship between financial development and energy consumption by incorporating economic growth, agriculture and modern sectors in Pakistan over the period of 1972-2011. The Autoregressive Distributive Lag (ARDL) bounds testing approach to cointegration, assuming structural breaks, confirms cointegration. Innovation accounting approach, used to examine the direction of causality, shows that economic growth causes energy demand. We also find bidirectional causality between financial development and energy consumption; and between modern sector growth and energy consumption. Energy consumption Granger causes agriculture growth. The results offer valuable insights for policymakers in crafting appropriate energy policy for Pakistan.

**Web URL:** [https://mpra.ub.uni-muenchen.de/62848/1/MPRA\\_paper\\_62848.pdf](https://mpra.ub.uni-muenchen.de/62848/1/MPRA_paper_62848.pdf)

**29. Ahad, M., Afza, T., & Shahbaz, M. (2017). Financial Development and Estimation of Import Demand Function in Pakistan: Evidence from Combined Cointegration and Causality Tests. *Global Business Review*, 18(1), 118-131.**

**ABSTRACT:**

This article explores the relationship between financial development and imports focusing on economic growth and import prices as potential contributors to this relationship. We have applied combined cointegration and causality tests using multivariate model for long-run and augmented Dickey–Fuller (ADF) as well as *Phillips–Perron* (PP) unit root to test the order of integration of the variables. The empirical evidence confirms the presence of a long-run

relationship among the series. Financial development increases imports demand. Economic growth and imports prices decrease imports consumption. Imports are negatively affected by relative prices.

**Web URL:** <http://journals.sagepub.com/doi/abs/10.1177/0972150916666909>

### **30. Munir, S. CAN SPEAKING UP REALLY HINDER THE PERFORMANCE.**

#### **ABSTRACT:**

In today's dynamic environment, employees are becoming the most valuable asset to the organizations, because they are the main source who can add value to their organization by their commitment, creativity and high performance. But this all depends on how the employees are being treated by their organizations. (Burriss, E. 2012). Sometimes employees tend to speak up and express what they feel about their work setting. Managers play a fundamental role in the voice process because they are supposed to have the power to address the raised issue (Ashford, Sutcliffe, & Christianson, 2009; Detert& Burriss, 2007). The present study focuses on positive side of employee voice and the way it should be dealt with in order to gain more value for the organization This study investigates that how employee voice can lead to a better performance. It was assumed that the stance of employee voice depends on the manager/team lead/ supervisor of that employee as how the raised voice has been perceived and resultantly it can affect the performance of that employee. The validity of the instrument has been test through Confirmatory factor analysis in AMOS 19 and hypotheses were being tested by applying regression analysis on SPSS 19. In a sample of 239 employees of telecom sector of Pakistan, as hypothesized, employees who raised supportive type of voice were being considered as loyal to the organization and eventually they performed better. Employees who tend to raise challengeable voice were considered as threat and hence it hindered their performance.

**Web URL:** <http://www.ciitlahore.edu.pk/Papers/Abstracts/539-8587398458801182058.pdf>

**31. Sadiq, M. W., & Abbasi, A. S. (2016). DIVERSITY MANAGEMENT IN TODAY'S CHINA: A CRITICAL ASSESSMENT OF CHINESE POLICIES FROM DIVERSITY POINT OF VIEW. *Science International*, 28(2).**

**ABSTRACT:**

This research study gathers and assembles the different discussions and history happenings from literature regarding China and its five main regions which are Hong Kong, Taiwan, Tibet, Xinjiang and Inner Mongolia, and then debates on this literature from diversity management point of view, using argumentative research methodology. This study wants to determine, whether the diversity management policies used by China in these five regions could be considered as a role model strategy for international community to follow, or it's a recipe of failure. Evaluation of Chinese policies from diversity point of view in these five regions which includes religion, culture, language, ethnicity, dress code, politics & socio economic status, will be useful to identify the problem and its solution in a precise way for China and its regions. Literature shows that Chinese diversity management policies are not up to mark and they are not reasonably successful, leading towards the disagreements between these five regions with China, and this disagreement could ultimately lead towards the altered geography of China in coming future. China needs to overcome the gaps in its policies related to diversity management with combined consent of all regions, so that China and these regions could finally attain peace and harmony.

**Web URL:** <http://www.ciitlahore.edu.pk/Papers/Abstracts/539-8587398467936338308.pdf>

**32. Munir, S., Abbasi, A. S., & Hassan, S. S. (2016). IMPLICATIONS OF MANAGERIAL PERCEPTION, EMPLOYEE VOICE AND ORGANIZATIONAL COMMITMENT IN TELECOM SECTOR OF PAKISTAN. *Science International*, 28(2).**

**ABSTRACT:** This study aims to investigate the relationship between managerial perception and organizational commitment of the employees of telecom sector of Pakistan. When an employee raises a voice it will be either challenging to the status quo or supportive for the organizational context. Likewise, manager will perceive the employee as a threat or being loyal to the organization based on the raised voice. It was hypothesized that employees will be more committed towards their organizations if they are perceived as loyal by their supervisors/team leads/managers as compared to those who were perceived as a threat based on their voice behavior. A sample of 300 employees from telecom sector was being studied to gauge their

commitment towards their organizations in both cases i.e. when perceived as loyal and when perceived as threat. The reliability of the scale was measured through Cronbach alpha test in SPSS 19 and validity of the scale was measured by Confirmatory Factor Analysis (CFA) in AMOS 19. The regression analysis was conducted in SPSS 19 to see the relationship between managerial perception and organizational commitment of employees. The results show that employees are more attached to their organizations because they are perceived as loyal by their managers and on the other hand employees are less committed with their organizations when their managers think that they are threat to the organization.

**Web URL:** <http://www.sci-int.com/Search?catid=65>

**33. Nazeer, S., & Abbasi, A. S. (2016). IS FREEWILL FREE IN PHILOSOPHICAL PERSPECTIVE?. *Science International*, 28(2).**

**ABSTRACT:** Determinism, theological fatalism, and problem of evil all negate the existence of freewill. But belief in freewill persuades individuals to indulge in moral behavior. Also, one cannot hold a person morally responsible for an action without freewill. Subsequent developments to resolve the matter, mostly in the probabilistic predictions in quantum mechanics, have muddied the waters more than clarifying them. The study has proved the existence of freewill by providing arguments from Islamic thoughts. Using deductive method from logical reasoning, the study concludes compatibility of freewill with determinism and problem of evil. On the other hand, theological fatalism and indeterminism have been proved as only speculative beliefs on freewill. Both are concluded to be the logical fallacies based on false assumptions. Limitations on freewill emerging from the discussion have been capitalized to discuss how is will free and its implications for employeremployee relationship.

**Web URL:** <http://www.sci-int.com/Search?catid=65>

**34. Nazeer, S., & Abbasi, A. S. (2016). SCRUTINIZING UNITED STATES FROM DIVERSITY PERSPECTIVE: REFLECTIONS FROM DOMESTIC AND GLOBAL PRACTICES. *Science International*, 28(2).**

**ABSTRACT:**

The current study investigates the local and global ethnic diversity management practices of the United States and tries to answer the question that can United States be the role model for global community in ethnic diversity management practices? By analyzing secondary data and surveying existing literature relevant to ethnic diversity practices of United States from its independence till today, the study analyzes different events and concludes that United States does not qualify as a leader for the rest of the world in ethnic diversity management practices. The results are validated both in local and global contexts. Finally, the present study recommends that United States should pursue multicultural policies with positive discrimination aimed at removing blockade that limit a particular group entry into key managerial positions and into moneyspinning professions. Internationally, United States must abide by the laws laid by human rights organizations towards respecting otherness of global nations. The current study investigates the local and global ethnic diversity management practices of the United States and tries to answer the question that can United States be the role model for global community in ethnic diversity management practices? By analyzing secondary data and surveying existing literature relevant to ethnic diversity practices of United States from its independence till today, the study analyzes different events and concludes that United States does not qualify as a leader for the rest of the world in ethnic diversity management practices. The results are validated both in local and global contexts. Finally, the present study recommends that United States should pursue multicultural policies with positive discrimination aimed at removing blockade that limit a particular group entry into key managerial positions and into moneyspinning professions. Internationally, United States must abide by the laws laid by human rights organizations towards respecting otherness of global nations.

**Web URL:** <http://www.ciitlahore.edu.pk/Papers/Abstracts/539-8587398461252119558.pdf>

**35. Naqvi, S. M., Abbas, K., & Ahmad, A. (2016). Riba Free Loan in Islamic Finance: Key to Social Development and Welfare. *European Online Journal of Natural and Social Sciences*, 5(2), pp-559.**

**ABSTRACT:**

Worldwide Islamic financial institutions (IFIs) do not offer loan for avoiding interest/usury, confine their Shariah interpretations to a particular school of thought and offer products for rich people only. Loans are however demanded by the underdeveloped social actors in economy for welfare and development. As per Islam usury (Riba) free loan (Qard – e – Hassan or Dain) is a key to social development. Modern implicit and explicit shapes of master-servant relation among individuals and institutions are legal phenomena with diversified standards and patterns. As per Jaferia school of thought, Islam allows presetting Hadya (gift) in loans among master-servant. These options were utilized by our study for proposing a Pro-Hadya Riba Free Loan among masterservant. Such model of loaning can help stakeholders of Islamic finance improving the existing landscape from pro-commercial creed to pro - social development approach. It is further a potential replacement of fixed rate of interest/usury with Hadya. Such loan can be utilized for turning pension, gratuity, provident fund and other investment schemes Shariah based easily by taking advantage of master-servant setup. Findings and recommendations of this study contributes novel and further invites future research on its engineered model of loaning.

**Web URL:** <http://european-science.com/eojnss/article/view/3117>

**36. Mahmood, H. Z., Abbas, K., Fatima, M., & Asghar, S. (2016). Does Islamic Microfinance Go beyond the Self-employability? An Appraisal from Lahore, Pakistan. *Journal of Creating Value*, 2(2), 268-286.**

**ABSTRACT:**

Unemployment is a syndrome which is a common feature of all developing nations. Masses are either unemployed or self-employed due to lack of opportunities and distorted public policies regarding employment generation in these countries. Microenterprises financing through microfinance institutions are playing a pivotal role in creating employment opportunities for their target households. This study observes the impact of Islamic microfinance on self, family and community employment generation activities. In this regard, data were collected from 168 clients of three pioneering Islamic microfinance institutions working in Lahore, Pakistan. The study uses descriptive analysis and probability econometric modeling to achieve its objectives. The results show that the Islamic microfinance played a significant role in starting and

extending existing businesses of the target households. Moreover, it also helps households and community members to get absorbed in the microenterprises apart from borrowers themselves. Therefore, it is concluded that Islamic microfinance does go beyond self-employability.

**Web URL:**

<http://journals.sagepub.com/doi/abs/10.1177/2394964316655238?journalCode=jcva>

**37. Yahya, F., Ali, S. A., & Ghazali, Z. (2016). The relevance of agency conflicts in small and medium enterprises. *International Journal of Advanced and Applied Sciences*, 3(7), 41-45.**

**ABSTRACT:**

The agency theory posits that the separation of control and ownership in firms leads to agency conflicts. Previous studies have focused on the relevance of these conflicts in large public listed companies; however, very few studies have demonstrated the role of agency conflicts in small and medium enterprises. This paper has presented theoretical and conceptual arguments regarding to types of agency conflicts prevail in SMEs and the solutions to mitigate them. Firstly, this study has demonstrated the conflicts of interest emerge between creditors and managers. It is postulated that underinvestment (debt overhang) issue can be resolved through short-term debts, the asset substitution (risk-shifting) problem can be mitigated by aligning the economic life of asset with debt maturity and overinvestment issue is likely to be reduced by increasing debt maturity. Secondly, to overcome principal-agent conflict, it is recommended that SMEs should have demand for voluntary external auditing regardless of their size to improve the monitoring mechanisms in the firms. This paper has also specified the directions for futuristic research especially in the context of developing economies.

**Web URL:** <http://www.science-gate.com/IJAAS/V3I7/Yahya.html>

**38. Raza, N., Shahzad, S. J. H., Tiwari, A. K., & Shahbaz, M. (2016). Asymmetric impact of gold, oil prices and their volatilities on stock prices of emerging markets. *Resources Policy*, 49, 290-301.**

**ABSTRACT:**

This paper examines the asymmetric impact of gold prices, oil prices and their associated volatilities on stock markets of emerging economies. Monthly data are used for the period January 2008 till June 2015. The nonlinear ARDL approach is applied in order to find short-run and long-run asymmetries. The empirical results indicate that gold prices have a positive impact on stock market prices of large emerging BRICS economies and a negative impact on the stock markets of Mexico, Malaysia, Thailand, Chile and Indonesia. Oil prices have a negative impact on stock markets of all emerging economies. Gold and oil volatilities have a negative impact on stock markets of all emerging economies in both the short- and the long-run. The results indicate that the stock markets in the emerging economies are more vulnerable to bad news and events that result in uncertain economic conditions.

**Web URL:** [https://www.researchgate.net/profile/Naveed\\_Raza2/publication/308947769\\_1-s20-S0301420716300617-main/links/57f93338e08ae91deaa6167f9.pdf](https://www.researchgate.net/profile/Naveed_Raza2/publication/308947769_1-s20-S0301420716300617-main/links/57f93338e08ae91deaa6167f9.pdf)

**39. Shahzad, S. J. H., Kumar, R. R., Zakaria, M., & Hurr, M. (2017). Carbon emission, energy consumption, trade openness and financial development in Pakistan: A revisit. *Renewable and Sustainable Energy Reviews*, 70, 185-192.**

**ABSTRACT:**

The paper empirically examines the cointegrating relationship between carbon emissions, energy consumption, trade openness and financial development in Pakistan using ARDL bounds test for cointegration procedure. Annual time series data is used for the period 1971–2011. The results reveal an inverted U-shaped relationship between carbon emission and energy consumption with a maximum threshold value of energy consumption per capita 640 kg of oil equivalent. Currently, the economy is operating below this level and therefore it is expected that carbon emission will continue to rise gradually over some time until the threshold level is reached. The lower than threshold level of energy consumption implies that scale and composition effects dominate the technology effect in terms of energy use. Further, the long-run results indicate that one percent increase in trade openness and financial development will increase carbon emission by 0.247% and 0.165%, respectively. The short-run elasticities are

0.122% and 0.087% for trade openness and financial development, respectively. The Granger causality results indicate a unidirectional causality from energy consumption, trade openness and financial development to carbon emission; and a bi-directional causality between energy consumption and financial development. In line with the results and given the growing focus on climate change effects in Pakistan, the paper discusses some policy issues for consideration and highlights the need to interpret elasticities with caution.

**Web URL:** <http://www.sciencedirect.com/science/article/pii/S1364032116308401>

**40. Damalas, C. A., & Khan, M. (2016). Farmers' attitudes towards pesticide labels: implications for personal and environmental safety. *International Journal of Pest Management*, 62(4), 319-325.**

**ABSTRACT:**

The label of pesticide containers is a major source of information for the use of pesticides, but research on whether farmers use this information is scarce. A survey of small-scale cotton farmers was conducted in the area of Punjab, Pakistan, to study attitudes related with the use of pesticide labels. The majority of the farmers (97%) stated that they were using pesticide products purchased in their original containers and accompanied by written information for use. However, 73% of the farmers reported that they usually do not read this information. Elderly, less educated, and experienced farmers in chemical pest control, but without previous training, were found to be less likely to read the labels. A large part of the farmers (34%) stated that they primarily rely on information of pesticide retailers for pesticide use, while nearly four out of ten said they usually rely on other sources of information or their own experience with pesticides. A sizeable proportion of the farmers (9%) mentioned that there is no need to receive information on such issues. Effective pesticide risk communication conveyed through label information is important so that potential risks from pesticide handling may be mitigated at the point of use.

**Web URL:**

<http://www.tandfonline.com/doi/abs/10.1080/09670874.2016.1195027?needAccess=true#aH>

[R0cDovL3d3dy50YW5kZm9ubGluZS5jb20vZG9pL3BkZi8xMC4xMDgwLzA5NjcwODc0LjIwMTYuMTE5NTAyNz9uZWVkQWNjZXNzPXRydWVAQEAw](https://www.researchgate.net/profile/Waqar_Akram2/publication/308366093_ESTIMATING_PRODUCTIVITY_OF_BT_COTTON_AND_ITS_IMPACT_ON_PESTICIDE_USE_IN_PUNJAB_PAKISTAN/links/57e22d2e08ae9e25307d5635.pdf)

**41. Bakhsh, K., Akram, W., Jahanzeb, A., & Khan, M. (2016). ESTIMATING PRODUCTIVITY OF BT COTTON AND ITS IMPACT ON PESTICIDE USE IN PUNJAB (PAKISTAN). *Pakistan Economic and Social Review*, 54(1), 15.**

**ABSTRACT:**

The present study is designed to determine the impact of Bt cotton seed on pesticide use and cotton productivity in the Punjab province of Pakistan. Cross-sectional data for two cropping seasons of 2008 and 2009 are gathered from three districts of cotton growing region of the province. Modified exponential damage control production function is employed to estimate the effect of Bt cotton seed. Results of the production function show that farmers using Bt cotton seed obtain higher yield as compared to non-users of Bt cotton seed. Fertilizer and irrigation variables are positively related with cotton yield whereas location dummies indicate that cotton growers from Multan district have low productivity as compared to those from Rahim Yar Khan and Mianwali districts. Age, farming experience and farm size are found increasing cotton productivity. So, the study concludes that in addition to traditional inputs and socioeconomic factors, Bt cotton can fetch higher benefits to cotton growers, provided that farmers have access to quality Bt cotton seed in the market.

**Web URL:**

[https://www.researchgate.net/profile/Waqar\\_Akram2/publication/308366093\\_ESTIMATING\\_PRODUCTIVITY\\_OF\\_BT\\_COTTON\\_AND\\_ITS\\_IMPACT\\_ON\\_PESTICIDE\\_USE\\_IN\\_PUNJAB\\_PAKISTAN/links/57e22d2e08ae9e25307d5635.pdf](https://www.researchgate.net/profile/Waqar_Akram2/publication/308366093_ESTIMATING_PRODUCTIVITY_OF_BT_COTTON_AND_ITS_IMPACT_ON_PESTICIDE_USE_IN_PUNJAB_PAKISTAN/links/57e22d2e08ae9e25307d5635.pdf)

**42. Mahmood, A., Hussan, S. G., Sarfraz, M., Abdullah, M. I., & Basheer, M. F. (2016). Rewards Satisfaction, Perception about Social Status and Commitment of Nurses in Pakistan. *European Online Journal of Natural and Social Sciences*, 5(4), pp-1049.**

**ABSTRACT:**

This research is undertaken to approve or reject the general perception of masses about commitment of employees and to identify those factors, which effect commitment of employees in general and of nurses in particular. In previous research of Allen and Myere (1990), the factor of social status was not addressed. In this study target audience is nurses. Whereas, it is a proven fact that psychological perception effects individual's attitudes and behaviors, so to see that how satisfaction with rewards/ benefits and perception about social status effect commitment of employees, this research was undertaken. Satisfaction level varies from person to person. The empirical results have proved that commitment of employees is affected due to satisfaction with rewards/ benefits and perception about social Status.

**Web URL:** <http://european-science.com/eojnss/article/view/4747/pdf>

**43. Sarfraz, M., Liu, S., & Abdullah, M. I. (2016). Coping with Information Overload: A Business Perspective. *European Online Journal of Natural and Social Sciences*, 5(3), pp-878.**

**ABSTRACT:**

Study examines the sources and origins of information overload, its effects on knowledge workers, and its overall implications for business companies. The main argument presented in this study is that information overload is not a singular issue but that it arises out of a combination of excessive amount of both sought information and supplied information (i.e. interruptions and distractions). An empirical study conducted as a part of the research revealed that information overload is a widespread problem at modern workplace. Furthermore, the empirical research suggests that the level of perceived information overload depends on both the nature of performed work task and individual personality disposition.

**Web URL:** <http://european-science.com/eojnss/article/view/3167>

**44. Shahzad, S. J. H., Nor, S. M., Hammoudeh, S., & Shahbaz, M. (2017). Directional and bidirectional causality between US industry credit and stock markets and their determinants. *International Review of Economics & Finance*, 47, 46-61.**

**ABSTRACT:**

We examine the causal links between U.S. industry-wise credits and stock markets. The full sample bootstrap Granger causality results show that all stock markets Granger cause their CDS counterparts and there is also bidirectional causality for the banking, healthcare and material industries. The short-run parametric stability tests highlight that the full sample parameters are not stable and hence less reliable. The bootstrap rolling window estimations confirm the inconsistency in the CDS-stock causality relationships where bidirectional causalities are also found between the credit and stock markets that vary over different sub-samples. Finally, we analyze the impact of different financial and macroeconomic determinants on the CDS-stock causality through a probit model. Overall, the business conditions, stock market volatility, default premiums, Treasury bond rate and the slope of the yield curve are major drivers of the CDS-stock nexus. Our findings provide possible explanation for varying and mixed previous empirical findings in the existing literature, and hence have useful investment implications.

**Web URL:** [https://mpra.ub.uni-muenchen.de/74705/1/MPRA\\_paper\\_74705.pdf](https://mpra.ub.uni-muenchen.de/74705/1/MPRA_paper_74705.pdf)

**45. Paramati, S. R., Shahbaz, M., & Alam, M. S. (2017). Does tourism degrade environmental quality? A comparative study of Eastern and Western European Union. *Transportation Research Part D: Transport and Environment*, 50, 1-13.**

**ABSTRACT:**

The purpose of this paper is to investigate the effect of tourism on economic growth and carbon dioxide emissions in Eastern and Western European Union (EU) countries by incorporating FDI and trade in the production and CO<sub>2</sub> emission functions. We apply panel econometric techniques which account for cross-sectional dependence and heterogeneity. The results of Westerlund panel cointegration test confirm a long-run equilibrium relationship among the variables. Results from long-run elasticities suggest that tourism stimulates economic growth in Eastern and Western EU countries. However, tourism increases CO<sub>2</sub> emissions in Eastern EU but decreases in Western EU. This indicates that tourism has an adverse effect on the environment in Eastern EU. Finally, short-run heterogeneous panel causality test results suggest that tourism causes CO<sub>2</sub> emissions in Eastern EU while economic

growth and CO<sub>2</sub> emissions cause tourism in Western EU. Overall, our findings suggest that tourism plays an important role in accelerating economic growth; however, its role on CO<sub>2</sub> emissions largely depends on the adaptation of sustainable tourism policies and efficient management.

**Web URL:** <http://www.sciencedirect.com/science/article/pii/S1361920915301747>

**46. Sbia, R., Shahbaz, M., & Ozturk, I. (2016). Economic Growth, Financial Development, Urbanization and Electricity Consumption Nexus in UAE.**

**ABSTRACT:**

This study aims to explore the relationship between economic growth, urbanization, financial development and electricity consumption in United Arab Emirates for 1975-2011 period. ARDL bounds testing approach is employed to examine long run relationship between the variables in the presence of structural breaks. The VECM Granger causality is applied to investigate the direction of causal relationship between the variables. Our empirical exercise validated the cointegration between the series in case of United Arab Emirates. Further, results reveal that inverted U-shaped relationship is found between economic growth and electricity consumption. Financial development adds in electricity consumption. The relationship between urbanization and electricity consumption is also inverted U-shaped. This implies that urbanization increases electricity consumption initially and after a threshold level of urbanization, electricity demand falls. The causality analysis finds feedback hypothesis between economic growth and electricity consumption i.e. economic growth and electricity consumption are interdependent. The bidirectional causality is found between financial development and electricity consumption. Economic growth and urbanization Granger cause each other. The feedback hypothesis is also found between urbanization and financial development, financial development and economic growth and same is true for electricity consumption and urbanization.

**Web URL:** [https://mpra.ub.uni-muenchen.de/74790/1/MPRA\\_paper\\_74790.pdf](https://mpra.ub.uni-muenchen.de/74790/1/MPRA_paper_74790.pdf)

**47. Khraief, N., Shahbaz, M., Mallick, H., & Loganathan, N. (2016). Estimation of electricity demand function for Algeria: Revisit of time series analysis. *Renewable and Sustainable Energy Reviews*.**

**ABSTRACT:**

This paper aims to empirically re-examine whether economic growth has effect on electricity consumption for Algerian economy. We have incorporated urbanisation and trade openness in electricity demand function as additional determinants of electricity consumption for the period of 1971-2012. For empirical purpose, we have applied the recently developed combined cointegration test proposed by Bayer and Hanck (2013) and bounds testing approach to cointegration by Pesaran et al. (2001) for establishing the cointegration between the variables by accommodating structural breaks. The results expose that income growth leads to higher electricity demand along with urbanization being another major contributing factor of rising electricity demand. In contrast, trade openness leads to reduce electricity demand. The causal association between the variables is further examined with the application of innovation accounting approach of Vector Autoregressive (VAR). The empirical evidence indicates the presence of the neutral effect between income growth and electricity use. Urbanization causes electricity use and electricity use causes urbanization in Granger sense.

**Web URL:** [https://mpra.ub.uni-muenchen.de/74870/1/MPRA\\_paper\\_74870.pdf](https://mpra.ub.uni-muenchen.de/74870/1/MPRA_paper_74870.pdf)

**48. Shahbaz, M., Khan, S., Ali, A., & Bhattacharya, M. (2015). The Impact of Globalization on CO2 Emissions in China. *The Singapore Economic Review*, 1740033.**

**ABSTRACT:**

This paper examines the Environmental Kuznets Curve (EKC) hypothesis for China in the presence of globalization. We have applied Bayer and Hanck combined cointegration test as well as the ARDL bounds testing approach to cointegration by accommodating structural breaks in the series. The causal relationship among the variables is investigated by applying the VECM causality framework. The study covers the period of 1970-2012. The results confirm the presence of cointegration among the variables. Furthermore, the EKC hypothesis is valid in

China both in short-and-long runs. Coal consumption increases CO2 emissions significantly. The overall index and sub-indices of globalization indicate that globalization in China is decreasing CO2 emissions. The causality results reveal that economic growth causes CO2 emissions confirming the existence of the EKC hypothesis. The feedback effect exists between coal consumption and CO2 emissions. CO2 emissions Granger causes globalization (social, economic and political).

**Web URL:** [https://mpra.ub.uni-muenchen.de/64450/1/MPRA\\_paper\\_64450.pdf](https://mpra.ub.uni-muenchen.de/64450/1/MPRA_paper_64450.pdf)

**49. Khan, N. Z. A., Imran, A., & Nisar, Q. A. (2016). Emotional Exhaustion as Stressor agent for Job Stress in Call Centers: Empirical evidence from perspective of Job Satisfaction and Turnover Intention as Work Outcomes. *European Online Journal of Natural and Social Sciences*, 5(4), 908.**

**ABSTRACT:**

The purpose of the study is to analyze job burnout component emotional exhaustion as a probable stressor agent that causes job stress and their impact on job satisfaction and turnover intention as work outcomes. The scales were adapted from that measure to analyze the effect of emotional exhaustion causing job stress, also highlights the evidence in support of the conceptual model. Data was collected by the survey that generated 220 respondents. The sample chosen for this research are employees working in telecommunication call centers of Lahore city region in Pakistan. SPSS regression analysis was employed for data analysis. The results showed that emotional exhaustion carried negative and significant relation with job satisfaction ( $\beta = -.354, p < .05$ ) and significant positive relation with turnover intention ( $\beta = .290, p < .05$ ) also significant relation between dependent variables followed by mediating effect of two dimensions of job stress analyzed by PROCESS procedure of bootstrapping technique contained no and full mediation between emotional exhaustion in relation with job satisfaction and turnover intention respectively. Outcome from the conducted study depicted that stress did not affected the level of satisfaction of employees as they are well trained and informed that job stress is the part of their work activities in call centers and the stress in organizations is needed to be dealt with.

**Web URL:**

[https://www.researchgate.net/profile/Qasim\\_Nisar/publication/309348349\\_Emotional\\_Exhaustion\\_as\\_Stressor\\_agent\\_for\\_Job\\_Stress\\_in\\_Call\\_Centers\\_Empirical\\_evidence\\_from\\_perspective\\_of\\_Job\\_Satisfaction\\_and\\_Turnover\\_Intention\\_as\\_Work\\_Outcomes/links/580a29f008aecba934f9528f.pdf](https://www.researchgate.net/profile/Qasim_Nisar/publication/309348349_Emotional_Exhaustion_as_Stressor_agent_for_Job_Stress_in_Call_Centers_Empirical_evidence_from_perspective_of_Job_Satisfaction_and_Turnover_Intention_as_Work_Outcomes/links/580a29f008aecba934f9528f.pdf)

**50. HAZIQ, M., AZMAN, K., AZEEM, F., NAREJO, G., JOYO, M., JAFFERY, M., ...& TARIQ, A. (2016). An Analysis of Islanded Hybrid Microgrid Implementation Using Canals as Micro Hydro Power Source with Solar PV for Rural Areas of Pakistan. *Sindh University Research Journal-SURJ (Science Series)*, 48(4D).**

**ABSTRACT:**

Modern technological expansions and human reliance on it has made impossible for the existing infrastructure to fulfil electric power supplies. Besides human living standards are increasing day by day which upsurges per capita electric power consumption. Existing electric power infrastructure cannot be protracted anymore to achieve electric power requirements in the rural areas where it does not exist yet. On the other hand power generation using conventional means is not the preferred option due to its depletion and more significantly due to environmental cautions. To cater the demand of rural community, microgrid utilizing renewable energy resources is one of the viable options to overcome the identified problem. Special emphasis for the implementation of rural microgrids in Pakistan has been given in the paper. This paper deals with the proposed model of Solar Photovoltaic (PV) and micro hydro based hybrid microgrid that can be implemented in the specific area. Paper presents the overview of technical and socioeconomic aspects that are noteworthy for the implementation of microgrids in rural areas of Pakistan. One of the site ideal for microgrid has been selected for the case study. Requirements like Demand side management, load forecasting and controls of renewable energy resource has been discussed for the implementation of microgrid in Punjab Pakistan.

**Web URL:** <http://sujo.usindh.edu.pk/index.php/SURJ/article/download/2740/2160>

# DEPARTMENT OF CHEMICAL ENGINEERING

## Journal Papers

1. Qu, L. L., Geng, Y. Y., Bao, Z. N., Riaz, S., & Li, H. (2016). Silver nanoparticles on cotton swabs for improved surface-enhanced Raman scattering, and its application to the detection of carbaryl. *Microchimica Acta*, 183(4), 1307-1313.

**ABSTRACT:**

We describe the preparation of a cotton swab for use in surface enhanced Raman scattering (SERS) by assembling silver nanoparticles (Ag-NPs) on common cotton. The flexibility of such cotton swabs allows for a close contact with sample surfaces by swabbing. This can considerably improve the sample collection efficiency. These cotton swabs exhibit excellent SERS activity as shown by the detection of rhodamine 6G at 0.81 pM concentration. The reproducibility of the intensity of SERS peaks is within 10 %. The applicability is demonstrated by in-situ detection of the fungicide carbaryl on a cucumber with an irregular surface. This combination of superior SERS activity, high reproducibility, accessibility in irregularly-shaped matrices and low-cost production indicates that such swabs offer a large potential in analytical SERS.

**Web URL:** <https://link.springer.com/article/10.1007/s00604-016-1760-4>

2. Ahmad, Z., Patel, F., Mastoi, N. R., & Saddiqa, A. (2016). Effect of sandblasting, annealing and hydrophobic treatment on the nano-mechanical and corrosion behaviour of n-TiO<sub>2</sub>-coated 316L stainless steel. *Current science*, 110(3), 353.

**ABSTRACT:**

In this article, the effect of hydrophobic coated and uncoated surfaces on the corrosion resistance, tribological property, and surface morphology and nanomechanical properties is

presented. A hierarchical surface (micro/nano) was prepared by ultra shot penning of 316L stainless steel at 20 kHz. Chemical vapour deposition technique was used for deposition of the coating, and coating thickness of 0.5  $\mu\text{m}$  was obtained. A maximum hardness of 6.7 and 6.32 GPa was exhibited by the sandblasted (SB), annealed (SBA) and coated (SBAT) samples respectively. The beneficial effect of annealing and surface roughness was clearly indicated by the sandblasted, annealed and coated specimens. They showed the highest value of reduced modulus maximum resistance to scratch tests and a high adhesion as indicated by scratch path profiles. The lowest corrosion rates were obtained by SBAT specimens (1.32 mpy) in 3.5 wt% NaCl. After application of 3.5% fluoroalkylsilane (FAS13), the corrosion rate was reduced to 0.04 mpy with no evidence of localized pitting. The water contact angle using DSA-100 system was measured to be 120° for SBAT and 80–90° for the samples.

**Web URL:** <http://www.currentscience.ac.in/Volumes/110/03/0353.pdf>

**3. Jeong, Y., Jang, N., Yasin, M., Park, S., & Chang, I. S. (2016). Intrinsic kinetic parameters of *Thermococcus onnurineus* NA1 strains and prediction of optimum carbon monoxide level for ideal bioreactor operation. *Bioresource technology*, 201, 74-79.**

**ABSTRACT:**

This study determines and compares the intrinsic kinetic parameters ( $K_s$  and  $K_i$ ) of selected *Thermococcus onnurineus* NA1 strains (wild-type (WT), and mutants MC01, MC02, and WTC156T) using the substrate inhibition model.  $K_s$  and  $K_i$  values were used to find the optimum dissolved CO ( $C_L$ ) conditions inside the reactor. The results showed that in terms of the maximum specific CO consumption rates ( $q_{\text{CO}}^{\text{max}}$ ) of WT, MC01, MC02, and WTC156T the optimum activities can be achieved by maintaining the  $C_L$  levels at 0.56 mM, 0.52 mM, 0.58 mM, and 0.75 mM, respectively. The  $q_{\text{CO}}^{\text{max}}$  value of WTC156T at 0.75 mM was found to be 1.5-fold higher than for the WT strain, confirming its superiority. Kinetic modeling was then used to predict the conditions required to maintain the optimum  $C_L$  levels and high cell concentrations in the reactor, based on the kinetic parameters of the WTC156T strain.

**Web URL:** <http://www.sciencedirect.com/science/article/pii/S0960852415015564>

4. Ashfaq, M., Khan, K. N., Rasool, S., Mustafa, G., Saif-Ur-Rehman, M., Nazar, M. F., ...& Yu, C. P. (2016). Occurrence and ecological risk assessment of fluoroquinolone antibiotics in hospital waste of Lahore, Pakistan. *Environmental toxicology and pharmacology*, 42, 16-22.

**ABSTRACT:**

In the present study, wastewater and sludge samples of two major hospitals of Lahore, Pakistan were analyzed by developing an HPLC-UV method for the possible occurrence of five frequently used fluoroquinolone antibiotics i.e. ofloxacin, ciprofloxacin, sparfloxacin, moxifloxacin and gemifloxacin. The highest detected concentration was for moxifloxacin in both wastewater (224 g/L) and sludge samples (219 g/kg). The highest concentration of ofloxacin, ciprofloxacin, sparfloxacin and gemifloxacin were found to be 66, 18, 58 and 0.2 g/L respectively. Risk quotient(RQ) was also calculated based on maximum measured concentrations and the RQ values were very high particularly for ofloxacin and ciprofloxacin. The maximum RQ values for ofloxacin against *Vibrio fisheri*, *Pseudomonas putida*, fish, *Daphnia*, Green algae and *Pseudokirchneriella subcapitata* were 3300, 66,000, 124, 46, 3300 and 6000, respectively. In case of ciprofloxacin, RQ values were found to be 1750 and 3500 against green algae and *Microcystis aeruginosa*, respectively.

**Web URL:**

[https://www.researchgate.net/profile/Muhammad\\_Saif\\_Ur\\_Rehman2/publication/287966343\\_Occurrence\\_and\\_ecological\\_risk\\_assessment\\_of\\_fluoroquinolone\\_antibiotics\\_in\\_hospital\\_waste\\_of\\_Lahore\\_Pakistan/links/581948dd08aee7cdc685f2c0/Occurrence-and-ecological-risk-assessment-of-fluoroquinolone-antibiotics-in-hospital-waste-of-Lahore-Pakistan.pdf](https://www.researchgate.net/profile/Muhammad_Saif_Ur_Rehman2/publication/287966343_Occurrence_and_ecological_risk_assessment_of_fluoroquinolone_antibiotics_in_hospital_waste_of_Lahore_Pakistan/links/581948dd08aee7cdc685f2c0/Occurrence-and-ecological-risk-assessment-of-fluoroquinolone-antibiotics-in-hospital-waste-of-Lahore-Pakistan.pdf)

5. Saif Ur Rehman, M., Kim, I., Rashid, N., Adeel Umer, M., Sajid, M., & Han, J. I. (2016). Adsorption of Brilliant Green dye on biochar prepared from lignocellulosic bioethanol plant waste. *CLEAN–Soil, Air, Water*, 44(1), 55-62.

**ABSTRACT:**

This study was aimed at the adsorption of Brilliant Green (BG) on hydrolyzed rice straw biochar, which was obtained from a lignocellulosic bioethanol process. Rice straw biochar (RBC)

possessed surface properties such as a Brunauer–Emmett–Teller (BET) surface area of 232.31 m<sup>2</sup>/g, a total pore volume of 0.30 cm<sup>3</sup>/g, and an average pore width of 5.22 nm. Adsorption studies were carried out to investigate the effect of experimental factors such as pH (2–10), biochar dose (0.05–1.25 g/L), contact time (30–480 min), and temperature (30 to –50°C) on the adsorption of BG. The Langmuir isotherm ( $R^2 = 0.998$ ) fitted well to the adsorption data for initial dye concentrations of 20–500 mg/L, implying that BG adsorption occurred in the form of a monolayer on RBC. Adsorption kinetics was well fitted by the pseudo-second order kinetic model ( $R^2 \geq 0.988$ ) for all tested dye concentrations. The thermodynamic study revealed that BG adsorption on RBC was spontaneous, favorable, and a physical process. The maximum adsorption capacity of RBC was found to be 111.11 mg/g. These results showed that RBC, prepared from the waste of the bioethanol process, can be effectively used as a promising cheap adsorbent to remove dyes from aqueous solution. This approach of product diversification (bioethanol along with biochar) may lead to a cost effective and cleaner production of bioethanol.

**Web URL:** <http://onlinelibrary.wiley.com/doi/10.1002/clen.201300954/epdf>

**6. Ahmed, M. A., Kim, I., Kim, G. Y., Rehman, M. S. U., & Han, J. I. (2016). Ammonium carbonate as a catalyst for lignocellulose pretreatment and a nitrogen source for fermentation. *Sustainable Energy Technologies and Assessments*, 16, 64-68.**

**ABSTRACT:**

In this work, ammonium carbonate (AC), a product released during the regeneration of ammonia-based carbon capture process, was evaluated as an alkaline catalyst for the pretreatment of lignocellulose; and as a nitrogen source in the subsequent fermentation process for bioethanol production. Response surface methodology was employed to attain an optimum pretreatment condition in terms of AC concentration (15–25%), reaction time (5–15 h) and temperature (60–100 °C). The highest enzymatic digestibility of 59.9% was achieved with AC concentration of 20.0% at 79.5 °C of treatment temperature for 9.46 h of reaction time. A fermentation medium containing ammonium ion derived from the liquid hydrolysate after the AC-based pretreatment was found to enhance the final concentration of ethanol produced

by *Saccharomyces cerevisiae* from 9.13 g/L to 13.30 g/L. These results indicate that AC can indeed serve as a catalyst option for pretreating lignocellulosic biomass and has an added advantage of being used as a nitrogen source for the fermentation process.

**Web URL:** <http://www.sciencedirect.com/science/article/pii/S2213138816300248>

**7. Khan, A. L., Li, X., Ilyas, A., Raza, M. T., & Vankelecom, I. F. (2016). Novel sulfonated and fluorinated PEEK membranes for CO<sub>2</sub> separation. *Separation and Purification Technology*, 167, 1-5.**

**ABSTRACT:**

Polymeric membranes containing sulfonated and fluorinated poly (ether ether ketone) were prepared by solution casting method. The monomers were pre-sulfonated before the polymerization to avoid the side-effects of polymer post-sulfonation, like low degree of sulfonation and poor mechanical and thermal properties. The degree of sulfonation was varied from 20% to 40% to study its influence on the membrane performance. Pure and mixed gas permeation experiments were performed to evaluate the potential of this novel polymer in separation of CO<sub>2</sub> from mixtures containing CH<sub>4</sub> and N<sub>2</sub>. Increasing degree of sulfonation improved the CO<sub>2</sub> permeability and selectivity for both gas pairs. The incorporation of fluorinated groups further enhanced the performance of membranes by simultaneous increase in gas permeability and selectivity. Diffusion and solubility measurements were also performed in order to get further insight into the role of sulfonic and fluorinated groups in membrane performance. The comparison of results with literature revealed the promising characteristics of the polymer in industrially relevant gas separations.

**Web URL:** <http://www.sciencedirect.com/science/article/pii/S1383586616302234>

**8. Ahmad, M. S., Bazmi, A. A., Bhutto, A. W., Shahzadi, K., & Bukhari, N. (2016). Students' responses to improve environmental sustainability through recycling: quantitatively improving qualitative model. *Applied Research in Quality of Life*, 11(1), 253-270.**

**ABSTRACT:**

This study attempts to contemplate the respondents' behaviors regarding recycling, with the purpose of identifying the factors that influence their behaviors. The study is based on a survey that was conducted with 230 nationwide university students and guidelines borrowed from the Theory of Planned Behavior and The Theory of Reasoned action. The data collected was evaluated by applying the Structure Equation Modelling technique. The study concluded that peoples' attitudes are largely subject to the moral values and general norms of their own society. Additionally, an individual's response towards recycling is greatly determined by the extent of his/her awareness towards the environment, as well as his/her personal knowledge. Another conclusion was that an individual's past experience towards recycling contributes to his/her attitude (willingness or apprehension about recycling) in the future. Furthermore, although the convenience and cost of recycling were found to be reasonably significant determinants about one's recycling behavior, it was determined that time commitment is the most decisive factor that influences an individual's willingness to or not to recycle. The study's findings have not only established the authority of Theory of Planned

**Web URL:**

[https://www.researchgate.net/profile/Ahmad\\_Muhammd\\_Shakil/publication/284825684\\_Students'\\_Responses\\_to\\_Improve\\_Environmental\\_Sustainability\\_Through\\_Recycling\\_Quantitatively\\_Improving\\_Qualitative\\_Model/links/56655ef308ae192bbf91ff09.pdf](https://www.researchgate.net/profile/Ahmad_Muhammd_Shakil/publication/284825684_Students'_Responses_to_Improve_Environmental_Sustainability_Through_Recycling_Quantitatively_Improving_Qualitative_Model/links/56655ef308ae192bbf91ff09.pdf)

**9. Bhutto, A. W., Qureshi, K., Abro, R., Harijan, K., Zhao, Z., Bazmi, A. A., ...& Yu, G. (2016). Progress in the production of biomass-to-liquid biofuels to decarbonize the transport sector—prospects and challenges. *Rsc Advances*, 6(38), 32140-32170.**

**ABSTRACT:**

Annually the transport sector consumes a quarter of global primary energy and is responsible for related greenhouse gas emissions. Presently, petroleum derived liquid fuels are the overwhelming source of energy for the transport sector. Liquid biofuels are a viable substitution for petroleum-derived fuels in the transport sector and an important option to mitigate greenhouse gas emissions, especially CO<sub>2</sub> emissions. Substituting petroleum-derived fuels with liquid biofuel is also anticipated

to reduce the dependency of the transport sector on fossil fuels. Different options are available for the production liquid biofuels. However, the production of liquid biofuels from lignocellulosic biomass has certain advantages. These advantages include the high abundance, availability, low procurement cost and current under-utilization of lignocellulosic biomass. However, the potential for successful deployment of technologies to produce liquid biofuel from lignocellulosic biomass and their cost reductions are surrounded by large uncertainties. High cost of production of liquid fuels from lignocellulosic biomass and their commercial immaturity are major obstacles for the widespread application of liquid biofuels in transportation. Other obstacles include the lack of infrastructure and lack of political as well as public support. This article reviews the obstacles behind the limited production of biomass to liquid (BTL) fuels and their diffusion in the transport sector. The potential approaches to make the production of lignocellulosic-based liquid biofuels economically attractive are also discussed. An approach that focuses on integrating individual operations and processes and adequately modelling these processes evaluated on the bases of the entire pathway can help in realizing the large scale commercial production of liquid biofuels through cleaner production.

**Web URL:**

<http://pubs.rsc.org/en/content/articlelanding/2016/ra/c5ra26459f/unauth#!divAbstract>

**10. Iqbal, J., Ali, Z., Hussain, M., Sheikh, R., Majeed, K., Khan, A. U., & Ulrich, J. (2016). Formation of crystalline particles from phase change emulsion: Influence of different parameters. *Chinese Journal of Chemical Engineering*, 24(7), 929-936.**

**ABSTRACT:**

Solidification or crystallization of phase change emulsion in the form of fine emulsion drops in a direct contact coolant at temperatures below their freezing point was studied. This work is mainly focused on the size and shape of the generated particles from phase change emulsified fats. Size of the particles is the major or key factor being considered during their formation, however, other factors that govern the particles size and shape were also observed. The operating parameters of the process were optimized in order to obtain particles of smaller size ranges in the window of current operating conditions. The crystallization of complex emulsion

matrices is very difficult to control in the bulk at desired requirement. Hence, the emulsion drop to particle formation has advantage in comparison with the bulk solidification or crystallization. The main objective of this work is to achieve spherical emulsion particles in a direct contact cooling system. Parameters like: stability, characterization, viscosity, and the effect of different energy inputs were examined. Moreover, the effects of the capillary size, interfacial tension, temperature of the emulsion on the particle size were also monitored.

**Web URL:**

[https://www.researchgate.net/profile/Asad\\_Khan27/publication/288873974\\_Formation\\_of\\_crystalline\\_particles\\_from\\_phase\\_change\\_emulsion\\_Influence\\_of\\_different\\_parameters/links/56b87e1108ae44bb330d2883.pdf](https://www.researchgate.net/profile/Asad_Khan27/publication/288873974_Formation_of_crystalline_particles_from_phase_change_emulsion_Influence_of_different_parameters/links/56b87e1108ae44bb330d2883.pdf)

**11. Ali, Z., Le, H. H., Iqbal, J., Hussain, M., Hussain, H., Mahmood, N., ...& Radusch, H. (2016). Dynamics of migration and phase selective localization of nanoclay in HNBR/ENR blends. *Journal of Applied Polymer Science*, 133(41).**

**ABSTRACT:**

The phase specific selective localization and dynamics of migration of nanoclay in hydrogenated acrylonitrile butadiene rubber (HNBR)/epoxidized natural rubber (ENR) blend systems is investigated. The phase specific dispersion of clay particles is monitored through measuring the online measured electrical conductance (OMEC) during mixing by means of a sensor system installed inside the chamber of an internal mixer. The results of different characterization techniques, such as atomic force microscopy, transmission electron microscopy, and small angle X-ray scattering have been used to understand and interpret the OMEC behaviors of nanoclay-filled rubber compounds individually (HNBR and ENR) and their blend systems. The observed online conductance is ionic in nature that arises due to the release of surfactant molecules from the clay galleries. It is observed that the OMEC behavior depends mainly on two factors: the localization of nanoclay in specific phase of the blend system and on the gradual development of blend morphology. The OMEC behavior and the supported data from the microscopic methods, clearly reveal the migration of organoclay from the ENR to HNBR phase during the mixing process, particularly localizing near the interface of the blend. Further,

the localization of organoclay is also evaluated by applying the surface tension measurements based model, which also predicts the favorable localization of organoclay in HNBR phase of the blend. The work clearly suggests the OMEC method to be a powerful online tool to monitor and control the nanoclay dispersion and localization in rubber based nanocomposites during the melt mixing process.

**Web URL:** <http://onlinelibrary.wiley.com/doi/10.1002/app.44074/epdf>

**12. Akhter, P., Farkhondehfal, M. A., Hernández, S., Hussain, M., Fina, A., Saracco, G., ...& Russo, N. (2016). Environmental issues regarding CO<sub>2</sub> and recent strategies for alternative fuels through photocatalytic reduction with titania-based materials. *Journal of Environmental Chemical Engineering*, 4(4), 3934-3953.**

**ABSTRACT:**

Carbon dioxide (CO<sub>2</sub>) is considered one of the main contributors to the greenhouse effect and is currently a key challenge throughout the world. Therefore, the CO<sub>2</sub> complications associated with the environment have in particular been focused on in this review, and various strategies regarding CO<sub>2</sub> mitigation, or the utilization of different technologies to produce renewable fuels or useful chemicals to overcome the energy crisis, have been considered together with the recent developments in the photocatalytic reduction of CO<sub>2</sub> by means of different titania photocatalysts to produce various energy-bearing products. The problems, progress and future prospects regarding CO<sub>2</sub> utilization are presented. This present review indicates that the development of efficient active photocatalysts for this technology is still under way and that better efficiency of the desired products could be accomplished. It is also shown that this technique is still at an embryonic stage, due to a lack of proficiency, and that the yield discrimination is very low. It can therefore be concluded that further research efforts are needed to boost this process towards commercialization in the near future.

**Web URL:** <http://www.sciencedirect.com/science/article/pii/S2213343716303256>

**13. Majeed, K., Hassan, A., Bakar, A. A., & Jawaid, M. (2016). Effect of montmorillonite (MMT) content on the mechanical, oxygen barrier, and thermal properties of rice husk/MMT hybrid**

filler-filled low-density polyethylene nanocomposite blown films. *Journal of Thermoplastic Composite Materials*, 29(7), 1003-1019.

**ABSTRACT:**

Montmorillonite (MMT)/rice husk (RH) hybrid filler-filled low-density polyethylene (LDPE) nanocomposite films, containing 0, 2, 3, 4, 5, and 6 wt% MMT (based on the total weight) were prepared by extrusion blown film. The films were characterized by morphological, mechanical, oxygen (O<sub>2</sub>) barrier, and thermal properties. The delamination of MMT layers evidenced from X-ray diffraction results suggests an increase in the interlayer distance and shows intercalated structure of the nanocomposites. Adding MMT did not adversely affect the interfacial morphology, as confirmed by scanning electron microscopy. Addition of MMT into the LDPE/RH system improved the mechanical and O<sub>2</sub> barrier properties. For instance, tensile strength, tensile modulus, and tear strength increased by 8, 10, and 5%, respectively, with the addition of 3 wt% MMT. Further, the O<sub>2</sub> barrier of the composite films improved more than twofold by adding 4 wt% MMT. Initial degradation temperature of LDPE/RH composites increased with the incorporation.

**Web URL:**

[https://www.researchgate.net/profile/Dr\\_Mohammad\\_Jawaid/publication/266739785\\_Effect\\_of\\_MMT\\_content\\_on\\_the\\_mechanical\\_oxygen\\_barrier\\_and\\_thermal\\_properties\\_of\\_rice\\_husk\\_MMT\\_hybrid\\_filler\\_filled\\_low\\_density\\_polyethylene\\_nanocomposite\\_blown\\_films/links/54462e1b0cf22b3c14de1155.pdf](https://www.researchgate.net/profile/Dr_Mohammad_Jawaid/publication/266739785_Effect_of_MMT_content_on_the_mechanical_oxygen_barrier_and_thermal_properties_of_rice_husk_MMT_hybrid_filler_filled_low_density_polyethylene_nanocomposite_blown_films/links/54462e1b0cf22b3c14de1155.pdf)

14.Ahmad, R., Ahmad, Z., Khan, A. U., Mastoi, N. R., Aslam, M., & Kim, J. (2016). Photocatalytic systems as an advanced environmental remediation: Recent developments, limitations and new avenues for applications. *Journal of Environmental Chemical Engineering*, 4(4), 4143-4164.

**ABSTRACT:**

Heterogeneous photocatalysis is a promising technology especially for environmental remediation. Despite more than a decade of worldwide research in developing photocatalytic efficiency improving techniques, many questions regarding the large scale application of

photocatalytic reactors still remain unanswered. Recently, improving the photocatalytic efficiency has gained scientific attention because it might lead to more economical and robust photocatalytic operation for environmental remediation. In this review, fundamental and comprehensive assessments of the photocatalytic concepts and their applications for environmental remediation are reviewed. The existing challenges and strategies to improve the photocatalytic efficiency are discussed. Further, recent developments and future research prospects on photocatalytic systems for environmental applications are also addressed.

**Web URL:** <http://www.sciencedirect.com/science/article/pii/S221334371630330X>

**15. Inuwa, I. M., Arjmandi, R., Ibrahim, A. N., Haafiz, M. M., Wong, S. L., Majeed, K., & Hassan, A. (2016). Enhanced mechanical and thermal properties of hybrid graphene nanoplatelets/multiwall carbon nanotubes reinforced polyethylene terephthalate nanocomposites. *Fibers and Polymers*, 17(10), 1657-1666.**

**ABSTRACT:**

The effects of graphene nanoplatelets (GNP) and multiwall carbon nanotube (MWCNT) hybrid nanofillers on the mechanical and thermal properties of reinforced polyethylene terephthalate (PET) have been investigated. The nanocomposites were melt blended using the counter rotating twin screw extruder followed by injection molding. Their morphology, mechanical and thermal properties were characterized. Combination of the two nanofillers in composites formulation supplemented each other which resulted in the overall improvement in adhesion between fillers and matrix. The mechanical properties and thermal stability of the hybrid nanocomposites (PET/GNP1.5/MWCNT1.5) were significantly improved compared to PET/GNP3 and PET/MWCNT3 single filler nanocomposites. However, it was observed that GNP was better in improving the mechanical properties but MWCNT resulted in higher thermal stability of Nanocomposite. The transmission electron microscopy (TEM) and field emission scanning electron microscopy (FESEM) revealed uniform dispersion of the hybrid fillers in PET/GNP1.5/MWCNT1.5 nanocomposites while agglomeration was observed at higher filler content. The MWCNT prevented the phenomenal stacking of the GNPs by forming a bridge between adjacent GNP planes resulting in higher dispersion of fillers. This complimentary

geometrical structure is responsible for the significant improvement in the thermal stability and mechanical properties of the hybrid nanocomposites

**Web URL:**

[https://www.researchgate.net/profile/Reza\\_Arjmandi/publication/309744441\\_Enhanced\\_mechanical\\_and\\_thermal\\_properties\\_of\\_hybrid\\_graphene\\_nanoplatelets\\_multiwall\\_carbon\\_nanotubes\\_reinforced\\_polyethylene\\_terephthalate\\_nanocomposites/links/5823c7b108ae61258e3cc5da.pdf](https://www.researchgate.net/profile/Reza_Arjmandi/publication/309744441_Enhanced_mechanical_and_thermal_properties_of_hybrid_graphene_nanoplatelets_multiwall_carbon_nanotubes_reinforced_polyethylene_terephthalate_nanocomposites/links/5823c7b108ae61258e3cc5da.pdf)

16. Akhtar, M. A., Riaz, S., Hayat, A., Nasir, M., Muhammad, N., Rahim, A., & Nawaz, M. H. (2017). Poly (ethylene oxide) tethered trans-porphyrin: Synthesis, self-assembly with fullerene (C 60) and DNA binding studies. *Journal of Molecular Liquids*, 225, 235-239.

**ABSTRACT:**

trans-Porphyrin containing phenyl group at both ends was synthesized via corresponding dipyrromethanes (DPM) in the presence of TFA and DDQ. The polyethyleneglycole (PEG) chains were attached at the trans positions of ABA type porphyrinic moiety. The prepared PEGylated porphyrin (with PEG arms at the periphery) P-(PEO)<sub>2</sub> was self-assembled into spheres of uniform diameter while their DMF solution was dialyzed into water. Furthermore, the addition of fullerene (C<sub>60</sub>) to P-(PEO)<sub>2</sub> caused complexation between porphyrin and fullerene which lead to interesting and trenchant morphology having worm like lateral aggregates. The assembly process and the as-prepared edifices were characterized using UV-vis absorption spectroscopy and the morphology of these assemblies was investigated using transmission electron microscope (TEM). Furthermore, the DNA binding with porphyrin aggregates has been demonstrated via electrochemical (cyclic voltammetric) response of screen printed electrodes modified. The obvious increase in redox current disclosed the intermolecular interactions of the adducts with the DNA. These studies of unprecedented adducts can further be explored for potential applications in biosensors.

**Web URL:** <http://www.ciitlahore.edu.pk/Papers/Abstracts/815-8587210166462645319.pdf>

17. Riaz, S., Feng, W., Khan, A. F., & Nawaz, M. H. (2016). Sonication-induced self-assembly of polymeric porphyrin-fullerene: Formation of nanorings. *Journal of Applied Polymer Science*.

**ABSTRACT:**

In this article, we detail the sonication-induced self-assembly of polymeric porphyrin and fullerenes into distinct nanorings in solution form. The formation of these trenchant superstructures was the result of the delicate choice of different assembly protocols, solvents, and polymeric tails associated with porphyrin and fullerene. In this study, the sonication supposedly directed the lateral aggregation into uniform ring formation. The sonication time was found to be the key parameter in ring formation. Furthermore, the flexibility of polymeric arms and electronic interactions of porphyrin–fullerene gave rise to synergistically enhanced molecular interactions, and this resulted in discrete morphologies. Key optical data, including the absorption maxima of the complexes, and microscopic studies attested to the nature and morphology of the self-assembled complexes. This introduction of polymeric arms and sonication protocols in the porphyrin self-assembly was expected to allow the easy formation of diverse morphologies. Because of the facile fabrication process and uniform morphology, the resulting composite architectures might show promising applications in drugdelivery and advance materials. VC 2016 Wiley Periodicals, Inc. *J. Appl. Polym.Sci.* 2016, 133, 43537.

**Web URL:** <http://onlinelibrary.wiley.com/doi/10.1002/app.43537/pdf>

**18. Kertik, A., Khan, A. L., & Vankelecom, I. F. (2016). Mixed matrix membranes prepared from non-dried MOFs for CO<sub>2</sub>/CH<sub>4</sub> separations. *RSC Advances*, 6(115), 114505-114512.**

**ABSTRACT:**

Mixed matrix membranes (MMMs) aim at combining the processibility of polymers with the molecular sieving of fillers to improve gas separation performance. Metal–organic frameworks (MOFs) are a new family of materials with promising potential as fillers. The first part of this work reports on exploiting the versatility of MOF synthesis routes by forming ZIF-8 particles in polymer solutions to subsequently cast membranes directly from the solution. Although MOFs can be synthesised in a polymer medium, the decline in the synthesis yield does not allow for high loading in the MMMs. The second part describes a method for preparing MMMs with the commercial polyimide (PI) Matrimid® and ZIF-8, ZIF-7 and NH<sub>2</sub>-MIL-53(Al) as non-dried filler with 30 wt% and 50 wt% loading. A comparison of this method with the conventional approach of drying MOFs prior to

incorporation exhibits the flexibility MOFs provide in membrane synthesis, in contrast to *e.g.* zeolites which intrinsically have to be calcined to become useful. The membranes with non-dried MOFs show some improvement in performance as compared to the unfilled polymer-only membranes, while those with dried MOFs even lose the inherent selectivity of the polymer.

**Web URL:**

<http://pubs.rsc.org/is/content/articlelanding/2016/ra/c6ra23013j/unauth#!divAbstract>

**19. Lu, S. C., Khan, A. L., & Vankelecom, I. F. (2016). Polysulfone-ionic liquid based membranes for CO<sub>2</sub>/N<sub>2</sub> separation with tunable porous surface features. *Journal of Membrane Science*, 518, 10-20.**

**ABSTRACT:**

A surprisingly simple, yet effective blending method for ionic liquids (ILs) and polysulfone (PSf) is presented in this paper. Not only is the IL properly immobilised in the polymer matrix, which is crucial in high-pressure gas separation applications, but this method also produces tunable porous surfaced membranes that can be useful in several other applications. The size and distribution of the pores are dependent on the type and amount of IL incorporated into the PSf. A membrane formation mechanism is proposed to explain the presence of such a regular surface pore structure. Several commercially available ILs were tested to examine their compatibility with the polymer, and the CO<sub>2</sub>/N<sub>2</sub> gas separation performance of the resulting membrane was screened. ATR-FTIR spectroscopy, FTIR microscopy, and SEM imaging were also employed to shed light on the observed membrane structures.

**Web URL:** <http://www.sciencedirect.com/science/article/pii/S0376738816307323>

**20. Waheed, N., Mushtaq, A., Tabassum, S., Gilani, M. A., Ilyas, A., Ashraf, F., ...& Khan, A. L. (2016). Mixed matrix membranes based on polysulfone and rice husk extracted silica for CO<sub>2</sub> separation. *Separation and Purification Technology*, 170, 122-129.**

**ABSTRACT:**

Mesoporous silica particles after extraction from rice husk ash were used as fillers in polysulfone based mixed-matrix membranes (MMMs). The fillers were functionalized with 4-aminophenazone (4-AMP) to enhance the CO<sub>2</sub>-philic properties. The attractive feature of this

research was the utility of extracted silica from a biological waste -the rice husk ash. A good dispersion and adhesion of the filler within the polymer matrix were confirmed by the gas permeation results, SEM images and FTIR analysis. The results revealed that all MMMs showed high permeabilities in comparison to pristine polysulfone membrane. The higher gas permeabilities were attributed to the presence of large mesopores in the filler that led to faster diffusion of the penetrant gas. The functionalized silica showed significantly higher CO<sub>2</sub>/CH<sub>4</sub> and CO<sub>2</sub>/N<sub>2</sub> selectivities. The highest ideal selectivities obtained for CO<sub>2</sub>/N<sub>2</sub> and CO<sub>2</sub>/CH<sub>4</sub> at a maximum of 40% filler loading, were 32.79 and 33.31 respectively. All synthesized membranes were tested at various operating temperatures and their activation energies were also calculated. The highly ordered structures with short and straight pore channels and improved gas permeation properties, warrant the silica extracted from rice husk as promising filler for industrial gas separation under varying conditions of temperature.

**Web URL:**

[https://www.researchgate.net/profile/Asad\\_Khan27/publication/304356246\\_Mixed\\_Matrix\\_Membranes\\_Based\\_on\\_Polysulfone\\_and\\_Rice\\_Husk\\_Extracted\\_Silica\\_for\\_CO2\\_Separation/links/5772240a08ae6219474a663c.pdf](https://www.researchgate.net/profile/Asad_Khan27/publication/304356246_Mixed_Matrix_Membranes_Based_on_Polysulfone_and_Rice_Husk_Extracted_Silica_for_CO2_Separation/links/5772240a08ae6219474a663c.pdf)

**21. Lee, J., Jang, N., Yasin, M., Lee, E. Y., Chang, I. S., & Kim, C. (2016). Enhanced mass transfer rate of methane via hollow fiber membrane modules for *Methylosinus trichosporium* OB3b fermentation. *Journal of Industrial and Engineering Chemistry*, 39, 149-152.**

**ABSTRACT:**

Polyvinylidene fluoride (PVDF) hollow fiber membranes were employed to enhance mass transfer rate of methane in water for the fermentation of *Methylosinus trichosporium* OB3b. Compared to common alumina bubbler, hollow fiber membrane modules (HFMMs) afforded smaller methane bubble size and larger methane–water volumetric mass transfer coefficient (kLa) as high as 150.1 h<sup>-1</sup>. Furthermore, cell growth rate and maximum optical density of *M. trichosporium* OB3b were increased by 67.3 and 77.4%, respectively, by adapting forty HFMMs, compared to those of alumina bubbler.

**Web URL:**

[https://www.researchgate.net/profile/Choongik\\_Kim/publication/303634058\\_Enhanced\\_mass\\_transfer\\_rate\\_of\\_methane\\_via\\_hollow\\_fiber\\_membrane\\_modules\\_for\\_Methylosinus\\_trichosporium\\_OB3b\\_fermentation/links/5785c82708aef321de2a9f89.pdf](https://www.researchgate.net/profile/Choongik_Kim/publication/303634058_Enhanced_mass_transfer_rate_of_methane_via_hollow_fiber_membrane_modules_for_Methylosinus_trichosporium_OB3b_fermentation/links/5785c82708aef321de2a9f89.pdf)

**22. Bhatti, I., Qureshi, K., Kamarudin, K. S. N., Bazmi, A. A., Bhutto, A. W., Ahmad, F., & Lee, M. (2016). Innovative method to prepare a stable emulsion liquid membrane for high CO<sub>2</sub> absorption and its performance evaluation for a natural gas feed in a rotating disk contactor. *Journal of Natural Gas Science and Engineering*, 34, 716-732.**

**ABSTRACT:**

This paper presents an innovative method to prepare a stable emulsion liquid membrane (ELM) for high CO<sub>2</sub> absorption in a natural gas feed. This new method achieved high throughput at low power consumption. The ELM prepared using this new method was characterized by determining the effects of the concentration of the ELM constituents, emulsification time, and speed on the emulsion droplet size (EDS) and stability. This was followed by a parametric study of the process parameters for CO<sub>2</sub> separation from natural gas in a rotating disk contactor (RDC)-based setup to evaluate the performance of a stable ELM. The results suggest that the retention time of the stable ELM in a RDC increases with increasing amount of absorbed CO<sub>2</sub>. The results support the fundamental development of the ELM process to achieve a high overall separation efficiency of CO<sub>2</sub> removal from natural gas with a relatively small contact time. This is the first parametric study of CO<sub>2</sub> absorption from a gas stream in ELM using a RDC as the contracting equipment. The results of the parametric study suggested that the factors of time, TEA concentration and RDC speed have significant effect on the CO<sub>2</sub> absorption from natural gas feed. It was identified that 4% TEA in ELM, 30 min operational time and 700 rpm speed of modified RDC system is suitable for maximum CO<sub>2</sub> absorption from gas mixture of CO<sub>2</sub>/CH<sub>4</sub>. Furthermore, the study suggested that the ELM containing 4% TEA can absorb 5.6 kmol/m<sup>3</sup> CO<sub>2</sub>.

**Web URL:** <http://www.sciencedirect.com/science/article/pii/S1875510016304711>

**23. Bhatti, I., Bhutto, A. W., Qureshi, K., Kamarudin, K. S. N., Bazmi, A. A., & Ahmad, F. (2016). Hydrodynamics study of the modified rotating disc contactor for CO<sub>2</sub> absorption from**

natural gas using emulsion liquid membrane. *Chemical Engineering Research and Design*, **111**, 465-478.

**ABSTRACT:**

This study modified the rotating disc contactor (RDC) structure to optimize its performance for CO<sub>2</sub> separation from natural gas feed using stable emulsion liquid membrane (ELM). Based on parametric study of absorption of CO<sub>2</sub> from natural gas feed into ELM, the mass transfer behavior in the RDC system was optimized. Rotor diameter, stator inner diameter, and minimum free area of RDC were modified to achieve maximum contact between dispersed liquid phase and gas feed phase, which was necessary to achieve maximum mass transfer. The problem of rupture of the emulsion droplet due to pressure created by direct dispersion of gas at the bottom of conventional RDC extraction system was addressed by adding an impeller at the bottom compartment of RDC. The impeller provided continuous mixing of emulsion and a gas sparger was fitted along the impeller's side that maintained the dispersed aqueous phase miscible in system. The hydrodynamic behavior of a modified RDC was optimized for CO<sub>2</sub> absorption from natural gas in ELM, which indicated that modified design dimensions can provide a maximum liquid–gas contact. Beside the concentration of CO<sub>2</sub> in natural gas feed, it was observed that the speed of RDC and run time significantly influence CO<sub>2</sub> absorption from natural gas using ELM. When all the parameters optimized for CO<sub>2</sub> absorption from natural gas feed this study is useful in extending the application of RDC in liquid–gas system. In this study, the use of ELM in RDC can be effective for CO<sub>2</sub> when applied under proper conditions.

**Web URL:** [http://www.cherd.ichemejournals.com/article/S0263-8762\(16\)30130-7/fulltext](http://www.cherd.ichemejournals.com/article/S0263-8762(16)30130-7/fulltext)

**24. Abbas, N., Shao, G. N., Haider, M. S., Imran, S. M., Park, S. S., & Kim, H. T. (2016). Sol–gel synthesis of TiO<sub>2</sub>-Fe<sub>2</sub>O<sub>3</sub> systems: Effects of Fe<sub>2</sub>O<sub>3</sub> content and their photocatalytic properties. *Journal of Industrial and Engineering Chemistry*, **39**, 112-120.**

**ABSTRACT:**

An inexpensive sol–gel technique to synthesize TiO<sub>2</sub>-Fe<sub>2</sub>O<sub>3</sub> nanocomposites with improved structural and photochemical properties is introduced. A series of TiO<sub>2</sub>-Fe<sub>2</sub>O<sub>3</sub> nanocomposites with different Fe<sub>2</sub>O<sub>3</sub> contents were prepared through cheap TiO<sub>2</sub> precursor titanium oxychloride (TiOCl<sub>2</sub>). The physicochemical properties of the samples were examined by XRD,

XRF, SEM, EDX, HRTEM, UV–vis DRS, FTIR, TGA and nitrogen gas physisorption studies. The effects of calcination temperatures and Fe<sub>2</sub>O<sub>3</sub> content on the mesostructure and photocatalytic strength of the prepared TiO<sub>2</sub>-Fe<sub>2</sub>O<sub>3</sub> composites were investigated. Results showed that composites with distinct structural, optical and photochemical properties can be formed by varying Fe<sub>2</sub>O<sub>3</sub> content.

**Web URL:** [https://www.researchgate.net/profile/Nadir\\_Abbas/publication/303634915\\_Sol-gel\\_synthesis\\_of\\_TiO2-Fe2O3\\_systems\\_Effects\\_of\\_Fe2O3\\_content\\_and\\_their\\_photocatalytic\\_properties/links/57970f1c08aeb0ffcd05a46d.pdf](https://www.researchgate.net/profile/Nadir_Abbas/publication/303634915_Sol-gel_synthesis_of_TiO2-Fe2O3_systems_Effects_of_Fe2O3_content_and_their_photocatalytic_properties/links/57970f1c08aeb0ffcd05a46d.pdf)

**25. Imran, S. M., Shao, G. N., Haider, M. S., Hwang, H. J., Choa, Y. H., Hussain, M., & Kim, H. T. (2016). Carbon nanotube-based thermoplastic polyurethane-poly (methyl methacrylate) nanocomposites for pressure sensing applications. *Polymer Engineering & Science*, 56(9), 1031-1036.**

**ABSTRACT:**

We have synthesized unique flexible pressure-sensitive nanocomposites by means of a solution mixing method, by adding multiwalled carbon nanotubes (MWCNTs) into a thermoplastic urethane (TPU) matrix along with poly(- methyl methacrylate) (PMMA) microbeads of various sizes. The influence of the various PMMA bead sizes on the pressure sensing properties of the nanocomposites was studied over a range of pressures. The PMMA microbeads were used to achieve an early percolation threshold at low loadings of MWCNTs. We used scanning electron microscopy to study the nanocomposites' morphology, and conducted differential scanning calorimetry analyses to investigate their thermal properties. The nanocomposites' electrical and thermal conductivities were also measured under various applied pressures. The nanocomposites displayed repeatable electrical responses under various applied pressures, demonstrating their suitability for use as pressure sensing materials. The proposed material is an ideal candidate for use in the preparation of pressure-sensitive devices.

**Web URL:**

[https://www.researchgate.net/profile/Hee-Taik-Kim/publication/303799780\\_Carbon\\_nanotub](https://www.researchgate.net/profile/Hee-Taik-Kim/publication/303799780_Carbon_nanotub)

[e-based thermoplastic polyurethane-poly methyl methacrylate nanocomposites for pressure sensing applications/links/575a9b9e08aec91374a603de.pdf](http://www.ijser.org/researchpaper/Bioelectrochemical-Reduction-of-Carbon-Dioxide-to-Organic-Compounds.pdf)

**26. Farooq, R., Jabeen, G., Siddique, M., Shaukat, S. F., & Rehman, S. U. (2016) Bioelectrochemical Reduction of Carbon Dioxide to Organic Compounds 2, *International Journal of Scientific & Engineering Research*, 7(10), 2229-5518**

**ABSTRACT:**

The present study demonstrates bioelectrochemical reduction of inorganic carbon dioxide to organic compounds using 6 *SporomusaOvata* in a tube shaped bioelectrochemical cell (BEC). Among biosynthesized products acetate, ethanol, n-butyric acid and iso- 7 pentanoic acid, 142.9 mg/L of acetate produced in 72 hours. This increase in acetate yield is attributed to improved parameters adopted 8 during reactor design. Average bioelectrochemical acetate synthesis rate was found to be  $1.3 \pm 0.67 \text{ mgL}^{-1} \text{ h}^{-1}$ . Cyclic voltameteric study 9 confirmed redox activity of *S.Ovata* on poised biocathode. The percentage electron recovery as total organic compounds is found to be in 10 the range of  $84 \pm 13\%$  to  $65 \pm 11\%$ . The second major product is ethanol, formed by the conversion of acetaldehyde into ethanol. The 11 presence of ethanol assumed to be due to electro activity and metabolic shift from acetate to ethanol in the biochemical-producing *S.Ovata* 12 in BEC. The current research opens up the prospects of improving processes for bioelectrosynthesis of electron dense organic compounds 13 from renewable energies and waste greenhouse gases instead of synthesizing them from non-renewable and energy rich compounds.

**Web URL:** <http://www.ijser.org/researchpaper/Bioelectrochemical-Reduction-of-Carbon-Dioxide-to-Organic-Compounds.pdf>

**27. Ahmad, Z. Farooq, R. Rasheed, K. Khan, A. Fatima, U & Irfan, M. (20116). *Journal of Petroleum & J Environmental Biotechnology*, 7(5).2157-7463**

**ABSTRACT:**

This paper reviews the recent development in green materials employed for eco-friendly construction in the context of developing countries, where climatic change and limited resource demand cost effective and sustainable materials of construction. The paper reviews some of the important fundamentals on which green engineering is based and shows how the advantages offered by green materials can be harnessed for societal, economic and technological benefits. The proliferation of nanotechnology in construction has filled many of the holes left by traditional technologies. The mountain and hilly regions is the primary target in South Asia in this review as these areas in Pakistan and similar geographical regions are still far behind in harnessing the benefits of green engineering. New methods of collection of safe drinking water, using Nano materials and treatment of snow melted and rain water are reviewed. The design of roofs in cold and snow bound areas and new green materials developed for such areas are also discussed. The article describes the latest Nano eco-friendly materials which may be employed to minimize energy, increase life cycle and decrease carbon foot points for longer and healthier lives. This paper also dwells on the proper use of green Nano materials for constructing houses in developing countries.

**Web URL:** <https://www.omicsonline.org/open-access/harnessing-green-engineering-for-ecofriendly-housing-and-utilities-in-southasian-countries-2157-7463-1000295.php?aid=81141>

**28. Jabeen, G., & Farooq, R. (2016). Bio-electrochemical synthesis of commodity chemicals by autotrophic acetogens utilizing CO<sub>2</sub> for environmental remediation. *Journal of biosciences*, 41(3), 367-380.**

**ABSTRACT:**

Bio-electrochemical synthesis (BES) is a technique in which electro-autotrophic bacteria such as *Clostridium ljungdahlii* utilize electric currents as an electron source from the cathode to reduce CO<sub>2</sub> to extracellular, multicarbon, exquisite products through autotrophic conversion. The BES of volatile fatty acids and alcohols directly from CO<sub>2</sub> is a sustainable alternative for non-renewable, petroleum-based polymer production. This conversion of CO<sub>2</sub> implies reduction of greenhouse gas emissions. The synthesis of heptanoic acid, heptanol, hexanoic acid and hexanol, for the first time, by *Clostridium ljungdahlii* was a remarkable achievement of BES. In our study, these microorganisms were cultivated on the cathode of a bio-electrochemical cell at

–400 mV by a DC power supply at 37°C, pH 6.8, and was studied for both batch and continuous systems. Pre-enrichment of bio-cathode enhanced the electroactivity of cells and resulted in maximizing extracellular products in less time. The main aim of the research was to investigate the impact of low-cost substrate CO<sub>2</sub>, and the longer cathode recovery range was due to bacterial reduction of CO<sub>2</sub> to multicarbon chemical commodities with electrons driven from the cathode. Reactor design was simplified for cost-effectiveness and to enhance energy efficiencies. The Coulombic recovery of ethanoic acid, ethanol, ethyl butyrate, hexanoic acid, heptanoic acid and hexanol being in excess of 80% proved that BES was a remarkable technology.

**Web URL:** <http://www.ias.ac.in/article/fulltext/jbsc/041/03/0367-0380>

**29. Haroon, H., Ashfaq, T., Gardazi, S. M. H., Sherazi, T. A., Ali, M., Rashid, N., & Bilal, M. (2016). Equilibrium kinetic and thermodynamic studies of Cr (VI) adsorption onto a novel adsorbent of *Eucalyptus camaldulensis* waste: Batch and column reactors. *Korean Journal of Chemical Engineering*, 33(10), 2898-2907.**

**ABSTRACT:**

Cr(VI) adsorption onto *Eucalyptus camaldulensis* sawdust (ECS) waste was investigated in batch and column reactors. Various parameters, including the adsorbent dose, pH, initial concentration, particle size, contact time and temperature were optimized. The maximum adsorption capacity (35.58mg g<sup>-1</sup>, 71.16%) was achieved at pH 2.0. Data fitted well to Freundlich and Halsey's models (R<sup>2</sup>=0.992), indicating the multilayer adsorption of Cr(VI). It obeys the pseudo-second order kinetics. Endothermic and non-spontaneous nature of Cr(VI) adsorption was observed with positive values of changes in enthalpy (9.83 kJ mol<sup>-1</sup>), and Gibbs-free energy (1.52, 1.38, 1.24, 1.10 and 0.97 kJ mol<sup>-1</sup>), respectively. In this column study, the breakthrough curve time increased from 670 to 1,270min by increasing the bed height from 5 to 15 cm, respectively. Column data was found well fitted to bed depth service time model. Adsorption capacity at 60% breakthrough was 2,443.636mg L<sup>-1</sup>. The study indicates that ECS waste can be a promising adsorbent for Cr(VI) remediation from industrial effluents.

**Web URL:** <https://link.springer.com/article/10.1007/s11814-016-0160-0>

**30. Hussain Gardazi, S. M., Ashfaq Butt, T., Rashid, N., Pervez, A., Mahmood, Q., Maroof Shah, M., & Bilal, M. (2016). Effective adsorption of cationic dye from aqueous solution using low-cost corncob in batch and column studies. *Desalination and Water Treatment*, 57(59), 28981-28998.**

**ABSTRACT:**

Dye effluents and their degradation products disrupt the aquatic ecosystem functioning. Corncob was used as a low-cost biosorbent for decolorization of methylene blue (MB) dye. Batch and fixed-bed column adsorption were performed by varying temperature, pH, initial dye concentration, adsorbent dose, particle size, and bed height, flow rate and inlet dye concentration, respectively. High MB adsorption capacities of corncob were attained at pH 9, i.e. 45.86 mg g<sup>-1</sup>, 91.7%. Equilibrium data was best described by Langmuir II ( $R^2 = 0.999$ ) followed by Freundlich ( $R^2 = 0.994$ ) and Halsey ( $R^2 = 0.994$ ) isotherm models, which indicates the favorable adsorption of MB dye onto corncob adsorbent. Moreover, chemisorption nature of corncob was confirmed through Dubinin–Radushkevich ( $E = 16.01 \text{ kJ mol}^{-1}$ ) and the best fit of pseudo-second-order kinetic model. Thermodynamic studies revealed spontaneous ( $\Delta G < 0$ ) and endothermic ( $\Delta H > 0$ ) nature of reaction with increased randomness ( $\Delta S > 0$ ) at the solid–liquid interface. The breakthrough curves were predicted using Thomas and BDST models. BDST reflected that 2.26 min were required to exhaust 1 cm of the fixed-bed column. MB dye-loaded corncob adsorbent could be regenerated (80%) and reused using 0.1 M acetic acid.

**Web URL:** <http://www.tandfonline.com/doi/abs/10.1080/19443994.2016.1188730>

**31. Rahman, Z., Rashid, N., Nawab, J., Ilyas, M., Sung, B. H., & Kim, S. C. (2016). Escherichia coli as a fatty acid and biodiesel factory: current challenges and future directions. *Environmental Science and Pollution Research*, 23(12), 12007-12018.**

**ABSTRACT:**

Biodiesel has received widespread attention as a sustainable, environment-friendly, and alternative source of energy. It can be derived from plant, animal, and microbial organisms in the form of vegetable oil, fats, and lipids, respectively. However, biodiesel production from such sources is not economically feasible due to extensive downstream processes, such as

trans-esterification and purification. To obtain cost-effective biodiesel, these bottlenecks need to be overcome. *Escherichia coli*, a model microorganism, has the potential to produce biodiesel directly from ligno-cellulosic sugars, bypassing trans-esterification. In this process, *E. coli* is engineered to produce biodiesel using metabolic engineering technology. The entire process of biodiesel production is carried out in a single microbial cell, bypassing the expensive downstream processing steps. This review focuses mainly on production of fatty acid and biodiesel in *E. coli* using metabolic engineering approaches. In the first part, we describe fatty acid biosynthesis in *E. coli*. In the second half, we discuss bottlenecks and strategies to enhance the production yield. A complete understanding of current developments in *E. coli*-based biodiesel production and pathway optimization strategies would reduce production costs for biofuels and plant-derived chemicals.

**Web URL:** <https://link.springer.com/article/10.1007/s11356-016-6367-0>

**32. Farooq, R., Shaukat, S. F., Yaqoob, A., & Farooq, U. (2016). U.S. Patent No. 9,512,012. Washington, DC: U.S. Patent and Trademark Office.**

**ABSTRACT:**

A process for removal of heavy metals at contamination level (50-500 mg/L) using ultrasonic energy and electrolysis, as a measure to decontaminate industrial waste, is described.

**Web URL:** <https://www.google.com/patents/US9512012>

**33. Farooq, R., & Shaukat, S. F. (2016). U.S. Patent No. 9,340,434. Washington, DC: U.S. Patent and Trademark Office.**

**ABSTRACT:**

Nickel is recovered from pickling acid solutions of crude ore using boric acid as catalyst by ultrasound assisted electrolysis.

**Web URL:** <https://www.google.com/patents/US9340434>

**34. Abdullah, M. A., Nazir, M. S., Raza, M. R., Wahjoedi, B. A., & Yussof, A. W. (2016). Autoclave and ultra-sonication treatments of oil palm empty fruit bunch fibers for cellulose extraction and its polypropylene composite properties. *Journal of Cleaner Production*, 126, 686-697.**

**ABSTRACT:**

Accumulation of residual plastics and the biomass wastes from agricultural sectors are causing serious global environmental problems if not addressed effectively. Cellulose with polypropylene as biocomposite material is an elegant strategy for value-added utilization of wastes. In this study, green isolation of cellulose from oil palm empty fruit bunches by autoclave-based and ultrasonication pretreatments were developed to replace the non-green chlorite method. Ultrasonic treatment with hydrogen peroxide yielded 49% cellulose with 91.3%  $\alpha$ -cellulose content and 68.7% crystallinity, as compared to 64% cellulose with autoclave treatment. Based on field emission scanning electron microscope, the ultrasonic and the autoclave-treated fibers showed complete separation of cellulose fibrils, with punctures and pores on the surface. High resolution transmission electron microscope and X-ray diffraction studies suggested monoclinic unitary crystal structure. The cellulose/polypropylene composite fabrications were achieved by using injection-molding technique where the composites with 25% cellulose loading gave high tensile strength of 27 MPa, without any addition of coupling agents. Thermogravimetric analysis study showed that the thermal stability of composites was enhanced by 150 C as compared to singular cellulose and polypropylene. The low water and diesel uptake suggested the compact structure of the composites. This study has developed green techniques combining heat and eco-friendly chemical treatment for cellulose extraction from agro-lignocellulosic wastes. The cellulose/ polypropylene composites developed with high tensile strength, high thermal stability, and low water and diesel sorption have great potentials for conversion into eco-composite products such as polymeric material insulated cables for high voltage engineering, automotive parts, sports tools and other household or office items.

**Web URL:**

[https://www.researchgate.net/profile/Dr\\_Muhammad\\_Shahid\\_Nazir/publication/301277361\\_Autoclave\\_and\\_Ultrasonication\\_treatments\\_of\\_Oil\\_Palm\\_Empty\\_Fruit\\_Bunch\\_fibres\\_for\\_cellulose\\_extraction\\_and\\_its\\_polypropylene\\_composite\\_properties/links/571dc87208aee3ddc56acfff.pdf](https://www.researchgate.net/profile/Dr_Muhammad_Shahid_Nazir/publication/301277361_Autoclave_and_Ultrasonication_treatments_of_Oil_Palm_Empty_Fruit_Bunch_fibres_for_cellulose_extraction_and_its_polypropylene_composite_properties/links/571dc87208aee3ddc56acfff.pdf)

35. Yadzir, Z. H. M., Shukor, M. Y., Ahmad, A., Nazir, M. S., Shah, S. M. U., & Abdullah, M. A. (2016). Phenol removal by newly isolated *Acinetobacter baumannii* strain Serdang 1 in a packed-bed column reactor. *Desalination and Water Treatment*, 57(28), 13307-13317.

**ABSTRACT:**

A newly isolated *Acinetobacter baumannii* strain Serdang 1 was explored for its potential in phenol remediation in batch and continuous system. An immobilization cell system has been successfully developed to remove phenol in a batch system as high as 2,000 mg/L in 12 d at a rate of 6.04 mg/L/h. Repeated use of immobilized cells as many as five cycles was shown without any loss of activity. The continuous system in a packed-bed reactor achieved 65–77% phenol removal at the rate of 38.4 mg/L/h for 200 mg/L influent, which was almost three fold higher than the batch system. Low influent flow rate at 1.5 mL/min and bed height-to-diameter ratio of 15.2 reached steady state faster than the higher flow rate, and the percentage of phenol removal was also higher.

**Web URL:** <http://www.tandfonline.com/doi/abs/10.1080/19443994.2015.1063459>

36. Ahmed, M. A., Seo, Y. H., Terán-Hilares, R., Rehman, M. S. U., & Han, J. I. (2016). Persulfate based pretreatment to enhance the enzymatic digestibility of rice straw. *Bioresource technology*, 222, 523-526.

**ABSTRACT:**

Oxidation induced by potassium persulfate was evaluated as an economic substitute for the Fenton-like reaction for the purpose of rice straw pretreatment in terms of temperature (80–140 °C), potassium persulfate concentration (5–100 mM) and process time (0.5–3 h), an optimal pretreatment condition was identified: 120 °C for 2 h with 75 mM potassium persulfate concentration and yielded 91% enzymatic digestibility using 25.2 FPU/g of biomass. Crystallinity index, SEM and SEM-EDS analyses revealed that biomass was indeed disrupted and components like silica were exposed. All this suggested that this persulfate-based pretreatment method, which is distinctively advantageous in terms of effectiveness and economics, can indeed be a competitive option.

**Web URL:** <http://www.sciencedirect.com/science/article/pii/S096085241631389X>

# DEPARTMENT OF MATHEMATICS

## Journal Papers

1. Khan, M. A. A., & Kalsoom, A. (2016). Existence and higher arity iteration for total asymptotically nonexpansive mappings in uniformly convex hyperbolic spaces. *Fixed Point Theory and Applications*, 2016(1), 3.

**ABSTRACT:**

This paper provides a fixed point theorem and iterative construction of a common fixed point for a general class of nonlinear mappings in the setup of uniformly convex hyperbolic spaces. We translate a multi-step iteration, essentially due to Chidume and Ofoedu (J. Math. Anal. Appl. 333:128-141, 2007) in such a setting for the approximation of common fixed points of a finite family of total asymptotically nonexpansive mappings. As a consequence, we establish strong and  $\Delta$ -convergence results which extend and generalize various corresponding results established in the current literature.

**Web URL:**

<https://fixedpointtheoryandapplications.springeropen.com/articles/10.1186/s13663-015-0483-2>

2. Younis, M., & Rizvi, S. T. R. (2016). Optical Soliton Like-Pulses in Ring-Cavity Fiber Lasers of Carbon Nanotubes. *Journal of Nanoelectronics and Optoelectronics*, 11(3), 276-279.

**ABSTRACT:**

A nonlinear schrödinger system in the optical fiber laser communications, with the second-order dispersion coefficient, mode locking with the use of an saturable absorber, including the gain dispersion, losses for the cavity and fiber, group-velocity dispersion, self-phase modulation and two-photon absorption, is analyzed through the  $G'/G$ -expansion scheme. It is the governing system of ring-cavity fiber laser using carbon nanotubes for passive mode locking. Soliton solutions for that system are found to be of different kinds: kink, inverse kink, tangent and cotangent forms solitary wave. The obtained optical soliton solutions are very interesting and valuable in the field of research pertaining to nonlinear optics.

**Web URL:**

<http://www.ingentaconnect.com/content/asp/jno/2016/00000011/00000003/art00004>

3. Sardar, A., Ali, K., Rizvi, S. T. R., Younis, M., Zhou, Q., Zerrad, E., ...& Bhrawy, A. (2016). Dispersive Optical Solitons in Nanofibers with Schrödinger-Hirota Equation. *Journal of Nanoelectronics and Optoelectronics*, 11(3), 382-387.

**ABSTRACT:**

This paper studies dispersive solitons in optical nanofibers that are modeled by Schrödinger-Hirota equation. The tanh-coth integration algorithm obtains soliton solutions to the model that are studied with Kerr law and power law nonlinearity. There are constraint conditions that fall out for these solitons to exist.

**Web URL:**

<http://www.ingentaconnect.com/content/asp/jno/2016/00000011/00000003/art00021>

4. Rizvi, S. T. R., Ali, I., Ali, K., & Younis, M. (2016). Saturation of the nonlinear refractive index for optical solitons in two-core fibers. *Optik-International Journal for Light and Electron Optics*, 127(13), 5328-5333.

**ABSTRACT:**

This article studies the dynamics of optical solitons in two-core fibers with saturation of the nonlinear refractive index describe by dual power law. The decoupled model is considered with group velocity dispersion, linear coupling coefficients and spatio-temporal dispersion. As the result bright, dark and two forms if singular optical 1-solitons are extracted using ansatz approach. Additionally, the constraint conditions for the existence of these solutions are also listed.

**Web URL:** <http://www.sciencedirect.com/science/article/pii/S0030402616302121>

5. Rani, S., & Jawad, A. (2016). Noncommutative Wormhole Solutions in Einstein Gauss-Bonnet Gravity. *Advances in High Energy Physics*, 2016.

**ABSTRACT:**

We explore static spherically symmetric wormhole solutions in the framework of  $n$ -dimensional Einstein Gauss-Bonnet gravity. Our objective is to find out wormhole solutions that satisfy energy conditions. For this purpose, we consider two frameworks such as Gaussian distributed and Lorentzian distributed noncommutative geometry. Taking into account constant redshift function, we obtain solutions in the form of shape function. The fifth and sixth dimensional solutions with positive as well as negative GaussBonnet coefficient are discussed. Also, we check the equilibrium condition for the wormhole solutions with the help of generalized Tolman-Oppenheimer-Volkoff equation. It is interesting to mention here that we obtain fifth dimensional stable wormhole solutions in both distributions that satisfy the energy conditions.

**Web URL:**

[https://scholar.google.com.pk/scholar?q=Noncommutative+Wormhole+Solutions+in+Einstein+Gauss-Bonnet+Gravity&btnG=&hl=en&as\\_sdt=0%2C5](https://scholar.google.com.pk/scholar?q=Noncommutative+Wormhole+Solutions+in+Einstein+Gauss-Bonnet+Gravity&btnG=&hl=en&as_sdt=0%2C5)

6. Jawad, A., Momeni, D., Rani, S., & Myrzakulov, R. (2016). Dynamical instability of cylindrical symmetric collapsing star in generalized teleparallel gravity. *Astrophysics and Space Science*, 361(4), 1-10.

**ABSTRACT:**

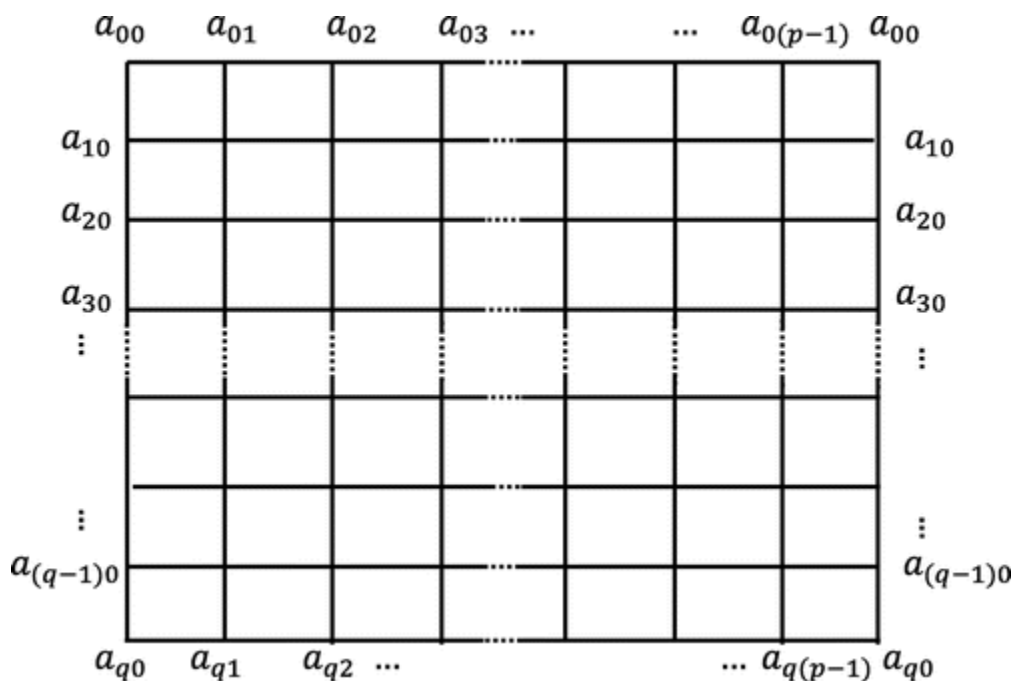
This paper is devoted to analyze the dynamical instability of a self-gravitating object undergoes to collapse process. We take the framework of generalized teleparallel gravity with cylindrical symmetric gravitating object. The matter distribution is represented by locally anisotropic energy-momentum tensor. We develop basic equations such as dynamical equations along with matching conditions and Harrison-Wheeler equation of state. By applying linear perturbation strategy, we construct collapse equation which is used to accomplish the instability ranges in Newtonian and post-Newtonian regimes. We find these ranges for isotropic pressure as well as reduce the results in general relativity. The unstable behavior depends on matter, metric, mass and torsion based terms.

**Web URL:** <https://arxiv.org/pdf/1511.03655.pdf>

7. Ahmad, S., Ahmad, U., Imran, M., & Farah, N. (2016). The Omega and Sadhana polynomials of TUC4 [p, q] nanotubes. *Canadian Journal of Chemistry*, 94(5), 490-493.

**ABSTRACT:**

The counting polynomials are useful in topological description of benzenoid structures. The uasi-orthogonal cut strips could account for the helicity of nanotubes and nanotori. It also helps to describe its topological indices by virtue of quasi-orthogonal cuts of the edge strips in the polycyclic graphs. In this article, we give a complete description of the Omega and Sadhana polynomials of the nanotube  $TUC_4[p,q]$  and provide its mathematical proof. We also give explicit formulae for the PI and the theta polynomial of  $TUC_4[p,q]$  nanotubes.



**Web URL:** <http://www.nrcresearchpress.com/doi/abs/10.1139/cjc-2015-0573#.WTjYrZKGPIU>

8. Ahmad, S. (2016). ON THE CHAIN BLOCKERS OF A POSET. *MATHEMATICAL REPORTS*, 18(2), 205-215.

**ABSTRACT:**

Let  $P = C_a \times C_b$  be a poset where  $C_i$  is the chain  $1 < \dots < i$ . A chain blocker of  $P$  is an inclusionwise minimal subset  $B \subseteq P$  with the property that every maximal chain in  $P$  contains at least one element of  $B$ . In [1] the chain blockers of  $P$  are being expressed in term of the Catalan numbers and  $k$  fold convolution of the Catalan numbers. In this paper we give a complete

description of the chain blockers of  $Ca \times Cb$ , where  $a \leq 4$  and  $b \geq 1$ . In the end algebraic consequences of the chain blockers are also provided. AMS 2010 Subject Classification: 05E40, 13F20, 13F55.

**Web URL:** [http://imar.ro/journals/Mathematical\\_Reports/Pdfs/2016/2/6.pdf](http://imar.ro/journals/Mathematical_Reports/Pdfs/2016/2/6.pdf)

**9. Maqbool, K., Bég, O. A., Sohail, A., & Idrees, S. (2016). Analytical solutions for wall slip effects on magnetohydrodynamic oscillatory rotating plate and channel flows in porous media using a fractional Burgers viscoelastic model. *The European Physical Journal Plus*, 131(5), 1-17.**

**ABSTRACT:**

The theoretical analysis of magnetohydrodynamic (MHD) incompressible flows of a Burgers fluid through a porous medium in a rotating frame of reference is presented. The constitutive model of a Burgers fluid is used based on a fractional calculus formulation. Hydrodynamic slip at the wall (plate) is incorporated and the fractional generalized Darcy model deployed to simulate porous medium drag force effects. Three different cases are considered: namely, the flow induced by a general periodic oscillation at a rigid plate, the periodic flow in a parallel plate channel and, finally, the Poiseuille flow. In all cases the plate(s) boundary(ies) are electrically non-conducting and a small magnetic Reynolds number is assumed, negating magnetic induction effects. The well-posed boundary value problems associated with each case are solved via Fourier transforms. Comparisons are made between the results derived with and without slip conditions. Four special cases are retrieved from the general fractional Burgers model, viz. *Newtonian fluid, general Maxwell viscoelastic fluid, generalized Oldroyd-B fluid and the conventional Burgers viscoelastic model*. Extensive interpretation of graphical plots is included. We study explicitly the influence of the wall slip on primary and secondary velocity evolution. The model is relevant to MHD rotating energy generators employing rheological working fluids.

**Web URL:** <https://link.springer.com/article/10.1140/epjp/i2016-16140-5>

**10. Ahmad, S., & Welker, V. (2016). Chain Blockers and Convolved Catalan Numbers. *Order*, 33(2), 347-358.**

**ABSTRACT:**

We give new interpretations of Catalan and convoluted Catalan numbers in terms of trees and chain blockers. For a poset  $P$  we say that a subset  $A \subseteq P$  is a chain blocker if it is an inclusionwise minimal subset of  $P$  that contains at least one element from every maximal chain. In particular, we study the set of chain blockers for the class of posets  $P = C_a \times C_b$  where  $C_i$  is the chain  $1 < \dots < i$ . We show that subclasses of these chain blockers are counted by Catalan and convoluted Catalan numbers.

**Web URL:** <https://link.springer.com/article/10.1007/s11083-015-9370-z>

**11. Cheemaa, N., Mehmood, S. A., Rizvi, S. T. R., & Younis, M. (2016). Single and combined optical solitons with third order dispersion in Kerr media. *Optik-International Journal for Light and Electron Optics*, 127(20), 8203-8208.**

**ABSTRACT:**

The article studies the dynamics of single and combined optical solitons in perturbed nonlinear Schrödinger equation with third order dispersion and nonlinear dispersion term. It has been demonstrated that this equation admits a rich variety of exact solutions for a different range of five parameters. The solutions are of qualitatively different nature, depending on the parameters, which are soliton-type solutions, triangular-type solutions, doubly periodic-like solutions, single and combined non-degenerate Jacobi elliptic function like solutions. Additionally, the constraint conditions for the existence of the solutions are also listed. It is also noted that the Jacobi elliptic functions degenerate into combined optical solitons and combined periodic singular solutions in limiting case when modulus  $m$  approaches to 1 and 0, respectively. The reported results are new and interesting in the field of nonlinear optics.

**Web URL:** <http://www.sciencedirect.com/science/article/pii/S0030402616306738>

**12. Sardar, A., Rizvi, S. T. R., Younis, M., Milovic, D., Majid, F. B., Biswas, A., Belich, M. (2016). Thirring optical solitons in birefringent fibers with parabolic law nonlinearity. *Optoelectronics and advanced materials – rapid communications*, 10(5-6), 327-331**

**ABSTRACT:**

This paper obtains dark and singular soliton solutions to Thirring model that is studied with parabolic law nonlinearity. The integration scheme employed is  $(G'/G)$ -expansion method. Apart from soliton solutions, singular periodic solutions and plane wave solutions are also obtained as a byproduct. The constraint conditions hold these solitons in place.

**Web URL:** <https://oam-rc.inoe.ro/index.php?option=magazine&op=view&idu=2825&catid=96>

**13. Sangawi, A. W., Nazar, K., & Murid, A. H. (2015). A Numerical Method for Locating the Zeros of Ahlfors Map for Doubly Connected Regions. *Indian Journal of Science and Technology*, 8(32).**

**ABSTRACT:**

The Ahlfors map of an  $n$ -connected region is a  $n$ -to-one map from the region onto the unit disk. The Ahlfors map being  $n$ -to-one map has  $n$  zeros. Previously, the exact zeros of the Ahlfors map are known only for the annulus region. The zeros of the Ahlfors map for general bounded doubly connected regions has been unknown for many years. This paper presents a numerical method for computing the zeros of the Ahlfors map of any bounded doubly connected region. The method depends on the values of Szego kernel, its derivative and the derivative of boundary correspondence function of the Ahlfors map. The Ahlfors map and Szego kernel are both classically related to each other. Ahlfors map can be computed using Szego kernel without relying on the zeros of Ahlfors map. The Szego kernel is a solution of a Fredholm integral equation of the second kind with the Kerzman-Stein kernel. The numerical examples presented here prove the effectiveness of the proposed method.

**Web URL:** <http://www.indjst.org/index.php/indjst/article/viewFile/92149/70104>

**14. Siddiqui, A. M., Sohail, A., Ashraf, A., & Azim, Q. A. (2016). Drag flow analysis of Oldroyd eight constant fluid. *Alexandria Engineering Journal*, 55(3), 2909-2918.**

**ABSTRACT:**

This article presents the steady drag flow problems. The incompressible Oldroyd eight constant fluid flow is considered between two infinite parallel plates. Three flow problems including the Couette flow, Poiseuille flow and Couette–Poiseuille flow are modeled. The source term appearing in the nonlinear differential equation for each case is simplified with the application

of modified homotopy perturbation method, and thus the general solution is obtained. The validity of second order approximate analytic solutions is tested with the aid of a numerical technique. The order of accuracy has been obtained in tabular form and the graphs are presented to demonstrate the difference between the three flow regimes.

**Web URL:** <http://www.sciencedirect.com/science/article/pii/S1110016816301387>

**15. Jawad, A., & Shahzad, M. U. (2016). Accretion onto some well-known regular black holes. *The European Physical Journal C*, 76(3), 1-11.**

**ABSTRACT:**

In this work, we discuss the accretion onto static spherically symmetric regular black holes for specific choices of the equation of state parameter. The underlying regular black holes are charged regular black holes using the Fermi–Dirac distribution, logistic distribution, nonlinear electrodynamics, respectively, and Kehagias–Sfetsos asymptotically flat regular black holes. We obtain the critical radius, critical speed, and squared sound speed during the accretion process near the regular black holes. We also study the behavior of radial velocity, energy density, and the rate of change of the mass for each of the regular black holes.

**Web URL:**

[http://download.springer.com/static/pdf/63/art%253A10.1140%252Fepjc%252Fs10052-016-3967-2.pdf?originUrl=http%3A%2F%2Flink.springer.com%2Farticle%2F10.1140%2Fepjc%2Fs10052-016-3967-2&token2=exp=1496903044~acl=%2Fstatic%2Fpdf%2F63%2Fart%25253A10.1140%25252Fepjc%25252Fs10052-016-3967-2.pdf%3ForiginUrl%3Dhttp%253A%252F%252Flink.springer.com%252Farticle%252F10.1140%252Fepjc%252Fs10052-016-3967-2\\*~hmac=bd6f38ee9dc601902d21e4cf7d115445a43e273af0464ccd0a629add55096758](http://download.springer.com/static/pdf/63/art%253A10.1140%252Fepjc%252Fs10052-016-3967-2.pdf?originUrl=http%3A%2F%2Flink.springer.com%2Farticle%2F10.1140%2Fepjc%2Fs10052-016-3967-2&token2=exp=1496903044~acl=%2Fstatic%2Fpdf%2F63%2Fart%25253A10.1140%25252Fepjc%25252Fs10052-016-3967-2.pdf%3ForiginUrl%3Dhttp%253A%252F%252Flink.springer.com%252Farticle%252F10.1140%252Fepjc%252Fs10052-016-3967-2*~hmac=bd6f38ee9dc601902d21e4cf7d115445a43e273af0464ccd0a629add55096758)

**16. Salako, I. G., & Jawad, A. (2016). Superresonance phenomenon from acoustic black holes in neo-Newtonian theory. *International Journal of Modern Physics D*, 25(05), 1650055.**

**ABSTRACT:**

We explore the possibility of the acoustic analogue of a super-radiance like phenomenon, i.e. the amplification of a sound wave by reflection from the ergo-region of a rotating acoustic black hole in the fluid draining bathtub model in the presence of the pressure to be amplified or reduced in agreement with the value of the parameter  $(\gamma=1+knpn-10c2)(\gamma=1+knp0n-1c2)$ . We remark that the interval of frequencies depend upon the neo-Newtonian parameter  $\gamma$  ( $\bar{\Omega} H=21+\gamma\Omega H\bar{\Omega} H=21+\gamma\Omega H$ ) and becomes narrow in this work. As a consequence, the tuning of the neo-Newtonian parameter  $(\gamma=1+knpn-10c2)(\gamma=1+knp0n-1c2)$  changes the rate of loss of the acoustic black hole mass.

**Web URL:**

<http://www.worldscientific.com/doi/abs/10.1142/S0218271816500553?journalCode=ijmpd>

**17. Alia, I., Chighoub, F., & Sohail, A. (2016). A characterization of equilibrium strategies in continuous-time mean–variance problems for insurers. *Insurance: Mathematics and Economics*, 68, 212-223.**

**ABSTRACT:**

In this work, we study the equilibrium reinsurance/new business and investment strategy for mean–variance insurers with constant risk aversion. The insurers are allowed to purchase proportional reinsurance, acquire new business and invest in a financial market, where the surplus of the insurers is assumed to follow a jump–diffusion model and the financial market consists of one riskless asset and a multiple risky assets whose price processes are driven by Poisson random measures and independent Brownian motions. By using a version of the stochastic maximum principle approach, we characterize the open loop equilibrium strategies via a stochastic system which consists of a flow of forward–backward stochastic differential equations (FBSDEs in short) and an equilibrium condition. Then by decoupling the flow of FSBDEs, an explicit representation of an equilibrium solution is derived as well as its corresponding objective function value.

**Web URL:** <http://www.sciencedirect.com/science/article/pii/S0167668715303437>

**18. Ali, K., Rizvi, S. T. R., & Semanicová-Fenovčíková, A. (2016). C-4-SUPERMAGIC LABELINGS OF DISJOINT UNION OF PRISMS. *Mathematical Reports.*, to appear.**

**ABSTRACT:**

A simple graph  $G$  admits an  $H$ -covering if every edge in  $E(G)$  belongs to a subgraph of  $G$  isomorphic to  $H$ . An  $H$ -magic labeling of a graph  $G$  admitting an  $H$ -covering is a bijective function from the vertex set  $V(G)$  and the edge set  $E(G)$  of the graph  $G$  onto the set of integers  $\{1, 2, \dots, |V(G)| + |E(G)|\}$  such that for all subgraphs  $H_0$  isomorphic to  $H$ , the sum of labels of all the edges and vertices belonged to  $H_0$  are the same. Such a labeling is called  $H$ -supermagic if the smallest possible labels appear on the vertices. In this paper, we will deal with  $C_4$ -supermagic labeling for the disjoint union of  $l$  isomorphic copies of prism graphs  $C_n \times P_m$  for  $m \geq 2$  and  $n \geq 3$ ,  $n \neq 4$ ,  $l \geq 1$ .

**Web URL:** [https://www.researchgate.net/profile/Syed\\_Rizvi43/publication/273766229\\_C\\_4\\_-\\_Supermagic\\_Labelings\\_of\\_Disjoint\\_Union\\_of\\_Prisms/links/550babb90cf290bdc111fcf5.pdf](https://www.researchgate.net/profile/Syed_Rizvi43/publication/273766229_C_4_-_Supermagic_Labelings_of_Disjoint_Union_of_Prisms/links/550babb90cf290bdc111fcf5.pdf)

**19. Abbas, M., Chema, I. Z., & Razani, A. (2016). Existence of common fixed point for b-metric rational type contraction. *Filomat*, 30(6), 1413-1429.**

**ABSTRACT:**

The necessary conditions for existence of a common fixed point of two mappings satisfying generalized b-order contractive condition in the setting of a partially ordered b-complete b-metric space are presented. Also, we study well-posedness of common fixed point problem for generalized b-order contractive mappings. We employ our result to establish an existence of a solution of an integral equation.

**Web URL:** <http://www.doiserbia.nb.rs/img/doi/0354-5180/2016/0354-51801606413A.pdf>

**20. Rafiullah, M., & Jabeen, D. (2016). New Eighth and Sixteenth Order Iterative Methods to Solve Nonlinear Equations. *International Journal of Applied and Computational Mathematics*, 1-10.**

**ABSTRACT:**

In this work we proposed two new higher order iterative methods to solve nonlinear equations. These methods based on the method Rafiullah (Numer Anal Appl 4(3):239–243, 2011) which is fifth-order. The Lagrange interpolation is used to improve the convergence order and efficiency

index of the method. Convergence order of new methods are proved analytically. Some test problems are given to show the efficiency of the proposed methods.

**Web URL:** <https://link.springer.com/article/10.1007/s40819-016-0245-9>

**21. Qayyum, M., Ashraf, S., & Kerre, E. (2016). Measure of intuitionistic fuzzy inclusion. *COMPTES RENDUS DE L ACADEMIE BULGARE DES SCIENCES*, 69(8), 973-982.**

**ABSTRACT:**

This paper introduces some new fuzzy measures for intuitionistic fuzzy sets which are then applied to define a degree of inclusion of one IFS into another. The results highlight that some properties are extended conditionally from their fuzzy counterparts.

**Web URL:** <https://biblio.ugent.be/publication/8122103>

**22. Zubair, M., & Abbas, G. (2016). Some interior models of compact stars in  $f(R, T)$  gravity. *Astrophysics and space science*, 361(10), 342.**

**ABSTRACT:**

This paper constitutes the investigations regarding possible formation of compact stars in  $f(R, T)$  theory of gravity, where  $R$  is Ricci scalar and  $T$  is trace of energy momentum tensor. In this connection, we use analytic solution of Krori and Barua metric (Krori and Barua 1975) to spherically symmetric anisotropic star in context of  $f(R, T)$  gravity. The masses and radii of compact stars models namely model 1, model2 and model 3 are employed to incorporate with unknown constants in Krori and Barua metric. The physical features such as regularity at center, anisotropy measure, causality and well-behaved condition of above mentioned class of compact stars are analyzed. Moreover, we have also discussed energy conditions, stability and surface redshift in  $f(R, T)$  gravity

**Web URL:** <https://arxiv.org/pdf/1512.05202.pdf>

**23. Zubair, M., Sardar, I. H., Rahaman, F., & Abbas, G. (2016). Interior solutions of fluid sphere in  $f(R, T)$ . *Astrophysics and Space Science*, 361(7), 1-6.**

**ABSTRACT:**

We discuss the interior solutions of fluid Sphere in  $f(R, T)$  gravity admitting conformal killing vectors, where  $R$  is Ricci scalar and  $T$  is trace of energy momentum tensor. The solutions

corresponding to isotropic and anisotropic configurations have been investigated explicitly. Further, the anisotropic case has been dealt by the utilization of linear equation of state. The results for both cases have been interpreted graphically. The equation of state parameter, integration constants and other parameters of the theory have been chosen to find the central density equal to standard value of central density of the compact objects. The energy conditions as well as stability of the solutions have been investigated in the background of  $f(R, T)$  gravity.

**Web URL:** <https://arxiv.org/pdf/1610.01754.pdf>

**24. Zubair, M., Waheed, S., & Ahmad, Y. (2016). Static spherically symmetric wormholes in  $f(R, T)$  gravity. *The European Physical Journal C*, 76(8), 444.**

**ABSTRACT:**

In this work, we explore wormhole solutions in  $f(R, T)$  theory of gravity, where  $R$  is the scalar curvature and  $T$  is the trace of stress-energy tensor of matter. To investigate this, we consider a static spherically symmetric geometry with matter contents as anisotropic, isotropic, and barotropic fluids in three separate cases. By taking into account the Starobinsky  $f(R)$  model, we analyze the behavior of energy conditions for these different kinds of fluids. It is shown that the wormhole solutions can be constructed without exotic matter in few regions of space-time. We also give the graphical illustration of the results obtained and discuss the equilibrium picture for the anisotropic case only. It is concluded that the wormhole solutions with anisotropic matter are realistic and stable in this theory of gravity.

**Web URL:** <https://link.springer.com/article/10.1140/epjc/s10052-016-4288-1/fulltext.html>

**25. Zubair, M., Ali Hassan, S. M., & Abbas, G. (2016). Bianchi type I and V solutions in  $f(R, T)$  gravity with time-dependent deceleration parameter. *Canadian Journal of Physics*, 94(12), 1289-1296.**

**ABSTRACT:**

In this paper, our attention is to reconstruct an appropriate model for Bianchi type I and Bianchi V space-times in  $f(R, T)$  gravity with the help of special law of deceleration parameter in connection to  $f(R, T)$  gravity (where  $R$  is the Ricci scalar and  $T$  is the trace of energy-momentum

tensor). We solve the modified Einstein field equations for anisotropic and homogeneous Bianchi type V space–time. The solution of field equations facilitates finding out the physical as well as kinematical quantities. We explore the behavior of null energy condition, energy density, and deceleration parameter to present cosmic picture.

**Web URL:** <http://www.nrcresearchpress.com/doi/abs/10.1139/cjp-2016-0575#.WUIQFZKGPIU>

**26. Bég, O. A., Ali, N., Zaman, A., Bég, E. T., & Sohail, A. (2016). Computational modeling of heat transfer in an annular porous medium solar energy absorber with the P1-radiative differential approximation. *Journal of the Taiwan Institute of Chemical Engineers*, 66, 258-268.**

**ABSTRACT:**

We study the steady, laminar thermal convection flow in a participating, absorbing-emitting fluid-saturated porous medium occupying a cylindrical annulus with significant thermal radiation effects as a simulation of a solar energy absorber system. The dimensionless incompressible, viscous conservation equations for mass, axial momentum, radial momentum, heat conservation and radiative transfer equation are presented with appropriate boundary conditions in an axisymmetric (X, R) coordinate system. The Traugott P1-Differential radiative transfer model is used which reduces the general integro-differential equation for radiation heat transfer to a partial differential equation. The Darcy–Forchheimer isotropic porous medium drag force model is employed to simulate resistance effects of the solar porous medium with constant permeability in both the radial (R) and axial (X) direction. A numerical finite difference (FTCS) scheme is used to compute the velocity (U,V), temperature ( $\Theta$ ) and dimensionless zero moment of intensity ( $I_0$ ) distributions for the effects of conduction–radiation parameter (N), Darcy parameter (Da), Forchheimer parameter (Fs), Rayleigh buoyancy number (Ra), aspect ratio (A) and Prandtl number (Pr). The computations have shown that increasing aspect ratio increases both axial and radial velocities and elevates the radiative moment of intensity. Increasing Darcy number accelerates both axial and radial flow whereas increasing Forchheimer number decelerates the axial and radial flow. Higher values of optical thickness induce a weak deceleration in the radial flow whereas they increase both axial flow

velocity and temperature. Increasing optical thickness also reduces radial radiative moment of intensity at intermediate axial coordinate values but enhances them at low and high axial coordinate values. Extensive validation is conducted with the network thermo-electric simulation program RAD-SPICE. The model finds important applications in solar energy porous wafer absorber systems, crystal growth technologies and also chemical engineering thermal technologies.

**Web URL:** <http://www.sciencedirect.com/science/article/pii/S1876107016302115>

**27. Jawad, A., Salako, I. G., & Sohail, A. (2016). Ghost dark energy models in specific modified gravity. *The European Physical Journal Plus*, 131(9), 299.**

**ABSTRACT:**

The paper is devoted to the study of the cosmic acceleration through ghost dark energy models (its simple and generalized form) in the dynamical Chern-Simons modified gravity. In order to check the reliability of this scenario, we explore different cosmological parameters, such as deceleration, equation of state parameters and squared speed of sound. The cosmological planes  $\omega_D$  and  $r_s$  are also investigated in this framework. The obtained results are consistent with observational data of various schemes (WMAP+eCAMB+BAO+ $H_0$ ).

**Web URL:** <https://link.springer.com/article/10.1140/epjp/i2016-16299-7>

**28. Khan, A. A., Sohail, A., Rashid, S., Rashidi, M. M., & Khan, N. A. (2016). Effects of Slip Condition, Variable Viscosity and Inclined Magnetic Field on the Peristaltic Motion of a Non-Newtonian Fluid in an Inclined Asymmetric Channel. *Journal of Applied Fluid Mechanics*, 9(3), 1381-1393.**

**ABSTRACT:**

The peristaltic motion of a third order fluid due to asymmetric waves propagating on the sidewalls of a inclined asymmetric channel is discussed. The key features of the problem includes long-wavelength and low-Reynolds number assumptions. A mathematical analysis has been carried out to investigate the effect of slip condition, variable viscosity and magnetohydrodynamics (MHD). Followed by the nondimensionalization of the nonlinear governing equations along with the nonlinear boundary conditions, a perturbation analysis is

made. For the validity of the approximate solution, a numerical solution is obtained using the iterative collocation technique.

**Web URL:**

<https://www.researchgate.net/publication/274195697> Effects of slip condition variable viscosity and inclined magnetic field on the peristaltic motion of a non-Newtonian fluid in an inclined asymmetric channel

**29. Akram, M., Farooq, A., & Shum, K. P. (2016). ON m-POLAR FUZZY LIE SUBALGEBRAS. *ITALIAN JOURNAL OF PURE AND APPLIED MATHEMATICS*, (36), 445-454.**

**ABSTRACT:**

The notion of an m-polar fuzzy set is a generalization of a bipolar fuzzy set. We apply the concept of m-polar fuzzy sets to Lie algebras. We introduce the concept of m-polar fuzzy Lie subalgebras of a Lie algebra and investigate some of their properties. We also present the homomorphisms between the Lie subalgebras of a Lie algebra and their relationship between the domains and the co-domains of the m-polar fuzzy subalgebras under these homomorphisms

**Web URL:** [http://ijpam.uniud.it/online\\_issue/201636/38-AkramFarookShum.pdf](http://ijpam.uniud.it/online_issue/201636/38-AkramFarookShum.pdf)

**30. Akram, M., & Farooq, A. (2016). Bipolar fuzzy trees. *New trends in mathematical sciences*, 4(3), 58-72.**

**ABSTRACT:**

Connectivity has an important role in different disciplines of computer science including computer network. In the design of a network, it is important to analyze connections by the levels. The structural properties of bipolar fuzzy graphs provide a tool that allows for the solution of operations research problems. In this paper, we introduce various types of bipolar fuzzy bridges, bipolar fuzzy cut-vertices, bipolar fuzzy cycles and bipolar fuzzy trees in bipolar fuzzy graphs, and investigate some of their properties. Most of these various types are defined in terms of levels. We also describe comparison of these types.

**Web URL:**

<http://www.ntmsci.com/AjaxTool/GetArticleByPublishedArticleId?PublishedArticleId=7167>

**31. Farooq, A., Ali, G., & Akram, M. (2016). On  $m$ -polar fuzzy groups. *International Journal of Algebra and Statistics*, 5(2), 115-127.**

**ABSTRACT:**

We introduce the concept of  $m$ -polar fuzzy subgroup, and investigate some of its properties. We describe the concept of an  $m$ -polar fuzzy coset and  $m$ -polar fuzzy quotient subgroup. We also present an  $m$ -polar fuzzy analog of Lagrange's theorem.

**Web URL:** <http://www.m-sciences.com/index.php?journal=ijas&page=article&op=view&path%5B%5D=1177&path%5B%5D=1045>

**32. Ali, H., Siddiqui, H. M. A., & Shafiq, M. K. (2016). On Degree-Based Topological Descriptors of Oxide and Silicate Molecular Structures.**

**ABSTRACT:**

In this Paper, we study general Zagreb, Zagreb inequality, augmented Zagreb, logarithm of first, second and modified first multiplicative Zagreb indices for Chain Oxide,  $COX_n$ , Chain Silicate,  $CS_n$ , Sheet Oxide,  $OX_n$  and Sheet Silicate,  $SL_n$  molecular structures for the first time. Moreover, analytically closed formulae for these structures are determined.

**Web URL:** <http://brisjast.com/wp-content/uploads/2016/09/MRR-Aug.-2-2016.pdf>

**33. Nadeem, I., & Shaker, H. (2016). On eccentric connectivity index of  $TiO_2$  nanotubes. *Acta Chimica Slovenica*, 63(2), 363-368.**

**ABSTRACT:**

The eccentric connectivity index (ECI) is a distance based molecular structure descriptor that was recently used for mathematical modeling of biological activities of diverse nature. The ECI has been shown to give a high degree of predictability compare to Wiener index with regard to diuretic activity and anti-inflammatory activity. The prediction accuracy rate of ECI is better than the Zagreb indices in case of anticonvulsant activity. Titania nanotubular materials are of high interest metal oxide substances due to their widespread technological applications. The numerous studies on the use of this material also require theoretical studies on the other properties of such materials. Recently, the Zagreb indices were studied of an infinite class of

titanium (TiO<sub>2</sub>) nanotubes [32]. In this paper, we study the eccentric connectivity index of these nanotubes.

**Web URL:** <https://journals.matheo.si/index.php/ACSi/article/viewFile/2337/950>

**34. Butt, S. I., Pečarić, J., & Vukelić, A. (2016). Generalization of Popoviciu-Type Inequalities Via Fink's Identity. *Mediterranean journal of mathematics*, 4(13), 1495-1511.**

**ABSTRACT:**

We obtained useful identities via Fink's identity, by which the inequality of Popoviciu for convex functions is generalized for higher order convex functions. We investigate the bounds for the identities related to the generalization of the Popoviciu inequality using inequalities for the Čebyšev functional. Some results relating to the Grüss- and Ostrowski-type inequalities are constructed. Further, we also construct new families of exponentially convex functions and Cauchy-type means by looking at linear functional associated with the obtained inequalities.

**Web URL:** [https://www.infona.pl/resource/bwmeta1.element.springer-doi-10\\_1007-S00009-015-0573-8](https://www.infona.pl/resource/bwmeta1.element.springer-doi-10_1007-S00009-015-0573-8)

**35. Zubair, M., Abbas, G., & Noureen, I. (2015). Possible Formation of Compact Stars in  $f(R, T)$  Gravity. *arXiv preprint arXiv:1512.05202*. (Published in 2016)**

**ABSTRACT:**

This paper constitutes the investigations regarding possible formation of compact stars in  $f(R, T)$  theory of gravity, where  $R$  is Ricci scalar and  $T$  is trace of energy momentum tensor. In this connection, we use analytic solution of Krori and Barua metric (Krori and Barua 1975) to spherically symmetric anisotropic star in context of  $f(R, T)$  gravity. The masses and radii of compact stars models namely model 1, model 2 and model 3 are employed to incorporate with unknown constants in Krori and Barua metric. The physical features such as regularity at center, anisotropy measure, causality and well-behaved condition of above mentioned class of compact stars are analyzed. Moreover, we have also discussed energy conditions, stability and surface redshift in  $f(R, T)$  gravity.

**Web URL:** <https://arxiv.org/pdf/1512.05202.pdf>

**36. Zubair, M., & Abbas, G. (2015). Analytic models of Anisotropic Strange Stars in  $f(T)$  Gravity with Off-diagonal tetrad. *arXiv preprint arXiv:1507.00247*. (Published in 2016)**

**ABSTRACT:**

This paper is devoted to study the analytic models of anisotropic compact stars in  $f(T)$  gravity (where  $T$  is torsion scalar), with nondiagonal tetrad. By taking the anisotropic source inside the spherically symmetric star, the equations of motions have been derived in the context of  $f(T)$  gravity. Krori and Barua metric which satisfies the physical requirement of a realistic star, has been applied to describe the compact objects like strange stars. We use the power law form of  $f(T)$  model to determine explicit relations of matter variables. Further, we have found the anisotropic behavior, energy conditions, stability and surface redshift of stars. Using the masses and radii of 4U1820-30, Her X-1, SAX J 1808-3658, we have determined the constants involved in metric components. Finally we discuss the graphical behavior of the analytic description of strange star candidates.

**Web URL:** <https://arxiv.org/pdf/1507.00247.pdf>

**37. Zubair, M. (2016). Phantom crossing with collisional matter in  $f(T)$  gravity. *International Journal of Modern Physics D*, 25(05), 1650057.**

**ABSTRACT:**

We study the late-time cosmological evolution of  $f(T)f(T)$  (where  $TT$  is the torsion scalar) theories with matter contents consisting of collisional self-interacting matter and radiations. The power law, exponential and logarithmic  $f(T)f(T)$  models are considered to explore the evolution of Hubble parameter  $H(z)H(z)$ , dark energy (DE) equation of state (EoS)  $\omega_{DE}\omega_{DE}$  and effective EoS parameter  $\omega_{eff}\omega_{eff}$ . We show that crossing of phantom divide line can be realized in the presence of collisional matter as compared to the results obtained for the choice of noncollisional matter [K. Bamba, C.-Q. Geng, C.-C. Lee and L.-W. Luo, *J. Cosmol. Astropart. Phys.* **01** (2011) 021; K. Bamba, C.-Q. Geng and C.-C. Lee, arXiv:1008.4036]. The evolutionary behavior of  $\omega_{DE}\omega_{DE}$  is consistent with the one developed in [P. Wu and H. Yu, *Eur. Phys. J. C* **71** (2011) 1552] and recent observational data [U. Alam, V. Sahni and A. A. Starobinsky, *J. Cosmol. Astropart. Phys.* **0406** (2004) 008; S. Nesseris and L. Perivolaropoulos, *J. Cosmol. Astropart. Phys.* **0701** (2007) 018; P. Wu and H. Yu, *Phys. Lett. B* **643** (2006) 315; U. Alam,

V. Sahni and A. A. Starobinsky, *J. Cosmol.Astropart.Phys.* **0702** (2007) 011; H. K. Jassal, J. S. Bagla and T. Padmanabhan, *Mon. Not.R. Astron. Soc.* **405** (2010) 2639].

**Web URL:**

<http://www.worldscientific.com/doi/abs/10.1142/S0218271816500577?journalCode=iimpd>

**38. Arshad, S., Sohail, A., & Maqbool, K. (2016). Nonlinear shallow water waves: A fractional order approach. *Alexandria Engineering Journal*, 55(1), 525-532.**

**ABSTRACT:**

Nonlinear partial differential equations governing the obscure phenomena of shallow water waves are discussed in this article. Time fractional model is considered to understand the upcoming solutions on the basis of all historical states of the solution. A semi-analytic technique, Homotopy Perturbation Transform Method (HPTM) is used in conjunction with a numerical technique to validate the approximate solutions. With the aid of graphical interpretation, the favorable wave parameters, to avoid wave breaking are estimated.

**Web URL:** <http://www.sciencedirect.com/science/article/pii/S1110016815001696>

**39.Sohail, A., Uddin, M. J., & Rashidi, M. M. (2015). Numerical study of free convective flow of a nanofluid over a chemically reactive porous flat vertical plate with a second-order slip model. *Journal of Aerospace Engineering*, 29(2), 04015047. (Published in 2016)**

**ABSTRACT:**

A mathematical model for free convective boundary-layer flow of a nanofluid with second-order velocity slip over a permeable vertical flat plate has been presented. The system of governing equations is first nondimensionalized, and then similarity transformations are used to convert the governing partial differential equations into a set of coupled ordinary differential equations. A numerical algorithm is applied to this boundary value problem (BVP) of coupled ordinary differential equations. Collocation method is used for the solution of the nonlinear ordinary BVP. The dimensionless analysis revealed that the dimensionless field variables (velocity, temperature, and nanoparticle volume fraction), and the flow characteristics (skin friction factor, heat transfer, and nanoparticle volume fraction transfer) in the respective

boundary layers depend on the Prandtl number ( $Pr$ ), the Lewis numbers ( $Le$ ), the thermophoresis parameter ( $Nt$ ), the Brownian motion parameter ( $Nb$ ), the buoyancy ratio parameter ( $Nr$ ), the convective parameter ( $\gamma$ ), the reaction parameter ( $KK$ ), first-order velocity slip parameter ( $aa$ ), and second-order velocity slip parameter ( $bb$ ). Flow field and physical quantities strongly depend on the governing parameters. The present problem has applications in nanofluid synthesis for medicine. A tabular validation of the present numerical approach with the existing results in the literature is provided as a limiting case.

**Web URL:** [http://ascelibrary.org/doi/abs/10.1061/\(ASCE\)AS.1943-5525.0000544](http://ascelibrary.org/doi/abs/10.1061/(ASCE)AS.1943-5525.0000544)

**40. Bashir, Y., Nadeem, F., & Shabbir, A. (2016). Highly non-concurrent longest paths in lattices. *Turkish Journal of Mathematics*, 40(1), 21-31.**

**ABSTRACT:**

In this paper we consider graphs in which any pair of vertices is missed by some longest path. We are proving the existence of such graphs in the infinite triangular, square and hexagonal lattices in the plane. Moreover, we extend our investigation to lattices on several surfaces such as the torus, the Möbius strip and the Klein bottle.

**Web URL:** <http://journals.tubitak.gov.tr/math/issues/mat-16-40-1/mat-40-1-2-1502-32.pdf>

**41. Nadeem, M. F., Zafar, S., & Zahid, Z. (2016). On topological properties of the line graphs of subdivision graphs of certain nanostructures. *Applied Mathematics and Computation*, 273, 125-130.**

**ABSTRACT:**

In the study of QSAR/QSPR, topological indices such as Shultz index, generalized Randic index, Zagreb index, general sum-connectivity index, atom-bond connectivity (ABC) index and geometric–arithmetic (GA) index are exploited to estimate the bioactivity of chemical compounds. A topological index attaches a chemical structure with a numeric number. There are numerous applications of graph theory in this field of research. In this paper we computed generalized Randic, general Zagreb, general sum-connectivity,  $ABC$ ,  $GA$ ,  $ABC_4$  and  $GA_5$  indices of the line graphs of 2D-lattice, nanotube and nanotorus of  $TUC_4C_8[p, q]$  by using the concept of subdivision.

**Web URL:** <http://www.sciencedirect.com/science/article/pii/S0096300315013429>

**42. Nadeem, M. F., Zafar, S., & Zahid, Z. (2016). ON THE EDGE VERSION OF GEOMETRIC-ARITHMETIC INDEX OF NANOCONES. *Studia Universitatis Babes-Bolyai, Chemia*, 61(1).**

**ABSTRACT:**

In this paper, the edge version geometric-arithmetic index of certain nanocones is presented.

**Web URL:**

<http://web.b.ebscohost.com/abstract?direct=true&profile=ehost&scope=site&authtype=crawler&jrnl=12247154&AN=115445722&h=zd%2bcm5h19uQsMC%2fzP2iwfscXc1Gerui2SU1MWrgAoEyHSPAfSUZtvatb6BM91cHamPV2Ufz843hYgCLmO48zw%3d%3d&crl=c&resultNs=AdminWebAuth&resultLocal=ErrCrlNotAuth&crlhashurl=login.aspx%3fdirect%3dtrue%26profile%3dehost%26scope%3dsite%26authtype%3dcrawler%26jrnl%3d12247154%26AN%3d115445722>

**43. Butt, S. I., Numan, M., & Qaisar, S. (2016). Labelings of type (1, 1, 1) for Klein bottle fullerenes. *Journal of Mathematical Chemistry*, 54(2), 428-441.**

**ABSTRACT:**

In this paper we deal with the problem of labeling the vertices, edges and faces of a Klein bottle fullerenes  $K_{nm}K_{mn}$  with  $mn$  hexagons by the consecutive integers from 1 up to  $|V(K_{nm})| + |V(K_{mn})| + |E(K_{nm})| + |E(K_{mn})| + |F(K_{nm})| + |F(K_{mn})|$  in such a way that the label of a 6-sided face and the labels of the vertices and edges surrounding that face all together add up to a weight of that face. These face-weights then form an arithmetic progression with common difference  $d$ . The paper examines the existence of such labelings for several differences  $d$ .

**Web URL:** <https://link.springer.com/article/10.1007/s10910-015-0568-5>

**44. Butt, S. I., Khan, K. A., & Pecaric, J. (2016). Popoviciu type inequalities via Green function and Taylor polynomial. *Turkish Journal of Mathematics*, 40(2), 333-349.**

**ABSTRACT:**

The well-known Taylor polynomial is used to construct the identities coming from Popoviciu type inequalities for convex functions via the Green function. The bounds for the new identities

are found using the Chebyshev functional  $\chi$  to develop the Grüss and Ostrowski type inequalities. Further, more exponential convexity together with Cauchy means is presented for linear functionals associated with the obtained inequalities.

**Web URL:** <http://journals.tubitak.gov.tr/math/issues/mat-16-40-2/mat-40-2-9-1501-38.pdf>

**45. Zubair, M., & Hassan, S. M. A. (2016). Dynamics of Bianchi type I, III and Kantowski-Sachs solutions in  $f(R, T)$  gravity. *Astrophysics and Space Science*, 361(4), 149.**

**ABSTRACT:**

In this paper, we reconstruct a suitable model in  $f(R, T)$  gravity, (where  $R$  is the Ricci scalar and  $T$  is the trace of the energy momentum tensor) which depict the current cosmic picture in more consistent way. The dynamical field equations are solved for generic anisotropic space-time. The solution of field equations helps us to determine the future cosmic evolution for both physical and kinematical quantities. We explore the nature of deceleration parameter, NEC and energy density for three different cases representing Bianchi type I, III and Kantowski-Sachs universe model. We find that this study favors the phantom cosmic evolution in all cases.

**Web URL:** <https://link.springer.com/article/10.1007/s10509-016-2737-9>

**46. Zubair, M., & Kousar, F. (2016). Cosmological reconstruction and energy bounds in  $f(R, R_{\alpha\beta}, \phi)$  gravity. *The European Physical Journal C*, 76(5), 254.**

**ABSTRACT:**

We discuss the cosmological reconstruction of  $f(R, R_{\alpha\beta}, \phi)$  (where  $R$ ,  $R_{\alpha\beta}$ , and  $\phi$  represent the Ricci scalar, the Ricci invariant, and the scalar field) corresponding to a power law and de Sitter evolution in the framework of the FRW universe model. We derive the energy conditions for this modified theory which seem to be more general and can be reduced to some well-known forms of these conditions in general relativity,  $f(R)$  and  $f(R, \phi)$  theories. We have presented the general constraints in terms of recent values of the snap, jerk, deceleration, and Hubble parameters. The energy bounds are analyzed for reconstructed as well as known models in this theory. Finally, the free parameters are analyzed comprehensively.

**Web URL:** <https://link.springer.com/article/10.1140/epjc/s10052-016-4104-y>

**47. Jawad, A., Azhar, N., & Rani, S. (2017). Entropy corrected holographic dark energy models in modified gravity. *International Journal of Modern Physics D*, 26(04), 1750040.**

**ABSTRACT:**

We consider the power law and the entropy corrected holographic dark energy (HDE) models with Hubble horizon in the dynamical Chern–Simons modified gravity. We explore various cosmological parameters and planes in this framework. The Hubble parameter lies within the consistent range at the present and later epoch for both entropy corrected models. The deceleration parameter explains the accelerated expansion of the universe. The equation of state (EoS) parameter corresponds to quintessence and cold dark matter ( $\Lambda$ CDM) limit. The  $\omega_\Lambda - \omega' / \omega_\Lambda - \omega_\Lambda'$  approaches to  $\Lambda$ CDM limit and freezing region in both entropy corrected models. The statefinder parameters are consistent with  $\Lambda$ CDM limit and dark energy (DE) models. The generalized second law of thermodynamics remain valid in all cases of interacting parameter. It is interesting to mention here that our results of Hubble, EoS parameter and  $\omega_\Lambda - \omega' / \omega_\Lambda - \omega_\Lambda'$  plane show consistency with the present observations like Planck, WP, BAO, H0H0, SNLS and nine-year WMAP.

**Web URL:** <http://www.worldscientific.com/doi/abs/10.1142/S0218271817500407>

**48. Rani, S., Jawad, A., & Amin, M. B. (2016). Charged Noncommutative Wormhole Solutions via Power-Law  $f(T)$  Models. *Communications in Theoretical Physics*, 66(4), 411.**

**ABSTRACT:**

In this paper, we explore static spherically symmetric charged wormhole solutions in extended teleparallel gravity taking power-law  $f(T)$  models. We consider noncommutative geometry under Lorentzian distribution. In order to obtain matter components, we develop field equations using effective energy-momentum tensor for non-diagonal tetrad. We explore solutions by considering various viable power-law  $f(T)$  models, which also include teleparallel gravity case. The violation of energy conditions obtain by exotic matter to form wormhole solutions in teleparallel case while, physical acceptable wormhole solutions exist for charged noncommutative wormhole solutions for some cases of power-law models. The effective

energy-momentum tensor and charge are responsible for the violation of the energy conditions. Also, we check the equilibrium condition for these solutions. The equilibrium condition meets for the teleparallel case and some power-law solutions while remaining solutions are either in less equilibrium or in disequilibrium situation.

**Web URL:** <http://iopscience.iop.org/article/10.1088/0253-6102/66/4/411/pdf>

**49. Rani, S., Jawad, A., Salako, I. G., & Azhar, N. (2016). Non-flat pilgrim dark energy FRW models in modified gravity. *Astrophysics and Space Science*, 361(9), 286.**

**ABSTRACT:**

We study the cosmic acceleration in dynamical Chern-Simons modified gravity in the framework of non-flat FRW universe. The pilgrim dark energy (with future event and apparent horizons) interacted with cold dark matter is being considered in this work. We investigate the cosmological parameters (equation of state, deceleration) and planes (statefinders,  $\omega_{\vartheta} - \omega_{\vartheta}'$ ) in the present scenario. It is interesting to mention here that the obtained results of various cosmological parameters are consistent with various observational schemes. The validity of generalized second law of thermodynamics for present dark energy models is also being analyzed.

**Web URL:** <https://link.springer.com/article/10.1007/s10509-016-2868-z>

**50. Jawad, A., Rani, S., & Nawaz, T. (2016). Interacting new holographic dark energy in dynamical Chern-Simons modified gravity. *The European Physical Journal Plus*, 131(8), 282.**

**ABSTRACT:**

In this paper, we explore various cosmological parameters (equation of state, squared speed of sound,  $Om$ -diagnostic) and cosmological planes ( $\omega_{\vartheta} - \omega_{\vartheta}'$ , where  $\omega_{\vartheta}'$  is the evolutionary equation of state parameter, statefinder). We consider the framework of dynamical Chern-Simons modified gravity with the new holographic dark energy model. It is observed that the equation of state parameter gives consistent ranges by using different observational schemes. We check the stability of the model using the squared speed of sound. In the present scenario, the squared speed of sound shows a stable solution. The  $\omega_{\vartheta} - \omega_{\vartheta}'$  and statefinder planes also present consistent results. We would like to

mention here that our results of cosmological parameters show consistency with previous different observational data like Planck,  $H_0$ , SNLS and WMAP.

**Web URL:** <https://link.springer.com/article/10.1140/epjp/i2016-16282-4>

**51. Rani, S., Nawaz, T., & Jawad, A. (2016). Thermodynamics in dynamical Chern-Simons modified gravity with canonical scalar field. *Astrophysics and Space Science*, 361(9), 285.**

**ABSTRACT:**

We take the scalar field dark energy model possessing a non-canonical kinetic term in the framework of modified Chern-Simon gravity. We assume the flat FRW universe model and interacting scenario between dark matter and non-canonical dark energy part. Under this scenario, we check the stability of the model using squared speed of sound which represents the stable behavior for a specific choice of model parameters. We also discuss the validity of generalized second law of thermodynamics by assuming the usual entropy and its corrected forms (logarithmic and power law) at the apparent horizon. This law satisfied for all cases versus redshift parameter at the present as well as later epoch.

**Web URL:** <https://link.springer.com/article/10.1007/s10509-016-2861-6>

**52. Jawad, A., Rani, S., & Mohsaneen, S. (2016). Generalized cosmic Chaplygin gas inspired intermediate standard scalar field inflation. *Astrophysics and Space Science*, 361(8), 1-9.**

**ABSTRACT:**

We study the warm intermediate inflationary regime in the presence of generalized cosmic Chaplygin gas and an inflaton decay rate proportional to the temperature. For this purpose, we consider standard scalar field model during weak and strong dissipative regimes. We explore inflationary parameters like spectral index, scalar and tensor power spectra, tensor to scalar ratio and decay rate in order to compare the present model with recent observational data. The physical behavior of inflationary parameters is presented and found that all the results are agreed with recent observational data such as WMAP7, WMAP9 and Planck 2015.

**Web URL:** <https://link.springer.com/article/10.1007/s10509-016-2852-7>

**53. Jawad, A., Butt, S., & Rani, S. (2016). Chaplygin gas inspired scalar fields inflation via well-known potentials. *Astrophysics and Space Science*, 361(8), 1-12.**

**ABSTRACT:**

Brane inflationary universe models in the context of modified Chaplygin gas and generalized cosmic Chaplygin gas are being studied. We develop these models in view of standard scalar and tachyon fields. In both models, the implemented inflationary parameters such as scalar and tensor power spectra, scalar spectral index and tensor to scalar ratio are derived under slow roll approximations. We also use chaotic and exponential potential in high energy limits and discuss the characteristics of inflationary parameters for both potentials. These models are compatible with recent astronomical observations provided by WMAP7+9 WMAP7+9 and Planck data,

i.e.,  $\eta_s=1.027\pm 0.051, 1.009\pm 0.049, 0.096\pm 0.025$   $\eta_s=1.027\pm 0.051, 1.009\pm 0.049, 0.096\pm 0.025$  and  $r < 0.38, 0.36, 0.11$   $r < 0.38, 0.36, 0.11$ .

**Web URL:** <https://link.springer.com/article/10.1007/s10509-016-2843-8>

**54. Jawad, A., Rani, S., & Mohsaneen, S. (2016). Generalized cosmic Chaplygin inflationary model on the brane. *The European Physical Journal Plus*, 131(7), 1-7.**

**ABSTRACT:**

The generalized cosmic Chaplygin model in the context of brane-inflationary background is being considered by taking the standard scalar field as matter field. We develop the modified first Friedmann equation and conservation equation under slow-roll approximations. We also discuss the feature of the generalized cosmic Chaplygin gas model in the presence of chaotic potential in the high-energy limit. Various inflationary parameters, such as slow-roll parameters, scalar and tensor power spectra, scalar spectral index and tensor-to-scalar ratio are evaluated. To this end, Planck results are used to constraint new parameters.

**Web URL:** <https://link.springer.com/article/10.1140/epjp/i2016-16234-0>

**55. Jawad, A., Rani, S., Salako, I. G., & Gulshan, F. (2016). Aspects of some new versions of pilgrim dark energy in DGP braneworld. *The European Physical Journal Plus*, 131(7), 1-12.**

**ABSTRACT:**

The illustration of cosmic acceleration under two interacting dark energy models (pilgrim dark energy with Granda-Oliveros cutoff and its generalized ghost version) in the DGP braneworld

framework is presented. In the current scenario, the equation of state parameter, deceleration parameter,  $\omega_D$  -  $\omega'_D$  plane and statefinder diagnosis are investigated. The equation of state parameter behaves like the phantom era of the universe. The deceleration parameter shows the accelerated expansion of the universe in both models. The cosmological planes, like  $\omega_D$  -  $\omega'_D$ , and the statefinder correspond to the  $\Lambda$  CDM limit. To conclude, we remark that our results support the phenomena of pilgrim dark energy and cosmic acceleration. Also, the results are consistent with observational data.

**Web URL:** <https://link.springer.com/article/10.1140/epjp/i2016-16236-x>

**56. Jawad, A., Chattopadhyay, S., & Rani, S. (2016). Viscous pilgrim  $f(T)$  gravity models. *Astrophysics and Space Science*, 7(361), 1-8.**

**ABSTRACT:**

The present paper reports a study on the cosmological consequences of pilgrim dark energy model in the framework of generalized teleparallel gravity. We consider a reconstruction scheme for  $f(T)$  models with power law scale factor taking Hubble horizon and Nojiri-Odintsov length as infrared cutoffs. We consider a time dependent viscous model through effective pressure in order to incorporate the effect of viscosity in the models. We study accelerated expansion of the universe through effective equation of state parameter, which represents cosmological constant and phantom behavior consistent with the observational data. To check the stability of the models we use squared speed of sound parameter, which shows that the model is stable for higher values of scale factor parameter. Analysis of the plane containing effective equation of state parameter with its evolutionary parameter indicates freezing region of the accelerated expansion and viability of the model has been tested through observational data.

**Web URL:** <https://link.springer.com/content/pdf/10.1007/s10509-016-2814-0.pdf>

**57. Rani, S., & Jawad, A. (2016). Cosmological implications of DGP braneworld via well-known holographic dark energy models. *International Journal of Modern Physics D*, 25(14), 1650102.**

**ABSTRACT:**

The cosmological analysis is being studied in the present work in Dvali–Gabadadze–Porrati (DGP) braneworld scenario by taking various interacting modified holographic dark energy (HDE) models. We discuss the various cosmological parameters such as deceleration parameter, equation-of-state (EoS) parameter and squared speed of sound. It is found that the trajectories of deceleration parameter exhibit in accelerated phase of the universe for all models. The EoS parameter corresponds to various phases of cosmic acceleration like quintessence, vacuum, phantom and also exhibits consistency with observational data. The squared speed of sound also gives stability of models in the current scenario. The  $\omega_{\text{eff}} - \omega'_{\text{eff}}/\omega_{\text{eff}}$  also gives consistent results with various observational schemes. The statefinders plane also exhibits the cosmic acceleration. It is interesting to remark here that some of our results shows consistency with observational data like WMAP+CMB+BAO+H0H0+SNe.

**Web URL:** <http://www.worldscientific.com/doi/abs/10.1142/S0218271816501029>

**58. Jawad, A., Ilyas, A., & Rani, S. (2016). Dynamics of bulk viscous pressure effected inflation in braneworld scenario. *Astroparticle Physics*, 81, 61-71.**

**ABSTRACT:**

The main goal of the present work is to examine the possible realization of warm chaotic inflation and logamediate inflation within the framework of a modified Chaplygin gas braneworld model. In this respect, the slow-roll parameters, number of e-folds, scalar-tensor power spectra, spectral indices, tensor–scalar ratio and running of scalar spectral index is being evaluated. These parameters are being analyzed for variable as well as constant dissipation and bulk viscous coefficients. Further, the trajectories among the inflationary parameters such as  $n_s - \varphi$ ,  $n_s - r$ ,  $\alpha_s - \varphi$  and  $n_s - \alpha_s$  are also developed to examine their behavior as well as physical cosmology. Some of results of inflationary parameters in all cases are:  $r < 0.11$ ,  $n_s = 0.96 \pm 0.025$  and  $\alpha_s = -0.019 \pm 0.025$ . It is interesting to mention here that the results of inflationary parameters are consistent with BICEP2, WMAP (7+9) and Planck data.

**Web URL:** <http://www.sciencedirect.com/science/article/pii/S0927650516300640>

**59. Jawad, A., Butt, S., & Rani, S. (2016). Dynamics of warm Chaplygin gas inflationary models with quartic potential. *The European Physical Journal C*, 76(5), 274.**

**ABSTRACT:**

Warm inflationary universe models in the context of the generalized Chaplygin gas, the modified Chaplygin gas, and the generalized cosmic Chaplygin gas are being studied. The dissipative coefficient of the form  $\Gamma \propto T^{\alpha}$ , and the weak and the strong dissipative regimes are being considered. We use the quartic potential,  $\lambda \phi^4$ , which is ruled out by current data in cold inflation but in our models by analysis it is seen to be in agreement with the WMAP9 and the latest Planck data. In these scenarios, the power spectrum, the spectral index, and the tensor-to-scalar ratio are being examined in the slow-roll approximation. We show the dependence of the tensor–scalar ratio  $r$  on the spectral index  $n_s$  and observe that the range of the tensor–scalar ratio is  $r < 0.05$  in the generalized Chaplygin gas,  $r < 0.15$  in the modified Chaplygin gas, and  $r < 0.12$  in the generalized cosmic Chaplygin gas models. Our results are in agreement with recent observational data like WMAP9 and the latest Planck data.

**Web URL:** <https://link.springer.com/article/10.1140/epjc/s10052-016-4121-x>

**60. Jawad, A., Rani, S., & Mohsaneen, S. (2016). Modified Chaplygin gas inspired inflationary model in braneworld scenario. *Astrophysics and Space Science*, 361(5), 158.**

**ABSTRACT:**

We investigate the modified Chaplygin gas inspired inflationary regime in the brane-world framework in the presence of standard and tachyon scalar fields. We consider the intermediate inflationary scenario and construct the slow-roll parameters, e-folding numbers, spectral index, scalar and tensor power spectra, tensor to scalar ratio for both scalar field models. We develop the  $n_s$ – $r$  and  $r$ – $N$  planes and concluded that  $n_s \approx 0.96 - 0.5 + 0.5$  and  $r \leq 0.0016$  for  $N \approx 60 - 5 + 5$  in both cases of scalar field models as well as for all values of  $m$ . These constraints are consistent with observational data such as WMAP7, WMAP9 and Planck data.

**Web URL:** <https://link.springer.com/article/10.1007/s10509-016-2751-y>

**61. Salako, I. G., Houndjo, M. J. S., & Jawad, A. (2016). Generalized Mattig’s relation in Brans–Dicke–Rastall gravity. *International Journal of Modern Physics D*, 25(07), 1650076.**

**ABSTRACT:**

The geodesic deviation equation (GDE) is being studied in Brans–Dicke–Rastall (BDR) gravity. We briefly discuss the BDR gravity and then construct GDE for FLRW metric. In this way, the obtained geodesic deviation equation will correspond to the BDR gravity. Eventually, we solve numerically the null vector GDE to obtain from Mattig relation, the deviation vector  $\eta(z)\eta(z)$  and observer area distance  $r_0(z)r_0(z)$  and compare the results with  $\Lambda$ CDM model.

**Web URL:** <http://www.worldscientific.com/doi/abs/10.1142/S0218271816500760>

**62. Jawad, A., & Rani, S. (2016). Anisotropic inflationary scenario via generalized Chaplygin gas model. *Communications in Theoretical Physics*, 65(5), 653.**

**ABSTRACT:**

We investigate generalized chaplygin gas for warm inflationary scenario in the context of locally rotationally symmetric Bianchi type I universe model. We assume two different cases of dissipative coefficient, i.e., constant as well as function of scalar field. We construct dynamical equations as well as a relationship between scalar and radiation energy densities under slow-roll approximation. We also derive slow-roll parameters, scalar and tensor power spectra, scalar spectral index, tensor to scalar ratio for analyzing inflationary background during high dissipative regime. We also use the WMAP7 data for the discussion of our parameters.

**Web URL:** <http://iopscience.iop.org/article/10.1088/0253-6102/65/5/653/meta>

**63. Javaid, M., Bhatti, A. A., & Hussain, M. (2016). Further results on super edge-magic total labeling of extended w-trees. *UTILITAS MATHEMATICA*, 100, 179-192.**

**ABSTRACT: Not Found**

**Web URL:**

**64. Wajid, H. A. (2016). Simulations of the Helmholtz equation at any wave number for adaptive grids using a modified central finite difference scheme. *Turkish Journal of Mathematics*, 40(4), 806-815.**

**ABSTRACT:**

In this paper, a modified central finite difference scheme for a three-point nonuniform grid is presented for the one-dimensional homogeneous Helmholtz equation using the Bloch wave property. The modified scheme provides highly accurate solutions at the nodes of the nonuniform grid for very small to very large range of wave numbers irrespective of how the grid is adapted throughout the domain. A variety of numerical examples are considered to validate the superiority of the modified scheme for a nonuniform grid over a standard central finite difference scheme.

**Web URL:** <http://journals.tubitak.gov.tr/math/issues/mat-16-40-4/mat-40-4-9-1506-24.pdf>

**65. Wajid, H. A., & Sohail, A. (2016). Compact Modified Implicit Finite Element Schemes for Wave Propagation Problems with Superior Dispersive Properties. *Arabian Journal for Science and Engineering*, 41(11), 4613-4624.**

**ABSTRACT:**

In this paper, we study in detail dispersive properties of the widely used implicit scheme called Newmark trapezoidal rule in conjunction with modified mass matrix to enjoy superior dispersive properties keeping the finite element stencil compact. We call such schemes *compact modified implicit finite element scheme*. In case of one-dimensional propagation, following contributions are made: (a) for modified finite element (MFE) scheme, we find an optimal value of dispersion controlling parameter depending on Courant–Friedrichs–Lewy (CFL) number which provides exact solutions at the nodes of spatial grid; (b) for standard finite element (SFE) scheme optimal value of CFL number is obtained which provides fourth-order accurate solutions. Moreover, in case of two-dimensional propagation following contributions are made: (c) we have found optimal value of CFL number for all angles in case of both SFE and MFE schemes; (d) superior dispersive behaviour is evident in case of MFE scheme in comparison with SFE scheme. Furthermore, the MFE scheme can be efficiently implemented using non-standard quadrature rules or just updating mass matrix which does not require to write brand new code and makes it computationally very attractive. Also for specific value of parameter, i.e.  $\tau = 0$ , the MFE scheme leads back to the SFE scheme.

**Web URL:** <https://link.springer.com/article/10.1007/s13369-016-2220-5>

**66. Abid, M., Saeed, J., & Wajid, H. A. (2016). Sediment and Cavitation Erosion Studies through Dam Tunnels. *Journal of Engineering, 2016*.**

**ABSTRACT:**

This paper presents results of sediment and cavitation erosion through Tunnel 2 and Tunnel 3 of Tarbela Dam in Pakistan. Main bend and main branch of Tunnel 2 and outlet 1 and outlet 3 of Tunnel 3 are concluded to be critical for cavitation and sediment erosion. Studies are also performed for increased sediments flow rate, concluding 5 kg/sec as the critical value for sudden increase in erosion rate density. Erosion rate is concluded to be the function of sediment flow rate and head condition. Particulate mass presently observed is reasonably low, hence presently not affecting the velocity and the flow field.

**Web URL:** <https://www.hindawi.com/journals/je/2016/8645789/abs/>

**67. Abid, M., Khan, A., Nash, D. H., Hussain, M., & Wajid, H. A. (2016). Optimized bolt tightening strategies for gasketed flanged pipe joints of different sizes. *International Journal of Pressure Vessels and Piping, 139, 22-27*.**

**ABSTRACT:**

Achieving a proper preload in the bolts of a gasketed bolted flanged pipe joint during joint assembly is considered important for its optimized performance. This paper presents results of detailed non-linear finite element analysis of an optimized bolt tightening strategy of different joint sizes for achieving proper preload close to the target stress values. Industrial guidelines are considered for applying recommended target stress values with TCM (torque control method) and SCM (stretch control method) using a customized optimization algorithm. Different joint components performance is observed and discussed in detail.

**Web URL:** <http://www.sciencedirect.com/science/article/pii/S030801611630076X>

**68. Rani, S., Amin, M. B., & Jawad, A. (2016). Exponential and logarithmic  $f(T)$  wormhole solutions in Lorentzian noncommutative background. *The European Physical Journal Plus, 131(12), 436*.**

**ABSTRACT:**

In this paper, we take noncommutative geometry under Lorentzian distribution and explore static spherically symmetric wormhole solutions in the extended teleparallel gravity by taking exponential and logarithmic  $f(T)$  models. For matter components, we use effective energy-momentum tensor for a nondiagonal tetrad and develop field equations. We work to explore solutions by considering various viable  $f(T)$  models and conclude that there exists a possibility of physically acceptable wormhole solutions under noncommutative background for these models. We observe that the effective energy-momentum tensor is responsible for the violation of the energy conditions. Also, we check the stability for these solutions by equilibrium condition. The equilibrium condition does not meet properly for any obtained solutions. Therefore solutions are in less equilibrium situation.

**Web URL:** <https://link.springer.com/article/10.1140/epjp/i2016-16436-4>

**69. Jawad, A., Ali, F., Shahzad, M. U., & Abbas, G. (2016). Dynamics of particles around time conformal Schwarzschild black hole. *The European Physical Journal C*, 76(11), 586.**

**ABSTRACT:**

In this work, we present the new technique for discussing the dynamical motion of neutral as well as charged particles in the absence/presence of a magnetic field around the time conformal Schwarzschild black hole. Initially, we find the numerical solutions of geodesics of the Schwarzschild black hole and the time conformal Schwarzschild black hole. We observe that the Schwarzschild spacetime admits the time conformal factor  $e^{\epsilon f(t)}e^{\epsilon f(t)}$ , where  $f(t)$  is an arbitrary function and  $\epsilon$  is very small, which causes a perturbation in the spacetimes. This technique also re-scales the energy content of spacetime. We also investigate the thermal stability, horizons and energy conditions corresponding to time conformal Schwarzschild spacetime. Also, we examine the dynamics of a neutral and charged particle around a time conformal Schwarzschild black hole. We investigate the circumstances under which the particle can escape from the vicinity of a black hole after collision with another particle. We analyze the effective potential and effective force of a particle in the presence of a magnetic field with angular momentum graphically.

**Web URL:** <https://link.springer.com/article/10.1140/epjc/s10052-016-4422-0>

**70. Jawad, A., Ali, F., Jamil, M., & Debnath, U. (2016). Dynamics of Particles Around a Regular Black Hole with Nonlinear Electrodynamics. *Communications in Theoretical Physics*, 66(5), 509..**

**ABSTRACT:**

We investigate the dynamics of a charged particle being kicked off from its circular orbit around a regular black hole by an incoming massive particle in the presence of magnetic field. The resulting escape velocity, escape energy and the effective potential are analyzed. It is shown that the presence of even a very weak magnetic field helps the charged particles in escaping the gravitational field of the black hole. Moreover the effective force acting on the particle visibly reduces with distance. Thus particle near the black hole will experience higher effective force as compared to when it is far away.

**Web URL:** <http://iopscience.iop.org/article/10.1088/0253-6102/66/5/509/meta>

**71. Jawad, A., & Iqbal, A. (2016). Viscous Chaplygin gas models as spherical top-hat collapsing fluids. *International Journal of Modern Physics D*, 25(06), 1650074.**

**ABSTRACT:**

We study the spherical top-hat collapse in Einstein gravity and loop quantum cosmology (LQC) by taking the nonlinear evolution of viscous modified variable Chaplygin gas (CG) and viscous generalized cosmic chaplygin gas (GCCG). We calculate the equation of state (EoS) parameter, square speed of sound, perturbed (EoS) parameter, perturbed square speed of sound, density contrast and divergence of peculiar velocity in perturbed region and discussed their behavior. It is observed that both CG models support the spherical collapse (SC) in Einstein as well as LQC because density contrast remains positive in both cases and the perturbed EoS parameter remains positive at the present epoch as well as near future. It is remarked here that these parameters provide consistent results for both CG models in both gravities.

**Web URL:** <http://www.worldscientific.com/doi/abs/10.1142/S0218271816500747>

**72. Butt, S. I., & PRALJAK, M. (2016). REVERSED HARDY INEQUALITY FOR C-MONOTONE FUNCTIONS. *JOURNAL OF MATHEMATICAL INEQUALITIES*, 10(3), 603-622.**

**ABSTRACT:**

In this paper, we will give general Hardy and reversed Hardy type inequalities for a generalized class of monotone functions. Moreover we will give  $n$ -exponential convexity, exponential convexity and related results for some functionals obtained from the differences of these inequalities. At the end we will give mean value theorems and Cauchy means for these functionals.

**Web URL:** <http://files.ele-math.com/articles/jmi-10-49.pdf>

**73. AGARWAL, R. P., BUTT, S. I., PECARI C, J. & VUKELIC, A. (2016). GENERALIZATION OF POPOVICIU TYPE INEQUALITIES VIA GREEN'S FUNCTION AND FINK'S IDENTITY. *Mathematical Inequalities and Applications*. 19(4). 1247-1256.**

**ABSTRACT:**

We obtain some useful identities via Green's function and Fink's identity, and apply them to generalize the known Popoviciu's inequality for convex functions to higher order convex functions. Then we investigate the bounds for the identities related to the generalization of the Popoviciu inequality by using inequalities for the Chebyshev functional. Some results relating to the Grüss and Ostrowski type inequalities are also obtained. Finally, we construct new families of exponentially convex functions and Cauchy-type means by exploring at linear functionals associated with the obtained inequalities.

**Web URL:** <http://mia.ele-math.com/volume/19/issue/4>

**74. Butt, S. I., & KVESI, L. (2016). GENERALIZATION OF MAJORIZATION THEOREM VIA TAYLOR'S FORMULA. *Mathematical Inequalities & Applications*, 1257.**

**ABSTRACT:**

We give generalization of majorization theorem for the class of  $n$ -convex functions by using Taylor's formula. We use inequalities for the Chebyshev functional to obtain bounds for the identities related to generalizations of majorization inequalities. We present mean value theorems and  $n$ -exponential convexity for the functional obtained from the generalized majorization inequalities. At the end we discuss the results for particular families of function and give means.

**Web URL:** <http://narod.hr/wp-content/uploads/2016/11/mia19-4.pdf#page=121>

**75. Butt, S. I., Khan, K. A., & Pecaric, J. (2016). POPOVICIU TYPE INEQUALITIES VIA HERMITE'S POLYNOMIAL. *M athematical I nequalities & Applications*, 1309.**

**ABSTRACT:**

We obtain useful identities via Hermite interpolation polynomial, by which the inequality of Popoviciu for convex functions is generalized for higher order convex functions. We investigate the bounds for the identities extracted by the generalization of the Popoviciu inequality using inequalities for the Chebyshev functional. Some results relating to the Grüss and Ostrowski type inequalities are constructed.

**Web URL:** <http://narod.hr/wp-content/uploads/2016/11/mia19-4.pdf#page=173>

**76. Khan, M. A. A. (2016). Construction of a common element for the set of solutions of fixed point problems and generalized equilibrium problems in Hilbert spaces. *Annales Universitatis Paedagogicae Cracoviensis. Studia Mathematica*, 15(1), 79-96.**

**ABSTRACT:**

In this paper, we propose and analyse an iterative algorithm for the approximation of a common solution for a finite family of  $k$ -strict pseudocontractions and two finite families of generalized equilibrium problems in the setting of Hilbert spaces. Strong convergence results of the proposed iterative algorithm together with some applications to solve the variational inequality problems are established in such setting. Our results generalize and improve various existing results in the current literature.

**WebURL:** <https://www.degruyter.com/view/j/aupcsm.2016.15.issue-1/aupcsm-2016-0007/aupcsm-2016-0007.xml>

**77. Younis, M., Cheemaa, N., Mahmood, S. A., & Rizvi, S. T. (2016). On optical solitons: the chiral nonlinear Schrödinger equation with perturbation and Bohm potential. *Optical and Quantum Electronics*, 48(12), 542.**

**ABSTRACT:**

The chiral nonlinear Schrödinger equation, with perturbation term and a coefficient of Bohm potential, has been studied analytically. The perturbation term produces quantum behaviour,

such that quantum features are closely related to its special properties and gives the introduction of hidden variable theory in Quantum Mechanics. The equation admits a rich variety of families of exact solutions for a range of five parameters. The solutions are of qualitatively different nature, depending on the parameters. During the analytical treatment the wave solutions namely: soliton like solutions, triangular type solutions, single and combined non degenerate jacobi elliptic function like solutions are derived along with their constraint conditions. Additionally, a couple of other solutions known as singular periodic solutions, fall out as a by-product.

**Web URL:** <https://link.springer.com/article/10.1007/s11082-016-0809-2>

**78. Abid, M. (2016). STAMINA OF A GASKETED BOLTED FLANGED PIPE JOINT UNDER DYNAMIC LOADING. *IIUM Engineering Journal*, 17(2), 137-155.**

**ABSTRACT:**

Gasketed bolted flange joints are the most critical components in pipelines for their sealing and strength under operating conditions. Most of the work available in literature is under static loading, whereas in industry, cyclic loads are applied due to the vibrating machinery such as motors, pumps, sloshing in offshore applications and in the ships etc. In this study a three dimensional finite element analysis of a gasketed joint is carried out using a spiral wound gasket under bolt up and dynamic operating conditions (internal pressure, axial and bending) singly and in combination. The cyclic axial loads are concluded relatively more challenging for both the sealing and strength of the joint. Higher magnitudes of loads and frequencies are also observed more challenging to the joints performance.

**Web URL:** <file:///C:/Users/abc/Downloads/565-3210-1-PB.pdf>

**79. Rafiullah, M., D. K. R Babajee and Dur-e-Jabeen (2016).NINTH ORDER METHOD FOR NONLINEAR EQUATIONS AND ITS DYNAMIC BEHAVIOUR.*Acta Universitatis Apulensis*, 45, 73-86**

**ABSTRACT:**

The aim of this paper is to construct a new efficient iterative method to solve nonlinear equations and discuss the dynamic behaviour of it. This method is based on "A<sub>n</sub>-th-order

iterative method for solving nonlinear equations, *Numerical Analysis and Applications*, 4 (3) (2011), pp. 239{243". The finite difference and Hermite interpolation are used to improve the convergence order and efficiency index of this method. The new method is of the ninth order of convergence and it is compared with other ninth order methods. Some numerical test problems are given to show the accuracy and fast convergence of the method proposed. The dynamic behavior of the methods for finding the roots of unity are also studied.

**Web URL:**

[https://www.researchgate.net/publication/299657382\\_Ninth\\_Order\\_Method\\_for\\_Nonlinear\\_Equations\\_and\\_its\\_Dynamic\\_Behaviour](https://www.researchgate.net/publication/299657382_Ninth_Order_Method_for_Nonlinear_Equations_and_its_Dynamic_Behaviour)

**80. Riasat, A., Kanwal, S., & Javed, S. (2016). On odd-graceful labeling of disjoint union of graphs. *UTILITAS MATHEMATICA*, 101, 189-214.**

**ABSTRACT:**

Let  $G = (V, E)$  be a finite, simple and undirected graph having  $v = |V(G)|$  and  $e = |E(G)|$ . A graph  $G$  with  $q$  edges is said to be odd-graceful if there is an injection  $f$  : Motivated by the work of Z. Gao [6], we have defined odd graceful labeling for some other union of graphs. In this paper we formulate odd-graceful labeling for disjoint unions of graphs consisting of generalized combs, ladder, star, bistar, caterpillar and path.

**Web URL:** [https://www.researchgate.net/publication/314950487\\_On\\_odd-graceful\\_labeling\\_of\\_disjoint\\_union\\_of\\_graphs\\_1](https://www.researchgate.net/publication/314950487_On_odd-graceful_labeling_of_disjoint_union_of_graphs_1)

**81. Jawad, A., & Rani, S. (2016). Non-minimal coupling of torsion–matter satisfying null energy condition for wormhole solutions. *The European Physical Journal C*, 76(12), 704.**

**ABSTRACT:**

We explore wormhole solutions in a non-minimal torsion–matter coupled gravity by taking an explicit non-minimal coupling between the matter Lagrangian density and an arbitrary function of the torsion scalar. This coupling describes the transfer of energy and momentum between matter and torsion scalar terms. The violation of the null energy condition occurred through an effective energy-momentum tensor incorporating the torsion–matter non-minimal coupling, while normal matter is responsible for supporting the respective wormhole

geometries. We consider the energy density in the form of non-monotonically decreasing function along with two types of models. The first model is analogous to the curvature–matter coupling scenario, that is, the torsion scalar with  $T$ -matter coupling, while the second one involves a quadratic torsion term. In both cases, we obtain wormhole solutions satisfying the null energy condition. Also, we find that the increasing value of the coupling constant minimizes or vanishes on the violation of the null energy condition through matter.

**Web URL:** <https://link.springer.com/article/10.1140/epjc/s10052-016-4560-4#authorsandaffiliations>

**82. Ahmad, A., Baca, M., & Nadeem, M. F. (2016). ON EDGE IRREGULARITY STRENGTH OF TOEPLITZ GRAPHS. UNIVERSITY POLITEHNICA OF BUCHAREST SCIENTIFIC BULLETIN-SERIES A-APPLIED MATHEMATICS AND PHYSICS, 78(4), 155-162.**

**ABSTRACT:**

An edge irregular  $k$ -labeling of a graph  $G$  is a labeling of the vertices of  $G$  with labels from the set  $\{1, 2, \dots, k\}$  in such a way that for any two different edges  $xy$  and  $x_0y_0$  their weights  $w(xy)$  and  $w(x_0y_0)$  are distinct. The weight  $w(xy)$  of an edge  $xy$  in  $G$  is the sum of the labels of the end vertices  $x$  and  $y$ . The minimum  $k$  for which the graph  $G$  has an edge irregular  $k$ -labeling is called the edge irregularity strength of  $G$ , denoted by  $es(G)$ . In this paper, we study the edge irregular  $k$ -labeling for Toeplitz graphs and determine the exact value for several classes of Toeplitz graphs.

**Web URL:** [https://www.scientificbulletin.upb.ro/rev\\_docs\\_arhiva/full15e\\_507690.pdf](https://www.scientificbulletin.upb.ro/rev_docs_arhiva/full15e_507690.pdf)

**83. Zubair, M., Kousar, F., & Bahamonde, S. (2016). Thermodynamics in  $f(R, R_{\alpha\beta}R^{\alpha\beta}, \varphi)$  theory of gravity. Physics of the Dark Universe, 14, 116-125.**

**ABSTRACT:**

First and second laws of black hole thermodynamics are examined at the apparent horizon of FRW spacetime in  $f(R, R_{\alpha\beta}R^{\alpha\beta}, \varphi)$  gravity, where  $R$ ,  $R_{\alpha\beta}R^{\alpha\beta}$  and  $\varphi$  are the Ricci invariant, Ricci tensor and the scalar field respectively. In this modified theory, Friedmann equations are formulated for any spatial curvature. These equations can be presented into the form of first law of thermodynamics for  $ThdS^h + ThdiS^h + WdV = dE$ , where  $diS^h$  is an extra entropy term

because of the non-equilibrium presentation of the equations and  $\text{ThdS}^h + \text{WdV} = dE$  for the equilibrium presentation. The generalized second law of thermodynamics (GSLT) is expressed in an inclusive form where these results can be represented in GR,  $f(R)$  and  $f(R, \varphi)$  gravities. Finally to check the validity of GSLT, we take some particular models and produce constraints of the parameters.

**Web URL:** <http://www.sciencedirect.com/science/article/pii/S2212686416300541>

**84. Nadeem, I., & Shaker, H. (2016). On topological indices of tri-hexagonal boron nanotubes. *JOURNAL OF OPTOELECTRONICS AND ADVANCED MATERIALS*, 18(9-10), 893-898.**

**ABSTRACT:**

Several chemical indices have been introduced in theoretical chemistry to measure the properties of molecular structures, such as atom bond connectivity (ABC) index and geometric-arithmetic (GA) index. Boron nanotubes are attractive because of their novel electronic properties due to the presence of multicenter bonds. Their thermal stability and mechanical properties are important issues in nanodevice applications and thus require intensive study. Y. Liu et al. [30] predicted a new class of boron nanotubes, called the Tri-Hexagonal boron nanotubes, which are constructed from triangles and hexagons. In this paper, we present the ABC index, the fourth version of ABC index, GA index and the fifth version of GA index for the Tri-Hexagonal boron nanotubes.

**Web URL:**

[https://www.researchgate.net/profile/Imran\\_Nadeem4/publication/316878812\\_On\\_topological\\_indices\\_of\\_tri-hexagonal\\_boron\\_nanotubes/links/59158a11a6fdcc963e832f58/On-topological-indices-of-tri-hexagonal-boron-nanotubes.pdf](https://www.researchgate.net/profile/Imran_Nadeem4/publication/316878812_On_topological_indices_of_tri-hexagonal_boron_nanotubes/links/59158a11a6fdcc963e832f58/On-topological-indices-of-tri-hexagonal-boron-nanotubes.pdf)

**85. Nazar, K., Murid, A. H. M., & Sangawi, A. W. K. (2015). Integral Equation for the Ahlfors map on Multiply Connected Region. *Journal Teknologi*, 73(1), 1-9.**

**ABSTRACT:**

This paper presents a new boundary integral equation with the adjoint Neumann kernel associated with where is the boundary correspondence function of Ahlfors map of a bounded multiply connected region onto a unit disk. The proposed boundary integral equation is

constructed from a boundary relationship satisfied by the Ahlfors map of a multiply connected region. The integral equation is solved numerically for using combination of Nystrom method, GMRES method, and fast multiple method. From the computed values of we solve for the boundary correspondence function which then gives the Ahlfors map. The numerical examples presented here prove the effectiveness of the proposed method.

**Web URL:**

[https://www.researchgate.net/profile/Kashif\\_Nazar/publication/275222398\\_Integral\\_Equation\\_for\\_the\\_Ahlfors\\_Map\\_on\\_Multiply\\_Connected\\_Regions/links/5669073b08ae8d6928fbcdae.pdf](https://www.researchgate.net/profile/Kashif_Nazar/publication/275222398_Integral_Equation_for_the_Ahlfors_Map_on_Multiply_Connected_Regions/links/5669073b08ae8d6928fbcdae.pdf)

**86. Khan, A. A., Sohail, A., Rashid, S., Rashidi, M. M., & Khan, N. A. (2016). Effects of Slip Condition, Variable Viscosity and Inclined Magnetic Field on the Peristaltic Motion of a Non-Newtonian Fluid in an Inclined Asymmetric Channel. *Journal of Applied Fluid Mechanics*, 9(3), 1381-1393.**

**ABSTRACT:**

The peristaltic motion of a third order fluid due to asymmetric waves propagating on the sidewalls of a inclined asymmetric channel is discussed. The key features of the problem includes long-wavelength and low-Reynolds number assumptions. A mathematical analysis has been carried out to investigate the effect of slip condition, variable viscosity and magnetohydrodynamics (MHD). Followed by the nondimensionalization of the nonlinear governing equations along with the nonlinear boundary conditions, a perturbation analysis is made. For the validity of the approximate solution, a numerical solution is obtained using the iterative collocation technique.

**Web URL:**

[https://www.researchgate.net/publication/274195697\\_Effects\\_of\\_slip\\_condition\\_variable\\_viscosity\\_and\\_inclined\\_magnetic\\_field\\_on\\_the\\_peristaltic\\_motion\\_of\\_a\\_non-Newtonian\\_fluid\\_in\\_an\\_inclined\\_asymmetric\\_channel](https://www.researchgate.net/publication/274195697_Effects_of_slip_condition_variable_viscosity_and_inclined_magnetic_field_on_the_peristaltic_motion_of_a_non-Newtonian_fluid_in_an_inclined_asymmetric_channel)

**87. Maqbool, K., Sohail, A., Manzoor, N., & Ellahi, R. (2016). Hall effect on Falkner—Skan boundary layer flow of FENE-P fluid over a stretching sheet. *Communications in Theoretical Physics*, 66(5), 547.**

**ABSTRACT:**

The Falkner—Skan boundary layer steady flow over a flat stretching sheet is investigated in this paper. The mathematical model consists of continuity and the momentum equations, while a new model is proposed for MHD Finitely Extensible Nonlinear Elastic Peterlin (FENE-P) fluid. The effects of Hall current with the variation of intensity of non-zero pressure gradient are taken into account. The governing partial differential equations are first transformed to ordinary differential equations using appropriate similarity transformation and then solved by Adomian decomposition method (ADM). The obtained results are validated by generalized collocation method (GCM) and found to be in good agreement. Effects of pertinent parameters are discussed through graphs and tables. Comparison with the existing studies is made as a limiting case of the considered problem at the end.

**Web URL:** <http://iopscience.iop.org/article/10.1088/0253-6102/66/5/547/meta>

**88. Wajid, H. A., & Sohail, A. (2016). Compact Modified Implicit Finite Element Schemes for Wave Propagation Problems with Superior Dispersive Properties. *Arabian Journal for Science and Engineering*, 41(11), 4613-4624.**

**ABSTRACT:**

In this paper, we study in detail dispersive properties of the widely used implicit scheme called Newmark trapezoidal rule in conjunction with modified mass matrix to enjoy superior dispersive properties keeping the finite element stencil compact. We call such schemes *compact modified implicit finite element scheme*. In case of one-dimensional propagation, following contributions are made: (a) for modified finite element (MFE) scheme, we find an optimal value of dispersion controlling parameter depending on Courant–Friedrichs–Lewy (CFL) number which provides exact solutions at the nodes of spatial grid; (b) for standard finite element (SFE) scheme optimal value of CFL number is obtained which provides fourth-order accurate solutions. Moreover, in case of two-dimensional propagation

following contributions are made: (c) we have found optimal value of CFL number for all angles in case of both SFE and MFE schemes; (d) superior dispersive behaviour is evident in case of MFE scheme in comparison with SFE scheme. Furthermore, the MFE scheme can be efficiently implemented using non-standard quadrature rules or just updating mass matrix which does not require to write brand new code and makes it computationally very attractive. Also for specific value of parameter, i.e.  $\tau = 0$ , the MFE scheme leads back to the SFE scheme.

**Web URL:** <https://link.springer.com/article/10.1007/s13369-016-2220-5>

**89. Yan, L., Li, Y., Hayat, S., Siddiqui, H. M. A., Imran, M., Ahmad, S., & Farahani, M. R. (2016). On Degree-Based and Frustration Related Topological Indices of Single-Walled Titania Nanotubes. *Journal of Computational and Theoretical Nanoscience*, 13(11), 9027-9032.**

**ABSTRACT:**

In theoretical and computational chemistry, a molecular descriptor is a numerical representation of a chemical structure while a topological descriptor correlates certain physico-chemical characteristics of underlying chemical compounds besides its numerical representation. Valency based topological descriptors like atom-bond connectivity index and geometric-arithmetic index play an important role in the stability analysis of linear alkanes. The prediction power of frustration indices for stability of various chemical and nanostructures like fullerenes is better than some valency based topological descriptors. In this paper, certain valency based and frustration related topological descriptors for titania nanotubes are studied.

**Web URL:**

<http://www.ingentaconnect.com/contentone/asp/jctn/2016/00000013/00000011/art00171>

**90. Ahmad, U., Ahmad, S., & Yousaf, R. (2016). Computation of Zagreb and atom–bond connectivity indices of certain families of dendrimers by using automorphism group action. *J. Serb. Chem. Soc.*, 82(2), 151-162.**

**ABSTRACT:**

In QSAR/QSPR studies, topological indices are utilized to predict the bioactivity of chemical compounds. In this paper, the closed forms of different Zagreb indices and atom–bond connectivity indices of regular dendrimers  $G[n]$  and  $H[n]$  in terms of a given parameter  $n$  are determined by using the auto-morphism group action. It was reported that these connectivity indices are correlated with some physicochemical properties and are used to measure the level of branching of the molecular carbon-atom skeleton.

**Web URL:** <http://shd-pub.org.rs/index.php/JSCS/article/download/3398/416>

# DEPARTMENT OF ELECTRICAL ENGINEERING

## Journal Papers

1. Khan, A. A., & Brown, A. K. (2016). Sector nulling in planar irregular sub-arrayed sparse array antennas. *IET Microwaves, Antennas & Propagation*, 10(1), 25-30.

**ABSTRACT:**

This study concerns wide angular sector (higher order) null synthesis in planar irregular sparse antenna arrays when aperture distributed sub-arrays are used to reduce the computational load. A hybrid optimisation tool has been used to find array element excitations to achieve as low as possible sector nulls for the desired sector width. Performance comparisons have been made for three sub-array configurations based on the obtained numerical results. Various interference jamming scenarios have been considered including single and dual sectors for single-dimensional ( $\vartheta$ ) (1D) and two-dimensional ( $\vartheta, \phi$ ) (2D) nulls. The proposed optimisation scheme has shown to be successful for the synthesis of 1D and 2D sector nulls with depths as low as  $-100$  dB for the given configuration with reduced computational time when compared with the full array. The comparison of achieved null depths for different sub-array sizes and convergence time has also been presented and discussed.

**Web URL:** <http://digital-library.theiet.org/content/journals/10.1049/iet-map.2014.0712>

2. Ijaz, S., Hamayun, M. T., Yan, L., & Mumtaz, M. F. (2016). Fractional Order Modeling and Control of Twin Rotor Aero Dynamical System using Nelder Mead Optimization. *Journal of Electrical Engineering & Technology*, 11(6), 1863-1871.

**ABSTRACT:**

This paper presents an application of fractional order controller for the control of multi input multi output twin rotor aerodynamic system. Dynamics of the considered system are highly nonlinear and there exists a significant cross-coupling between the horizontal and vertical axes (pitch & yaw). In this paper, a fractional order model of twin rotor aerodynamic system is identified using input output data from nonlinear system. Based upon identified FO model, a fractional order PID controller is designed to control the angular position of level bar of twin

rotor aerodynamic system. The parameters of controller are tuned using Nelder-Mead optimization and compared with particle swarm optimization techniques. Simulation results on the nonlinear model show a significant improvement in the performance of fractional order PID controller as compared to a classical PID controller.

**Web URL:**

<http://www.jeet.or.kr/LTKPSWeb/uploadfiles/be/201605/270520161625030941250.pdf>

**3. Masood, M. H., Ahmad, M., Kathia, M. A., Zafar, R. Z., & Zahid, A. N. (2016). BRAIN COMPUTER INTERFACE BASED SMART HOME CONTROL USING EEG SIGNAL. *Science International*, 28(3), 2219-2219.**

**ABSTRACT:**

The paper presents the Brain-Computer Interface (BCI) based home control system. The proposed system is used to facilitate the handicapped and needy persons. Neurosky headset is used to detect Electroencephalogram (EEG) signal from brain activity. Recognizing the brain activity for certain thoughts and eye blinking patterns, we managed to correlate them with the switching and regulation of certain home appliances like fan, bulb, etc. BCI based systems can yield the accuracy from (80 to 100) %.

**Web URL:**

<https://pdfs.semanticscholar.org/f1f5/c52d15359c05ea73632c1495e06ea1e9291a.pdf>

**4. Masood, B., Haider, A., & Baig, S. (2017). Modeling and Characterization of Low Voltage Access Network for Narrowband Powerline Communications. *Journal of Electrical Engineering & Technology*, 12(1), 443-450.**

**ABSTRACT:**

Nowadays, Power Line Communication (PLC) is gaining high attention from industry and electric supply companies for the services like demand response, demand side management and Advanced Metering Infrastructure (AMI). The reliable services to consumers using PLC can be provided by utilizing an efficient PLC channel for which sophisticated channel modeling is very important. This paper presents characterization of a Low Voltage (LV) access network for

Narrowband Power Line Communications (NB-PLC) using transmission line (TL) theory and a Simulink model. The TL theory analysis not only includes the constant parameters but frequency selectivity is also introduced in these parameters such as resistance, conductance and impedances. However, the proposed Simulink channel model offers an analysis and characterization of capacitive coupler, network impedance and channel transfer function for NB-PLC. Analysis of analytical and simulated results shows a close agreement of the channel transfer function. In the absence of a standardized NBPLC channel model, this research work can prove significant in improving the efficiency and accuracy of NB-PLC communication transceivers for Smart Grid communications.

**Web URL:**

<http://www.jeet.or.kr/LTKPSWeb/uploadfiles/be/201605/130520161459574535000.pdf>

**5. Asif, M. R., Chun, Q., Hussain, S., & Fareed, M. S. (2016). Multiple licence plate detection for Chinese vehicles in dense traffic scenarios. *IET Intelligent Transport Systems*, 10(8), 535-544.**

**ABSTRACT:**

In this paper, we propose a real time multiple license plate detection algorithm for dense traffic conditions which is of vital importance in this modern era due to increased traffic congestion. The chromatic component of YDbDr color space is proposed to detect the blue regions whereas a simple yet effective color detection method is used to identify yellow License Plate (LP) regions. The low intensity pixel values are eliminated as a pre-processing step to enhance the LP regions and Otsu method is used to obtain the binary image. The candidate regions are acquired by using the connected component analysis. The false candidate regions are by large rejected by inspecting the area and aspect ratio of LPs. Additionally, a two-layered false LP detection approach has been introduced to remove fake LP regions. Experimental results in practical scenarios carried out in various weather conditions show that the proposed method is highly effective in coping with various illumination conditions to accurately detect the multiple vehicle LPs with an accuracy of 93.86%. The average processing time per image is 0.33s that can achieve real time performance.

**Web URL:**

[https://www.researchgate.net/profile/M\\_Fareed/publication/303432672\\_Multiple\\_License\\_Plate\\_Detection\\_for\\_Chinese\\_Vehicles\\_in\\_Dense\\_Traffic\\_Scenarios/links/5742d71608ae298602e615e.pdf](https://www.researchgate.net/profile/M_Fareed/publication/303432672_Multiple_License_Plate_Detection_for_Chinese_Vehicles_in_Dense_Traffic_Scenarios/links/5742d71608ae298602e615e.pdf)

**6. Hussain, S., Chun, Q., Asif, M. R., & Khan, M. S. (2016). Active contours for image segmentation using complex domain-based approach. *IET Image Processing*, 10(2), 121-129.**

**ABSTRACT:**

A complex domain-based approach of active contour model has been proposed for image segmentation which deforms iteratively to partition an image into various useful regions. A new region-based complex pressure force function has been designed which gives shape to the dynamic active contour using image forces, and efficiently control the propagation of moving interface. This model makes the level set function binary, uses Gaussian smoothing kernel to regulate and avoid re-initialisation procedure. The working scheme of the model is as: the real image data is converted into complex data by  $i$  times and the average  $i$  times of horizontal and vertical components of gradient is inserted in the model to develop complete complex gradient. The proposed model can be implemented by simple finite difference scheme. The efficiency and robustness of the authors model have been verified.

**Web URL:** <http://digital-library.theiet.org/content/journals/10.1049/iet-ipr.2014.0730>

**7. Aslam, M. H., Farooq, U., Awais, M. N., Bhatti, M. K., & Shehzad, N. (2016). Exploring the Effect of LUT Size on the Area and Power Consumption of a Novel Memristor-Transistor Hybrid FPGA Architecture. *Arabian Journal for Science and Engineering*, 41(8), 3035-3049.**

**ABSTRACT:**

Field-programmable gate arrays (FPGAs) have come a long way from being used as glue logic to complete system solution. This is mainly because of their generalized reconfigurable nature, low non-recurring engineering (NRE) cost, and rapid time to market. However, their advantages come at the cost of larger area and higher power consumption eventually making them unsuitable for area and power critical applications. In this work, we propose a novel

memristor-transistor hybrid FPGA architecture. Memristor-transistor-based building blocks of FPGA architecture are designed and simulated using HSPICE in this work. Results show that hybrid blocks on average take 30.3 % less area and consume 64.3 % less power compared to transistor-only blocks. Hybrid blocks are combined together to construct logic blocks [i.e., look-up tables (LUTs) and configurable logic blocks] and routing switches of hybrid FPGA architecture. Furthermore, a generalized exploration environment is developed to explore the effect of LUT size on the area and power consumption of memristor-transistor hybrid FPGA architecture. For experimental purpose, sixteen largest MCNC benchmarks are used and LUT size is varied from three to seven. Experimental results show that LUT-4 gives the best area and power results for memristor-transistor hybrid FPGA architecture.

**Web URL:** <https://link.springer.com/article/10.1007/s13369-016-2068-8>

**8. Aslam, M. H. & Farooq, U., (2016) A Novel FPGA Architecture using Memristor-Transistor Hybrid Approach. Journal of Electronic Systems, 5(3).**

**ABSTRACT:**

This work focuses on the design of a novel FPGA architecture based on memristor-transistor hybrid approach. A lot of research has been carried out in the field of FPGA that has focused on decreasing the size and power consumption of FPGAs. However, still FPGAs are larger in area, slower in speed and more power consuming. In this work, basic building blocks like MUX, NOR gate, D flip flop, NOT gate and buffer are designed and implemented using memristor-transistor hybrid approach. These basic building blocks are combined to form Configurable Logic Blocks (CLBs), Switch Boxes (SBs) and Connection Boxes (CBs) of FPGA. Proposed hybrid basic building blocks of FPGA are smaller in size and lower in power consumption as compared to the conventional transistor-only building blocks. For experimental purpose, first we compare the area and power of conventional and proposed basic building blocks and achieve the average area and power efficiency of 30% and 60% respectively. Similarly, the area gain of a 2 input single tile based on proposed basic building block is 39%. Then, we also explore the overall area of memristortransistor hybrid FPGA architecture for sixteen largest MCNC benchmarks and present the results.

**Web URL:** [http://www.dline.info/jes/fulltext/v5n3/v5n3\\_3.pdf](http://www.dline.info/jes/fulltext/v5n3/v5n3_3.pdf)

**9. Khan, A. A., Razaq, A., Ali, J., Arshad, F., Mumtaz, M., & Khan, S. (2016). Antenna miniaturization using pulp fibres as a substrate for dual band operation. *Microwave and Optical Technology Letters*, 58(9), 2146-2148.**

**ABSTRACT:**

Reduced size dual band patch antenna is designed on pulp fibers-based substrate, obtained from a self-growing plant, *Typha angustifolia*. The proposed design is low cost and has <10 dB return loss at 2.4 and 5.7 GHz, with 6.9 dBi antenna gain and also has potential for conformal designs

**Web URL:** <http://onlinelibrary.wiley.com/doi/10.1002/mop.30002/full>

**10. Khosa, I., & Pasero, E. (2016). A Machine Vision System for Quality Inspection of Pine Nuts. *INTERNATIONAL JOURNAL OF ADVANCED COMPUTER SCIENCE AND APPLICATIONS*, 7(9), 253-267.**

**ABSTRACT:**

Computers and artificial intelligence have penetrated in the food industry since last decade, for intellectual automatic processing and packaging in general, and in assisting for quality inspection of the food itself in particular. The food quality assessment task becomes more challenging when it is about harmless internal examination of the ingredient, and even more when its size is also minute. In this article, a method for automatic detection, extraction and classification of raw food item is presented using x-ray image data of pine nuts. Image processing techniques are employed in developing an efficient method for automatic detection and then extraction of individual ingredient, from the source x-ray image which comprises bunch of nuts in a single frame. For data representation, statistical texture analysis is carried out and attributes are calculated from each of the sample image on the global level as features. In addition co-occurrence matrices are computed from images with four different offsets, and hence more features are extracted by using them. To find fewer meaningful characteristics, all the calculated features are organized in several combinations and then tested. Seventy percent of image data is used for training and 15% each for cross-validation and test purposes. Binary

classification is performed using two state-of-the-art non-linear classifiers: Artificial Neural Network (ANN) and Support Vector Machines (SVM). Performance is evaluated in terms of classification accuracy, specificity and sensitivity. ANN classifier showed 87.6% accuracy with correct recognition rate of healthy nuts and unhealthy nuts as 94% and 62% respectively. SVM classifier produced the similar accuracy achieving 86.3% specificity and 89.2% sensitivity rate. The results obtained are unique itself in terms of ingredient and promising relatively. It is also found that feature set size can be reduced up to 57% by compromising 3.5% accuracy, in combination with any of the tested classifiers.

**Web URL:** <http://thesai.org/Publications/ViewIssue?volume=7&issue=9&code=IJACSA>

**11. Saeed, A., Ahmadiania, A., & Just, M. (2016). Secure On-Chip Communication Architecture for Reconfigurable Multi-Core Systems. *Journal of Circuits, Systems and Computers*, 25(08), 1650089.**

**ABSTRACT:**

Security is becoming the primary concern in today's embedded systems. Network-on-chip (NoC)-based communication architectures have emerged as an alternative to shared bus mechanism in multi-core system-on-chip (SoC) devices and the increasing number and functionality of processing cores have made such systems vulnerable to security attacks. In this paper, a secure communication architecture has been presented by designing an identity and address verification (IAV) security module, which is embedded in each router at the communication level. IAV module verifies the identity and address range to be accessed by incoming and outgoing data packets in an NoC-based multi-core shared memory architecture. Our IAV module is implemented on an FPGA device for functional verification and evaluated in terms of its area and power consumption overhead. For FPGA-based systems, the IAV module can be reconfigured at run-time through partial reconfiguration. In addition, a cycle-accurate simulation is carried out to analyze the performance and total network energy consumption overhead for different network configurations. The proposed IAV module has presented reduced area and power consumption overhead when compared with similar existing solutions.

**Web URL:**

<http://www.worldscientific.com/doi/abs/10.1142/S0218126616500894?journalCode=jcsc>

**12. Farooq-I-Azam, M., Ni, Q., & Ansari, E. A. (2016). Intelligent energy efficient localization using variable range beacons in industrial wireless sensor networks. *IEEE Transactions on Industrial Informatics*, 12(6), 2206-2216.**

**ABSTRACT:**

In many applications of industrial wireless sensor networks, sensor nodes need to determine their own geographic position coordinates so that the collected data can be ascribed to the location from where it was gathered. We propose a novel intelligent localization algorithm which uses variable range beacon signals generated by varying the transmission power of beacon nodes. The algorithm does not use any additional hardware resources for ranging and estimates position using only radio connectivity by passively listening to the beacon signals. The algorithm is distributed, so each sensor node determines its own position and communication overhead is avoided. As the beacon nodes do not always transmit at maximum power and no transmission power is used by unknown sensor nodes for localization, the proposed algorithm is energy efficient. It also provides control over localization granularity. Simulation results show that the algorithm provides good accuracy under varying radio conditions.

**Web URL:** <http://eprints.lancs.ac.uk/81858/1/RippleLocalizationAlgorithm.pdf>

**13. Kamal, A., Rafiq, M. A., Rafiq, M. N., Usman, M., Waqar, M., & Anwar, M. S. (2016). Structural and impedance spectroscopic studies of CuO-doped (K<sub>0.5</sub>Na<sub>0.5</sub>Nb<sub>0.995</sub>Mn<sub>0.005</sub>O<sub>3</sub>)<sub>1-x</sub>CuO lead-free piezoelectric ceramics. *Applied Physics A*, 122(12), 1037.**

**ABSTRACT:**

Polycrystalline lead-free  $(1 - x)(K_{0.5}Na_{0.5})(Nb_{0.995}Mn_{0.005}O_3)_{1-x}CuO$  ceramics where  $0 \leq x \leq 2\%$  were synthesized using the conventional solid-state reaction method. X-ray diffraction analysis confirmed the presence of single-phase possessing monoclinic symmetry for all the synthesized compositions. Scanning electron microscopy revealed a dense microstructure along with increase in grains size with Cu doping in the KNNMn ceramics. Impedance spectroscopy (IS) showed that Cu doping was found to be helpful in increasing the grain boundary resistance. A temperature-dependent and non-Debye-type relaxation process was

also revealed by IS studies. The relaxation time for both bulk and grain boundary decreased with temperature indicating a hopping conduction mechanism. The activation energy was found to be 0.4–0.5 eV, indicating conduction of oxygen vacancies through hopping mechanism. Insights gained from this work could be useful in designing the optimum composition and microstructure of KNN-based ceramics for practical applications.

**Web URL:** <https://link.springer.com/article/10.1007/s00339-016-0564-z>

**14. Bhatti, M. K., Oz, I., Popov, K., Brorsson, M., & Farooq, U. (2016). Scheduling of Parallel Tasks with Proportionate Priorities. *Arabian Journal for Science and Engineering*, 41(8), 3279-3295.**

**ABSTRACT:**

Parallel computing systems promise higher performance for computationally intensive applications. Since programmes for parallel systems consist of tasks that can be executed simultaneously, task scheduling becomes crucial for the performance of these applications. Given dependence constraints between tasks, their arbitrary sizes, and bounded resources available for execution, optimal task scheduling is considered as an NP-hard problem. Therefore, proposed scheduling algorithms are based on *heuristics*. This paper presents a novel list scheduling heuristic, called the *Noodle* heuristic. Noodle is a simple yet effective scheduling heuristic that differs from the existing list scheduling techniques in the way it assigns task priorities. The priority mechanism of Noodle maintains a *proportionate fairness* among all ready tasks belonging to all paths within a task graph. We conduct an extensive experimental evaluation of Noodle heuristic with task graphs taken from Standard Task Graph. Our experimental study includes results for task graphs comprising of 50, 100, and 300 tasks per graph and execution scenarios with 2-, 4-, 8-, and 16-core systems. We report results for average Schedule Length Ratio (SLR) obtained by producing variations in Communication to Computation cost Ratio. We also analyse results for different degree of parallelism and number of edges in the task graphs. Our results demonstrate that Noodle produces schedules that are within a maximum of 12 % (in worst-case) of the optimal schedule for 2-, 4-, and 8-core systems. We also compare Noodle with existing scheduling

heuristics and perform comparative analysis of its performance. Noodle outperforms existing heuristics for average SLR values.

**Web URL:** <https://link.springer.com/article/10.1007/s13369-016-2180-9>

**15. Ghou, I., & Xiang, Z. (2015). Reliable  $H_\infty$  control of 2-D continuous nonlinear systems with time varying delays. *Journal of the Franklin Institute*, 352(12), 5758-5778.**

**ABSTRACT:**

This paper investigates the reliable  $H_1$  stabilization problem for a class of two-dimensional (2-D) continuous nonlinear state-delayed systems represented by the Roesser state-space model, where the nonlinear function satisfies the sector bounded condition. By choosing an appropriate Lyapunov–Krasovskii functional, sufficient conditions for asymptotical stability with  $H_1$  performance of the given system are derived. Then, a reliable controller is proposed such that the resulting closed-loop system is asymptotically stable and has a prescribed  $H_1$  performance level  $\gamma$  in the presence of actuator failures. Finally, an example is given to illustrate the effectiveness of the proposed method.

**Web URL:**

[https://www.researchgate.net/profile/Imran\\_Ghou/publication/283122259\\_Reliable\\_H\\_control\\_of\\_2-D\\_continuous\\_nonlinear\\_systems\\_with\\_time\\_varying\\_delays/links/56346e3608aeb786b70179ed.pdf](https://www.researchgate.net/profile/Imran_Ghou/publication/283122259_Reliable_H_control_of_2-D_continuous_nonlinear_systems_with_time_varying_delays/links/56346e3608aeb786b70179ed.pdf)

**16. Ghou, I., & Xiang, Z. (2016).  $H_\infty$  control of a class of 2-D continuous switched delayed systems via state-dependent switching. *International Journal of Systems Science*, 47(2), 300-313.**

**ABSTRACT:**

This paper addresses the problem of state feedback  $H_\infty$  stabilisation of 2-D (two-dimensional) continuous switched state delayed systems represented by the Roesser model using the multiple Lyapunov functional approach. First, an asymptotical stability condition of 2-D continuous switched systems with state-dependent switching is derived. Second, a sufficient condition for  $H_\infty$  performance of the underlying system is established. Third, a state feedback

controller is proposed to ensure that the resulting closed-loop system has a prescribed  $H_\infty$  performance level under a state-dependent switching signal. All the results are developed in terms of linear matrix inequalities. Finally, three examples are provided to demonstrate the validity and effectiveness of the proposed method.

**Web URL:** <http://www.tandfonline.com/doi/abs/10.1080/00207721.2015.1068882>

**17. Ghaus, I., Huang, S., & Xiang, Z. (2016). State Feedback  $L_1$ -Gain Control of Positive 2-D Continuous Switched Delayed Systems Via State-Dependent Switching. *Circuits, Systems, and Signal Processing*, 35(7), 2432-2449.**

**ABSTRACT:**

This paper investigates the stability and  $L_1$ -gain control of two-dimensional (2-D) continuous positive switched delayed systems. Firstly, by constructing an appropriate co-positive Lyapunov–Krasovskii functional, a sufficient condition for asymptotical stability of the system under consideration is derived. Secondly,  $L_1$ -gain performance analysis of the underlying system is investigated. Thirdly, a design methodology for state feedback controller is proposed to ensure that the closed-loop system is asymptotically stable with  $L_1$ -gain performance. Finally, an example is provided to show the effectiveness of the proposed method.

**Web URL:** <https://link.springer.com/article/10.1007/s00034-015-0161-y>

**18. Ghaus, I., Xiang, Z., & Karimi, H. R. (2017).  $H_\infty$  control of 2-D continuous Markovian jump delayed systems with partially unknown transition probabilities. *Information Sciences*, 382, 274-291.**

**ABSTRACT:**

This study focuses on stochastic stability and  $H_\infty$  control of two-dimensional (2-D) continuous delayed Markovian jump systems (MJSs) with partial information on transition probability. At first, a sufficient condition for the stochastic stability of 2-D MJSs is proposed by choosing an appropriate Lyapunov–Krasovskii functional. Then, the results are developed by designing a state feedback controller that guarantees the stochastic stability of the resultant closed-loop

system with a prescribed  $H_\infty$ -performance level  $\gamma$ . Finally, the proposed results are validated with the help of examples.

**Web URL:** <http://www.sciencedirect.com/science/article/pii/S0020025516320369>

**19. Saeed, A., Ahmadiania, A., Javed, A., & Larijani, H. (2016). Intelligent intrusion detection in low-power IoTs. *ACM Transactions on Internet Technology (TOIT)*, 16(4), 27.**

**ABSTRACT:**

Security and privacy of data are one of the prime concerns in today's Internet of Things (IoT). Conventional security techniques like signature-based detection of malware and regular updates of a signature database are not feasible solutions as they cannot secure such systems effectively, having limited resources. Programming languages permitting immediate memory accesses through pointers often result in applications having memory-related errors, which may lead to unpredictable failures and security vulnerabilities. Furthermore, energy efficient IoT devices running on batteries cannot afford the implementation of cryptography algorithms as such techniques have significant impact on the system power consumption. Therefore, in order to operate IoT in a secure manner, the system must be able to detect and prevent any kind of intrusions before the network (i.e., sensor nodes and base station) is destabilised by the attackers. In this article, we have presented an intrusion detection and prevention mechanism by implementing an intelligent security architecture using random neural networks (RNNs). The application's source code is also instrumented at compile time in order to detect out-of-bound memory accesses. It is based on creating tags, to be coupled with each memory allocation and then placing additional tag checking instructions for each access made to the memory. To validate the feasibility of the proposed security solution, it is implemented for an existing IoT system and its functionality is practically demonstrated by successfully detecting the presence of any suspicious sensor node within the system operating range and anomalous activity in the base station with an accuracy of 97.23%. Overall, the proposed security solution has presented a minimal performance overhead.

**Web URL:** <http://dl.acm.org/citation.cfm?id=2990499>

**20. Khan, M. U. S., Abbas, A., Ali, M., Jawad, M., Khan, S. U., Li, K., & Zomaya, A. Y. (2016). On the Correlation of Sensor Location and Human Activity Recognition in Body Area Networks (BANs). *IEEE Systems Journal*.**

**ABSTRACT:**

Accurate recognition of patients' physical activities leads to correct diagnosis and treatments. However, currently deployed approaches are deficient in recognizing the activities requiring frequent interposture transitions, such as jogging, jumping, turning left, and going upstairs. The reason is that with the change in position and rotation, different activity signals are generated, which are difficult to distinguish from other activities and can therefore mislead the physicians. Therefore, we propose to employ a methodology that utilizes the energy expenditure for each activity and reduces the dimensions of the feature space to differentiate among the activities. In this regard, we employ a feature descriptor called local energy-based shape histogram to preserve the maximum information of local energy. Considering the high volumes of continuously generated data, our methodology integrates cloud computing services with the body area networks. We also investigate the effects of on-body sensors' location on the activity recognition accuracy and also identify the best sensor position for a certain activity with the maximum accuracy. We used the wearable action recognition database dataset to perform the experiments. Our analysis shows that for each activity to be recognized at a decent level, it is imperative to observe the activity recognition performance by simultaneously applying different combinations of sensors.

**Web URL:** <http://ieeexplore.ieee.org/abstract/document/7604065/?reload=true>

**21. Ali, S. M., Jawad, M., Khan, B., Mehmood, C. A., Zeb, N., Tanoli, A., ...& Khan, S. U. (2016). Wide area smart grid architectural model and control: A survey. *Renewable and Sustainable Energy Reviews*, 64, 311-328.**

**ABSTRACT:**

The catastrophic outages and time-variant load patterns have posed a complex problem for the energy management policy makers in the deregulated power market. The Wide Area Smart Grid Model (WASGM) is a plausible solution for the future Wide Area Systems (WASs) in terms

of the operation, monitoring, and control. This survey provides a comprehensive insight into the state-of-the-art research steered in the wide area control and stability. We present a technical overview of data metering and management classification in the WASs by covering topics, such as: (a) Smart Meters, (b) Smart Sensor Networks, (c) Phasor Measuring Units (PMUs), and (d) Phasor Data Concentrators (PDCs). We also survey the role of Supervisory Control and Data Acquisition (SCADA)/Energy Management System (EMS) in the WASs, to provide a taxonomy of the communication technologies for an efficient data flow in the Smart Grid (SG) network. Moreover, the wide area smart grid architectural model for the future electrical networks is also explored pertaining to the ongoing research in the vast sphere of the WASs. Furthermore, the technical aspects and distinguishing features of the non-linear control schemes utilized for the advanced Wide Area Controls (WACs) are also quantitatively analyzed.

**Web URL:** <http://www.sciencedirect.com/science/article/pii/S1364032116302209>

**22. Ali, S. M., Mehmood, C. A., Khan, B., Jawad, M., Farid, U., Jadoon, J. K., ...& Anwar, S. M. (2016). Stochastic and Statistical Analysis of Utility Revenues and Weather Data Analysis for Consumer Demand Estimation in Smart Grids. *PLoS one*, 11(6), e0156849.**

**ABSTRACT:**

In smart grid paradigm, the consumer demands are random and time-dependent, owing towards stochastic probabilities. The stochastically varying consumer demands have put the policy makers and supplying agencies in a demanding position for optimal generation management. The utility revenue functions are highly dependent on the consumer deterministic stochastic demand models. The sudden drifts in weather parameters effects the living standards of the consumers that in turn influence the power demands. Considering above, we analyzed stochastically and statistically the effect of random consumer demands on the fixed and variable revenues of the electrical utilities. Our work presented the Multi-Variate Gaussian Distribution Function (MVGDF) probabilistic model of the utility revenues with time-dependent consumer random demands. Moreover, the Gaussian probabilities outcome of the utility revenues is based on the varying consumer  $n$  demands data-pattern. Furthermore, Standard Monte Carlo (SMC) simulations are performed that validated the factor of accuracy in

the aforesaid probabilistic demand-revenue model. We critically analyzed the effect of weather data parameters on consumer demands using correlation and multi-linear regression schemes. The statistical analysis of consumer demands provided a relationship between dependent (demand) and independent variables (weather data) for utility load management, generation control, and network expansion.

**Web URL:** <http://journals.plos.org/plosone/article?id=10.1371/journal.pone.0156849>

**23. Ali, S. M., Jawad, M., Guo, F., Mehmood, A., Khan, B., Glower, J., & Khan, S. U. (2016). Exact feedback linearization-based permanent magnet synchronous generator control. *International Transactions on Electrical Energy Systems*, 26(9), 1917-1939.**

**ABSTRACT:**

This paper presents the technical aspects, theoretical analysis, and comparisons of two new permanent magnet synchronous generator (PMSG) grid-interfaced models named PMSG boost and PMSG rectifier-inverter. The exact feedback linearization (EFL) control scheme is used for the effective design and stability analysis of the aforementioned models. The complexity of the EFL control laws is discussed in the light of the nonlinear coordinate transformations and linearization (local and global) of the PMSG models. We also discussed the effectiveness of the EFL control over the output Direct Current (DC) link voltage of the PMSG during the electrical grid faults and the mechanical perturbations. Moreover, we compared the aforementioned models and concluded that the stability of the PMSG rectifier-inverter is higher compared with the PMSG boost during the variation of wind speed values from minimum to maximum. Furthermore, the robustness of the EFL control scheme for the PMSG rectifier-inverter is compared with the conventional proportional and integral controller and state-feedback controller. The EFL controller reports a faster output response, better accuracy, and quicker settling time of the output DC link voltage as compared with the proportional integral controller.

**Web URL:** <http://onlinelibrary.wiley.com/doi/10.1002/etep.2185/full>

**24. Zafar, M., Naeem Awais, M., Naeem Awais, M., Asif, Amin, G. (2017). Fabrication and characterization of piezoelectric nanogenerator based on Al/ZnO/Au structure. *Microelectronics International*, 34(1), 35-39.**

**ABSTRACT:**

**Purpose**

The purpose of this research work is to harvest energy using the piezoelectric properties of ZnO nanowires (NW). Fabrication and characterization of the piezoelectric nanogenerator (NG), based on Al/ZnO/Au structure without using hosting layer, were done to harvest energy. The proposed method has full potential to harvest the cost-effective energy.

**Design/methodology/approach**

ZnO NW were fabricated between the thin layers of Al- and Au-coated substrates for the development of piezoelectric NG. To grow ZnO NW, ZnO seed layer was prepared on the Al-coated substrate, and then ZnO NW were grown by aqueous chemical growth method. Finally, Au top electrode was used to conclude the Al/ZnO/Au NG structure. The Al and Au electrodes were used to establish the ohmic and Schottky contacts with ZnO NW, respectively.

**Findings**

Surface morphology of the fabricated device was done by using scanning electron microscopy, and electrical characterization of the sample was performed with digital oscilloscope, picoammeter and voltmeter. The energy harvesting experiment was performed to excite the presented device. The fabricated piezoelectric-sensitive device revealed the maximum open circuit voltage up to 5 V and maximum short circuit current up to 30 nA, with a maximum power of 150 nW. Consequently, it was also shown that the output of the fabricated device was increased by applying the stress. The presented work will help for the openings to capture the mechanical energy from the surroundings to power up the nano/micro-devices. This research work shows that NGs have the competency to build the self-powered nanosystems. It has potential applications in biosensing and personal electronics.

**Originality/value**

The fabrication of simple and cost-effective piezoelectric NG is done with a structure of Al/ZnO/Au without using hosting layer. The presented method elucidates an efficient and cost-effective approach to harvest the mechanical energy from the native environment.

**Web URL:** <http://www.emeraldinsight.com/doi/abs/10.1108/MI-11-2015-0092>

**25. Awais, M. N., Mustafa, M., Shehzad, M. N., Farooq, U., Hamayun, M. T., & Choi, K. H. (2016). Resistive-switching and current-conduction mechanisms in F8BT polymer resistive switch. *Micro & Nano Letters*, 11(11), 712-714.**

**ABSTRACT:**

Poly[(9,9-di-n-octylfluorenyl-2,7-diyl)-alt-(benzo[2,1,3]thiadiazol-4,8-diyl)] (F8BT) polymer has been investigated to elucidate the resistive-switching properties in a sandwiched structure of indium tin oxide (ITO)/F8BT/aluminium (Al). An active layer of F8BT polymer was deposited on the ITO-coated polyethylene terephthalate through spin coating. Morphologically, the layer was characterised with field emission scanning electron microscope. The fabricated sample showed resistive-switching properties within  $\pm 5$  V with an OFF/ON ratio of 10:1. The switching characteristics were attributed to the transition of trap-limited space charge-limited conduction (SCLC) to trap-filled SCLC. It is shown through energy band diagram that memory effects in the fabricated sample were due to the trapping of electrons in the F8BT active layer that were injected from the top Al electrode.

**Web URL:** <http://digital-library.theiet.org/content/journals/10.1049/mnl.2016.0165>

**26. Muhammad, Q. K., Waqar, M., Rafiq, M. A., Rafiq, M. N., Usman, M., & Anwar, M. S. (2016). Structural, dielectric, and impedance study of ZnO-doped barium zirconium titanate (BZT) ceramics. *Journal of Materials Science*, 51(22), 10048-10058.**

**ABSTRACT:**

Polycrystalline lead-free  $\text{BaZr}_{0.15}\text{Ti}_{0.85}\text{O}_3$  ceramics doped with ZnO ( $0 \leq x \leq 2$  wt%) were produced via mixed oxide solid-state reaction method. X-ray diffraction confirmed the presence of a single phase having tetragonal symmetry and having space group P4 mm.

Scanning electron microscopy confirmed an increase in the density of microstructure and enlargement of grains with increase in ZnO concentration. Complex impedance spectroscopy revealed non-Debye type relaxation phenomenon. It was observed that an increase in the resistance of grain boundaries and decrease in that of grain interior (bulk) occurred with an increase in temperature. Relaxation time decreased with increase in temperature for both grain boundaries and grain interior. Understandings obtained from this work might be helpful in engineering the microstructure of BZT-based ceramics for useful applications.

**Web URL:** <https://link.springer.com/article/10.1007/s10853-016-0231-y>

# DEPARTMENT OF COMPUTER SCIENCE

## Journal Papers

1.Tahir, T., Rasool, G., & Gencel, C. (2016). A systematic literature review on software measurement programs. *Information and Software Technology, 73*, 101-121.

### **ABSTRACT:**

#### **Context**

Software measurement programs (MPs) are an important means for understanding, evaluating, managing, and improving software processes, products and resources. However, implementing successful MPs still remains a challenge.

#### **Objectives**

To make a comprehensive review of the studies on MPs for bringing into light the existing measurement planning models and tools used for implementing MPs, the accumulated knowledge on the success/failure factors of MPs and mitigation strategies to address their challenges.

#### **Methods**

A Systematic Literature Review (SLR) was conducted. In total, 65 primary studies were reviewed and analyzed.

#### **Results**

We identified 35 measurement planning models and 11 associated tools, most of which either proposed extensions or improvements for goal based approaches. The identified success factors include (a) organizational adoption of MP, (b) integration of MP with SDLC, (c) synchronization of MP with SPI and (d) design of MP. The mostly mentioned mitigation strategies for addressing challenges are effective change management and measurement stakeholder management, automated tool support and incorporation of engineering

mechanisms for designing sustainable, effective, scalable and extendible MPs, and measurement expertise and standards development.

### **Conclusion**

Most of the success factors and mitigation strategies have interdependencies. Therefore, for successful MP implementation, software organizations should consider these factors in combination and make a feasibility study at the very beginning.

**Web URL:** <http://www.sciencedirect.com/science/article/pii/S0950584916300131>

**2. Chaudhry, M. T., Yong, C. C., Ling, T. C., Rasheed, S., & Kim, J. (2016). Thermal prediction models for virtualized data center servers by using thermal-profiles. *Malaysian Journal of Computer Science*, 29(1).**

### **ABSTRACT:**

The energy dissipated as heat for each utilization level of a data center server is empirically measured and stored as the thermal-profile. These thermal-profiles are used to predict the outlet temperatures of the related servers for current and future utilization. The predicted outlet temperature is an important parameter for energy efficient thermal-aware workload scheduling and workload migration in green data centers. This paper presents three models for outlet temperature prediction on virtualized data center servers based on thermal-profile. The best case scenario managed to predict the outlet temperature with a negligible error of 0.3 degree Celsius.

**Web URL:** [http://e-journal.um.edu.my/filebank/published\\_article/9608/1587.pdf](http://e-journal.um.edu.my/filebank/published_article/9608/1587.pdf)

**3. Ali, A., Jalil, A., Niu, J., Zhao, X., Rathore, S., Ahmed, J., & Iftikhar, M. A. (2016). Visual object tracking—classical and contemporary approaches. *Frontiers of Computer Science*, 10(1), 167-188.**

### **ABSTRACT:**

Visual object tracking (VOT) is an important subfield of computer vision. It has widespread application domains, and has been considered as an important part of surveillance and

security system. VOA facilitates finding the position of target in image coordinates of video frames. While doing this, VOA also faces many challenges such as noise, clutter, occlusion, rapid change in object appearances, highly maneuvered (complex) object motion, illumination changes. In recent years, VOT has made significant progress due to availability of low-cost high-quality video cameras as well as fast computational resources, and many modern techniques have been proposed to handle the challenges faced by VOT. This article introduces the readers to 1) VOT and its applications in other domains, 2) different issues which arise in it, 3) various classical as well as contemporary approaches for object tracking, 4) evaluation methodologies for VOT, and 5) online resources, i.e., annotated datasets and source code available for various tracking techniques.

**Web URL:** <https://link.springer.com/article/10.1007/s11704-015-4246-3>

**4. Hussain, I., Chen, L., Mirza, H. T., Wang, L., Chen, G., & Memon, I. (2016). Chinese-Based Spearcons: Improving Pedestrian Navigation Performance in Eyes-Free Environment. *International Journal of Human-Computer Interaction*, 32(6), 460-469.**

**ABSTRACT:**

This article presents nonspeech audio (i.e., English-based spearcons and Chinese-based spearcons) to represent distance, and forward-direction for pedestrian navigation in an eyes-free environment. Experiment in the field is carried out with the involvement of 10 participants (i.e., native Chinese) using within-subject design to evaluate English-based spearcons, Chinese-based spearcons, and Chinese text-to-speech (TTS). Results from the experiment suggest that Chinese-based spearcons are efficient in task completion compared to Chinese TTS. Moreover, Chinese-based spearcons are more effective in conveying distance and forward-direction compared to English-based spearcons in pedestrian navigation. Overall, participants have shown their satisfaction with Chinese-based spearcons as an auditory feedback in pedestrian navigation.

**Web URL:** <http://www.tandfonline.com/doi/abs/10.1080/10447318.2016.1160669>

5. Shahbaz, M., Rasool, G., Ahmed, K., & Mahalik, M. K. (2016). Considering the effect of biomass energy consumption on economic growth: fresh evidence from BRICS region. *Renewable and Sustainable Energy Reviews*, 60, 1442-1450.

**ABSTRACT:**

This paper investigates the relationship between biomass energy consumption and economic growth by incorporating capital and trade openness in production function for the case of BRICS countries. In doing so, unit root and cointegration tests have been used in order to examine unit root properties and long run relationship between the series for the period of 1991Q1–2015Q4. The results confirm the presence of long-run equilibrium relationship between the variables. Moreover, biomass energy consumption stimulates economic growth. Capital increments economic growth and trade openness spurs economic growth. The feedback effect exists between biomass energy consumption and economic growth. Trade openness Granger causes economic growth, capital and biomass energy consumption. The policy to adopt biomass as the primary source of renewable energy helps BRICS countries to achieve sustainable development goal in both short-run and long-run. However, the key innovative point of this study is to establish the sign for Granger causality test.

**Web URL:** <http://www.sciencedirect.com/science/article/pii/S1364032116002720>

6. Rathore, S., Hussain, M., Iftikhar, M. A., & Jalil, A. (2015). Novel structural descriptors for automated colon cancer detection and grading. *Computer methods and programs in biomedicine*, 121(2), 92-108.

**ABSTRACT:**

The histopathological examination of tissue specimens is necessary for the diagnosis and grading of colon cancer. However, the process is subjective and leads to significant inter/intra observer variation in diagnosis as it mainly relies on the visual assessment of histopathologists. Therefore, a reliable computer-aided technique, which can automatically classify normal and malignant colon samples, and determine grades of malignant samples, is required. In this paper, we propose a novel colon cancer diagnostic (CCD) system, which initially classifies colon biopsy images into normal and malignant classes, and then automatically determines the

grades of colon cancer for malignant images. To this end, various novel structural descriptors, which mathematically model and quantify the variation among the structure of normal colon tissues and malignant tissues of various cancer grades, have been employed. Radial basis function (RBF) kernel of support vector machines (SVM) has been employed as classifier in order to classify/grade colon samples based on these descriptors. The proposed system has been tested on 92 malignant and 82 normal colon biopsy images. The classification performance has been measured in terms of various performance measures, and quite promising performance has been observed. Compared with previous techniques, the proposed system has demonstrated better cancer detection (classification accuracy = 95.40%) and grading (classification accuracy = 93.47%) capability. Therefore, the proposed CCD system can provide a reliable second opinion to the histopathologists.

**Web URL:** <http://www.sciencedirect.com/science/article/pii/S0169260715001510>

**7. Rathore, S., & Iftikhar, M. A. (2016). CBISC: A Novel Approach for Colon Biopsy Image Segmentation and Classification. *Arabian Journal for Science and Engineering*, 41(12), 5061-5076.**

**ABSTRACT:**

The morphology of epithelial cells plays a vital role in distinguishing malignant colon tissues from the normal ones. Epithelial cells have near elliptic shape in normal colon tissues, whereas they deform into an amorphous shape in malignant tissues. The information about the morphology of epithelial cells may be incorporated in order to obtain an effective segmentation of colon biopsy images. In this research study, we propose a novel colon biopsy image segmentation and classification (CBISC) technique that does so. The proposed CBISC technique comprises two main modules, namely, segmentation and classification. The segmentation module exploits the background information about morphology of epithelial cells, and detects elliptic and nearly elliptic epithelial cells in four orientations. It further calculates three novel features, namely, semi-major axis, direction, and area occurrence for each image pixel. Finally, it grows and merges regions based on these features, and demarcates final region boundaries. Genetic algorithm has been employed to optimize

several parameters used in the segmentation process. A dataset comprising 300 colon biopsy images has been used for the evaluation of proposed segmentation module, and improved performance has been observed compared to previously reported techniques. To validate the effectiveness of segmentation, moments of gray-level histogram and gray-level co-occurrence matrix-based features have been extracted from 710 segmented patches of the images, and have been used for the classification of segmented regions into normal and malignant classes. Radial basis function kernel of support vector machines has been used for classification, and reasonable classification results have been obtained.

**Web URL:** <https://link.springer.com/article/10.1007/s13369-016-2187-2>

**8. Nawab, R. M. A., Stevenson, M., & Clough, P. (2016). An ir-based approach utilising query expansion for plagiarism detection in medline. *IEEE/ACM transactions on computational biology and bioinformatics*.**

**ABSTRACT:**

The identification of duplicated and plagiarised passages of text has become an increasingly active area of research. In this paper we investigate methods for plagiarism detection that aim to identify potential sources of plagiarism from MEDLINE, particularly when the original text has been modified through the replacement of words or phrases. A scalable approach based on Information Retrieval is used to perform candidate document selection - the identification of a subset of potential source documents given a suspicious text - from MEDLINE. Query expansion is performed using the ULMS Metathesaurus to deal with situations in which original documents are obfuscated. Various approaches to Word Sense Disambiguation are investigated to deal with cases where there are multiple Concept Unique Identifiers (CUIs) for a given term. Results using the proposed IR-based approach outperform a state-of-the-art baseline based on Kullback-Leibler Distance.

**Web URL:** <http://ieeexplore.ieee.org/abstract/document/7434600/>

9. Asghar, K., Habib, Z., & Hussain, M. (2017). Copy-move and splicing image forgery detection and localization techniques: a review. *Australian Journal of Forensic Sciences*, 49(3), 281-307.

**ABSTRACT:**

Digital image acquisition is now a simple task and information in the form of digital images is drastically increasing on social media, which has both positive and negative impacts on a society in many different ways. Advanced user-friendly tools have made it easy to manipulate image content in order to gain illegal advantage or to make false propaganda, and digital images and videos are not acceptable in courts of law as evidence without reliable forensic analysis. A lot of research has been done in order to address this problem and many techniques exist that detect and localize copy-move and splicing forgeries. However, it is very important to know whether these methods are robust, properly modelling the structural changes that have occurred in images due to copy-move and/or splicing forgeries, and can reliably classify a digital image as a genuine or modified image. In this paper, we present an extensive literature review of the state-of-the-art techniques on copy-move and splicing forgeries, highlighting their limitations, and we provide future research directions.

**Web URL:** <http://www.tandfonline.com/doi/abs/10.1080/00450618.2016.1153711>

10. Rasool, G., & Arshad, Z. (2017). A Lightweight Approach for Detection of Code Smells. *Arabian Journal for Science and Engineering*, 42(2), 483-506.

**ABSTRACT:**

The accurate removal of code smells from source code supports activities such as refactoring, maintenance, examining code quality etc. A large number of techniques and tools are presented for the specification and detection of code smells from source code in the last decade, but they still lack accuracy and flexibility due to different interpretations of code smell definitions. Most techniques target just detection of few code smells and render different results on the same examined systems due to different informal definitions and threshold values of metrics used for detecting code smells. We present a flexible and lightweight approach based on multiple searching techniques for the detection and

visualization of all 22 code smells from source code of multiple languages. Our approach is lightweight and flexible due to application of SQL queries on intermediate repository and use of regular expressions on selected source code constructs. The concept of approach is validated by performing experiments on eight publicly available open source software projects developed using Java and C# programming languages, and results are compared with existing approaches. The accuracy of presented approach varies from 86–97 % on the eight selected software projects.

**Web URL:** <https://link.springer.com/article/10.1007/s13369-016-2238-8>

**11. Qadri, S., Khan, D. M., Ahmad, F., Qadri, S. F., Babar, M. E., Shahid, M., ...& Ahmad, S. (2016). A Comparative Study of Land Cover Classification by Using Multispectral and Texture Data. *BioMed research international*, 2016.**

**ABSTRACT:**

The main objective of this study is to find out the importance of machine vision approach for the classification of five types of land cover data such as bare land, desert rangeland, green pasture, fertile cultivated land, and Sutlej river land. A novel spectra-statistical framework is designed to classify the subjective land cover data types accurately. Multispectral data of these land covers were acquired by using a handheld device named multispectral radiometer in the form of five spectral bands (blue, green, red, near infrared, and shortwave infrared) while texture data were acquired with a digital camera by the transformation of acquired images into 229 texture features for each image. The most discriminant 30 features of each image were obtained by integrating the three statistical features selection techniques such as Fisher, Probability of Error plus Average Correlation, and Mutual Information (F + PA + MI). Selected texture data clustering was verified by nonlinear discriminant analysis while linear discriminant analysis approach was applied for multispectral data. For classification, the texture and multispectral data were deployed to artificial neural network (ANN: n-class). By implementing a cross validation method (80-20), we received an accuracy of 91.332% for texture data and 96.40% for multispectral data, respectively.

**Web URL:** <https://www.hindawi.com/journals/bmri/2016/8797438/abs/>

**12. Sharjeel, M., Nawab, R. M. A., & Rayson, P. (2016). COUNTER: corpus of Urdu news text reuse. *Language Resources and Evaluation*, 1-27.**

**ABSTRACT:**

Text reuse is the act of borrowing text from existing documents to create new texts. Freely available and easily accessible large online repositories are not only making reuse of text more common in society but also harder to detect. A major hindrance in the development and evaluation of existing/new mono-lingual text reuse detection methods, especially for South Asian languages, is the unavailability of standardized benchmark corpora. Amongst other things, a gold standard corpus enables researchers to directly compare existing state-of-the-art methods. In our study, we address this gap by developing a benchmark corpus for one of the widely spoken but under resourced languages i.e. Urdu. The COpus of Urdu News TExt Reuse (COUNTER) corpus contains 1200 documents with real examples of text reuse from the field of journalism. It has been manually annotated at document level with three levels of reuse: wholly derived, partially derived and non derived. We also apply a number of similarity estimation methods on our corpus to show how it can be used for the development, evaluation and comparison of text reuse detection systems for the Urdu language. The corpus is a vital resource for the development and evaluation of text reuse detection systems in general and specifically for Urdu language.

**Web URL:** <https://link.springer.com/article/10.1007/s10579-016-9367-2>

**13. Khan, A., Noreen, I., & Habib, Z. (2017). On Complete Coverage Path Planning Algorithms for Non-holonomic Mobile Robots: Survey and Challenges. *Journal of Information Science & Engineering*, 33(1).**

**ABSTRACT:**

The problem of determining a collision free path within a region is an important area of research in robotics. One significant aspect of this problem is coverage path planning, which is a process to find a path that passes through each reachable position in the desired area. This task is fundamental to many robotic applications such as cleaning, painting, underwater operations, mine sweeping, lawn mowing, agriculture, monitoring, searching, and rescue operations. The

total coverage time is significantly influenced by total number of turns, optimization of backtracking sequence, and smoothness in the complete coverage path. There is no comprehensive literature review on backtracking optimization and path smoothing techniques used in complete coverage path planning. Although the problem of coverage path planning has been addressed by many researchers. However, existing state of the art needs to be significantly improve, particularly in terms of accuracy, efficiency, robustness, and optimization. This paper aims to present the latest developments, challenges regarding backtracking sequence optimization, smoothness techniques, limitations of existing approaches, and future research directions.

**Web URL:**

<http://web.b.ebscohost.com/abstract?direct=true&profile=ehost&scope=site&authtype=crawler&jrnl=10162364&AN=120961667&h=a96eysVgKIkO8uGa80Tyish9TmRgYvMBnCIWmOQWNYRywd2o9rpxNqMommZRcFudIJ7aXZPm9ldECOGvcGfrfA%3d%3d&crl=c&resultNs=AdminWebAuth&resultLocal=ErrCrlNotAuth&crlhashurl=login.aspx%3fdirect%3dtrue%26profile%3dehost%26scope%3dsite%26authtype%3dcrawler%26jrnl%3d10162364%26AN%3d120961667>

**14. Sargano, A. B., Angelov, P., & Habib, Z. (2016). Human action recognition from multiple views based on view-invariant feature descriptor using support vector machines. *Applied Sciences*, 6(10), 309.**

**ABSTRACT:**

This paper presents a novel feature descriptor for multiview human action recognition. This descriptor employs the region-based features extracted from the human silhouette. To achieve this, the human silhouette is divided into regions in a radial fashion with the interval of a certain degree, and then region-based geometrical and Hu-moments features are obtained from each radial bin to articulate the feature descriptor. A multiclass support vector machine classifier is used for action classification. The proposed approach is quite simple and achieves state-of-the-art results without compromising the efficiency of the recognition process. Our contribution is two-fold. Firstly, our approach achieves high recognition accuracy with simple silhouette-based representation. Secondly, the average

testing time for our approach is 34 frames per second, which is much higher than the existing methods and shows its suitability for real-time applications. The extensive experiments on a well-known multiview IXMAS (INRIA Xmas Motion Acquisition Sequences) dataset confirmed the superior performance of our method as compared to similar state-of-the-art methods.

**Web URL:** <http://www.mdpi.com/2076-3417/6/10/309/htm>

**15. Noreen, I., Khan, A., & Habib, Z. (2016). A Comparison of RRT, RRT\* and RRT\*-Smart Path Planning Algorithms. *International Journal of Computer Science and Network Security (IJCSNS)*, 16(10), 20.**

**ABSTRACT:**

Sampling based planning algorithm such as RRT and RRT\* are extensively used in recent years for path planning of mobile robots. They are probabilistic complete algorithms and have natural support for solving high dimensional complex problems. RRT\*-Smart is an extension of RRT\* with faster convergence as compared to its predecessors. This paper provides an analytical review of the three algorithms. Impact of different parameters on algorithm's performance is also evaluated. Moreover, a performance comparison for different optimality criteria such as path cost, run time and total number of nodes in tree is performed through simulation based experiments. Further, the comparative analysis is concluded with future research directions.

**Web URL:** [http://paper.ijcsns.org/07\\_book/201610/20161004.pdf](http://paper.ijcsns.org/07_book/201610/20161004.pdf)

**16. Saeed, Y., Ahmed, K., Lohi, M., Abbas, S., & Athar, A. (2016). Impact of Cognition on User Authentication Scheme in Vehicle using Fuzzy Logic and Artificial Neural Network. *International Journal of Computer Science and Information Security*, 14(10), 285.**

**ABSTRACT:**

Vehicular Ad hoc Network is an emerging area in the field of communication that provides key role in our transportation industry. One of the challenges in this domain is to incorporate human cognition in vehicles to authenticate the right user. This enables a vehicle to evolve with time and to make rational decisions in terms of user authenticity. We have proposed vehicle user authentication module from cognition perspective and utilized cognitive memories where

user episodes are learned, stored and accessed. Cognitive memories are going to store user authentication experiences that enable a vehicle to take rational decisions in different task environments. The more user authentication process takes place in different task environments, the more a vehicle populates its knowledge repository for better decision making. The ultimate goal is to make a shift from supervised mode to semi-supervised and unsupervised ultimately. From system administration point of view, the concept of controller is introduced and incorporated for performance enhancement. For validation, user authentication module based-case is devised and fuzzy logic is used to highlight the amount of fuzziness involved in authenticating a user due to the presence of cognitive instances that makes them fuzzified and to find under what circumstances better and worsts results are achieved. From learning perspective, artificial neural network is used to show that learning can be achieved in vehicular agency in order to make rational decisions.

**Web URL:**

[http://s3.amazonaws.com/academia.edu.documents/51179149/37\\_Paper\\_30091678\\_IJCSIS\\_C\\_amera\\_Ready\\_pp.\\_285-296.pdf?AWSAccessKeyId=AKIAIWOWYYGZ2Y53UL3A&Expires=1500544342&Signature=tW62niKoebWPea6IMR22DDckJUQ%3D&response-content-disposition=inline%3B%20filename%3DImpact\\_of\\_Cognition\\_on\\_User\\_Authenticati.pdf](http://s3.amazonaws.com/academia.edu.documents/51179149/37_Paper_30091678_IJCSIS_C_amera_Ready_pp._285-296.pdf?AWSAccessKeyId=AKIAIWOWYYGZ2Y53UL3A&Expires=1500544342&Signature=tW62niKoebWPea6IMR22DDckJUQ%3D&response-content-disposition=inline%3B%20filename%3DImpact_of_Cognition_on_User_Authenticati.pdf)

**17. Gul, M. T., Ali, A., Singh, D. K., Imtinan, U., Raza, I., Hussain, S. A., ...& Lee, J. W. (2016). Merge-and-forward: a cooperative multimedia transmissions protocol using RaptorQ codes. *IET Communications*, 10(15), 1884-1895.**

**ABSTRACT:**

Recently, nodes cooperation has emerged as a popular means for improving the quality of multimedia delivery over fifth-generation cellular networks. However, in the conventional relaying scheme such as amplify-and-forward (AaF), there is a higher probability of duplicate packets at the receiver node which affect the decoding probability and consequently deteriorate the quality of multimedia transmission. In this study, the authors propose a cooperative multimedia transmission protocol based on a novel merge-and-forward relaying and the best relay selection (RS) schemes. Their best RS scheme is based on two important

parameters: (i) two-hop link distances and (ii) minimum block error rate value. Moreover, to combat the packet loss for enhanced and reliable video delivery, they adopt application layer forward error correction scheme which is based on the most improved and advanced version of fountain codes (i.e. RaptorQ codes). They evaluate the performance of the proposed scheme under different time-sharing scenarios between the direct and best indirect transmission links in terms of decoding failure probability, decoding overhead, peak signal-to-noise ratio, and mean opinion score. Simulation results show that the proposed scheme outperforms the conventional AaF relaying scheme.

**Web URL:** <http://digital-library.theiet.org/content/journals/10.1049/iet-com.2016.0146>

**18. Hussain, S. A., Khan, N. A., Sadiq, A., & Ahmad, F. (2016). Simulation, modeling and analysis of master node election algorithm based on signal strength for VANETs through Colored Petri nets. *Neural Computing and Applications*, 1-17.**

**ABSTRACT:**

The broadcast storm problem causes redundancy, contention and collision of messages in a network, particularly in vehicular ad hoc networks (VANETs) where number of participants can grow arbitrarily. This paper presents a solution to this problem in which a node is designated as a master through an election process. Moreover, an algorithm is proposed for asynchronous VANETs to select a master node, where the participants (i.e., vehicles) can communicate with each other directly (single-hop). The proposed algorithm is extremal-finding in a way that a node having maximum signal strength is elected as a master node and each vehicle continues communication with the master until the master node keeps its signal strength at the highest level and remains operational too. This paper further presents the Petri net-based modeling of the proposed algorithm for evaluation which is going to be presented for the first time in leader election algorithm in VANETs. Verification of the proposed algorithm is carried out through state space analysis technique.

**Web URL:** <https://link.springer.com/article/10.1007/s00521-016-2622-z>

**19. Shah, N., Abid, S. A., Qian, D., & Mehmood, W. (2017). A survey of P2P content sharing in MANETs. *Computers & Electrical Engineering*, 57, 55-68.**

**ABSTRACT:**

Recently, several approaches have been proposed for Peer-to-peer (P2P) content/file sharing in mobile ad hoc networks (MANETs). In this article, we apprise a comprehensive survey of researches related to P2P overlay networks for sharing the content at the application layer in MANETs. We compare and contemplate the features, vitality, and vulnerability of these approaches and highlight indispensable research challenges that are imperative to address and will have substantial advantages. The fallout of the analysis would serve as a substantial guide for anyone willing to delve into research on the topic of P2P overlay over MANETs.

**Web URL:** <http://www.sciencedirect.com/science/article/pii/S004579061631062X>

**20. Afzal, H., Waqas, M., & Naz, T. (2016). OWLMap: Fully Automatic Mapping of Ontology into Relational Database Schema. *INTERNATIONAL JOURNAL OF ADVANCED COMPUTER SCIENCE AND APPLICATIONS*, 7(11), 7-15.**

**ABSTRACT:**

Semantic web is becoming a controversial issue in current research era. There must be an automated approach to transform ontology constructs into relational database so that it can be queried efficiently. The previous research work based on transformation of RDF/OWL concepts into relational database contains flaws in complete transformation of ontology constructs into relational database. Some researchers claim that their technique of transformation is entirely automated, however their approach of mapping is incomplete and miss essential OWL constructs. This paper presents a tool called OWLMap that is fully automatic and provides lossless approach for transformation of ontology into relational database format. Number of experiments have been performed for ontology to relational database transformation. Experiments show that proposed approach is fully automatic, effective and quick. Our OWLMap is based on an approach that is lossless as well as it does not lose data, data types and structure.

**Web URL:**

<http://thesai.org/Publications/ViewPaper?Volume=7&Issue=11&Code=IJACSA&SerialNo=2>

**21. Sajid, M., Taj, I. A., Bajwa, U. I., & Ratyal, N. I. (2016). The role of facial asymmetry in recognizing age-separated face images. *Computers & Electrical Engineering*, 54, 255-270.**

**ABSTRACT:**

Recognition of age-separated face images is a challenging and open research problem. In this paper we propose a facial asymmetry based matching-score space (MSS) approach for recognition of age-separated face images. Motivated by its discriminatory information, we evaluate facial asymmetry across small and large temporal variations and use asymmetric facial features to recognize age-separated face images. We extract three different facial features including holistic feature descriptors using Principal Component Analysis (PCA), local feature descriptors using Local Binary Patterns (LBP), and Densely Sampled Asymmetric Features (DSAF) to represent face images. Then we develop MSS to discriminate genuine and imposter classes using support vector machine (SVM) as a classifier. Experimental results on three widely used face aging databases, the FERET, MORPH and FG-NET, show that proposed approach has superior performance compared to some existing state-of-the-art approaches.

**Web URL:** <http://www.sciencedirect.com/science/article/pii/S0045790616000033>

**22. Khan, N. A., Ahmad, F., Hussain, S. A., & Naseer, M. (2016). Hierarchical Coloured Petri Net based Random Direction Mobility Model for Wireless Communications. *TIIIS*, 10(8), 3656-3671.**

**ABSTRACT:**

Most of the research in the area of wireless communications exclusively relies on simulations. Further, it is essential that the mobility management strategies and routing protocols should be validated under realistic conditions. Most appropriate mobility models play a pivotal role to determine, whether there is any subtle error or flaw in a proposed model. Simulators are the standard tool to evaluate the performance of mobility models however sometimes they suffer from numerous documented problems. To accomplish the widely acknowledged lack of formalization in this domain, a Coloured Petri nets (CPNs) based random direction mobility model for specification, analysis and validation is presented in this paper for wireless communications. The proposed model does not suffer from any border effect or speed decay

issues. It is important to mention that capturing the mobility patterns through CPN is challenging task in this type of the research. Further, an appropriate formalism of CPNs supported to analyze the future system dynamic status. Finally the formal model is evaluated with the state space analysis to show how predefined behavioral properties can be applied. In addition, proposed model is evaluated based on generated simulations to track origins of errors during debugging.

**Web URL:**

[http://www.kpubs.org/article/articleDownload.kpubs?downType=pdf&articleANo=E1KOBZ\\_2016\\_v10n8\\_3656](http://www.kpubs.org/article/articleDownload.kpubs?downType=pdf&articleANo=E1KOBZ_2016_v10n8_3656)

**23. Sherazi, H. H. R., Iqbal, R., Ul Hassan, S., Chaudary, M. H., & Gilani, S. A. (2016). ZigBee's Received Signal Strength and Latency Evaluation under Varying Environments. *Journal of Computer Networks and Communications*, 2016.**

**ABSTRACT:**

Being self-configured, self-organized, and self-healing low power technology, ZigBee has obtained significant attention in last few years for achieving ubiquitous communication among various devices within a Personal Area Network (PAN). Even after a decade of its emergence, it has been well serving the communication needs of numerous modern applications belonging to multiple industries and is still a spotlight for the researchers working on certain aspects to enhance productivity along with a major cost reduction. Despite its robust communication nature, it heavily depends upon the context and is prone to the external effects that may cause a serious threat to prospective applications. This paper presents the novel experimental analysis conducted on real test beds to evaluate the impact of continuously changing communication environment on various parameters, for example, RSSI (Received Signal Strength Indicator) and latency in the presence of multiple obstacles that may lead to severe degradation in the overall performance. Eventually, we suggest a suitable frame size for ZigBee based on our results deduced from the experimental study.

**Web URL:** <https://www.hindawi.com/journals/icnc/2016/9409402/abs/>

**24. Noreen, I., Khan, A., & Habib, Z. (2016). Optimal Path Planning using RRT\* based Approaches: A Survey and Future Directions. *INTERNATIONAL JOURNAL OF ADVANCED COMPUTER SCIENCE AND APPLICATIONS*, 7(11), 97-107.**

**ABSTRACT:**

Optimal path planning refers to find the collision free, shortest, and smooth route between start and goal positions. This task is essential in many robotic applications such as autonomous car, surveillance operations, agricultural robots, planetary and space exploration missions. Rapidly-exploring Random Tree Star (RRT\*) is a renowned sampling based planning approach. It has gained immense popularity due to its support for high dimensional complex problems. A significant body of research has addressed the problem of optimal path planning for mobile robots using RRT\* based approaches. However, no updated survey on RRT\* based approaches is available. Considering the rapid pace of development in this field, this paper presents a comprehensive review of RRT\* based path planning approaches. Current issues relevant to noticeable advancements in the field are investigated and whole discussion is concluded with challenges and future research directions.

**Web URL:** [https://thesai.org/Downloads/Volume7No11/Paper\\_14-Optimal\\_Path\\_Planning\\_using\\_RRT\\_based\\_Approaches.pdf](https://thesai.org/Downloads/Volume7No11/Paper_14-Optimal_Path_Planning_using_RRT_based_Approaches.pdf)

**25. Abbas, S., Nawaz, B., Athar, A., Saeed, Y., & Khan, W. A. (2016). Intelligent Agent Navigation using Bluetooth Based Ad Hoc Communication. *International Journal of Computer Science and Information Security*, 14(11), 646.**

**ABSTRACT:**

Mobile phones are very common now a days and being used as a primary medium for communication. Therefore, intelligent agent navigation could be facilitated generally by mobile communication. However, agent communication using Wi-Fi access points, may be too costly. To minimize the cost of communication for intelligent agent navigation, this paper presents a Bluetooth based ad-hoc communication system using Wi-Fi access points to improve the agent navigation. The performance of an agent navigation may be compromised due to poor reception of GPS and Wi-Fi signals in indoor environment. The proposed agent navigation system may be

converted into an intelligent agent navigation system provided that Bluetooth based ad-hoc communication is taken as a secondary medium to support the navigation in agency.

**Web URL:**

[http://www.academia.edu/30927536/Intelligent\\_Agent\\_Navigation\\_using\\_Bluetooth\\_Based\\_Ad\\_Hoc\\_Communication](http://www.academia.edu/30927536/Intelligent_Agent_Navigation_using_Bluetooth_Based_Ad_Hoc_Communication)

**26. Abid, A., Hussain, N., Abid, K., Ahmad, F., Farooq, M. S., Farooq, U., ...& Sabir, N. (2016). A survey on search results diversification techniques. *Neural Computing and Applications*, 27(5), 1207-1229.**

**ABSTRACT:**

The quantity of information placed on the web has been greater than before and is increasing rapidly day by day. Searching through the huge amount of data and finding the most relevant and useful result set involves searching, ranking, and presenting the results. Most of the users probe into the top few results and neglect the rest. In order to increase user's satisfaction, the presented result set should not only be relevant to the search topic, but should also present a variety of perspectives, that is, the results should be different from one another. The effectiveness of web search and the satisfaction of users can be enhanced through providing various results of a search query in a certain order of relevance and concern. The technique used to avoid presenting similar, though relevant, results to the user is known as a diversification of search results. This article presents a survey of the approaches used for search result diversification. To this end, this article not only provides a technical survey of existing diversification techniques, but also presents a taxonomy of diversification algorithms with respect to the types of search queries.

**Web URL:** <https://link.springer.com/article/10.1007/s00521-015-1945-5>

**27. Khan, N. A., & Ahmad, F. (2016). Modeling and simulation of an improved random direction mobility model for wireless networks using colored Petri nets. *Simulation*, 92(4), 323-336.**

**ABSTRACT:**

Wireless networks have received increased attention from researchers due to their extensive set of applications and ubiquitous communication facility. The underlying mobility model plays a key role in mobility management, which is a prominent communication means in delivering services to mobile users accurately. Random direction is a synthetic mobility model that is widely used in simulators, while simulation is universally considered the most effective method for the design and analysis of the characteristics of mobility models. However, simulation is limited in its capabilities and it may generate unrealistic, error-prone results and consume more time. Further, the random direction mobility model produces unrealistic movement patterns due to a sharp turn problem and it forces the mobile host to travel to the edge of the terrain. To alleviate the issues of the random direction mobility model, this paper presents a colored Petri net (CPN)-based formal approach as an improved direction mobility model. Further, the proposed algorithm to tackle the sharp turn problem is implemented by using the CPN formalism. The formal semantics of the CPN allow a graphical, intuitive approach to design, simulate, execute, and validate the model.

**Web URL:** <http://journals.sagepub.com/doi/abs/10.1177/0037549716634435>

**28. Sohail, A., Dominic, P. D. D., & Shahzad, K. (2016). Business process analysis: a process warehouse-based resource preference evaluation method. *International Journal of Business Information Systems*, 21(2), 137-161.**

**ABSTRACT:**

In a working environment, resources are commonly shared between tasks, and sometime multiple resources are necessary to commence a single task, this scenario makes the resource utilisation complex. Existing studies on business process analysis and evaluations widely focused on competence of resource to measure work performance, but it is contended that the relationship of resource with task is not sufficiently understood due to not considering evaluations of all resource classes. Particularly, business intelligence-based approaches to BPI have not adequately explored this relationship. Subsequently, a set of relationships between human resources, non-human resources and tasks (named suitability, preference and competence) are presented. However, only human resources relationship with non-human resources (named preference) is presented in detail, as a resource preference model. The

model bundled with the presented preference evaluation method guides users for evaluation of resources preference. The applicability of the method is illustrated through a healthcare case study. Quality of data produces is evaluated though an empirical study, that is confirming the claim of highly relevant information generation.

**Web URL:** <http://www.inderscienceonline.com/doi/abs/10.1504/IJBIS.2016.074255>

**29. Rizwan, S. (2016). Smart Navigation System For Buses With Location for Pakistan. *Advances in Social Sciences Research Journal*, 3(6).**

**ABSTRACT:**

Road traffic is getting worse with every passing day, especially in major urban centers such as Lahore. In Pakistan, it is important to be aware of the traffic situation before setting out on a predetermined path. The smart navigation tool for buses will allow them to reach their destination and bus stops on time by determining the traffic flow along their routes, and suggesting an alternative route wherever possible. People get in to the long traffic jams as they are not informed of they have less knowledge about the condition of traffic in particular area. General public also get into difficulties in numerous ways. Firstly they are not sure that when the bus will come to the station which waste a lot of their time. Secondly they didn't know whether bus is coming to their station or not.. We are going to develop a smart navigation system which will use the maps provided by Google maps and will update the current situation of traffic for the correct information to the bus driver so that he can take an alternate path on his route on real time. A system must be built for bus drivers that can help them guide through their journey and show alternate routes when the original route cannot be followed due to traffic jams. Entire system is monitored by the admin which is another part for the better development, generating monthly reports is also significant to ensure the reliability of transport. They will help determine the average time a bus takes to travel on its route, the areas that host the heaviest traffic flow, the number of times an alternative route was taken and the factors that have an impact on a traveler's experience.

**Web URL:** <http://scholarpublishing.org/index.php/ASSRJ/article/view/2045>

# DEPARTMENT OF IRCBM

## Journal Papers

1. Yar, M., Gigliobianco, G., Shahzadi, L., Dew, L., Siddiqi, S. A., Khan, A. F., ...& MacNeil, S. (2016). Production of chitosan PVA PCL hydrogels to bind heparin and induce angiogenesis. *International Journal of Polymeric Materials and Polymeric Biomaterials*, 65(9), 466-476.

### **ABSTRACT:**

New blood vessel formation is an essential part of wound healing to provide cells with the nutrients and oxygen for their survival. Many nonhealing ulcers fail to heal because of poor blood supply and skin grafts will also fail to take on poorly vascularized wound beds. There is a real need for proangiogenic biomaterials to assist wound healing. *In vivo* heparin binds proangiogenic growth factors and helps regulate new blood vessel formation, hence heparin containing biomaterials are attractive. To achieve a hydrogel with high heparin binding capacity a composite of chitosan, poly(vinyl alcohol) (PVA) and polycaprolactone (PCL) was produced. Chitosan is a biodegradable natural polymer with great potential for biomedical applications due to its biocompatibility, high charge density and nontoxicity. PVA is biocompatible and nontoxic with good chemical stability, film-forming ability, and high hydrophilicity. PCL has physicochemical and mechanical properties comparable to those of the biological tissues and due its hydrophilic nature helps in the sustained release of drugs. Accordingly in this study we explored a range of PCL concentrations from 4% to 16% added to hydrogels composed of chitosan and PVA. Heparin was blended into the polymer mixture and the nanoporous structure was created by freeze-drying the PCL hydrogel. The physical properties of the hydrogels were evaluated by Fourier transform infrared spectroscopy (FTIR) and XPS confirmed the presence of sulfur on the surface of the hydrogels. Their porous morphology was investigated by scanning electron microscope (SEM). The Chick Chorionic Allantoic Membrane (CAM) assay was used to study the angiogenic potential of these materials and histology (H&E and Goldner trochome) was used to confirm the presence of new blood vessels inside the

hydrogels. We report that the addition of 8% PCL to the hydrogels gave porous structures containing heparin, which significantly increased new blood vessel formation into the hydrogels. These hydrogels offer a new approach to biomaterials, which could be added to wounds to improve vascularization.

**Web URL:** <http://www.tandfonline.com/doi/abs/10.1080/00914037.2015.1129959>

**2. Khan, Z. U. H., Khan, A., Shah, A., Chen, Y., Wan, P., ullah Khan, A., ...& Shah, H. U. (2016). Photocatalytic, antimicrobial activities of biogenic silver nanoparticles and electrochemical degradation of water soluble dyes at glassy carbon/silver modified past electrode using buffer solution. *Journal of Photochemistry and Photobiology B: Biology*, 156, 100-107.**

**ABSTRACT:**

In the present research work a novel, nontoxic and ecofriendly procedure was developed for the green synthesis of silver nano particle (AgNPs) using *Caruluma edulis* (*C. edulis*) extract act as reductant as well as stabilizer agents. The formation of AgNPs was confirmed by UV/Vis spectroscopy. The small and spherical sizes of AgNPs were conformed from high resolution transmission electron microscopy (HRTEM) analysis and were found in the range of 2–10 nm, which were highly dispersion without any aggregation. The crystalline structure of AgNPs was conformed from X-ray diffraction (XRD) analysis. For the elemental composition EDX was used and FTIR helped to determine the type of organic compounds in the extract. The potential electrochemical property of modified silver electrode was also studied. The AgNPs showed prominent antibacterial motion with MIC values of 125 µg/mL against *Bacillus subtilis* and *Staphylococcus aureus* while 250 µg/mL against *Escherichia coli*. High cell constituents' release was exhibited by *B. subtilis* with 2 × MIC value of silver nanoparticles. Silver nanoparticles also showed significant DPPH free radical scavenging activity. This research would have an important implication for the synthesis of more efficient antimicrobial and antioxidant agent. The AgNP modified electrode (GC/AgNPs) exhibited an excellent electro-catalytic activity toward the redox reaction of phenolic compounds. The AgNPs were evaluated for electrochemical degradation of bromothymol blue (BTB) dyes which showed a significant activity. From the strong reductive properties it is obvious that AgNPs can be used in water sanitization and converting some organic perilous in to non-hazardous materials. The AgNPs

showed potential applications in the field of electro chemistry, sensor, catalyst, nano-devices and medical.

**Web URL:** <http://www.sciencedirect.com/science/article/pii/S1011134416300148>

**3. Muhammad, N., Gao, Y., Iqbal, F., Ahmad, P., Ge, R., Nishan, U., ...& Ullah, Z. (2016). Extraction of biocompatible hydroxyapatite from fish scales using novel approach of ionic liquid pretreatment. *Separation and Purification Technology*, 161, 129-135.**

**ABSTRACT:**

In this study the waste fish scales (FS) were dissolved in 1-butyl-3-methylimidazolium acetate ionic liquid to obtain a valuable product of hydroxyapatite (HAp). The HAp was obtained in the yield of  $32 \pm 2\%$ . The obtained HAp was characterized using Fourier Transform Infrared Spectroscopy (FTIR), Powder X-rays Diffraction (PXRD), Thermal Gravimetric Analysis (TGA), Field Emission Scanning Microscopy (FE-SEM), Energy Dispersive X-rays spectroscopy (EDX), and Brunauer–Emmett–Teller (BET). The results of FTIR and XRD showed the characteristic peaks of the HAp. The thermal degradation temperature of the extracted HAp was relatively high. Furthermore, low weight loss was measured which confirmed the removal of organic part of FS during ionic liquid treatment. The FE-SEM result showed the particles with different morphologies and EDX analysis showed a Ca/P ratio of 1.60 for the extracted HAp. The biocompatibility of the extracted HAp was assessed through MTT cell viability assay using known Human Embryonic Kidney 293 cells (HEK cells) and epidermoid carcinoma cells (A431 cells).

**Web URL:** <http://www.sciencedirect.com/science/article/pii/S138358661630051X>

**4. Khan, A. U., Wei, Y., Ahmad, A., Khan, Z. U. H., Tahir, K., Khan, S. U., ... & Yuan, Q. (2016). Enzymatic browning reduction in white cabbage, potent antibacterial and antioxidant activities of biogenic silver nanoparticles. *Journal of Molecular Liquids*, 215, 39-46.**

**ABSTRACT:**

To produce economically benign and nontoxic enzymatic browning reducing and antimicrobial agents is the goal of nanotechnology. In this study we synthesized environmentally friendly silver nanoparticles (AgNPs) using Longan fruit juice as reducing and stabilizing agent. Silver

nanoparticles synthesis was monitored by UV–vis spectroscopy showing localized surface plasmon resonance at 443 nm. XRD (X-ray diffraction analysis), HRTEM (high resolution transmission electron microscopy) and EDX (energy dispersive X-ray analysis) were used to characterize crystalline structure, size (4–10 nm), shape and elemental composition of silver nanoparticles. Surface capped phytochemicals were characterized by FTIR. Silver nanoparticles have significant enzymatic browning reduction ( $p < 0.001$ ) using white cabbage as a model system. No research has been reported on the Enzymatic browning reduction of biosynthesized silver nanoparticles. The silver nanoparticles showed prominent antibacterial activity with MIC values of 31.25  $\mu\text{g/ml}$  against *Staphylococcus aureus* and *Basillus subtilus* while 62.5  $\mu\text{g/ml}$  against *Escherichia coli*. High cells constituents' release was exhibited by *B. subtilus* with  $2 \times$  MIC value of silver nanoparticles. Silver nanoparticles exhibited no hemolytic activity against Red blood cells of male Wistar albino rat. Silver nanoparticles also showed significant DPPH free radical scavenging activity. This research would have an important implication for the synthesis of more efficient antimicrobial, antioxidant and anti-enzymatic browning agents for food preservation, processing and other biomedical applications.

**Web URL:** <http://www.sciencedirect.com/science/article/pii/S0167732215305584>

**5. Hussain, R., Tabassum, S., Gilani, M. A., Ahmed, E., Sharif, A., Manzoor, F., ...& Siddiqi, S. A. (2016). In situ synthesis of mesoporous polyvinyl alcohol/hydroxyapatite composites for better biomedical coating adhesion. *Applied Surface Science*, 364, 117-123.**

**ABSTRACT:**

Hydroxyapatite (HA) shows diverse biomedical applications as bone filler and coating material for metal implants to enhance osteoconduction. Four different PVAHA composites were synthesized *in situ* by an economical co-precipitation wet methodology. The FTIR spectra of PVAHA composites showed characteristic signals of HA and PVA. The BET surface area of PVAHA composites were in range of 41.3–63.7  $\text{m}^2/\text{g}$ . The composites showed type IV nitrogen adsorption/desorption isotherm, a characteristic for mesoporous material. The pore diameter range (6.3–8.1 nm) of PVAHA composites also confirmed their mesoporous nature. The Barrett–Joyner–Halenda (BJH) pore size distribution curves indicated a narrow pore size distribution. To obtain a homogeneous crack free coating with EPD on stainless steel (SS) plates,

different parameters such as PVA percentages in PVAHA composites, solvent, deposition time and voltage were optimized. The PVAHA composites were stable after EPD as confirmed by FTIR spectra recorded before and after EPD. The SEM images of the coating showed a homogeneous morphology. The thickness of the coating was controlled by varying voltage and time. The best results were obtained with c-PVAHA composite at 30 volts for 5–10 min and current density was around 4.5 to 5 mA. The adhesion strength of c-PVAHA coating was measured by using ASTM standard F1044-99. The average value was approximately  $9.328 \pm 1.58$  MPa.

**Web URL:** <http://www.sciencedirect.com/science/article/pii/S0169433215030524>

**6. Lung, C. Y. K., Sarfraz, Z., Habib, A., Khan, A. S., & Matinlinna, J. P. (2016). Effect of silanization of hydroxyapatite fillers on physical and mechanical properties of a bis-GMA based resin composite. *Journal of the mechanical behavior of biomedical materials*, 54, 283-294.**

**ABSTRACT:**

To evaluate the physical and mechanical properties of an experimental *bis*-GMA-based resin composite incorporated with non-silanized and silanized nano-hydroxyapatite (nHAP) fillers. Experimental *bis*-GMA based resin composites samples which were reinforced with nHAP fillers were prepared. Filler particles were surface treated with a silane coupling agent. Five test groups were prepared: 1. Unfilled, 2. Reinforced with 10 wt% and 30 wt% non-silanized nHAP fillers, and 3. Reinforced with 10 wt% and 30 wt% silanized nHAP fillers. The samples were subjected to tests in dry condition and in deionized water, aged at 37 °C for 30 days. Prepared silanized and non-silanized nHAP were analyzed with Fourier Transform Infrared (FTIR) Spectroscopy and X-ray Photoelectron Spectroscopy (XPS). The micro-hardness and water sorption were evaluated. Data were analyzed by one-way ANOVA ( $p < 0.05$ ). The samples were characterized by FTIR Spectroscopy, Thermogravimetric Analysis and Differential Scanning Calorimetry. The surface morphology of sample surfaces was examined by Scanning Electron Microscope (SEM). The results showed that the water sorption for nHAP fillers reinforced resins was significantly lower than unfilled resins. Surface hardness for resins reinforced with silane treated fillers was superior to unfilled and untreated fillers resins. The resin matrix loaded with

30 wt% silanized-nHAP fillers would improve the physical and mechanical properties of a bis-GMA based resin.

**Web URL:** <http://www.sciencedirect.com/science/article/pii/S1751616115003707>

**7. Rasheed, S., Aziz, H. S., Khan, R. A., Khan, A. M., Rahim, A., Nisar, J., ... & Khan, A. R. (2016). Effect of Li–Cu doping on structural, electrical and magnetic properties of cobalt ferrite nanoparticles. *Ceramics International*, 42(2), 3666-3672.**

**ABSTRACT:**

CoFe<sub>2-2x</sub>Li<sub>x</sub>Cu<sub>x</sub>O<sub>4</sub> (x=0.00, 0.05, 0.1, 0.15, 0.2, 0.25) spinel ferrite nanoparticles have been synthesized using a CTAB assisted hydrothermal method. Structural characterization of the ferrite powders was carried out using X-ray diffraction (XRD) and scanning electron microscopy (SEM). Employing X-ray diffraction analysis, the synthesized samples were found to be in single crystalline phase with crystallite size of 25–29 nm. The microstructural analysis revealed that the shape of particles can be changed considerably by selecting proper content of the dopants. The room temperature resistivity of all the doped samples was observed to decrease with increase in Li–Cu doping up to a value of  $1.9 \times 10^6 \Omega \text{ cm}$ . The dielectric measurements showed the normal Maxwell Wagner type dielectric dispersion due to interfacial polarization. The optimum values of saturation magnetization ( $M_s$ ), remnant magnetization ( $M_r$ ) and coercivity ( $H_c$ ) were found as 46 emu/g, 12 emu/g and 284 Oe respectively for Li–Cu content of x=0.10.

**Web URL:** <http://www.sciencedirect.com/science/article/pii/S0272884215021100>

**8. Mutahir, S., Jończyk, J., Bajda, M., Khan, I. U., Khan, M. A., Ullah, N., ...& Yar, M. (2016). Novel biphenyl bis-sulfonamides as acetyl and butyrylcholinesterase inhibitors: Synthesis, biological evaluation and molecular modeling studies. *Bioorganic chemistry*, 64, 13-20.**

**ABSTRACT:**

A series of new biphenyl bis-sulfonamide derivatives **2a–3p** were synthesized in good to excellent yield (76–98%). The inhibitory potential of the synthesized compounds on acetylcholinesterase (AChE) and butyrylcholinesterase (BuChE) was investigated. Most of the screened compounds showed modest *in vitro* inhibition for both AChE and BChE. Compared to the reference compound eserine ( $IC_{50} 0.04 \pm 0.0001 \mu\text{M}$  for AChE) and ( $IC_{50} 0.85 \pm 0.0001 \mu\text{M}$

for BChE), the  $IC_{50}$  values of these compounds were ranged from  $2.27 \pm 0.01$  to  $123.11 \pm 0.04 \mu\text{M}$  for AChE and  $7.74 \pm 0.07$  to  $<400 \mu\text{M}$  for BuChE. Among the tested compounds, **3p** was found to be the most potent against AChE ( $IC_{50} 2.27 \pm 0.01 \mu\text{M}$ ), whereas **3g** exhibited the highest inhibition for BChE ( $IC_{50} 7.74 \pm 0.07 \mu\text{M}$ ). Structure–activity relationship (SAR) of these compounds was developed and elaborated with the help of molecular docking studies.

**Web URL:** <http://www.sciencedirect.com/science/article/pii/S004520681530033X>

**9. Mishra, R. K., Hayat, A., Catanante, G., Istamboulie, G., & Marty, J. L. (2016). Sensitive quantitation of Ochratoxin A in cocoa beans using differential pulse voltammetry based aptasensor. *Food chemistry*, 192, 799-804.**

**ABSTRACT:**

In this work, we propose for the first time a sensitive Ochratoxin A (OTA) detection in cocoa beans using competitive aptasensor by differential pulse voltammetry (DPV). In the proposed method, biotin labeled and free OTA competed to bind with immobilized aptamer onto the surface of a screen printed carbon electrode (SPCE), and percentage binding was calculated. The detection was performed after adding avidin-ALP to perform avidin–biotin reaction; the signal was generated through a suitable substrate 1-naphthyl phosphate (1-NP), for alkaline phosphatase (ALP). The cocoa samples were extracted and purified using molecular imprinted polymer (MIP) columns specifically designed for OTA. The developed aptasensor showed a good linearity in the range 0.15–5 ng/mL with the limit of detection (LOD) 0.07 ng/mL and 3.7% relative standard deviation (RSD). The aptasensor displayed good recovery values in the range 82.1–85% with 3.87% RSD, thus, demonstrated the efficiency of proposed aptasensor for such matrices.

**Web URL:** <http://www.sciencedirect.com/science/article/pii/S0308814615011139>

**10. Aziz, H. S., Rasheed, S., Khan, R. A., Rahim, A., Nisar, J., Shah, S. M., ...& Khan, A. R. (2016). Evaluation of electrical, dielectric and magnetic characteristics of Al–La doped nickel spinel ferrites. *RSC Advances*, 6(8), 6589-6597.**

**ABSTRACT:**

The paper reports the effects of lanthanum and aluminum ions, on the structural, electrical and magnetic properties of  $\text{NiFe}_2\text{O}_4$  spinel ferrite nanoparticles. The precursors have been synthesized *via* a hydrothermal route in the presence of ascorbic acid (AA) using urea as a reducing agent and fuel for maintaining the uniform morphology and equal particle size distribution. In order to find out the optimum temperature (1023 K) for the formation of the spinel phase of the doped nickel ferrite, thermogravimetric analysis (TGA) for the un-annealed samples was performed. The X-ray diffraction patterns show that  $\text{NiFe}_{2-2x}\text{Al}_x\text{La}_x\text{O}_4$  have been well crystallized to spinel ferrite crystal structure with the  $Fd3m$  space group. The average crystallite size obtained is in the range of 9–19 nm, a size useful for attaining a suitable signal-to-noise ratio in high-density recording media and in electrical devices. In order to render the synthesized samples for diminishing eddy current losses, we were able to enhance the room temperature resistivity through proper selection of dopant used. The dielectric constant and dielectric loss decreased with applied frequency for all the samples showing normal behavior of ferrites. The calculated magnetic parameters such as saturation magnetization ( $M_s$ ), remanence ( $M_r$ ) and coercivity ( $H_c$ ), showed increased values for some Al–La doped samples.

**Web URL:** <http://pubs.rsc.org/-/content/articlelanding/2016/ra/c5ra20981a/unauth#!divAbstract>

**11. Ahmad, P., Khandaker, M. U., Amin, Y. M., Khan, G., Ramay, S. M., Mahmood, A., ...& Muhammad, N. (2016). Catalytic growth of vertically aligned neutron sensitive  $^{10}\text{B}$  boron nitride nanotubes. *Journal of Nanoparticle Research*, 18(1), 25.**

**ABSTRACT:**

$^{10}\text{B}$  boron nitride nanotubes ( $^{10}\text{BNNTs}$ ) are a potential neutron sensing element in a solid-state neutron detector. The aligned  $^{10}\text{BNNT}$  can be used for its potential application without any further purification. Argon-supported thermal CVD is used to achieve vertically aligned  $^{10}\text{BNNT}$  with the help of nucleation sites produced in a thin layer of magnesium–iron alloy deposited at the top of Si substrate. FESEM shows vertically aligned  $^{10}\text{BNNTs}$  with ball-like catalytic tips at top. EDX reveals magnesium (Mg) contents in the tips that refer to catalytic growth of  $^{10}\text{BNNT}$ . HR-TEM shows tubular morphology of the synthesized  $^{10}\text{BNNT}$  with lattice fringes on its outer part having an interlayer spacing of  $\sim 0.34$  nm. XPS shows B 1 s

and N 1 s peaks at 190.5 and 398 eV that correspond to hexagonal <sup>10</sup>Boron nitride (<sup>10</sup>h-BN) nature of the synthesized <sup>10</sup>BNNT, whereas the Mg kll auger peaks at ~301 and ~311 eV represents Mg contents in the sample. Raman spectrum has a peak at 1390 (cm<sup>-1</sup>) that corresponds to E<sub>2g</sub> mode of vibration in <sup>10</sup>h-BN.

**Web URL:** <https://link.springer.com/article/10.1007/s11051-016-3326-0>

**12. Khan, S. U., Khan, F. U., Khan, I. U., Muhammad, N., Badshah, S., Khan, A., ...& Nasrullah, A. (2016). Biosorption of nickel (II) and copper (II) ions from aqueous solution using novel biomass derived from *Nannorrhops ritchiana* (Mazri Palm). *Desalination and Water Treatment*, 57(9), 3964-3974.**

**ABSTRACT:**

In the present research work, *Nannorrhops ritchiana* (Mazri Palm) was used as an effective biosorbent for removal of Cu<sup>2+</sup> and Ni<sup>2+</sup> ions from aqueous solution. *Nannorrhops ritchiana* (Mazri Palm), a dead biomass powder, was used as a low-cost adsorbent without any chemical treatment. In order to estimate the equilibrium parameters, the equilibrium adsorption data were analyzed using Freundlich, Langmuir, and Temkin isotherms. Freundlich isotherms indicated that the sorption capacities on the biomass surfaces increased with increasing initial concentrations of both metals. The adsorption isotherms were correlated with a comparison of linear and non-linear regression analysis. The squares of the errors (SSE) and chi-square test ( $\chi^2$ ) along with the coefficient of determination ( $R^2$ ) were used to determine the best fit isotherm. Langmuir type I was found the best fitting isotherm for adsorption of both Cu<sup>2+</sup> and Ni<sup>2+</sup> ions as compared to the other three Langmuir linear isotherms on the basis of the values for  $R^2$  and other error functions like SSE and  $\chi^2$  obtained from Langmuir-type I linear equation. The present study revealed that *Nannorrhops ritchiana* proved to be an effective, inexpensive, alternative, and environmentally friendly biosorbent for the removal of Cu<sup>2+</sup> and Ni<sup>2+</sup> ions from aqueous solution.

**Web URL:** <http://www.tandfonline.com/doi/abs/10.1080/19443994.2014.989268>

13. Najeeb, S., Khurshid, Z., Zafar, M. S., Khan, A. S., Zohaib, S., Martí, J. M. N., ...& Rehman, I. U. (2016). Modifications in glass ionomer cements: nano-sized fillers and bioactive nanoceramics. *International journal of molecular sciences*, 17(7), 1134.

**ABSTRACT:**

Glass ionomer cements (GICs) are being used for a wide range of applications in dentistry. In order to overcome the poor mechanical properties of glass ionomers, several modifications have been introduced to the conventional GICs. Nanotechnology involves the use of systems, modifications or materials the size of which is in the range of 1–100 nm. Nano-modification of conventional GICs and resin modified GICs (RMGICs) can be achieved by incorporation of nano-sized fillers to RMGICs, reducing the size of the glass particles, and introducing nano-sized bioceramics to the glass powder. Studies suggest that the commercially available nano-filled RMGIC does not hold any significant advantage over conventional RMGICs as far as the mechanical and bonding properties are concerned. Conversely, incorporation of nano-sized apatite crystals not only increases the mechanical properties of conventional GICs, but also can enhance fluoride release and bioactivity. By increasing the crystallinity of the set matrix, apatites can make the set cement chemically more stable, insoluble, and improve the bond strength with tooth structure. Increased fluoride release can also reduce and arrest secondary caries. However, due to a lack of long-term clinical studies, the use of nano-modified glass ionomers is still limited in daily clinical dentistry. In addition to the in vitro and in vivo studies, more randomized clinical trials are required to justify the use of these promising materials. The aim of this paper is to review the modification performed in GIC-based materials to improve their physicochemical properties.

**Web URL:** <http://www.mdpi.com/1422-0067/17/7/1134/htm>

14. Yar, M., Farooq, A., Shahzadi, L., Khan, A. S., Mahmood, N., Rauf, A., ...& ur Rehman, I. (2016). Novel meloxicam releasing electrospun polymer/ceramic reinforced biodegradable membranes for periodontal regeneration applications. *Materials Science and Engineering: C*, 64, 148-156.

**ABSTRACT:**

Periodontal disease is associated with the destruction of periodontal tissues, along with other disorders/problems including inflammation of tissues and severe pain. This paper reports the synthesis of meloxicam (MX) immobilized biodegradable chitosan (CS)/poly(vinyl alcohol) (PVA)/hydroxyapatite (HA) based electrospun (e-spun) fibers and films. Electrospinning was employed to produce drug loaded fibrous mats, whereas films were generated by solvent casting method. *In-vitro* drug release from materials containing varying concentrations of MX revealed that the scaffolds containing higher amount of drug showed comparatively faster release. During initial first few hours fast release was noted from membranes and films; however after around 5 h sustained release was achieved. The hydrogels showed good swelling property, which is highly desired for soft tissue engineered implants. To investigate the biocompatibility of our synthesized materials, VERO cells (epithelial cells) were selected and cell culture results showed that these all materials were non-cytotoxic and also these cells were very well proliferated on these synthesized scaffolds. These properties along with the anti-inflammatory potential of our fabricated materials suggest their effective utilization in periodontal treatments

**Web URL:** <http://www.sciencedirect.com/science/article/pii/S0928493116302478>

**15. Shah, A. T., Ahmad, S., Kashif, M., Khan, M. F., Shahzad, K., Tabassum, S., & Mujahid, A. (2016). In situ synthesis of copper nanoparticles on SBA-16 silica spheres. *Arabian Journal of Chemistry*, 9(4), 537-541.**

**ABSTRACT:**

A chemical method for in situ synthesis of copper nanoparticles on SBA-16 silica spheres under ambient conditions has been reported. The silica support has been introduced into copper precursor solution before chemical reduction. Metal ions diffuse into mesopores (pore diameter 5–7 nm) of silica where in situ reduction by hydrazine leads to formation of nanoparticles. These mesopores act as nanoreactor and their walls prevent metal particle's agglomeration by providing a physical barrier. The obtained copper nanoparticles have been investigated by electron microscopy, X-ray diffraction, UV–Visible spectroscopy, Fourier transform Infra-red spectroscopy and thermogravimetric analyzer. SEM, TEM and UV–Visible spectroscopic images revealed that nanosized particles have been successfully synthesized by

this method. Thermogravimetric investigations revealed that copper nanoparticles impregnated on silica were thermally more stable compared to unsupported nanoparticles. Silica not only helps in maintaining the particle size but also makes nanoparticles stable at high temperatures due to its thick pore walls. Macro sized silica support also makes separation/handling of nanoparticles easy and simple.

**Web URL:** <http://www.sciencedirect.com/science/article/pii/S1878535214000483>

**16. Bülbül, G., Hayat, A., Liu, X., & Andreescu, S. (2016). Reactivity of nanoceria particles exposed to biologically relevant catechol-containing molecules. *RSC Advances*, 6(65), 60007-60014.**

**ABSTRACT:**

The interaction of nanoceria particles with catechol-like molecules of physiological importance, including dopamine, norepinephrine, epinephrine, serotonin, 3,4 dihydroxyphenylacetic acid (DOPAC) and L-3-(3,4-dihydroxyphenylalanine) (L-DOPA) was studied to obtain predictive information of their behavior in biological systems. A suite of complementary techniques including UV-Vis spectroscopy, electrochemistry, dynamic light scattering (DLS), thermogravimetric analysis (TGA) and Fourier transform infrared spectroscopy (FTIR) demonstrated alteration in the spectral, redox and surface properties of nanoceria exposed to these molecules in an aqueous environment. Binding of catechol to the surface of nanoceria diminished the oxidase-like activity of these particles against an organic dye, TMB (3,3',5,5'-tetramethylbenzidine), but enhanced their ability to react with and inactivate reactive oxygen species. Therefore, the reactivity of these particles can be modulated by addition of catechol-like molecules. These findings can help develop predictive models of the behavior and potential effects of nanoceria particles in complex environments.

**Web URL:** <http://pubs.rsc.org/-/content/articlelanding/2016/ra/c6ra07279h/unauth#!divAbstract>

**17. Catanante, G., Mishra, R. K., Hayat, A., & Marty, J. L. (2016). Sensitive analytical performance of folding based biosensor using methylene blue tagged aptamers. *Talanta*, 153, 138-144.**

**ABSTRACT:**

This work demonstrates the development of a folding based electrochemical aptasensor using methylene blue (MB) tagged anti-Ochratoxin A (OTA) aptamers. Different aptamer coupling strategies were tested using Hexamethylenediamine, polyethylene glycol, simple adsorption and diazonium coupling mechanism. The best sensitivity was recorded by oxidation of amines using hexamethylenediamine (HDMA) on screen printed carbon electrode (SPCE). To achieve the direct detection of OTA, aptamer conjugated redox probe was used and detection was demonstrated based on the conformational changes in aptamer structure upon OTA sensing. Signaling in this class of sensors arises from changes in electron transfer efficiency upon target-induced changes in the conformation/flexibility of the aptamer probe. These changes can be readily recorded electrochemically. The developed aptasensor is unique in its own mechanism as redox probe tagged aptamer coupling such as MB has never been tried to immobilize using long carbon chain spacers as, addition of spacers would provide more sensitive detection methods. A good dynamic range 0.01–5 ng/ml was obtained for OTA with Limit of detection (LOD) 0.01 ng/ml and Limit of quantification (LOQ) of 0.03 ng/ml respectively. The good reproducibility was recorded with RSD% of 3.75. The obtained straight line equation was  $y=0.4035x+0.90311$ ,  $r=0.9976$ . We believe that the sensor design guidelines outlined here represents a general strategy for developing new folding-based electrochemical aptasensors. The developed aptasensor was extended to screen cocoa samples for OTA contamination. The cocoa samples were extracted and purified using molecular imprinted polymer (MIP) columns. The aptasensor displayed good recovery values in the range 84–85% thus, exhibited the effectiveness of proposed aptasensor for such complex matrices.

**Web URL:** <http://www.sciencedirect.com/science/article/pii/S0039914016301321>

**18. Khan, A. S., Man, Z., Bustam, M. A., Kait, C. F., Khan, M. I., Muhammad, N., ... & Ahmad, P. (2016). Impact of ball-milling pretreatment on pyrolysis behavior and kinetics of crystalline cellulose. *Waste and Biomass Valorization*, 7(3), 571-581.**

**ABSTRACT:**

Effect of ball-milling pretreatment on pyrolysis characteristics of cellulose was studied by thermogravimetric analysis (TGA) at four different heating rates; 5, 10, 20, and 40 K/min.

Variation in the thermal stability and activation energy of cellulose with ball-milling were calculated by TGA Kinetics using Kissinger, Kissinger–Akahira–Sunose, Flynn–Wall–Ozawa and Starink model free methods. Results demonstrated that ball-milling reduced the thermal stability and activation energy of cellulose. The original and ball-milled cellulose were thoroughly characterized by Fourier-transform infrared spectroscopy, X-ray diffraction, and Scanning electron microscopy. X-ray diffraction analysis revealed that ball-milling decreased the crystallinity of cellulose from 93 to 51 %. The results suggested that ball-milling pretreatment led to effective disruption of crystalline cellulose to amorphous cellulose. It is, therefore, concluded that the ball-milled cellulose can easily become a useful source of chemicals and energy than crystalline cellulose.

**Web URL:** [https://www.researchgate.net/publication/288827915\\_Impact\\_of\\_Ball-Milling\\_Pretreatment\\_on\\_Pyrolysis\\_Behavior\\_and\\_Kinetics\\_of\\_Crystalline\\_Cellulose](https://www.researchgate.net/publication/288827915_Impact_of_Ball-Milling_Pretreatment_on_Pyrolysis_Behavior_and_Kinetics_of_Crystalline_Cellulose)

19. Khan, F. U., Khanc, A. U., Hussain, J., Khan, I. U., Muhammad, N., Khan, A., ... & Gilani, A. H. (2016). Spasmolytic and Ca<sup>++</sup> Channel Blocking Potential of Nepetolide: Isolated from *Nepeta suaveis*. *Natural product communications*, 11(5), 591-592.

**ABSTRACT:**

*Nepeta suaveis* is used in traditional medicine for treatment of abdominal spasm (colic). The tricyclic clerodane type diterpene, nepetolide, isolated for the first time from *Nepeta suaveis*, was evaluated for Ca<sup>++</sup> antagonist and antispasmodic activities. When studied in isolated rabbit jejunum, nepetolide caused concentration-dependent (0.03-100 μM) relaxation of spontaneous and high K<sup>+</sup> (80 mM)-induced contractions, like that caused by verapamil, indicating that nepetolide exhibits spasmolytic activity, possibly mediated through Ca<sup>++</sup> channel blocking action, which provides scientific explanation for the medicinal application of *Nepeta suaveis* as an antispasmodic agent.

**Web URL:** <http://europepmc.org/abstract/med/27319124>

20. Bülbül, G., Hayat, A., & Andreescu, S. (2016). ssDNA-Functionalized Nanoceria: A Redox-Active Aptaswitch for Biomolecular Recognition. *Advanced healthcare materials*, 5(7), 822-828.

**ABSTRACT:**

Quantification of biomolecular binding events is a critical step for the development of biorecognition assays for diagnostics and therapeutic applications. This paper reports the design of redox-active switches based on aptamer conjugated nanoceria for detection and quantification of biomolecular recognition. It is shown that the conformational transition state of the aptamer on nanoceria, combined with the redox properties of these particles can be used to create surface based structure switchable aptasensing platforms. Changes in the redox properties at the nanoceria surface upon binding of the ssDNA and its target analyte enables rapid and highly sensitive measurement of biomolecular interactions. This concept is demonstrated as a general applicable method to the colorimetric detection of DNA binding events. An example of a nanoceria aptaswitch for the colorimetric sensing of Ochratoxin A (OTA) and applicability to other targets is provided. The system can sensitively and selectivity detect as low as  $0.15 \times 10^{-9}\text{M}$  OTA. This novel assay is simple in design and does not involve oligonucleotide labeling or elaborate nanoparticle modification steps. The proposed mechanism discovered here opens up a new way of designing optical sensing methods based on aptamer recognition. This approach can be broadly applicable to many bimolecular recognition processes and related applications.

**Web URL:** <http://onlinelibrary.wiley.com/doi/10.1002/adhm.201500705/full>

**21. Sharif, F., Rehman, I. U., Muhammad, N., & MacNeil, S. (2016). Dental materials for cleft palate repair. *Materials Science and Engineering: C*, 61, 1018-1028.**

**ABSTRACT:**

Numerous bone and soft tissue grafting techniques are followed to repair cleft of lip and palate (CLP) defects. In addition to the gold standard surgical interventions involving the use of autogenous grafts, various allogenic and xenogenic graft materials are available for bone regeneration. In an attempt to discover minimally invasive and cost effective treatments for cleft repair, an exceptional growth in synthetic biomedical graft materials have occurred. This study gives an overview of the use of dental materials to repair cleft of lip and palate (CLP). The eligibility criteria for this review were case studies, clinical trials and retrospective studies on the use of various types of dental materials in surgical repair of cleft palate defects. Any data

available on the surgical interventions to repair alveolar or palatal cleft, with natural or synthetic graft materials was included in this review. Those datasets with long term clinical follow-up results were referred to as particularly relevant. The results provide encouraging evidence in favor of dental and other related biomedical materials to fill the gaps in clefts of lip and palate. The review presents the various bones and soft tissue replacement strategies currently used, tested or explored for the repair of cleft defects. There was little available data on the use of synthetic materials in cleft repair which was a limitation of this study. In conclusion although clinical trials on the use of synthetic materials are currently underway the uses of autologous implants are the preferred treatment methods to date.

**Web URL:**

[https://www.researchgate.net/profile/Nawshad\\_Muhammad/publication/295086710\\_Dental\\_materials\\_for\\_cleft\\_palate\\_repair/links/570bda7c08ae8883a1ffdc9.pdf](https://www.researchgate.net/profile/Nawshad_Muhammad/publication/295086710_Dental_materials_for_cleft_palate_repair/links/570bda7c08ae8883a1ffdc9.pdf)

**22. Rehman, F., Gul, S., Hussain, S., & Khan, S. (2016). NEW SPECTROPHOTOMETRY METHOD FOR THE DETERMINATION OF MIRTAZAPINE IN PHARMACEUTICAL FORMULATIONS. *Journal of the Chilean Chemical Society*, 61(2), 2913-2915.**

**ABSTRACT:**

A simple extractive spectrophotometric method has been developed for the quantification of mirtazapine. This method is based on the formation of ion-association complex of mirtazapine drug with bromocresol purple dye. The absorbance of the complex was measured at 400 nm. The method was successfully applied to the determination of mirtazapine in their pharmaceutical formulations. The method shows a linear range from 0.2-10  $\mu\text{g mL}^{-1}$  with a molar absorptivity of  $1.53 \times 10^4 \text{ L mol}^{-1} \text{ cm}^{-1}$ . The limit of detection (LOD) and limit of quantification (LOQ) were found to be  $0.096 \mu\text{g mL}^{-1}$  and  $0.32 \mu\text{g mL}^{-1}$  respectively. The developed methodology was successfully applied for the determination of mirtazapine in commercial formulation and the percentage recovery was found  $99.91 \pm 0.15$ . The developed methodology promises a feasible, low cost and an efficient method for the routine analysis.

**Web URL:** [http://www.scielo.cl/scielo.php?pid=S0717-97072016000200013&script=sci\\_arttext](http://www.scielo.cl/scielo.php?pid=S0717-97072016000200013&script=sci_arttext)

23. Rhouati, A., Hayat, A., Mishra, R. K., Bueno, D., Shahid, S. A., Muñoz, R., & Marty, J. L. (2016). Ligand Assisted Stabilization of Fluorescence Nanoparticles; an Insight on the Fluorescence Characteristics, Dispersion Stability and DNA Loading Efficiency of Nanoparticles. *Journal of fluorescence*, 26(4), 1407-1414.

**ABSTRACT:**

This work reports on the ligand assisted stabilization of Fluospheres® carboxylate modified nanoparticles (FCMNPs), and subsequently investigation on the DNA loading capacity and fluorescence response of the modified particles. The designed fluorescence bioconjugate was characterized with enhanced fluorescence characteristics, good stability and large surface area with high DNA loading efficiency. For comparison purpose, bovine serum albumin (BSA) and polyethylene glycol (PEG) with three different length strands were used as cross linkers to modify the particles, and their DNA loading capacity and fluorescence characteristics were investigated. By comparing the performance of the particles, we found that the most improved fluorescence characteristics, enhanced DNA loading and high dispersion stability were obtained, when employing PEG of long spacer arm length. The designed fluorescence bioconjugate was observed to maintain all its characteristics under varying pH over an extended period of time. These types of bioconjugates are in great demand for fluorescence imaging and in vivo fluorescence biomedical application, especially when most of the synthesized fluorescence particles cannot withstand to varying in vivo physiological conditions with decreases in fluorescence response and DNA loading efficiency.

**Web URL:**

[https://www.researchgate.net/profile/Rupesh\\_Mishra6/publication/303462437\\_Ligand\\_Assisted\\_Stabilization\\_of\\_Fluorescence\\_Nanoparticles\\_an\\_Insight\\_on\\_the\\_Fluorescence\\_Characteristics\\_Dispersion\\_Stability\\_and\\_DNA\\_Loading\\_Efficiency\\_of\\_Nanoparticles/links/5747bc9b08aef66a78b08125/Ligand-Assisted-Stabilization-of-Fluorescence-Nanoparticles-an-Insight-on-the-Fluorescence-Characteristics-Dispersion-Stability-and-DNA-Loading-Efficiency-of-Nanoparticles.pdf](https://www.researchgate.net/profile/Rupesh_Mishra6/publication/303462437_Ligand_Assisted_Stabilization_of_Fluorescence_Nanoparticles_an_Insight_on_the_Fluorescence_Characteristics_Dispersion_Stability_and_DNA_Loading_Efficiency_of_Nanoparticles/links/5747bc9b08aef66a78b08125/Ligand-Assisted-Stabilization-of-Fluorescence-Nanoparticles-an-Insight-on-the-Fluorescence-Characteristics-Dispersion-Stability-and-DNA-Loading-Efficiency-of-Nanoparticles.pdf)

**24. Shah, A. T., Batool, M., Chaudhry, A. A., Iqbal, F., Javaid, A., Zahid, S., ... & ur Rehman, I. (2016). Effect of calcium hydroxide on mechanical strength and biological properties of bioactive glass. *Journal of the mechanical behavior of biomedical materials*, 61, 617-626.**

**ABSTRACT:**

In this manuscript for the first time calcium hydroxide ( $\text{Ca}(\text{OH})_2$ ) has been used for preparation of bioactive glass (BG-2) by co-precipitation method and compared with glass prepared using calcium nitrate tetrahydrate  $\text{Ca}(\text{NO}_3)_2 \cdot 4\text{H}_2\text{O}$  (BG-1), which is a conventional source of calcium. The new source positively affected physical, biological and mechanical properties of BG-2. The glasses were characterized by Fourier transform infrared (FTIR), X-Ray Diffractometer (XRD), Scanning Electron Microscopy (SEM), Thermogravimetric Analysis/Differential Scanning Calorimetry (TGA-DSC), BET surface area analysis and Knoop hardness. The results showed that BG-2 possessed relatively larger surface properties ( $100 \text{ m}^2 \text{ g}^{-1}$  surface area) as compared to BG-1 ( $78 \text{ m}^2 \text{ g}^{-1}$ ), spherical morphology and crystalline phases (wollastonite and apatite) after sintering at lower than conventional temperature. These properties contribute critical role in both mechanical and biological properties of glasses. The Knoop hardness measurements revealed that BG-2 possessed much better hardness ( $0.43 \pm 0.06 \text{ GPa}$  at  $680^\circ\text{C}$  and  $2.16 \pm 0.46 \text{ GPa}$  at  $980^\circ\text{C}$ ) than BG-1 ( $0.24 \pm 0.01$  at  $680^\circ\text{C}$  and  $0.57 \pm 0.07 \text{ GPa}$  at  $980^\circ\text{C}$ ) under same conditions. Alamar blue Assay and confocal microscopy revealed that BG-2 exhibited better attachment and proliferation of MG63 cells. Based on the improved biological properties of BG-2 as a consequent of novel calcium source selection, BG-2 is proposed as a bioactive ceramic for hard tissue repair and regeneration applications.

**Web URL:** <http://www.sciencedirect.com/science/article/pii/S1751616116300509>

**25. Nasrullah, A., Khan, H., Khan, A. S., Muhammad, N., Man, Z., Khan, F. U., & Ullah, Z. (2016). Calligonum polygonoides biomass as a low-cost adsorbent: surface characterization and methylene blue adsorption characteristics. *Desalination and Water Treatment*, 57(16), 7345-7357.**

**ABSTRACT:**

In this present research work, *Calligonum polygonoides* (CP) was used as an effective biosorbent for the methylene blue (MB) removal from aqueous solution. The biosorbent was

used without any chemical treatment. The biosorbent was characterized by various techniques, such as Fourier transform infrared spectroscopy, thermogravimetric analysis, and scanning electron microscopy (SEM). The particle size and surface area were measured by using particle size analyzer and Brunauer–Emmett–Teller (BET) equation. The SEM and BET results expressed that the adsorbent has porous nature. Effect of various experimental conditions, such as initial concentration of MB, initial pH, contact time, dosage of biosorbent, and stirring rate, were also investigated on adsorption capacity of MB on CP. The contact time experiment indicated that the rate of adsorption of MB is a rapid process and equilibrium is reached in 1 h. The kinetics study expressed that MB adsorption on biosorbent followed the pseudo-second order kinetic equation with correlation coefficient value ( $R^2$ ) of 0.999. The study revealed that CP proved to be an effective, inexpensive, alternative, and environmentally friendly biosorbent for MB from aqueous solution.

**Web URL:**

<http://www.tandfonline.com/doi/full/10.1080/19443994.2015.1024742?scroll=top&needAccess=true>

**26. Khan, Z. U. H., Khan, A., Shah, A., Wan, P., Chen, Y., Khan, G. M., ... & Khan, H. U. (2016). Enhanced photocatalytic and electrocatalytic applications of green synthesized silver nanoparticles. *Journal of Molecular liquids*, 220, 248-257.**

**ABSTRACT:**

A green facile, cheap, nontoxic and eco-friendly procedure was developed for the synthesis of silver nanoparticle (AgNPs) using extract of *Cirsium japonicum* that is useful than commonly used physiochemical methods. The extract of *C. japonicum* was used as reducing and stabilizing agent. The formation of AgNPs was confirmed by UV/vis spectroscopic technique. The formation of AgNPs was studied at different range of temperature and concentration. Size and distribution was confirmed by high resolution transmission electron microscopy (HRTEM) and were found to be small (2–8 nm), spherical and with no aggregation. X-ray diffraction (XRD) helped to confirm the crystalline nature AgNPs. For elemental composition of the material, EDX was used. FTIR spectroscopy was used to detect organic compounds capping AgNPs. The effect

of various experimental conditions, size and shape and catalytic amount were studied on the photodegradation of bromo phenyl blue. AgNPs are found significant photocatalysts and degraded 98% bromo phenyl blue in 12 min. From the strong reductive properties it is clear that AgNPs can be used in water purification and converting some organic hazardous to non-hazardous materials. Furthermore the AgNPs adapted electrode (Ag/GC) exhibited tremendous electro-catalytic properties to reduce phenolic compounds like hydroquinone. Cyclic voltammetric analysis of AgNPs was studied in acetate buffer solution. The result of modified AgNPs and standard glassy carbon electrode (GC) were compared. The conductivity of AgNPs was studied in 0.15 M acetate buffer solution. The synthesized AgNPs are stable and analogous in size. The synthesized AgNPs showed potential activities in the field of electrochemistry.

**Web URL:** <http://www.sciencedirect.com/science/article/pii/S0167732215312381>

**27. Catanante, G., Rhouati, A., Hayat, A., & Marty, J. L. (2016). An overview of recent electrochemical immunosensing strategies for mycotoxins detection. *Electroanalysis*, 28(8), 1750-1763.**

**ABSTRACT:**

Electrochemical immunosensors are affinity ligand based biosensors based on solid state devices in which immunochemical reactions are coupled to a transducer surface to generate the output electrochemical signal. The concept of immunosensor methodology is similar to conventional ELISA based immunoassays; however, in contrast to immunoassays, modern transducer technology permits the highly sensitive quantification of the immune complex in diverse ways. Mycotoxins are naturally occurring toxic secondary metabolites produced by fungi contaminating food and feed and are responsible for mycotoxicosis with symptoms of intoxication causing substantial effects on animal and human health. Based on the adverse effect, it has been very crucial to develop ultrasensitive sensing methodologies to ensure food safety and prevent risks in agro-food and environmental sector. For these purposes, many electrochemical immunosensors based on different analyzing techniques have been reported for mycotoxins monitoring. In this review paper, we provided a general overview on the practical aspects of electrochemical immunosensor designs such as assay format, choice of the transducer surface, immobilization methodologies, signal generating probe and type of output

electrochemical signal. In doing so, we also reviewed the recent development in electrochemical immunosensor applications for mycotoxin analysis.

**Web URL:** <http://onlinelibrary.wiley.com/doi/10.1002/elan.201600181/full>

**28. Goud, K. Y., Sharma, A., Hayat, A., Catanante, G., Gobi, K. V., Gurban, A. M., & Marty, J. L. (2016). Tetramethyl-6-carboxyrhodamine quenching-based aptasensing platform for aflatoxin B1: Analytical performance comparison of two aptamers. *Analytical biochemistry*, 508, 19-24.**

**ABSTRACT:**

In this study, a simple TAMRA (tetramethyl-6-carboxyrhodamine) quenching-based aptasensing platform was designed for the detection of aflatoxin B1 (AFB1). Here, we compared the analytical performance of two aptamer sequences: seqA and seqB. The AFB1 detection was based on the interactions of FAM (carboxyfluorescein)-labeled aptamer with TAMRA-labeled DNA complementary strand in the presence and absence of target analyte. Under optimized experimental conditions, TAMRA-labeled strand quenched the fluorescence response of FAM-labeled aptamer due to the noncovalent interaction between the two DNA strands. The binding of AFB1 induced the complex formation and weakened the interaction between FAM-labeled aptamer and TAMRA-labeled complementary strand, resulting in the fluorescence recovery. By using this principle concept, an assay was constructed for the detection of AFB1. The method exhibited good sensitivity, good selectivity with a limit of detection of  $0.2 \text{ ng ml}^{-1}$ , and a wide linear range from  $0.25$  to  $32 \text{ ng ml}^{-1}$ . For real sample application, the aptasensors were tested in beer and wine samples, with good recovery rates obtained for AFB1 detection.

**Web URL:** <http://www.sciencedirect.com/science/article/pii/S0003269716300938>

**29. Sharma, A., Catanante, G., Hayat, A., Istamboulie, G., Rejeb, I. B., Bhand, S., & Marty, J. L. (2016). Development of structure switching aptamer assay for detection of aflatoxin M1 in milk sample. *Talanta*, 158, 35-41.**

**ABSTRACT:**

The discovery of in-vitro systematic evolution of ligands by exponential enrichment (SELEX) process has considerably broaden the utility of aptamer as bio-recognition element, providing the high binding affinity and specificity against the target analytes. Recent research has

focused on the development of structure switching signaling aptamer assay, transducing the aptamer- target recognition event into an easily detectable signal. In this paper, we demonstrate the development of structure switching aptamer assay for determination of aflatoxin M1 (AFM1) employing the quenching-dequenching mechanism. Hybridization of fluorescein labelled anti-AFM1 aptamer (F-aptamer) with TAMRA labelled complementary sequences (Q-aptamer) brings the fluorophore and the quencher into close proximity, which results in maximum fluorescence quenching. On addition of AFM1, the target induced conformational formation of antiparallel G-quadruplex aptamer-AFM1 complex results in fluorescence recovery. Under optimized experimental conditions, the developed method showed the good linearity with limit of detection (LOD) at 5.0 ng kg<sup>-1</sup> for AFM1. The specificity of the sensing platform was carefully investigated against aflatoxin B1 (AFB1) and ochratoxin A (OTA). The developed assay platform showed the high specificity towards AFM1. The practical application of the developed aptamer assay was verified for detection of AFM1 in spiked milk samples. Good recoveries were obtained in the range from 94.40% to 95.28% (n=3) from AFM1 spiked milk sample.

**Web URL:**

[https://www.researchgate.net/profile/Atul\\_Sharma15/publication/303179679\\_Development\\_of\\_structure\\_switching\\_aptamer\\_assay\\_for\\_detection\\_of\\_aflatoxin\\_M1\\_in\\_milk\\_sample/links/574eb2af08ae789584d7173c/Development-of-structure-switching-aptamer-assay-for-detection-of-aflatoxin-M1-in-milk-sample.pdf](https://www.researchgate.net/profile/Atul_Sharma15/publication/303179679_Development_of_structure_switching_aptamer_assay_for_detection_of_aflatoxin_M1_in_milk_sample/links/574eb2af08ae789584d7173c/Development-of-structure-switching-aptamer-assay-for-detection-of-aflatoxin-M1-in-milk-sample.pdf)

**30. Shahzad, S., Shahzadi, L., Mahmood, N., Siddiqi, S. A., Rauf, A., Manzoor, F., ... & Yar, M. (2016). A new synthetic methodology for the preparation of biocompatible and organo-soluble barbituric-and thiobarbituric acid based chitosan derivatives for biomedical applications. *Materials Science and Engineering: C*, 66, 156-163.**

**ABSTRACT:**

Chitosan's poor solubility especially in organic solvents limits its use with other organo-soluble polymers; however such combinations are highly required to tailor their properties for specific biomedical applications. This paper describes the development of a new synthetic methodology

for the synthesis of organo-soluble chitosan derivatives. These derivatives were synthesized from chitosan (CS), triethyl orthoformate and barbituric or thiobarbituric acid in the presence of 2-butanol. The chemical interactions and new functional motifs in the synthesized CS derivatives were evaluated by FTIR, DSC/TGA, UV/VIS, XRD and  $^1\text{H}$  NMR spectroscopy. A cytotoxicity investigation for these materials was performed by cell culture method using VERO cell line and all the synthesized derivatives were found to be non-toxic. The solubility analysis showed that these derivatives were readily soluble in organic solvents including DMSO and DMF. Their potential to use with organo-soluble commercially available polymers was exploited by electrospinning; the synthesized derivatives in combination with polycaprolactone delivered nanofibrous membranes.

**Web URL:**

[https://www.researchgate.net/profile/Lubna\\_Shahzadi/publication/303088713\\_A\\_new\\_synthetic\\_methodology\\_for\\_the\\_preparation\\_of\\_biocompatible\\_and\\_organosoluble\\_barbituric\\_and\\_thiobarbituric\\_acid\\_based\\_chitosan\\_derivatives\\_for\\_biomedical\\_applications/links/573a912a08aea45ee83f93a5.pdf](https://www.researchgate.net/profile/Lubna_Shahzadi/publication/303088713_A_new_synthetic_methodology_for_the_preparation_of_biocompatible_and_organosoluble_barbituric_and_thiobarbituric_acid_based_chitosan_derivatives_for_biomedical_applications/links/573a912a08aea45ee83f93a5.pdf)

**31. Afzal, A., Atiq, S., Saleem, M., Ramay, S. M., Naseem, S., & Siddiqi, S. A. (2016). Structural and magnetic phase transition of sol-gel-synthesized  $\text{Cr}_2\text{O}_3$  and  $\text{MnCr}_2\text{O}_4$  nanoparticles. *Journal of Sol-Gel Science and Technology*, 80(1), 96-102.**

**ABSTRACT:**

$\text{Cr}_2\text{O}_3$  and  $\text{MnCr}_2\text{O}_4$  spinel chromite nanoparticles were synthesized using chemically derived sol-gel technique. Crystal structure was analyzed using X-ray diffraction, and phase transition from a rhombohedral symmetry (R-3c) for  $\text{Cr}_2\text{O}_3$  to a spinel cubic symmetry (Fd3 m) for  $\text{MnCr}_2\text{O}_4$  has been observed. Data obtained from diffraction were also utilized to evaluate the lattice parameters, crystallite size and unit cell volume. Micrographs obtained using a field emission scanning electron microscope exhibited well-shaped, homogeneously distributed 30–70-nm-sized nanoparticles, with well-defined grain. Stoichiometric composition of all the elements present in the samples was confirmed using energy-dispersive X-ray spectroscopy. Dynamic light scattering measurement was performed to corroborate the hydrodynamic diameter and distribution of  $\text{Cr}_2\text{O}_3$  and  $\text{MnCr}_2\text{O}_4$  nanoparticles. The magnetic behavior of

samples was scrutinized as a function of temperature and applied field. It was observed that Cr<sub>2</sub>O<sub>3</sub> exhibited paramagnetic behavior both at room temperature and at 5 K, while a magnetic phase transition from ferro to para was observed in MnCr<sub>2</sub>O<sub>4</sub> with a Curie temperature,  $T_c \approx 50$  K.

**Web URL:**

[https://www.researchgate.net/profile/Saadat\\_Anwar\\_Siddiqi/publication/303037013\\_Structural\\_and\\_magnetic\\_phase\\_transition\\_of\\_sol-gel-synthesized\\_Cr2O3\\_and\\_MnCr2O4\\_nanoparticles/links/573d952d08aea45ee842adf9.pdf](https://www.researchgate.net/profile/Saadat_Anwar_Siddiqi/publication/303037013_Structural_and_magnetic_phase_transition_of_sol-gel-synthesized_Cr2O3_and_MnCr2O4_nanoparticles/links/573d952d08aea45ee842adf9.pdf)

**32. Bueno, D., Mishra, R. K., Hayat, A., Catanante, G., Sharma, V., Muñoz, R., & Marty, J. L. (2016). Portable and low cost fluorescence set-up for in-situ screening of Ochratoxin A. *Talanta*, 159, 395-400.**

**ABSTRACT:**

The present article describes a portable and low cost fluorescence set-up designed and characterized for in-situ screening of Ochratoxin A (OTA) in cocoa samples at field settings. The sensing module (the set up) consists of a LED with the wavelength of 370–380 nm and a color complementary metal oxide semiconductor (CMOS) micro-camera inbuilt at upright position of a black box to obtain an image of the sensing molecule. It allows the user to get an image of the sensing analytes under excitation conditions and process the image in order to predict the toxicity of the samples. The image capturing and processing of the system was based on the OTA concentration in the sample and analyzed data can be presented as RGB values. For each concentration of the OTA, the R, G, B co-ordinates were obtained and plotted to quantify actual OTA presents in the sample. Moreover, the system was tested for real sample analysis using cocoa contaminated with OTA. The system could detect OTA as low as 1.25 ng/ml with the maximum recovery of 87.5% in cocoa samples. The OTA was extracted in 1% NaHCO<sub>3</sub> and cleaned up using molecular imprinted polymer column (MIP). The method demonstrated a good linear range between 1.25 and 10 ng/ml. The obtained results were cross validated using chromatographic method HPLC and also compared with commercially available fluorescence instrument. The developed fluorescence setup is simple, economical, and portable with added advantages of digital image processing. The system could be deployable to cocoa fields for

monitoring of OTA in quick successions. It is noteworthy to mention that this is the first report of such portable fluorescence setup where, OTA sensing was explored.

**Web URL:** <http://www.sciencedirect.com/science/article/pii/S0039914016304647>

**33. Shahzadi, L., Yar, M., Jamal, A., Siddiqi, S. A., Chaudhry, A. A., Zahid, S., ... & MacNeil, S. (2016). Triethyl orthoformate covalently cross-linked chitosan-(poly vinyl) alcohol based biodegradable scaffolds with heparin-binding ability for promoting neovascularisation. *Journal of biomaterials applications*, 31(4), 582-593.**

**ABSTRACT:**

There is a need to develop pro-angiogenic biomaterials to promote wound healing and to assist in regenerative medicine. To this end, various growth factors have been exploited which have the potential to promote angiogenesis. However, these are generally expensive and labile which limits their effectiveness. An alternative approach is to immobilize heparin onto biocompatible degradable hydrogels. The heparin in turn will then bind endogenous proangiogenic growth factors to induce formation of new blood vessels.

In this study, we continue our development of hydrogels for wound healing purposes by exploring covalently cross-linking chitosan and polyvinyl alcohol hydrogels using triethyl orthoformate. Two concentrations of triethyl orthoformate (4 and 16%) were compared for their effects on the structure of hydrogels – their swelling, pore size, and rate of degradation and for their ability to support the growth of cells and for their heparin-binding capacity and their effects on angiogenesis in a chick chorioallantoic membrane assay.

Hydrogels formed with 4 or 16% both triethyl orthoformate cross-linker were equally cyto-compatible. Hydrogels formed with 4% triethyl orthoformate absorbed slightly more water than those made with 16% triethyl orthoformate and broke down slightly faster than non-cross-linked hydrogels. When soaked in heparin the hydrogel formed with 16% triethyl orthoformate showed more blood vessel formation in the CAM assay than that formed with 4% triethyl orthoformate.

**Web URL:**

<http://journals.sagepub.com/doi/abs/10.1177/0885328216650125?journalCode=jbaa>

**34. Ahmad, P., Khandaker, M. U., Amin, Y. M., Muhammad, N., Khan, G., Khan, A. S., ... & Khan, A. (2016). Synthesis of hexagonal boron nitride fibers within two hour annealing at 500° C and two hour growth duration at 1000° C. *Ceramics International*, 42(13), 14661-14666.**

**ABSTRACT:**

Several advantageous features like low density, large surface area, high porosity and tight pore size make the nanofiber suitable for a wide range of applications from medical to consumer products and industrial to high-tech applications. Present study concerns the synthesis of hexagonal boron nitride fibers ( $\phi=70\text{--}350$  nm) from a mixture of Boron, Magnesium oxide and Iron oxide powders via a simple CVD technique. A relatively long annealing and growth duration of two hours at 500 °C and 1000 °C, respectively were utilized in this synthesis. The synthesized samples seem to have the BNFs of irregular curved human hair-like morphologies in lower resolution and solid cylinder-like structures in high resolution transmission electron microscopy. The presence of Boron and Nitrogen in the synthesized BNF's sample were confirmed via the B 1s peak at 190.7 eV and N 1s peak at 398.3 eV in the XPS survey whereas a major peak at 1370 ( $\text{cm}^{-1}$ ) in the Raman spectrum corresponds to the vibration of  $E_{2g}$  mode in h-BN. The sharp peaks in the XRD pattern verify the h-BN phase and highly crystalline nature of the synthesized BNFs.

**Web URL:** <http://www.sciencedirect.com/science/article/pii/S0272884216309221>

**35. Nawaz, M. A. H., Rauf, S., Catanante, G., Nawaz, M. H., Nunes, G., Marty, J. L., & Hayat, A. (2016). One Step Assembly of Thin Films of Carbon Nanotubes on Screen Printed Interface for Electrochemical Aptasensing of Breast Cancer Biomarker. *Sensors*, 16(10), 1651.**

**ABSTRACT:**

Thin films of organic moiety functionalized carbon nanotubes (CNTs) from a very well-dispersed aqueous solution were designed on a screen printed transducer surface through a single step directed assembly methodology. Very high density of CNTs was obtained on the

screen printed electrode surface, with the formation of a thin and uniform layer on transducer substrate. Functionalized CNTs were characterized by X-ray diffraction spectroscopy (XRD), Fourier transform infrared spectroscopy (FTIR), thermogravimetric analysis (TGA) and Brunauer–Emmett–Teller (BET) surface area analyzer methodologies, while CNT coated screen printed transducer platform was analyzed by scanning electron microscopy (SEM), atomic force microscopy (AFM), cyclic voltammetry (CV) and electrochemical impedance spectroscopy (EIS). The proposed methodology makes use of a minimum amount of CNTs and toxic solvents, and is successfully demonstrated to form thin films over macroscopic areas of screen printed carbon transducer surface. The CNT coated screen printed transducer surface was integrated in the fabrication of electrochemical aptasensors for breast cancer biomarker analysis. This CNT coated platform can be applied to immobilize enzymes, antibodies and DNA in the construction of biosensor for a broad spectrum of applications.

**Web URL:** <http://www.mdpi.com/1424-8220/16/10/1651/htm>

**36. Waheed, N., Mushtaq, A., Tabassum, S., Gilani, M. A., Ilyas, A., Ashraf, F., ... & Khan, A. L. (2016). Mixed matrix membranes based on polysulfone and rice husk extracted silica for CO<sub>2</sub> separation. *Separation and Purification Technology*, 170, 122-129.**

**ABSTRACT:**

Mesoporous silica particles after extraction from rice husk ash were used as fillers in polysulfone based mixed-matrix membranes (MMMs). The fillers were functionalized with 4-aminophenazone (4-AMP) to enhance the CO<sub>2</sub>-philic properties. The attractive feature of this research was the utility of extracted silica from a biological waste -the rice husk ash. A good dispersion and adhesion of the filler within the polymer matrix were confirmed by the gas permeation results, SEM images and FTIR analysis. The results revealed that all MMMs showed high permeabilities in comparison to pristine polysulfone membrane. The higher gas permeabilities were attributed to the presence of large mesopores in the filler that led to faster diffusion of the penetrant gas. The functionalized silica showed significantly higher CO<sub>2</sub>/CH<sub>4</sub> and CO<sub>2</sub>/N<sub>2</sub> selectivities. The highest ideal selectivities obtained for CO<sub>2</sub>/N<sub>2</sub> and CO<sub>2</sub>/CH<sub>4</sub> at a maximum of 40% filler loading, were 32.79 and 33.31 respectively. All synthesized membranes

were tested at various operating temperatures and their activation energies were also calculated. The highly ordered structures with short and straight pore channels and improved gas permeation properties, warrant the silica extracted from rice husk as promising filler for industrial gas separation under varying conditions of temperature.

**Web URL:**

[https://www.researchgate.net/profile/Asad\\_Khan27/publication/304356246\\_Mixed\\_Matrix\\_Membranes\\_Based\\_on\\_Polysulfone\\_and\\_Rice\\_Husk\\_Extracted\\_Silica\\_for\\_CO2\\_Separation/links/5772240a08ae6219474a663c/Mixed-Matrix-Membranes-Based-on-Polysulfone-and-Rice-Husk-Extracted-Silica-for-CO2-Separation.pdf](https://www.researchgate.net/profile/Asad_Khan27/publication/304356246_Mixed_Matrix_Membranes_Based_on_Polysulfone_and_Rice_Husk_Extracted_Silica_for_CO2_Separation/links/5772240a08ae6219474a663c/Mixed-Matrix-Membranes-Based-on-Polysulfone-and-Rice-Husk-Extracted-Silica-for-CO2-Separation.pdf)

**37. Tabassum, S., Zahid, S., Zarif, F., Gilani, M. A., Manzoor, F., Rehman, F., ... & ur Rehman, I. (2016). Efficient drug delivery system for bone repair by tuning the surface of hydroxyapatite particles. *RSC Advances*, 6(107), 104969-104978.**

**ABSTRACT:**

A limited blood flow to skeletal tissues results in minimal therapeutic effect of drugs being administered to a patient using conventional ways. To obtain sufficient amount of drug at an effected site, implanted drug delivery systems based on biomaterials can be used. In this study, surface modified hydroxyapatites (m-HA) were prepared and evaluated as drug delivery systems. The effect of modifiers on surface properties of HA and their *in vitro* drug delivery efficiency were investigated. For synthesis of m-HA, a simple *in situ* co-precipitation method was used. Hydroxyapatite was subjected to surface modification by various carboxylic acids such as adipic acid, malonic acid, succinic acid and stearic acid. This surface modification affected its surface properties such as surface area, pore size, pore volume, particle size and crystallinity. The m-HA were characterized by Fourier transform infrared spectroscopy (FT-IR), X-ray diffraction (XRD) and thermogravimetric analysis (TGA). Brunauer–Emmett–Teller (BET) technique was used to compute surface properties of m-HA. The highest BET surface area of 143 m<sup>2</sup> g<sup>-1</sup> has been found for HA modified with malonic acid and the lowest surface area of 37 m<sup>2</sup> g<sup>-1</sup> was calculated for stearic acid modified HA. The BET adsorption average pore size (17–20 nm) of m-HA confirmed its mesoporous nature. The biocompatible nature of the prepared m-HA was assessed by 3-(4,5)-dimethylthiaziazolo(-

z-yl)-3,5-di-phenyltetrazoliumromide (MTT) assay. To evaluate the influence of functional groups and surface properties of m-HA on drug delivery efficiency, ibuprofen was used as a model drug. *In vitro* drug delivery experimental results indicated that drug loading and release efficiency relied on functional groups, surface area, and porosity of m-HA. The percentage loading of ibuprofen was good for samples containing free  $-\text{COOH}$  groups and high surface area. A drug loading of  $22 \text{ mg g}^{-1}$  has been found for malonic acid modified HA (ma-HA) having high surface area, pore volume, whereas a poor loading of  $2.03 \text{ mg g}^{-1}$  has been observed for stearic acid modified HA (st-HA) sample having low surface area and pore volume. A sustained drug release profile showed that 61% drug had been released from malonic acid modified HA (ma-HA) in 24 hours. A 100% drug release was observed for st-HA in 8 hours. Succinic acid modified HA and adipic acid modified HA exhibited intermediate drug release profiles. The drug release behavior of m-HA followed Fick's laws of diffusion.

**Web URL:** <http://pubs.rsc.org/-/content/articlehtml/2016/ra/c6ra24551j>

**38. Sheikh, Z., Khan, A. S., Roohpour, N., Glogauer, M., & ur Rehman, I. (2016). Protein adsorption capability on polyurethane and modified-polyurethane membrane for periodontal guided tissue regeneration applications. *Materials Science and Engineering: C*, 68, 267-275.**

**ABSTRACT:**

Periodontal disease if left untreated can result in creation of defects within the alveolar ridge. Barrier membranes are frequently used with or without bone replacement graft materials for achieving periodontal guided tissue regeneration (GTR). Surface properties of barrier membranes play a vital role in their functionality and clinical success. In this study polyetherurethane (PEU) membranes were synthesized by using 4,4'-methylene-diphenyl diisocyanate (MDI), polytetramethylene oxide (PTMO) and 1,4-butane diol (BDO) as a chain extender via solution polymerization. Hydroxyl terminated polydimethylsiloxane (PDMS) due to having inherent surface orientation towards air was used for surface modification of PEU on one side of the membranes. This resulting membranes had one surface being PEU and the other being PDMS coated PEU. The prepared membranes were treated with solutions of bovine serum albumin (BSA) in de-ionized water at  $37^\circ\text{C}$  at a pH of 7.2. The surface protein adsorptive potential of PEU membranes was observed using Attenuated Total Reflectance Fourier

Transform Infrared Spectroscopy (ATR-FTIR), Raman spectroscopy and Confocal Raman spectroscopy. The contact angle measurement, tensile strength and modulus of prepared membranes were also evaluated. PEU membrane ( $89.86 \pm 1.62^\circ$ ) exhibited less hydrophobic behavior than PEU-PDMS ( $105.87 \pm 3.16^\circ$ ). The ultimate tensile strength and elastic modulus of PEU ( $27 \pm 1$  MPa and  $14 \pm 2$  MPa) and PEU-PDMS ( $8 \pm 1$  MPa and  $26 \pm 1$  MPa) membranes was in required range. The spectral analysis revealed adsorption of BSA proteins on the surface of non PDMS coated PEU surface. The PDMS modified PEU membranes demonstrated a lack of BSA adsorption. The non PDMS coated side of the membrane which adsorbs proteins could potentially be used facing towards the defect attracting growth factors for periodontal tissue regeneration. Whereas, the PDMS coated side could serve as an occlusive barrier for preventing gingival epithelial cells from proliferating and migrating into the defect space by facing the soft tissue flaps. This study demonstrates the potential of a dual natured PEU barrier membrane for use in periodontal tissue engineering applications and further investigations are required.

**Web URL:** <http://www.sciencedirect.com/science/article/pii/S0928493116304519>

**39. Goud, K. Y., Catanante, G., Hayat, A., Satyanarayana, M., Gobi, K. V., & Marty, J. L. (2016). Disposable and portable electrochemical aptasensor for label free detection of aflatoxin b1 in alcoholic beverages. *Sensors and Actuators B: Chemical*, 235, 466-473.**

**ABSTRACT:**

Aflatoxin B1 (AFB1) is the most prevalent and toxic contaminant for human beings and animals among all the aflatoxins (AFs). Additionally, AFB1 is documented as a highly carcinogenic and mutagenic contaminant in the literature. Therefore, it is of vital importance to monitor AFB1 contamination to reduce its health associated risks. In the present work, we have designed a label-free electrochemical impedimetric aptasensor for aflatoxin B1 detection. Herein, we compared the analytical performances of two aptamer sequences (seqA and seqB). The detection is based on specific recognition by the aptamer covalently-bound as compact monolayer on screen printed carbon electrodes (SPCEs) via diazonium coupling reaction. The quantification of AFB1 was achieved by using electrochemical impedance spectroscopy. A dynamic quantification range from  $0.125 \text{ ng mL}^{-1}$  to  $16 \text{ ng mL}^{-1}$  was obtained with both types of

aptamer sequences while the detection limits were  $0.12 \text{ ng mL}^{-1}$  and  $0.25 \text{ ng mL}^{-1}$  for seqA and seqB respectively. For real sample applications, the developed aptasensors were demonstrated in beer and wine samples, and good recovery levels in the range of 92–102% were recorded for AFB1 detection.

**Web URL:** <http://www.sciencedirect.com/science/article/pii/S0925400516307973>

**40. Rauf, S., Hayat Nawaz, M. A., Badea, M., Marty, J. L., & Hayat, A. (2016). Nano-Engineered Biomimetic Optical Sensors for Glucose Monitoring in Diabetes. *Sensors*, 16(11), 1931.**

**ABSTRACT:**

Diabetes is a rapidly growing disease that can be monitored at an individual level by controlling the blood glucose level, hence minimizing the negative impact of the disease. Significant research efforts have been focused on the design of novel and improved technologies to overcome the limitations of existing glucose analysis methods. In this context, nanotechnology has enabled the diagnosis at the single cell and molecular level with the possibility of incorporation in advanced molecular diagnostic biochips. Recent years have witnessed the exploration and synthesis of various types of nanomaterials with enzyme-like properties, with their subsequent integration into the design of biomimetic optical sensors for glucose monitoring. This review paper will provide insights on the type, nature and synthesis of different biomimetic nanomaterials. Moreover, recent developments in the integration of these nanomaterials for optical glucose biosensing will be highlighted, with a final discussion on the challenges that must be addressed for successful implementation of these nano-devices in the clinical applications is presented.

**Web URL:** <http://www.mdpi.com/1424-8220/16/11/1931/htm>

**41. Vasilescu, A., Nunes, G., Hayat, A., Latif, U., & Marty, J. L. (2016). Electrochemical affinity biosensors based on disposable screen-printed electrodes for detection of food allergens. *Sensors*, 16(11), 1863.**

**ABSTRACT:**

Food allergens are proteins from nuts and tree nuts, fish, shellfish, wheat, soy, eggs or milk which trigger severe adverse reactions in the human body, involving IgE-type antibodies.

Sensitive detection of allergens in a large variety of food matrices has become increasingly important considering the emergence of functional foods and new food manufacturing technologies. For example, proteins such as casein from milk or lysozyme and ovalbumin from eggs are sometimes used as fining agents in the wine industry. Nonetheless, allergen detection in processed foods is a challenging endeavor, as allergen proteins are degraded during food processing steps involving heating or fermentation. Detection of food allergens was primarily achieved via Enzyme-Linked Immuno Assay (ELISA) or by chromatographic methods. With the advent of biosensors, electrochemical affinity-based biosensors such as those incorporating antibodies and aptamers as biorecognition elements were also reported in the literature. In this review paper, we highlight the success achieved in the design of electrochemical affinity biosensors based on disposable screen-printed electrodes towards detection of protein allergens. We will discuss the analytical figures of merit for various disposable screen-printed affinity sensors in relation to methodologies employed for immobilization of bioreceptors on transducer surface.

**Web URL:** <http://www.mdpi.com/1424-8220/16/11/1863/htm>

**42. Ahmed, K., Rehman, F., Pires, C. T., Rahim, A., Santos, A. L., & Airoidi, C. (2016). Aluminum doped mesoporous silica SBA-15 for the removal of remazol yellow dye from water. *Microporous and Mesoporous Materials*, 236, 167-175.**

**ABSTRACT:**

Aluminum doped mesoporous silica SBA-15 was synthesized and characterized using nuclear magnetic resonance spectroscopy, nitrogen adsorption, X-rays diffraction, thermogravimetry, scanning and transmission electron microscopy. The modified mesoporous silicas [Al]SBA-15 and [2Al]SBA-15 showed high sorption capacities of remazol yellow dye (RY) of about 0.971 and 0.821 mmol g<sup>-1</sup> respectively, when compared to original precursor silica SBA-15 (0.725 mmol g<sup>-1</sup>). The sorption kinetic of RY dye was slow and the equilibrium reached in 4–5 h. The effect of pH on sorption process was studied at room temperature and maximum dye sorption was achieved at pH 7. Kinetic data of RY sorption onto mesoporous silica was best fitted to second-order kinetic model. The equilibrium data were fitted to the Langmuir, Freundlich and Sips isotherm models. The obtained results suggest that doped mesoporous

silica can be an efficient, cheap sorbent and convenient method for the removal of reactive dyes such as RY from industrial effluents.

**Web URL:** <http://www.sciencedirect.com/science/article/pii/S1387181116303754>

**43. Rehman, F., Rahim, A., Airoidi, C., & Volpe, P. L. (2016). Preparation and characterization of glycidyl methacrylate organo bridges grafted mesoporous silica SBA-15 as ibuprofen and mesalamine carrier for controlled release. *Materials Science and Engineering: C*, 59, 970-979.**

**ABSTRACT:**

Mesoporous silica SBA-15 was synthesized and functionalized with bridged polysilsesquioxane monomers obtained by the reaction of 3-aminopropyltriethoxy silane with glycidyl methacrylate in 2:1 ratio. The synthesized mesoporous silica materials were characterized by elemental analysis, infrared spectroscopy, nuclear magnetic resonance spectroscopy, nitrogen adsorption, X-ray diffraction, thermogravimetry and scanning electron microscopy. The nuclear magnetic resonance in the solid state is in agreement with the sequence of carbon distributed in the attached organic chains, as expected for organically functionalized mesoporous silica. After functionalization with organic bridges the BET surface area was reduced from 1311.80 to 494.2 m<sup>2</sup> g<sup>-1</sup> and pore volume was reduced from 1.98 to 0.89 cm<sup>3</sup> g<sup>-1</sup>, when compared to original precursor silica. Modification of the silica surface with organic bridges resulted in high loading capacity and controlled release of ibuprofen and mesalamine in biological fluids. The Korsmeyer–Peppas model better fits the release data indicating Fickian diffusion and zero order kinetics for synthesized mesoporous silica. The drug release rate from the modified silica was slow in simulated gastric fluid, (pH 1.2) where less than 10% of mesalamine and ibuprofen were released in initial 8 h, while comparatively high release rates were observed in simulated intestinal (pH 6.8) and simulated body fluids (pH 7.2). The preferential release of mesalamine at intestinal pH suggests that the modified silica could be a simple, efficient, inexpensive and convenient carrier for colon targeted drugs, such as mesalamine and also as a controlled drug release system.

**Web URL:** <http://www.sciencedirect.com/science/article/pii/S0928493115305373>

**44. Ahmad, P., Khandaker, M. U., Amin, Y. M., & Muhammad, N. (2016). Synthesis of highly crystalline multilayered boron nitride microflakes. *Scientific reports*, 6, 21403.**

**ABSTRACT:**

Boron nitride microflakes of 2–5  $\mu\text{m}$  in diameter and greater than 40  $\mu\text{m}$  in length with multilayer structure and highly crystalline nature are synthesized in two states of catalysts and dual role of nitrogen at 1100 °C. Most of the microflakes are flat, smooth and vertically aligned with a wall-like view from the top. Transmission electron microscopy shows overlapped layers of microflakes with an interlayer spacing of 0.34 nm. The h-BN components of the synthesized microflakes are verified from B 1s and N 1s peaks at 190.7 and 397.9 eV. Raman shift at 1370 ( $\text{cm}^{-1}$ ) and sharp peaks in the XRD pattern further confirm the h-BN phase and crystalline nature of the synthesized microflakes. Microflakes of h-BN with the above characteristics are highly desirable for the development of a solid state neutron detector with higher detection efficiency.

**Web URL:** [https://www.nature.com/articles/srep21403?WT.feed\\_name=subjects\\_sensors-and-biosensors](https://www.nature.com/articles/srep21403?WT.feed_name=subjects_sensors-and-biosensors)

**45. Mishra, R. K., Catanante, G., Hayat, A., & Marty, J. L. (2016). Evaluation of extraction methods for ochratoxin A detection in cocoa beans employing HPLC. *Food Additives & Contaminants: Part A*, 33(3), 500-508.**

**ABSTRACT:**

Cocoa is an important ingredient for the chocolate industry and for many food products. However, it is prone to contamination by ochratoxin A (OTA), which is highly toxic and potentially carcinogenic to humans. In this work, four different extraction methods were tested and compared based on their recoveries. The best protocol was established which involves an organic solvent-free extraction method for the detection of OTA in cocoa beans using 1% sodium hydrogen carbonate ( $\text{NaHCO}_3$ ) in water within 30 min. The extraction method is rapid (as compared with existing methods), simple, reliable and practical to perform without complex experimental set-ups. The cocoa samples were freshly extracted and cleaned-up using immunoaffinity column (IAC) for HPLC analysis using a fluorescence detector. Under the

optimised condition, the limit of detection (LOD) and limit of quantification (LOQ) for OTA were 0.62 and 1.25 ng ml<sup>-1</sup> respectively in standard solutions. The method could successfully quantify OTA in naturally contaminated samples. Moreover, good recoveries of OTA were obtained up to 86.5% in artificially spiked cocoa samples, with a maximum relative standard deviation (RSD) of 2.7%. The proposed extraction method could determine OTA at the level 1.5 µg kg<sup>-1</sup>, which surpassed the standards set by the European Union for cocoa (2 µg kg<sup>-1</sup>). In addition, an efficiency comparison of IAC and molecular imprinted polymer (MIP) column was also performed and evaluated.

**Web URL:** <http://www.tandfonline.com/doi/abs/10.1080/19440049.2015.1133933>

**46. Hayat, A., Rhouati, A., Mishra, R. K., Alonso, G. A., Nasir, M., Istamboulie, G., & Marty, J. L. (2016). An electrochemical sensor based on TiO<sub>2</sub>/activated carbon nanocomposite modified screen printed electrode and its performance for phenolic compounds detection in water samples. *International Journal of Environmental Analytical Chemistry*, 96(3), 237-246.**

**ABSTRACT:**

Herein, we reported a titanium oxide (TiO<sub>2</sub>) modified activated carbon nanocomposite that showed advantageous characteristics in terms of electro-conductivity, catalytic activity and surface area. The designed nanocomposite was employed to modify the screen printed carbon electrode transducer surface in the construction of an electrochemical sensor. The electrode surface modification was characterised by cyclic voltammetry and impedimetric studies. The modified transducer surface was subsequently used for the detection of four phenolic endocrine disruptors, *p*-nitrophenol, hydroquinone, catechol and 1-naphtol. Under optimal conditions, TiO<sub>2</sub> modified activated carbon sensor was evaluated by differential pulse voltammetry showing a good linearity with correlation coefficients higher than 0.99. It showed, in parallel, a high sensitivity where the detection limits were 348 ng/L, 110.1 ng/L, 3.3 ng/L and 7.2 µg/L for the respective studied compounds (S/N = 3). Finally, we validated the method with river water samples, and good recovery values were obtained showing the potential application of the reported biosensor.

**Web URL:** <http://www.tandfonline.com/doi/abs/10.1080/03067319.2015.1137910>

47. Siddiqi, S. A., Manzoor, F., Jamal, A., Tariq, M., Ahmad, R., Kamran, M., ... & Rehman, I. U. (2016). Mesenchymal stem cell (MSC) viability on PVA and PCL polymer coated hydroxyapatite scaffolds derived from cuttlefish. *RSC Advances*, 6(39), 32897-32904.

**ABSTRACT:**

In the present study, cuttlefish bones are used to prepare highly porous hydroxyapatite (HA) scaffolds *via* hydrothermal treatment at 200 °C. Raw cuttlefish bones (CB) and the hydrothermal products have been analyzed and compared for their composition and microstructure, using X-ray powder diffraction (XRD), Optical Microscopy (OM), Scanning Electron Microscopy (SEM), Fourier transform infrared spectroscopy (FTIR), porosity estimation and compressive strength measuring techniques. Characterization reveals that cuttlebone has high porosity approaching above 70%, and possesses the laminar structure of aragonite mixed with some organic materials. The compressive strength of the CB-HA is improved after coating with both polyvinyl alcohol (PVA) and polycaprolactone (PCL). Furthermore, our *in vitro* biocompatibility studies revealed that CB-HA and PVA coated CB-HA scaffolds are non-cytotoxic and support the adherence and proliferation of rMSCs, comparable to pure HA scaffolds. Altogether, our results suggest that naturally derived CB-HA, PVA and PCL coated CB-HA scaffolds are potential cheap candidates for bone tissue engineering applications, and also that PVA and PCL coatings provide better mechanical strength.

**Web URL:** <http://pubs.rsc.org/-/content/articlelanding/2016/ra/c5ra22423c/unauth#!divAbstract>

48. Gonfa, G., Bustam, M. A., Shariff, A. M., Muhammad, N., & Ullah, S. (2016). Quantitative structure–activity relationships (QSARs) for estimation of activity coefficient at infinite dilution of water in ionic liquids for natural gas dehydration. *Journal of the Taiwan Institute of Chemical Engineers*, 66, 222-229.

**ABSTRACT:**

Recently, ionic liquids (ILs) have been considered as alternative solvents to glycol in dehydration of natural gas. However, due to the unlimited structural variations and possible combinations of cations and anions of the ILs, selection of potential ILs for this separation process has been a

difficult task. Activity coefficient at infinite dilution is one of the most important thermodynamic properties for preliminary selection of suitable liquid desiccants for water absorption and designing of the natural gas dehydration process. In this paper, COSMO-RS based quantitative structure–property/activity relationship (QSPR/QSAR) models were developed for prediction of activity coefficient of water at infinite dilution in ILs over various temperatures. COSMO-RS based descriptors were generated for 53 ILs (318 data points) at various temperatures. Multiple linear regressions were applied to develop the models. The accuracies of the models were verified by different statistical tests. The model provides a better understanding of the effect of the structural variations of ILs on their affinity for water.

**Web URL:** <http://www.sciencedirect.com/science/article/pii/S1876107016302048>

**49. Riaz, T., Kanwal, F., Siddiqi, S. A., Gull, N., Jamil, T., Ali, A., ... & Thebo, K. H. (2016). Study of Conducting Properties of Chemically Synthesized Polyaniline/crystalline Silica Composites.**

**ABSTRACT:**

Conducting polyaniline (PANI) and polyaniline/SiO<sub>2</sub> composites with significantly high conductivity were synthesized via facile oxidative polymerization method using potassium dichromate (K<sub>2</sub>Cr<sub>2</sub>O<sub>7</sub>) as oxidizing agent at 0°C. PANI/SiO<sub>2</sub> composites with different weight ratios of crystalline silica were prepared in order to evaluate their electrical conductivity. Their structural and thermal properties were also investigated by using X-ray diffraction (XRD) and thermo gravimetric analysis (TGA) techniques. The insertion of silica into PANI up to specific weight percentages gives a 10 fold increase in conductivity. Microstructural analysis by scanning electron microscopy (SEM) reveals that a specific type of inter-connecting morphology is essential for obtaining an optimal electrical conductivity. Such a condition is attained with a specific amount of silica distribution in the composite. SEM study showed that polyaniline/SiO<sub>2</sub> composites maintain a conducting micro-structural network up to 20wt-% silica inclusion by giving a maximum electrical conductivity of 40S.cm<sup>-1</sup> due to better de-localisation of electrons and improvement of the inter-particle processes for the charge transport.

**Web URL:** <https://www.iiser.org/researchpaper/Study-of-Conducting-Properties-of-Chemically-Synthesized-Polyaniline-crystalline-Silica-Composites.pdf>

50. Zahid, S., Shah, A. T., Jamal, A., Chaudhry, A. A., Khan, A. S., Khan, A. F., ... & ur Rehman, I. (2016). Biological behavior of bioactive glasses and their composites. *RSC Advances*, 6(74), 70197-70214.

**ABSTRACT:**

Bioactive glasses (BGs) as third generation biomaterials have the ability to form an interfacial bonding more rapidly than other bioceramics between implant and host tissues in defect treatment. Therefore, BGs have shown great applications in the field of bone tissue engineering, dental materials, skin and other tissue regeneration. This review is based on inorganic and organic BG composites being used in bone tissue engineering and summarizes current developments in improving the biological behavior of BGs and their composites. A main focus was given to highlight the role of BGs and their composites in osteogenic differentiation and angiogenesis, followed by their cytotoxicity, protein adsorption ability and antibacterial properties. BGs were found to enhance the cell proliferation and cell attachment without any toxic effects with a significant increase in metabolic activity and possess osteogenic properties. Organic and inorganic dopants have been used to improve their cytocompatibility, osteoconductivity and promote stem cell differentiation towards the osteogenic lineage. BGs have also been used as graft materials because of their significant role in angiogenesis, as they stimulate relevant cells (*i.e.* fibroblasts, osteoblasts and endothelial cells) to release angiogenic growth factors. They show good protein adsorption because they act as templates for the adsorption of proteins which in turn depends upon surface properties. Antibacterial effects were also observed in BGs as a result of the high aqueous pH value in body fluids due to the presence of alkaline ions. There has been significant research work performed on silica-based bioactive glasses but not much literature can be found on phosphate- and borate-based bioactive glasses, which have good solubility and degradation, respectively.

**Web URL:**

<http://pubs.rsc.org/en/content/articlelanding/2016/ra/c6ra07819b/unauth#!divAbstract>

51. Farooq, A., Shahzadi, L., Bajda, M., Ullah, N., Rauf, A., Shahzad, S. A., ... & Yar, M. (2016). Organocatalyzed Novel Synthetic Methodology for Highly Functionalized Piperidines as Potent  $\alpha$ -Glucosidase Inhibitors. *Archiv der Pharmazie*, 349(9), 724-732.

**ABSTRACT:**

An efficient atom-economic one-pot synthesis of highly functionalized piperidines was achieved by catalytic multicomponent reaction. A wide range of heterogeneous and homogenous catalysts were explored; however, promising results were achieved when a  $\beta$ -keto-ester was reacted with selected aromatic aldehydes and anilines by using *N*-acetyl glycine (NAG) as catalyst. The implication of this methodology is straightforward since the products were precipitated out from the reaction solution, eliminating the need of column chromatography purifications. The synthesized piperidines were screened against  $\alpha$ -glucosidase inhibition, which revealed that these compounds were very active inhibitors, and some of the compounds showed even better inhibition than the reference compound, at low micromolar concentrations. *In silico* molecular modeling was also performed to investigate the binding modes of the compounds into the active sites of the target protein.

**Web URL:** <http://onlinelibrary.wiley.com/doi/10.1002/ardp.201600045/full>

**52. Hussain, S., Ullah, Z., Gul, S., Khattak, R., Kazmi, N., Rehman, F., ... & Khan, A. (2016). Adsorption Characteristics of Magnesium-Modified Bentonite Clay with Respect to Acid Blue 129 in Aqueous Media. *Polish Journal of Environmental Studies*, 25(5).**

**ABSTRACT:**

Locally available bentonite clay has been modified by magnesium and used to eliminate acid blue 129 from aqueous solutions. The adsorption was studied under different experimental conditions such as dye concentrations, temperature, and shaking time. The adsorption of the dye increased with time and followed the pseudo-first-order kinetic with rate constant "k" 0.126 min<sup>-1</sup> at 283 K. Thermodynamic parameters such as  $\Delta H^\circ$ ,  $\Delta S^\circ$ , and  $\Delta G^\circ$  were calculated from the slope and intercept of the linear plots of  $\ln K$  against  $1/T$ . Analysis of adsorption results obtained at temperatures of 283, 293, 303, and 313 K showed that the adsorption pattern on bentonite seems to follow Langmuir and Freundlich. The increase in temperature reduces adsorption capacity by magnesium-modified bentonite due to the enhancement of the desorption step in the mechanism. The activation energy of the adsorption process was found to be 3.55 kJ mol<sup>-1</sup>. The Mg-bentonite showed better adsorption than Ba and Al-bentonite. Our

study reveals that abundantly available local clay may be used to eliminate dyes from aqueous solutions.

**Web URL:** <http://www.pjoes.com/pdf/25.5/Pol.J.Environ.Stud.Vol.25.No.5.1947-1953.pdf>

**53. Khan, A. S., Man, Z., Bustam, M. A., Kait, C. F., Ullah, Z., Nasrullah, A., ... & Muhammad, N. (2016). Kinetics and thermodynamic parameters of ionic liquid pretreated rubber wood biomass. *Journal of Molecular Liquids*, 223, 754-762.**

**ABSTRACT:**

The impact of ionic liquids (ILs) namely 1-butyl-3-methylimidazolium chloride ([BMim][Cl]) and 1-butyl-3-methylimidazolium acetate ([BMIM][OAc]) on rubber wood pyrolysis kinetic and thermodynamic parameters were investigated using thermogravimetric analysis (TGA). The ILs treated and untreated samples were characterized with FT-IR and elemental (CHNS) analyses. The activation energy for untreated and ILs treated rubber wood (RW) were determined using the Flynn-Wall-Ozawa (FWO), Kissinger-Akahira-Sunose (KAS) and Starink methods. The average activation energy calculated using FWO, KAS and Starink methods for untreated rubber wood was 120.15 kJ/mol, 117.10 kJ/mol and 117.60 kJ/mol, [BMIM][Cl] treated rubber wood was 87.32 kJ/mol, 77.73 kJ/mol, and 81.16 kJ/mol, while [BMIM][OAc] treated rubber wood was 85.64 kJ/mol, 76.63 kJ/mol, and 80.47 kJ/mol, respectively. Starink method was further used to determine the pre-exponential factor and thermodynamic parameters of untreated and ILs treated samples. The thermo kinetics and thermodynamic parameters indicate that ILs pre-treatment decreases the thermal stability of the rubber wood. From FTIR analysis, it was observed that ILs pre-treatment affected the chemical composition of rubber wood. Elemental analysis showed that ILs treated RW has a higher content of Hydrogen/Carbon ratio because of the separation of lignin and hemicellulose during pre-treatment. It was concluded that ILs pre-treatment provided a potential way to improve the thermal conversion efficiency of rubber wood.

**Web URL:** <http://www.sciencedirect.com/science/article/pii/S0167732216307887>

**54. Ullah, Z., Bustam, M. A., Man, Z., Shah, S. N., Khan, A. S., & Muhammad, N. (2016). Synthesis, characterization and physicochemical properties of dual-functional acidic ionic liquids. *Journal of Molecular Liquids*, 223, 81-88.**

**ABSTRACT:**

In this manuscript the synthesis of four new ionic liquids (ILs) having the same cation (1,4-butane sultone methyl-benzimidazole) but different anions ( $\text{CH}_3\text{SO}_3^-$ ,  $\text{CF}_3\text{SO}_3^-$ ,  $\text{CF}_3\text{CO}_2^-$ ,  $\text{HSO}_4^-$ ) were synthesized and characterized. The ILs was characterized using NMR, elemental analysis (CHNS) and FTIR. The physicochemical properties for these ILs, such as viscosity, density, refractive index, surface tension and thermal stability were analysed in a wide temperature window. Moreover the effects of different anions on the physicochemical properties were studied as well. The density and surface tension values were further used to calculate other properties such as thermal expansion coefficient, surface enthalpy, surface entropy as well as the boiling point and critical temperature of the ILs. The thermal stability analyses were performed from (373.15–773.15) K.

**Web URL:** <http://www.sciencedirect.com/science/article/pii/S0167732216310121>

**55. Rhouati, A., Catanante, G., Nunes, G., Hayat, A., & Marty, J. L. (2016). Label-free aptasensors for the detection of mycotoxins. *Sensors*, 16(12), 2178.**

**ABSTRACT:**

Various methodologies have been reported in the literature for the qualitative and quantitative monitoring of mycotoxins in food and feed samples. Based on their enhanced specificity, selectivity and versatility, bio-affinity assays have inspired many researchers to develop sensors by exploring bio-recognition phenomena. However, a significant problem in the fabrication of these devices is that most of the biomolecules do not generate an easily measurable signal upon binding to the target analytes, and signal-generating labels are required to perform the measurements. In this context, aptamers have been emerged as a potential and attractive bio-recognition element to design label-free aptasensors for various target analytes. Contrary to other bioreceptor-based approaches, the aptamer-based assays rely on antigen binding-induced conformational changes or oligomerization states rather

than binding-assisted changes in adsorbed mass or charge. This review will focus on current designs in label-free conformational switchable design strategies, with a particular focus on applications in the detection of mycotoxins.

**Web URL:** <http://www.mdpi.com/1424-8220/16/12/2178/htm>

**56. Feroze, A., Idrees, M., Nadeem, M., Siddiqi, S. A., Saleem, M., Atif, M., ... & Shaukat, S. F. (2016). Origin of magnetic and dielectric response in single phase nano crystalline BiFeO<sub>3</sub>. *Materials Research Express*, 3(12), 125015.**

**ABSTRACT:**

Stoichiometric and single phase synthesis of BiFeO<sub>3</sub> is critical both in its particle industrial applications as well as in understanding the origin of its attractive dielectric and magnetic properties. In this study, BiFeO<sub>3</sub> has been obtained at temperatures as low as 400 °C. Zero Fe<sup>+2</sup>/Fe<sup>+3</sup> ratio, and absence of bismuth and oxygen non-stoichiometry have been probed by <sup>57</sup>Fe Mössbauer spectroscopy. The appearance of different magnetic phases in <sup>57</sup>Fe Mössbauer spectrum, MH hysteresis curve and exchange bias effect have been conferred on the basis of magneto-crystalline anisotropy and particle size distribution. Dependence of the dielectric response on the applied electric field reveals that the colossal dielectric response in BiFeO<sub>3</sub> is dominated by extrinsic effects at grain-grain interface.

**Web URL:** <http://iopscience.iop.org/article/10.1088/2053-1591/3/12/125015/meta>

**57. Riaz, S., Feng, W., Khan, A. F., & Nawaz, M. H. (2016). Sonication-induced self-assembly of polymeric porphyrin–fullerene: Formation of nanorings. *Journal of Applied Polymer Science*, 133(24).**

**ABSTRACT:**

In this article, we detail the sonication-induced self-assembly of polymeric porphyrin and fullerenes into distinct nanorings in solution form. The formation of these trenchant superstructures was the result of the delicate choice of different assembly protocols, solvents, and polymeric tails associated with porphyrin and fullerene. In this study, the sonication supposedly directed the lateral aggregation into uniform ring formation. The sonication time was found to be the key parameter in ring formation. Furthermore, the flexibility of polymeric

arms and electronic interactions of porphyrin–fullerene gave rise to synergistically enhanced molecular interactions, and this resulted in discrete morphologies. Key optical data, including the absorption maxima of the complexes, and microscopic studies attested to the nature and morphology of the self-assembled complexes. This introduction of polymeric arms and sonication protocols in the porphyrin self-assembly was expected to allow the easy formation of diverse morphologies. Because of the facile fabrication process and uniform morphology, the resulting composite architectures might show promising applications in drug-delivery and advance materials.

**Web URL:** <http://onlinelibrary.wiley.com/doi/10.1002/app.43537/full>

**58. Bhatti, N. U. A., Khan, M. J., Ahmad, J., Saleem, M., Ramay, S. M., & Siddiqi, S. A. Electrochemical Performance of Al-Mn<sub>2</sub>O<sub>3</sub> Based Electrode Materials. *World Academy of Science, Engineering and Technology, International Journal of Chemical, Molecular, Nuclear, Materials and Metallurgical Engineering*, 11(1), 41-45.**

**ABSTRACT:**

Manganese oxide is being recently used as electrode material for rechargeable batteries. In this study, Al incorporated Mn<sub>2</sub>O<sub>3</sub> compositions were synthesized to study the effect of Al doping on electrochemical performance of host material. Structural studies were carried out using X-ray diffraction analysis to confirm the phase stability and explore the lattice parameters, crystallite size, lattice strain, density and cell volume. Morphology and composition were analyzed using field emission scanning electron microscope and energy dispersive X-ray spectroscopy, respectively. Dynamic light scattering analysis was performed to observe the average particle size of the compositions. FTIR measurements exhibit the O-Al-O and OMn-O and Al-O bonding and with increasing the concentration of Al, the vibrational peaks of Mn-O become sharper. An enhanced electrochemical performance was observed in compositions with higher Al content.

**Web URL:** <http://www.waset.org/publications/10006152>

**59. Danish, M., Gu, X., Lu, S., Xu, M., Zhang, X., Fu, X., ... & Nasir, M. (2016). Role of reactive oxygen species and effect of solution matrix in trichloroethylene degradation from aqueous**

solution by zeolite-supported nano iron as percarbonate activator. *Research on Chemical Intermediates*, 42(9), 6959-6973.

**ABSTRACT:**

The role of reactive oxygen species (ROSs) and effect of solution matrix have been investigated for the degradation of trichloroethylene (TCE). Zeolite-supported nano iron (Z-nZVI) was synthesized as an activator to catalyze sodium percarbonate (SPC) with or without hydroxylamine, i.e. as reducing agent (RA). The probe tests confirmed the generation of OH<sup>•</sup> and O<sub>2</sub><sup>•-</sup> in the Z-nZVI activated SPC system in absence of the RA, while the presence of RA significantly increased the generation of OH<sup>•</sup> and O<sub>2</sub><sup>•-</sup> radicals. Scavenger tests demonstrated that OH<sup>•</sup> was the main ROS responsible for TCE degradation, whereas O<sub>2</sub><sup>•-</sup> also participated in TCE degradation. From the solution matrix perspective, the experimental results confirmed significant scavenging effects of Cl<sup>-</sup> (1.0, 10.0, and 100 mmol L<sup>-1</sup>) and HCO<sub>3</sub><sup>-</sup> (1.0 and 10.0 mmol L<sup>-1</sup>), whereas the scavenging effects were fairly impeded at 100 mmol L<sup>-1</sup> concentration of HCO<sub>3</sub><sup>-</sup>. On the other hand, a considerable decline in scavenging effect was observed in the presence of RA in tested Cl<sup>-</sup> and HCO<sub>3</sub><sup>-</sup> concentration ranges. In addition, negligible scavenging effects of NO<sub>3</sub><sup>-</sup> and SO<sub>4</sub><sup>2-</sup> anions were found in all tested concentrations. The effect of initial solution pH on catalytic activity indicated a significant increase in the TCE degradation in the presence of RA even at higher pH value of 9. The results indicated that the Z-nZVI activated SPC system in presence of RA can effectively degrade chlorinated organic solvents, but it is important to consider the intensive existence of anions in groundwater.

**Web URL:** <https://link.springer.com/article/10.1007/s11164-016-2509-8>

60. Nasir, M., Lei, J., Iqbal, W., & Zhang, J. (2016). Study of synergistic effect of Sc and C co-doping on the enhancement of visible light photo-catalytic activity of TiO<sub>2</sub>. *Applied Surface Science*, 364, 446-454.

**ABSTRACT:**

Scandium and carbon co-doped TiO<sub>2</sub> catalyst was prepared through a simple sol-gel synthesis method by using scandium nitrate as scandium dopant precursor, glucose as carbon precursor

and tetrabutyl orthotitanate as titanium precursor and calcined them at 450 °C for 3 h. The characterizations of the prepared samples were accomplished through X-ray diffraction (XRD), transmission electron microscopy (TEM), UV–visible diffuse reflectance spectroscopy (UV–Vis DRS), photoluminescence spectroscopy (PL), Fourier transformation infrared spectroscopy (FT-IR), X-ray photoelectron spectroscopy (XPS) and Brunauer–Emmett–Teller (BET). The X-ray diffraction results of the samples showed the decrease in the crystal size of the sample with the subsequent increase in the specific surface area as shown by Brunauer–Emmett–Teller. The UV–visible diffuse reflectance spectroscopy displayed the blue shift in the absorption together with the photoluminescence spectroscopy revealed the decrease in the recombination of electrons and holes by the addition of the scandium and then after the certain optimum value, the further increase of the scandium further increased the recombination of electrons and holes. The photo-catalytic activity of the samples was investigated with the help of photo-catalytic degradation of Acid orange 7 under visible light irradiation. The degradation of Acid orange 7 was highly increased for the Sc and C co-doped samples compared to the single C doped sample. And the sample 0.2 Sc/C-TiO<sub>2</sub> had the maximum increase. The enhanced photo-catalytic performance was due the decrease of the crystal size, increase of the surface area, increase in the surface hydroxyl groups, and increase of the lifetime of the electrons and holes because of the synergistic effect of the Sc and C co-doping in TiO<sub>2</sub>.

**Web URL:** <http://www.sciencedirect.com/science/article/pii/S0169433215031712>

**61. Sharma, A., Hayat, A., Mishra, R. K., Catanante, G., Shahid, S. A., Bhand, S., & Marty, J. L. (2016). Design of a fluorescence aptaswitch based on the aptamer modulated nano-surface impact on the fluorescence particles. *RSC Advances*, 6(70), 65579-65587.**

**ABSTRACT:**

The concept of DNA based stabilization of nanostructures to enhance the surface reactivity has been the focus of great interest in the design of colorimetric aptaswitches. Whereas, colorimetric methodologies have limited sensitivity, this concept is rarely considered for other sensing approaches such as those based on fluorescence detection. In this paper, we have investigated the impact of reversible assembly of a single strand DNA aptamer on nanoparticle surface chemistry, involving target tuneable electrostatic and steric repulsion phenomena for fluorescence based

detection of molecular interactions. In the same context, literature reported fluorescence based aptamer assays are prone to certain limitations such as complicated labelling chemistry, low conjugation yield, low binding affinity and elevated cost per assay. Alternatively, our designed aptaswitch capitalizes on the surface chemistry of nanoparticles to quench the response of fluorescence particles, eliminating the need of bioconjugation with a fluorophore. As a proof of concept, the proposed methodology was used for the detection of ochratoxin A with TiO<sub>2</sub> nanoparticles as a representative nanomaterial. We expect that this concept may pave a new way to probe aptamer-target binding events, since any nanomaterials with fluorescence quenching characteristics can be regulated in the same manner

**Web URL:** <http://pubs.rsc.org/-/content/articlelanding/2016/ra/c6ra10942j/unauth#!divAbstract>

**62. Kamil, A., Akhtar, S., Khan, A., Farooq, E., Nishan, U., Uddin, R., & Farooq, U. (2016). Synthesis, structure–activity relationship and antinociceptive activities of some 2-(2'-pyridyl) benzimidazole derivatives. *Medicinal Chemistry Research*, 25(6), 1216-1228.**

**ABSTRACT:**

In the present study, a new series of 2-(2'-pyridyl) benzimidazole derivatives **1–11** were resynthesized and evaluated for analgesic activity. The 2-(2'-pyridyl) benzimidazole was quaternized at its nitrogen atom in the ring with various substituted and unsubstituted phenacyl halides. As a result, eleven novel derivatives were synthesized. The structures of these new synthetic derivatives of 2-(2'-pyridyl) benzimidazole were confirmed by using different spectroscopic techniques i.e., UV/Visible, IR, <sup>1</sup>HNMR and Mass spectroscopy. Percentage of carbon, hydrogen and nitrogen was also determined by elemental analysis. All the synthetic compounds showed significant analgesic activity with dose-dependent manner.

**Web URL:** <https://link.springer.com/article/10.1007/s00044-016-1560-8>

**63. Shehzad, K., Hussain, T., Shah, A. T., Mujahid, A., Ahmad, M. N., Anwar, T., ... & Ali, A. (2016). Effect of the carbon nanotube size dispersity on the electrical properties and pressure sensing of the polymer composites. *Journal of Materials Science*, 51(24), 11014-11020.**

**ABSTRACT:**

Two different-diameter carbon nanotubes (CNTs), i.e., CNT-1 (diameter = 10–30 nm, length = 5–15  $\mu\text{m}$ ) and CNT-2 (diameter = 20–40 nm, length = 5–15  $\mu\text{m}$ ), were mixed in various relative concentrations to obtain series of hybrids with wider diameter disparity, which were subsequently melt blended with a polypropylene-based thermoplastic elastomer to fabricate their respective polymer composites. By changing the relative concentrations of CNTs in a polydisperse mixture, we were able to tune the percolation characteristics and the pressure–resistance sensitivity of the polymer composites. Percolation threshold, percolation window, and the minimum achievable resistivity value of the composites were found to be the function of relative concentration of CNTs in the polydisperse system. An important finding of this study is that percolation characteristics of composites with polydisperse system of CNTs prepared by mixing of two different CNTs with different relative concentrations can be explained by model of hybrid fillers. These findings may open a new pathway to design the conductive polymer composites with controlled electrical and sensing properties for various applications.

**Web URL:** <https://link.springer.com/article/10.1007/s10853-016-0322-9>

**64. Khan, S. U., Khan, F. U., Khan, I. U., Muhammad, N., Badshah, S., Khan, A., ... & Nasrullah, A. (2016). Biosorption of nickel (II) and copper (II) ions from aqueous solution using novel biomass derived from *Nannorrhops ritchiana* (Mazri Palm). *Desalination and Water Treatment*, 57(9), 3964-3974.**

**ABSTRACT:**

In the present research work, *Nannorrhops ritchiana* (Mazri Palm) was used as an effective biosorbent for removal of  $\text{Cu}^{2+}$  and  $\text{Ni}^{2+}$  ions from aqueous solution. *Nannorrhops ritchiana* (Mazri Palm), a dead biomass powder, was used as a low-cost adsorbent without any chemical treatment. In order to estimate the equilibrium parameters, the equilibrium adsorption data were analyzed using Freundlich, Langmuir, and Temkin isotherms. Freundlich isotherms indicated that the sorption capacities on the biomass surfaces increased with increasing initial concentrations of both metals. The adsorption isotherms were correlated with a comparison of linear and non-linear regression analysis. The squares of the errors (SSE) and

chi-square test ( $\chi^2$ ) along with the coefficient of determination ( $R^2$ ) were used to determine the best fit isotherm. Langmuir type I was found the best fitting isotherm for adsorption of both  $\text{Cu}^{2+}$  and  $\text{Ni}^{2+}$  ions as compared to the other three Langmuir linear isotherms on the basis of the values for  $R^2$  and other error functions like SSE and  $\chi^2$  obtained from Langmuir-type I linear equation. The present study revealed that *Nannorrhops ritchiana* proved to be an effective, inexpensive, alternative, and environmentally friendly biosorbent for the removal of  $\text{Cu}^{2+}$  and  $\text{Ni}^{2+}$  ions from aqueous solution.

**Web URL:** <http://www.tandfonline.com/doi/abs/10.1080/19443994.2014.989268>

**65. Gonfa, G., Bustam, M. A., Muhammad, N., & Ullah, S. (2015). Density and excess molar volume of binary mixture of thiocyanate-based ionic liquids and methanol at temperatures 293.15–323.15 K. *Journal of Molecular Liquids*, 211, 734-741.**

**ABSTRACT:**

Densities of binary mixture of three ionic liquids, 1-butyl-3-methylimidazolium thiocyanate ( $[\text{C}_4\text{C}_1\text{im}][\text{SCN}]$ ), 1-allyl-3-methylimidazolium thiocyanate ( $[\text{C}_1 = \text{C}_2]\text{C}_1\text{im}][\text{SCN}]$ ) and 3-(3-butyl-1H-imidazol-3-ium-1-yl)propanenitrile thiocyanate ( $[(\text{NC})^2\text{C}_2\text{C}_4\text{im}][\text{SCN}]$ ), with methanol were measured over a temperature range of 293.15 to 323.15 K and at atmospheric pressure. Excess molar volumes ( $V_m^E$ ) were calculated from density values and correlated with Redlich–Kister polynomial equation.

Partial molar volumes at infinite dilutions ( $V_{m,i}^\infty$ ) of the ILs and methanol were determined from the Redlich–Kister coefficients. For all the studied systems, the  $V_m^E$  is negative over the entire composition range. The  $V_m^E$  and  $V_{m,i}^\infty$  are interpreted in terms of intermolecular interactions in the binary mixture. Density functional theory has been used to investigate the interactions between methanol and the studied ILs.

**Web URL:** <http://www.sciencedirect.com/science/article/pii/S0167732215302798>

**66. Batool, M., Shah, A. T., Imran Din, M., & Li, B. (2016). Catalytic Pyrolysis of Low Density Polyethylene Using Cetyltrimethyl Ammonium Encapsulated Monovacant Keggin Units and ZSM-5. *Journal of Chemistry*, 2016.**

**ABSTRACT:**

The effect of the catalysts on the pyrolysis of commercial low density polyethylene (LDPE) has been studied in a batch reactor. The thermal catalytic cracking of the LDPE has been done using cetyltrimethyl ammonium encapsulated monovacant keggins units ( $C_{19}H_{42}N)_4H_3(PW_{11}O_{39})$ , labeled as CTA-POM and compared with the ZSM-5 catalyst. GC-MS results showed that catalytic cracking of LDPE beads generated oilier fraction over CTA-POM as compared to ZSM-5. Thus, the use of CTA-POM is more significant because it yields more useful fraction. It was also found that the temperature required for the thermal degradation of LDPE was lower when CTA-POM was used as a catalyst while high temperature was required for degradation over ZSM-5 catalyst. Better activity of CTA-POM was due to hydrophobic nature of CTA moiety which helps in catalyst mobility and increases its interaction with hydrocarbons.

**Web URL:** <https://www.hindawi.com/journals/ichem/2016/2857162/abs/>

**67. Al Kaisy, G. M., Mutalib, M. I. A., Bustam, M. A., Leveque, J. M., & Muhammad, N. (2016). Liquid-Liquid extraction of aromatics and sulfur compounds from base oil using ionic liquids. *Journal of Environmental Chemical Engineering*, 4(4), 4786-4793.**

**ABSTRACT:**

The viability of using ionic liquids (ILs) as extractive solvents to remove naphthalene (aromatics) and dibenzothiophene (DBT; Sulfur) from base oil by liquid-liquid extraction was investigated. The experiments were designed using Response Surface Methodology (RSM) with 1-butyl-3-methylpyridinium dicyanamide [BMPY][DCA], 1-butyl-3-methylimidazolium dicyanamide [BMIM][DCA], 1-butyl-3-methylimidazolium thiocyanate [BMIM][SCN] and 1-butyl-3-methylimidazolium dimethylphosphate [BMIM][DMP] ILs. The sulfur compound and aromatics were analyzed using Total Sulphur analyzer and High Performance Liquid Chromatography (HPLC) with high coefficient of determination i.e.  $R^2$  values of 0.964 and 0.997 respectively. The effects of different ILs, temperatures, and ILs to oil mass ratio (IL:Oil) were

optimized.[BMPY][DCA] appeared as the most promising medium with 94.3% of dibenzothiophene and 83.1% of naphthalene removal after a single extraction step. The aromatics and sulfur removal efficiency of [BMPY][DCA] IL was 54.3%, 78.3% and 82.9%, 93.8% at IL:Oil ratios of 0.4 and 1.8, respectively. An increase in temperature did not improve the extraction efficiency, but a slight decrease was noted. Results emphasized that extraction of aromatics and sulfur compounds from base oil can be achieved successfully using selected ionic liquids.

**Web URL:** <http://www.sciencedirect.com/science/article/pii/S2213343716304031>

# DEPARTMENT OF STATISTICS

## Journal Papers

1. Aleem, U., Shah, F. T., Kanwal, S., Idrees, F. , Khan, T. A. (2016). Employer Satisfaction on Employee's Project Management and Technical Skills: A Study on IT Sector in Punjab. *J. Appl. Environ. Biol. Sci.*, 6(4)111-122.

**ABSTRACT:**

This research measures the employer satisfaction about project management skills and technical skills in Information Technology industry of Punjab (Pakistan). Using a simple random sampling technique, survey is conducted to test hypothesized relationships among the mentioned constructs using Multiple Regression Analysis. Regression analysis shows significant positive relationship between employer satisfaction with project management skills and technical skills, therefore IT industry should develop collaboration with HEIs to develop curriculum for improved project management skills and technical skills.

**Web URL:**

[https://www.textroad.com/pdf/JAEBS/J.%20Appl.%20Environ.%20Biol.%20Sci.,%206\(4\)111-122,%202016.pdf](https://www.textroad.com/pdf/JAEBS/J.%20Appl.%20Environ.%20Biol.%20Sci.,%206(4)111-122,%202016.pdf)

2. Mohsin, M., Pilz, J., & Gebhardt, A. (2016). An Explicit Distribution to Model the Proportion of Heating Degree Day and Cooling Degree Day. *Communications in Statistics-Simulation and Computation*, 45(7), 2617-2624.

**ABSTRACT:**

With a view to estimating the energy consumption, we derive the explicit distribution of the proportion  $X/(X + Y)$  when  $X$  and  $Y$  follow the new Bivariate Affine-Linear Exponential distribution. An application of this distribution to model the proportion of heating using the heating degree day and the cooling degree day data in the State of Alabama for Appalachian Mountain is provided. Using intensive computations based on R-program, tabulation of some quantiles associated with this particular distribution of proportion is also provided, which is quite useful in estimating the proportion of energy required to heat a building.

**Web URL:** <http://www.tandfonline.com/doi/abs/10.1080/03610918.2014.915037>

3. Muhammad, W., Mahrukh, K., Yasir, H., Asim, S., & Irfan, S. M. (2016). FIXING JOB DEMANDS AS HINDRANCES OR CHALLENGES BY THE MODERATING EFFECT OF PERSONALITY TRAITS: LOOKING INTO THE LENS OF TRAIT THEORY. *Science International*, 28(3).

**ABSTRACT: Not Found**

**Web URL:**

4. Muhammad, W., Saleha, A., Rauf, S. M. I., & Yasir, H. (2016). JOB ENGAGEMENT OF FACULTY IN UNIVERSITIES OF PAKISTAN: A PERSPECTIVE FROM JOB DEMAND RECOURSE MODEL. *Science International*, 28(3).

**ABSTRACT: Not Found**

**Web URL:**

5. Gillani, A., Irfan, R. N. L. S., & Mehmood, Z. EXAMINING THE RELATIONSHIP BETWEEN SERVICE EXCELLENCE AND CUSTOMER DELIGHT: MEDIATING ROLE OF CUSTOMER SATISFACTION.

**ABSTRACT: Not Found**

**Web URL:**

6. Khan, R. S., Malik, A. A., Bashir, M. A., Sheikh, N. H., Irfan, S. M., & Humayun, A. MAGNITUDE OF ABORTION AND ITS ASSOCIATED HEALTH CARE SEEKING IN DYAL VILLAGE OF LAHORE, PAKISTAN. *education*, 28, 32-6.

**ABSTRACT:**

The issue of abortion is a threat to women's reproductive wellbeing and restrictive abortion laws are associated with increase in the percentage of abortions performed unsafely by unskilled persons. This study aims to identify prevalence of unsafe and safe abortions and to assess related health care seeking in ever-married women of reproductive age group residing in Dyal village Wahga town Lahore, Pakistan. Cross sectional study method is used to collect data from 86 women experiencing 120 abortions during last five years. Semi-structured questionnaire were used to gather the information for abortion variates and related health care

seeking. Results of this study provides insights that eighty-six women had 402 pregnancies. Among these 402 pregnancies, they experienced no of abortions were 127/402 (31.6%). Abortion rate 169 per 1000 reproductive age group during the last five years and 33.88 per 1000 reproductive age group females per year. According to legality status 66/120 (55%) were ill-legal abortions. According to safety status 46/120 (38.3%) abortions were unsafe. Among 88/120 (73.33%) abortions performed by health care providers, 70/88 (79.54%) were induced and 18/88 (20.45%) were spontaneous. Out of these 36/88 (40.90%) were performed by Dai(non-professional). Majority of these 30/88 (34.09%) were illegal. While 10/88 (11.36%) had self-medication.

**Web URL:** <http://www.sci-int.com/pdf/9621592001%20a%201%203549-3553%20Raozina%20paper--CO%20IRFAN.pdf>

**7. Sanaullah, A., ul Amin, M. N., Hanif, M., & Kadilar, C. (2016). Generalized Exponential Chain Ratio and Chain Product Estimators under Stratified Two-Phase Random Sampling for Non-Response. *International Journal of Applied Mathematics and Statistics™*, 55(2), 57-79.**

**ABSTRACT:**

In this paper, some generalized exponential chain-ratio and chain-product estimators have been proposed for estimating the finite population mean under the stratified two-phase random sampling method for two different cases under non-response case when information on only secondary auxiliary variable is available. The expressions for the bias and mean square error (MSE) of proposed estimators have been derived for two different situations under non-response case. The proposed class of generalized exponential estimators has been compared in theory with the adapted forms of Hansen-Hurwitz, ratio and product estimators to the stratified two-phase sampling method. An empirical study has also been given to demonstrate the performances of the estimators.

**Web URL:**

[http://s3.amazonaws.com/academia.edu.documents/41771356/Generalized\\_Exponential\\_Chain\\_Ratio\\_and\\_20160130-1816-13at9io.pdf?AWSAccessKeyId=AKIAIWOWYYGZ2Y53UL3A&Expires=1500531051&Signature=M6](http://s3.amazonaws.com/academia.edu.documents/41771356/Generalized_Exponential_Chain_Ratio_and_20160130-1816-13at9io.pdf?AWSAccessKeyId=AKIAIWOWYYGZ2Y53UL3A&Expires=1500531051&Signature=M6)

[QoM0d4%2BrKpwcJQHMMq46dUclU%3D&response-content-disposition=inline%3B%20filename%3DGeneralized\\_Exponential\\_Chain\\_Ratio\\_and.pdf](#)

8. Sanaullah, A., Hanif, M., & Asghar, A. (2016). Generalized Exponential Estimators for Population Variance Under Two-Phase Sampling. *International Journal of Applied and Computational Mathematics*, 2(1), 75-84.

**ABSTRACT:**

In this study, two-phase sampling is considered for estimating the population variance of study variable taking two auxiliary variables. The proposed generalized estimator and class of estimators are the exponential function of auxiliary variables. The mean square errors and biases equations have been obtained for the proposed estimators. The conditions for which proposed estimators are more efficient as compared to other estimators have been discussed. The empirical study showed that proposed estimators are more efficient as compared to the unbiased sample variance estimator, double sampling version of Isaki (J Am Stat Assoc 78:117–123, 1983) and Singh et al. (Ital. J. Pure Appl. Math. 28(N):101–108, 2011) generalized estimator.

**Web URL:** <https://link.springer.com/article/10.1007/s40819-015-0047-5>

9. Yasmeen, U., Noor-ul-Amin, M, & Hanif, M. (2016). Exponential ratio and product type estimators of finite population mean. *Journal of Statistics and Management Systems*, 19(1), 55-71.

**ABSTRACT:**

The improved exponential type estimators for finite population mean are proposed. The proposed estimators are based on the information from two transformed auxiliary variables using simple random sampling without replacement. The expression for the mean square error and bias of the proposed estimators has been derived, and the conditions have been obtained under which these estimators are more efficient than the existing estimators. Empirical study has also been conducted to show the improvement in efficiency of the proposed estimators.

**Web URL:** <http://www.tandfonline.com/doi/abs/10.1080/09720510.2015.1040249>

**10. Noor-ul-Amin, M., .Shahbaz, M. Q., & Kadilar, C. (2016). Ratio Estimators for Population Mean Using Robust Regression in Double Sampling. *Gazi University Journal of Science*, 29(4), 793-798.**

**ABSTRACT:**

In this article, ratio estimators for the population mean are suggested using the robust regression under the double sampling scheme. The mean squared error (MSE) expressions are obtained for the first degree of approximation. Theoretical comparisons show that the proposed estimators having the robust regression estimates are more efficient than the estimators using the least square method under the certain conditions. Theoretical findings are supported with the aid of a real life dataset in application and a simulation study is also conducted to evaluate the performance of the proposed estimators.

**Web URL:** <http://gujs.gazi.edu.tr/article/viewFile/5000188489/5000178056>

**11. Mushtaq, Nadia & Noor-ul-Amin, M & Hanif, Muhammad. (2016). Estimation of a population mean of a sensitive variable in stratified two-phase sampling. 32. 393-404.**

**ABSTRACT:**

In this study, we present the estimation of population mean of a sensitive variable in stratified sampling using two-phase sampling based on randomized response technique. We introduce a ratio, a regression and general class of estimators for the mean of sensitive variable using non-sensitive auxiliary variable based on randomized response technique in stratified two-phase sampling. Under stratified two phase sampling, the expression of bias and mean square error (MSE) up to the first-order approximations are derived. Simulation studies and real data are presented to demonstrate the performance of proposed estimators.

**Web URL:**

[https://www.researchgate.net/publication/311822674\\_Estimation\\_of\\_a\\_population\\_mean\\_of\\_a\\_sensitive\\_variable\\_in\\_stratified\\_two-phase\\_sampling](https://www.researchgate.net/publication/311822674_Estimation_of_a_population_mean_of_a_sensitive_variable_in_stratified_two-phase_sampling)

**12. Javaid,A. Noor-ul-Amin, M, Hanif, M. (2016) Two Parametric Ratio Estimator for Population Mean in Systematic Sampling. *Journal of Applied Statistical Sciences***

**ABSTRACT: Not found**

**Web URL:**

13. Shahbaz, S. H., Ismail, M., & Butt, N. S. (2016). The McDonald's Inverse Weibull Distribution. *Pakistan Journal of Statistics and Operation Research*, 12(4), 775-785.

**ABSTRACT:**

We have proposed a new Inverse Weibull distribution by using the generalized Beta distribution of McDonald (1984). Basic properties of the proposed distribution has been studied. Parameter estimation has been discussed alongside an illustrative example.

**Web URL:** [file:///C:/Users/shazia/Downloads/1650-6262-1-PB%20\(1\).pdf](file:///C:/Users/shazia/Downloads/1650-6262-1-PB%20(1).pdf)

14. Naeem, N., & Shabbir, J. (2016). Use of Scrambled Responses on Two Occasions Successive Sampling under Non-Response.

**ABSTRACT:**

In this paper, we deal with a problem of non-response on two successive occasions when the study character becomes sensitive in nature on second occasion. Estimators are formulated by considering two cases of non-response, (i) when non-response on both occasions, (ii) when non-response on current occasion only. Expressions for mean squared errors (MSEs) are derived under large sample approximation and the optimum replacement strategies are also discussed. A numerical study is carried out in support of the proposed technique.

**Web URL:** <http://www.hjms.hacettepe.edu.tr/uploads/32c18b80-275f-4b5a-a28d-6a5890eecac3.pdf>

# DEPARTMENT OF PHYSICS

## Journal Papers

1. Anjum, S., Nazli, H., Khurram, R., Zeeshan, T., Riaz, S., & Usman, A. (2016). Role of Zn substitution on structural, magnetic and dielectric properties of Cu–Cr spinel ferrites. *Indian Journal of Physics*, 90(8), 869-880.

**ABSTRACT:**

The Zn substituted copper chromium spinel ferrites with the chemical formula  $Zn_xCu_{1-x}Cr_{0.5}Fe_{1.5}O_4$  ( $x = 0-0.8$ ) have been fabricated using powder metallurgical route. The synthesized powders have been investigated by thermal analysis, X-ray diffraction, Fourier transform infrared spectroscopy, Field emission scanning electron microscopy, magnetic and electrical measurement. The X-ray diffraction has confirmed the formation of spinel structure. It has been observed that lattice parameter increases but both the bulk and X-ray density decrease with the increase of Zn concentration. FTIR spectra show two prominent bands in the range of 400–800  $cm^{-1}$  confirming the formation of spinel ferrites. The saturation magnetization increases up to  $x = 0.4$ . As the concentration of Zn increases further, the saturation magnetization decreases. The dielectric tangent loss and dielectric constant ( $\epsilon$ ) decreases while the ac conductivity increases with increasing frequency.

**Web URL:**

[https://www.researchgate.net/profile/Arslan\\_Usman/publication/289586595\\_Role\\_of\\_Zn\\_substitution\\_on\\_structural\\_magnetic\\_and\\_dielectric\\_properties\\_of\\_Cu-Cr\\_spinel\\_ferrites/links/56a6095608ae2c689d39a44b/Role-of-Zn-substitution-on-structural-magnetic-and-dielectric-properties-of-Cu-Cr-spinel-ferrites.pdf](https://www.researchgate.net/profile/Arslan_Usman/publication/289586595_Role_of_Zn_substitution_on_structural_magnetic_and_dielectric_properties_of_Cu-Cr_spinel_ferrites/links/56a6095608ae2c689d39a44b/Role-of-Zn-substitution-on-structural-magnetic-and-dielectric-properties-of-Cu-Cr-spinel-ferrites.pdf)

2. Irshad, M., Siraj, K., Raza, R., Ali, A., Tiwari, P., Zhu, B., ...& Usman, A. (2016). A Brief Description of High Temperature Solid Oxide Fuel Cell's Operation, Materials, Design, Fabrication Technologies and Performance. *Applied Sciences*, 6(3), 75.

**ABSTRACT:**

Today's world needs highly efficient systems that can fulfill the growing demand for energy. One of the promising solutions is the fuel cell. Solid oxide fuel cell (SOFC) is considered by many developed countries as an alternative solution of energy in near future. A lot of efforts have been made during last decade to make it commercial by reducing its cost and increasing its durability. Different materials, designs and fabrication technologies have been developed and tested to make it more cost effective and stable. This article is focused on the advancements made in the field of high temperature SOFC. High temperature SOFC does not need any precious catalyst for its operation, unlike in other types of fuel cell. Different conventional and innovative materials have been discussed along with properties and effects on the performance of SOFC's components (electrolyte anode, cathode, interconnect and sealing materials). Advancements made in the field of cell and stack design are also explored along with hurdles coming in their fabrication and performance. This article also gives an overview of methods required for the fabrication of different components of SOFC. The flexibility of SOFC in terms fuel has also been discussed. Performance of the SOFC with varying combination of electrolyte, anode, cathode and fuel is also described in this article.

**Web URL:** <http://www.mdpi.com/2076-3417/6/3/75/htm>

**3. Afaq, A., Iqbal, A., Rahman, A. U., Khan, N., & Ansari, M. M. (2016). Photodetachment Spectrum of Hydrogen Negative Ion Near a Partially Reflecting Spherical Surface. *Brazilian Journal of Physics*, 46(5), 489-495.**

**ABSTRACT:**

Photodetachment of negative ions near surfaces is of great interest in view of its fundamental significance and technological applications. We reinvestigate the dynamics of photoelectrons in H<sup>-</sup> photodetachment near a partially reflecting spherical surface by the semiclassical closedorbit theory. Reflection parameter R and curvature K is used to observe inelastic and spherical effects of the surface, respectively. The classical action is evaluated from the photodetached electron trajectories incident normally at the surface, arising simultaneously from the source and its image. The derived analytical formula of photodetachment cross

section correctly recovers the results of reflective spherical surface published recently based on theoretical imaging method.

**Web URL:**

[https://www.researchgate.net/profile/Amin\\_Rahman3/publication/306126315\\_Photodetachment\\_Spectrum\\_of\\_Hydrogen\\_Negative\\_Ion\\_Near\\_a\\_Partially\\_Reflecting\\_Spherical\\_Surface/links/57bbf58108ae9fdf82ef1ca9.pdf](https://www.researchgate.net/profile/Amin_Rahman3/publication/306126315_Photodetachment_Spectrum_of_Hydrogen_Negative_Ion_Near_a_Partially_Reflecting_Spherical_Surface/links/57bbf58108ae9fdf82ef1ca9.pdf)

**4. Rafique, M. Y., Ellahi, M., Iqbal, M. Z., & Pan, L. (2016). Gram scale synthesis of single crystalline nano-octahedron of NiFe<sub>2</sub>O<sub>4</sub>: Magnetic and optical properties. *Materials Letters*, 162, 269-272.**

**ABSTRACT:**

Gram scales Ni ferrite nano-octahedrons are prepared by cost effective and facile hydrothermal method. The mass of as-synthesized Ni ferrite nano-octahedron is about 1.37 g. Nano-octahedron of Ni ferrite are highly uniform and the edge length of octahedron is 80 nm. Transmission electron microscopy (TEM) and selected area electron diffraction (SAED) pattern confirm that octahedron nanoparticles are single crystalline. The direct and indirect band gaps are acquired to be 1.55 eV and 1.7 eV respectively. The saturation magnetization, coercivity, and remanent magnetization are obtained to be 55.1 emu/g, 69 Oe, and 9.8 emu/g respectively. This method is useful to synthesize the Ni ferrite nanostructure for commercial and industrial scale.

**Web URL:** [http://ac.els-cdn.com/S0167577X15306741/1-s2.0-S0167577X15306741-main.pdf?\\_tid=7b03b2a4-6d10-11e7-9d58-0000aab0f01&acdnat=1500530501\\_e04d34c664c29856d5f39605ba58ca6b](http://ac.els-cdn.com/S0167577X15306741/1-s2.0-S0167577X15306741-main.pdf?_tid=7b03b2a4-6d10-11e7-9d58-0000aab0f01&acdnat=1500530501_e04d34c664c29856d5f39605ba58ca6b)

**5. Rafique, M. Y., Pan, L., & Farid, A. (2016). From nano-dendrite to nano-sphere of Co<sub>100-x</sub>Ni<sub>x</sub> alloy: Composition dependent morphology, structure and magnetic properties. *Journal of Alloys and Compounds*, 656, 443-451.**

**ABSTRACT:**

Co<sub>100-x</sub>Ni<sub>x</sub> (x = 0, 10, 20, 30, ..., 100) alloy nanostructures with controlled composition are prepared by hydrothermal method. The effects of composition on crystal structure,

morphology, growth of nanostructure, and magnetic properties are described. The crystal structure is hexagonal closed pack (hcp) at  $x = 0$ , mixture of hcp and face-centered cubic (fcc) for  $0 < x < 0.3$ , and purely fcc for  $x = 1.0$ . The morphology is changed from nano-dendrite ( $x = 0$ ) to flower like structure composed on spherical core and nanorods ( $x = 0.5$ ) to nanosphere ( $x = 1.0$ ). The isotropic (spherical shape) character increases with Ni Content. Compositional analyses show the controlled composition in nanostructure. The saturation magnetization is 156 emu/g at  $x = 0$  and decreases linearly with alloy composition ( $x$ ) to 55 emu/g at  $x = 1.0$ . The coercivity is 285 Oe at  $x = 0$  (dendrite) and decrease gradually to 21 Oe at  $x = 0.8$ , and then increases to 146 Oe at  $x = 1.0$ . The effective anisotropy ( $K_{eff}$ ) constant decreases gradually with alloy composition and shows decaying exponential dependence on alloy-composition ( $x$ ). Magnetic and structural properties are explained by combined consequences of composition and nanoscale effects. This study reveals that the composition of alloy plays important role in growth, morphology, crystal structure and hence, properties of nanostructure.

**Web URL:**

[https://www.researchgate.net/profile/Muhammad\\_Farid10/publication/283680536\\_From\\_nano-dendrite\\_to\\_nano-sphere\\_of\\_Co100-xNi\\_x\\_alloy\\_Composition\\_dependent\\_morphology\\_structure\\_and\\_magnetic\\_properties/links/564ae54908ae127ff9870a3a.pdf](https://www.researchgate.net/profile/Muhammad_Farid10/publication/283680536_From_nano-dendrite_to_nano-sphere_of_Co100-xNi_x_alloy_Composition_dependent_morphology_structure_and_magnetic_properties/links/564ae54908ae127ff9870a3a.pdf)

6. Rasheed, A., Jamil, M., Areeb, F., Siddique, M., & Salimullah, M. (2016). Low frequency hybrid instability in quantum magneto semiconductor plasmas. *Journal of Physics D: Applied Physics*, 49(17), 175109.

**ABSTRACT:**

The excitation of electrostatic, comparatively low frequency, lower-hybrid waves (LHWs) induced by electron beam in semiconductor plasma is examined using a quantum hydrodynamic model. Various quantum effects are taken into account including the recoil effect, Fermi degenerate pressure, and exchange-correlation potential. The effects of different parameters like the electron-to-hole number density ratio, scaled electron beam temperature and streaming speed, propagation angle and cyclotron frequency over the growth, and phase

speed of LHWs are investigated. It is noticed that an increase in the electron number density and streaming speed enhance the instability. Similar effects are observed on decreasing the propagation angle with magnetic field.

**Web URL:** <http://iopscience.iop.org/article/10.1088/0022-3727/49/17/175109/meta>

**7. Ahmad, M. A., Azam, S., Aslam, S., Bukhari, S. H., Jamil, A., Mustafa, F., & Khan, S. N. (2016). Higher order squeezing as a measure of nonclassicality. *Optik-International Journal for Light and Electron Optics*, 127(5), 2992-2995.**

**ABSTRACT:**

Here, we have used a simplified criteria to study the possibilities of observing higher order squeezing for the superposition of two coherent states out of phase by  $\pi/2$  and  $3\pi/2$ . Remarkably, it is observed that the considered states exhibit higher order squeezing which reflects their nonclassical nature. It has been observed that the existence of higher order squeezing is dependent on the particular values of relative phase. Moreover, the squeezing effect gets stronger when relative phase of superposition is equal to the average photon number.

**Web URL:** [http://ac.els-cdn.com/S0030402615018616/1-s2.0-S0030402615018616-main.pdf?tid=7bdb1390-6d13-11e7-ab34-0000aab0f27&acdnat=1500531791\\_a3ad8bea02ab223436d96717fca58d1b](http://ac.els-cdn.com/S0030402615018616/1-s2.0-S0030402615018616-main.pdf?tid=7bdb1390-6d13-11e7-ab34-0000aab0f27&acdnat=1500531791_a3ad8bea02ab223436d96717fca58d1b)

**8. Raza, R., Akram, N., Javed, M. S., Rafique, A., Ullah, K., Ali, A., ...& Ahmed, R. (2016). Fuel cell technology for sustainable development in Pakistan—An over-view. *Renewable and Sustainable Energy Reviews*, 53, 450-461.**

**ABSTRACT:**

Fuel cell technology holds the combination of benefits, which are barely offered by any other energy generating technology. Because the fuel used in this technology is found in abundance in nature and can also be renewed/sustained. Pakistan is blessed with renewable energy resources which are suitable for fuel cell technology. Therefore, fuel cell technology offers a great opportunity to meet the demand of energy and for the sustainable development of Pakistan. The energy research group at COMSATS Institute of Information Technology (CIIT),

Lahore has made efforts to study the technical aspects of fuel cell technology and its commercial benefits. The research group is interested in finding ways and means of generating and storing the energy produced by using fuel cells. In this paper, the research activities on fuel cell technology in Pakistan have been reviewed and it is also discussed how this technology can resolve the current energy crises in Pakistan and can be the source of sustainable energy. It has been also reviewed that the country would greatly benefit from fuel cells and fuel cell hybrid system (environmental friendly technology), which could be the best solution for electricity production as well for automobile industry.

**Web URL:**

[https://www.researchgate.net/profile/Muhammad\\_Sufyan\\_Javed/publication/282131285\\_Fuel\\_cell\\_technology\\_for\\_sustainable\\_development\\_in\\_Pakistan\\_-\\_An\\_over-view/links/5604038c08aebfdb30b70a04/Fuel-cell-technology-for-sustainable-development-in-Pakistan-An-over-view.pdf](https://www.researchgate.net/profile/Muhammad_Sufyan_Javed/publication/282131285_Fuel_cell_technology_for_sustainable_development_in_Pakistan_-_An_over-view/links/5604038c08aebfdb30b70a04/Fuel-cell-technology-for-sustainable-development-in-Pakistan-An-over-view.pdf)

**9. Javed, M. S., Raza, R., Ahsan, Z., Rafique, M. S., Shahzadi, S., Shaukat, S. F., ...& Zhu, B. (2016). Electrochemical studies of perovskite cathode material for direct natural gas fuel cell. *International Journal of Hydrogen Energy*, 41(4), 3072-3078.**

**ABSTRACT:**

Natural gas is the most promising renewable energy source and its widespread availability ensured its importance for early applications in stationary fuel cells as a reliable and low cost fuel. Therefore it is very important to efficiently utilization of natural gas in low temperature fuel cells. Herein, we demonstrate the synthesis of perovskite material of Yttrium doped  $Sr_{0.92}Fe_xTi_{1-x}O_{3-d}$  ( $x = 0.25, 0.30$ ) (YSFT) by solid state reaction method and further investigated as a new cathode material for a low temperature solid oxide fuel cell fueled by natural gas. The YSFT is characterized by X-ray powder diffraction, BrunauereEmmetteTeller and scanning electron microscopy. The perovskite structure is achieved at relatively low temperature (850 C). The average crystalline size is found 28 nm and 36 nm for  $x = 0.25$  and 0.30 respectively. TGA results showed the lattice oxygen loss of YSFT is about 0.206% in its original weight in the temperature range of 25e1000 C. The maximum electronic conductivities of 2.3 Scm<sup>-1</sup> and 2.07 Scm<sup>-1</sup> are achieved for  $x = 0.25$  and  $x = 0.30$  at 550 C in air atmosphere

respectively. It is observed that the oxygen reduction is enhanced due to the perovskite crystal structure and oxygen vacancies play an important role in the redox reaction to improve the performance of fuel cell. The YSFT perovskite cathode material based fuel cell with natural gas have achieved the power density of 250 mW/cm<sup>2</sup> for  $x = 0.25$  at 550 °C. The fuel cell device has demonstrated very stable results by running continuously for 5 h with domestic available natural gas. Copyright © 2015, Hydrogen Energy Publications, LLC. Published by Elsevier Ltd. All rights reserved.

**Web URL:** [http://ac.els-cdn.com/S0360319915310831/1-s2.0-S0360319915310831-main.pdf?\\_tid=7b38549c-6d14-11e7-9340-0000aacb360&acdnat=1500532219\\_36f50532d0d734b56db31ff4263d6925](http://ac.els-cdn.com/S0360319915310831/1-s2.0-S0360319915310831-main.pdf?_tid=7b38549c-6d14-11e7-9340-0000aacb360&acdnat=1500532219_36f50532d0d734b56db31ff4263d6925)

**10. Irshad, M., Siraj, K., Raza, R., Javed, F., Ahsan, M., Shakir, I., & Rafique, M. S. (2016). High performance of SDC and GDC core shell type composite electrolytes using methane as a fuel for low temperature SOFC. *AIP Advances*, 6(2), 025202.**

**ABSTRACT:**

Nanocomposites Samarium doped Ceria (SDC), Gadolinium doped Ceria (GDC), core shell SDC amorphous Na<sub>2</sub>CO<sub>3</sub> (SDCC) and GDC amorphous Na<sub>2</sub>CO<sub>3</sub> (GDCC) were synthesized using co-precipitation method and then compared to obtain better solid oxide electrolytes materials for low temperature Solid Oxide Fuel Cell (SOFCs). The comparison is done in terms of structure, crystallinity, thermal stability, conductivity and cell performance. In present work, XRD analysis confirmed proper doping of Sm and Gd in both single phase (SDC, GDC) and dual phase core shell (SDCC, GDCC) electrolyte materials. EDX analysis validated the presence of Sm and Gd in both single and dual phase electrolyte materials; also confirming the presence of amorphous Na<sub>2</sub>CO<sub>3</sub> in SDCC and GDCC. From TGA analysis a steep weight loss is observed in case of SDCC and GDCC when temperature rises above 725 °C while SDC and GDC do not show any loss. The ionic conductivity and cell performance of single phase SDC and GDC nanocomposite were compared with core shell GDC/amorphous Na<sub>2</sub>CO<sub>3</sub> and SDC/ amorphous Na<sub>2</sub>CO<sub>3</sub> nanocomposites using methane fuel. It is observed that dual phase core shell electrolytes materials (SDCC, GDCC) show better performance in low temperature range than their

corresponding single phase electrolyte materials (SDC, GDC) with methane fuel. © 2016 Author(s). All article content, except where otherwise noted, is licensed under a Creative Commons Attribution 3.0 Unported License.

**Web URL:** <http://aip.scitation.org/doi/pdf/10.1063/1.4941676>

**11. Dong, W., Yaqub, A., Janjua, N. K., Raza, R., Afzal, M., & Zhu, B. (2016). All in one multifunctional perovskite material for next generation SOFC. *Electrochimica Acta*, 193, 225-230.**

**ABSTRACT:**

Multifunctional roles of La<sub>0.2</sub>Sr<sub>0.25</sub>Ca<sub>0.45</sub>TiO<sub>3</sub> (LSCT) perovskite material as anode, cathode, and electrolyte for low temperature solid oxide fuel cell (LT-SOFC) are discovered for the first time, and have been investigated via electrochemical impedance spectroscopy (EIS) and fuel cell (FC) measurements. LSCT resistance decreases prominently in FC environment as shown in this study. An improved performance was observed by compositing LSCT with samaria doped ceria (SDC) at 550 C when the FC power density increased from tens of mWcm<sup>2</sup> for the pure LSCT system up to hundreds of mWcm<sup>2</sup>. The improved conductivity of LSCT–SDC composite is highlighted. The multifunctionality of LSCT as cathode, anode and electrolyte could be attributed to different conducting behavior at high and low oxygen partial pressures and ionic conduction at intermediate oxygen partial pressures. These new discoveries not only indicate great potential for exploring multifunctional perovskites for the next generation SOFC, but also deepen SOFC science and develop new technologies.

**Web URL:**

[https://www.researchgate.net/profile/Bin\\_Zhu24/publication/294423159\\_All\\_in\\_One\\_Multifunctional\\_Perovskite\\_Material\\_for\\_Next\\_Generation\\_SOFC/links/56c6902f08ae408dfe4d6e71.pdf](https://www.researchgate.net/profile/Bin_Zhu24/publication/294423159_All_in_One_Multifunctional_Perovskite_Material_for_Next_Generation_SOFC/links/56c6902f08ae408dfe4d6e71.pdf)

**12. Akhtar, M. N., Sulong, A. B., Khan, M. A., Ahmad, M., Murtaza, G., Raza, M. R., ...& Kashif, M. (2016). Structural and magnetic properties of yttrium iron garnet (YIG) and yttrium aluminum iron garnet (YAIG) nanoferrites prepared by microemulsion method. *Journal of Magnetism and Magnetic Materials*, 401, 425-431.**

**ABSTRACT:**

Yttrium iron garnet (YIG) and yttrium aluminum iron garnet (YAIG) nanoferrite samples were synthesized by microemulsion method. The effect of sintering was examined by heating the samples at 900, 1000, and 1100 °C. The YIG and YAIG samples were then characterized using X-ray diffraction and field-emission scanning electron microscopy. Static and dynamic magnetic properties were measured by evaluating initial permeability, Q factor, and vibrating sample magnetometry properties of YIG and YAIG samples. YIG samples sintered at 1100 °C showed higher initial permeability and Q factor compared with YAIG samples. However, hysteresis loops also showed variations in the saturation magnetization, remanence, and coercivity of YIG and YAIG samples sintered at 900, 1000, and 1100 °C. The observed magnetic parameter such as saturation magnetization, coercivity and initial permeability are strongly affected by increasing temperature. The saturation magnetization and coercivity of YIG and YAIG nanoferrites were found in the range 11.56–19.92 emu/g and 7.30–87.70 Oe respectively. Furthermore, the decreasing trends in the static and magnetic properties of YAIG samples may be due to the introduction of Al ions in the YIG crystal lattice. Thus, YIG and YAIG sintered at 1100 °C can be used for wide-ranging frequency applications.

**Web URL:** [http://ac.els-cdn.com/S0304885315306946/1-s2.0-S0304885315306946-main.pdf?\\_tid=c1700436-6d15-11e7-9768-00000aab0f02&acdnat=1500532766\\_12b6c45eaa8074afcd638a3260684dfc](http://ac.els-cdn.com/S0304885315306946/1-s2.0-S0304885315306946-main.pdf?_tid=c1700436-6d15-11e7-9768-00000aab0f02&acdnat=1500532766_12b6c45eaa8074afcd638a3260684dfc)

**13. Khan, M. , Murtaza, G., Raza, R. & Kashif, M. (2016). Structural and Magnetic Properties of Yttrium Iron Garnet (YIG) and Yttrium Aluminum Iron Garnet (YAIG) Nanoferrites..., *Journal of Magnetism and Magnetic Materials*.**

**ABSTRACT:**

Yttrium iron garnet (YIG) and yttrium aluminum iron garnet (YAIG) nanoferrite samples were synthesized by microemulsion method. The effect of sintering was examined by heating the samples at 900, 1000, and 1100 °C. The YIG and YAIG samples were then characterized using X-ray diffraction and field-emission scanning electron microscopy. Static and dynamic magnetic properties were measured by evaluating initial permeability, Q factor, and vibrating sample magnetometry properties of YIG and YAIG samples. YIG samples sintered at 1100 °C showed

higher initial permeability and Q factor compared with YAIG samples. However, hysteresis loops also showed variations in the saturation magnetization, remanence, and coercivity of YIG and YAIG samples sintered at 900, 1000, and 1100 °C. The observed magnetic parameter such as saturation magnetization, coercivity and initial permeability are strongly affected by increasing temperature. The saturation magnetization and coercivity of YIG and YAIG nanoferrites were found in the range 11.56-19.92 emu/g and 7.30-87.70 Oe respectively. Furthermore, the decreasing trends in the static and magnetic properties of YAIG samples may be due to the introduction of Al ions in the YIG crystal lattice. Thus, YIG and YAIG sintered at 1100 °C can be used for wide-ranging frequency applications.

**Web URL:**

[https://www.researchgate.net/publication/282942535\\_Structural\\_and\\_Magnetic\\_Properties\\_of\\_Yttrium\\_Iron\\_Garnet\\_YIG\\_and\\_Yttrium\\_Aluminum\\_Iron\\_Garnet\\_YAIG\\_Nanoferrites\\_Prepared\\_by\\_Microemulsion\\_Method\\_Original\\_Research\\_Article](https://www.researchgate.net/publication/282942535_Structural_and_Magnetic_Properties_of_Yttrium_Iron_Garnet_YIG_and_Yttrium_Aluminum_Iron_Garnet_YAIG_Nanoferrites_Prepared_by_Microemulsion_Method_Original_Research_Article)

**14. Raza, M. R., Ahmad, F., Muhamad, N., Sulong, A. B., Omar, M. A., Akhtar, M. N., & Aslam, M. (2016). Effects of solid loading and cooling rate on the mechanical properties and corrosion behavior of powder injection molded 316 L stainless steel. *Powder Technology*, 289, 135-142**

**ABSTRACT:**

Solid loading and post-sintered cooling rates are two effective parameters used to control the mechanical properties of powder-injection molded parts. In the case of 316L stainless steel (SS), these parameters also influence mechanical properties and corrosion resistance. In this study, four formulations with powder loading above and below the critical powder loading were prepared and sintered at 1325 °C in vacuum with cooling rates varying from 3 °C/min to 10 °C/min. Solid loadings above the critical loading caused reductions in final properties (i.e. mechanical properties and corrosion resistance) because of increased porosity. The high cooling rate of 10 °C/min improved the mechanical properties due to the formation of large number of grains and corrosion resistance due to formation of chromium oxide layer at the surface of PIM

316L SS. Solid loading of 65 vol.% , sintered at 1325 °C with cooling rate of 10 °C/min showed improvements in terms of mechanical properties and corrosion resistance compared with conventional 316L SS. Such improvements were considered due to reduced grain sizes and formation of a chromium oxide layer on the sample surface. This study identify the solid loading

**Web URL:**

[https://www.researchgate.net/profile/Majid\\_Akhtar/publication/285280982\\_Effects\\_of\\_solid\\_loading\\_and\\_cooling\\_rate\\_on\\_the\\_mechanical\\_properties\\_and\\_corrosion\\_behavior\\_of\\_powder\\_injection\\_molded\\_316\\_L\\_stainless\\_steel/links/565d298b08aefe619b25509f/Effects-of-solid-loading-and-cooling-rate-on-the-mechanical-properties-and-corrosion-behavior-of-powder-injection-molded-316-L-stainless-steel.pdf](https://www.researchgate.net/profile/Majid_Akhtar/publication/285280982_Effects_of_solid_loading_and_cooling_rate_on_the_mechanical_properties_and_corrosion_behavior_of_powder_injection_molded_316_L_stainless_steel/links/565d298b08aefe619b25509f/Effects-of-solid-loading-and-cooling-rate-on-the-mechanical-properties-and-corrosion-behavior-of-powder-injection-molded-316-L-stainless-steel.pdf)

**15. Akhtar, M. N., Sulong, A. B., Ahmad, M., Khan, M. A., Ali, A., & Islam, M. U. (2016). Impacts of Gd–Ce on the structural, morphological and magnetic properties of garnet nanocrystalline ferrites synthesized via sol–gel route. *Journal of Alloys and Compounds*, 660, 486-495.**

**ABSTRACT:**

The effect of GdCe substitution on the structural, morphological and magnetic properties of garnet ferrites have been investigated in this study. The nanoferrites of GdCe with different substitution  $Gd_3Ce_{3x}Fe_5O_{12}$  ( $x = 0, 0.5, 1.0, 1.5, 2.0, 2.5$  and  $3.0$ ) were prepared using sol-gel route. X-ray diffraction (XRD), Field emission scanning electron microscopy (FESEM), Thermogravimetric (TG) and differential thermal (DT) analysis, Fourier transform infrared (FTIR) and Vibrating sample magnetometer (VSM) were used to measure the characteristics of GdCe substituted nanocrystalline powders. X-ray diffraction analysis revealed single phase structure of GdCe substituted garnet ferrites. However, lattice constant was not increased by increasing the Ce<sup>3+</sup> contents in the garnet structure which may be due to the nonreplacement of Fe<sup>3+</sup> ions. FTIR and TGA also confirm the garnet phase and nanocrystalline nature of Gd eCe substituted garnets respectively. Gd substituted ferrite without Ce<sup>3+</sup> contents shows better homogenous structure with well crystalline grains. The average particle size was in the range of 80-98 nm for all GdCe substituted nanocrystalline samples. Magnetic saturation, magnetic remanence, coercivity, Bohr magneton and magneto crystalline anisotropy constant (K) were

calculated from MH loops. It is noticed that the saturation magnetization, remanence decreased as concentration of Ce<sup>3+</sup> increased from x ¼ 0 to x ¼ 1.0 whereas at x ¼ 1.5 the saturation and remanence increased. Super paramagnetic behaviour was observed for Gd substituted ferrites. Furthermore, increase in coercivity in GdCe substituted nanocrystalline was observed from x ¼ 0 to x ¼ 2.5 whereas coercivity decreased at x ¼ 3.0. These GdCe substituted nanocrystalline garnet ferrites may play an important role for variety of applications.

**Web URL:** [http://ac.els-cdn.com/S0925838815317023/1-s2.0-S0925838815317023-main.pdf?\\_tid=cdc9ead4-6d16-11e7-b4c0-0000aacb35e&acdnat=1500533217\\_2de4039c779c66d6f2ca76eaf47c1f08](http://ac.els-cdn.com/S0925838815317023/1-s2.0-S0925838815317023-main.pdf?_tid=cdc9ead4-6d16-11e7-b4c0-0000aacb35e&acdnat=1500533217_2de4039c779c66d6f2ca76eaf47c1f08)

**16. S. Nisar , (2016) Study of  $J/\psi \rightarrow p\bar{p}$  at BESIII**

**ABSTRACT:** Not found

**Web URL:**

**17. Ablikim, M., Achasov, M. N., Ai, X. C., Albayrak, O., Albrecht, M., Ambrose, D. J., ...& Ferroli, R. B. (2016). Observation of the Singly Cabibbo-Suppressed Decay  $D^+ \rightarrow \omega \pi^+$  and Evidence for  $D^0 \rightarrow \omega \pi^0$ . *Physical review letters*, 116(8), 082001.**

**ABSTRACT:**

Based on  $2.93 \text{ fb}^{-1} e^+e^-$  collision data taken at center-of-mass energy of 3.773 GeV by the BESIII detector, we report searches for the singly Cabibbo-suppressed decays  $D^+ \rightarrow \omega \pi^+$  and  $D^0 \rightarrow \omega \pi^0$ . A double tag technique is used to measure the absolute branching fractions  $B(D^+ \rightarrow \omega \pi^+) = (2.79 \pm 0.57 \pm 0.16) \times 10^{-4}$  and  $B(D^0 \rightarrow \omega \pi^0) = (1.17 \pm 0.34 \pm 0.07) \times 10^{-4}$ , with statistical significances of  $5.5\sigma$  and  $4.1\sigma$ , respectively. We also present measurements of the absolute branching fractions for the related  $\eta \pi$  decay modes. We find  $B(D^+ \rightarrow \eta \pi^+) = (3.07 \pm 0.22 \pm 0.13) \times 10^{-3}$  and  $B(D^0 \rightarrow \eta \pi^0) = (0.65 \pm 0.09 \pm 0.04) \times 10^{-3}$ , which are consistent with the current world averages. The first and second uncertainties are statistical and systematic, respectively.

**Web URL:** <https://arxiv.org/pdf/1512.06998.pdf>

**18. Ablikim, M., Achasov, M. N., Ai, X. C., Albayrak, O., Albrecht, M., Ambrose, D. J., ...& Ferroli, R. B. (2016). Observation of  $e^+ e^- \rightarrow \omega \chi_{c1,2}$  near  $\sqrt{s} = 4.42$  and  $4.6$  GeV. *Physical Review D*, 93(1), 011102.**

**ABSTRACT:**

Based on data samples collected with the BESIII detector operating at the BEPCII storage ring at center-of-mass energies  $\sqrt{s} > 4.4$  GeV, the processes  $e^+ e^- \rightarrow \omega \chi_{c1,2}$  are observed for the first time. With an integrated luminosity of  $1074 \text{ pb}^{-1}$  near  $\sqrt{s} = 4.42$  GeV, a significant  $\omega \chi_{c2}$  signal is found, and the cross section is measured to be  $(20.9 \pm 3.2 \pm 2.5) \text{ pb}$ . With  $567 \text{ pb}^{-1}$  near  $\sqrt{s} = 4.6$  GeV, a clear  $\omega \chi_{c1}$  signal is seen, and the cross section is measured to be  $(9.5 \pm 2.1 \pm 1.3) \text{ pb}$ , while evidence is found for an  $\omega \chi_{c2}$  signal. The first errors are statistical and the second are systematic. <sup>3</sup> Due to low luminosity or low cross section at other energies, no significant signals are observed. In the  $\omega \chi_{c2}$  cross section, an enhancement is seen around  $\sqrt{s} = 4.42$  GeV. Fitting the cross section with a coherent sum of the  $\psi(4415)$  Breit-Wigner function and a phase space term, the branching fraction  $B(\psi(4415) \rightarrow \omega \chi_{c2})$  is obtained to be of the order of  $10^{-3}$

**Web URL:** <https://arxiv.org/pdf/1511.08564.pdf>

**19. Ablikim, M., Achasov, M. N., Ai, X. C., Albayrak, O., Albrecht, M., Ambrose, D. J., ...& Ferroli, R. B. (2016). Measurements of Absolute Hadronic Branching Fractions of the  $\Lambda^+ c$  Baryon. *Physical review letters*, 116(5), 052001.**

**ABSTRACT:**

We report the first measurement of absolute hadronic branching fractions of  $\Lambda^+ c$  baryon at the  $\Lambda^+ c$  production threshold, in the 30 years since the  $\Lambda^+ c$  discovery. In total, twelve Cabibbo-favored  $\Lambda^+ c$  hadronic decay modes are analyzed with a double-tag technique, based on a sample of  $567 \text{ pb}^{-1}$  of  $e^+ e^-$  collisions at  $\sqrt{s} = 4.599$  GeV recorded with the BESIII detector. A global least-squares <sup>3</sup> fitter is utilized to improve the measured precision. Among the measurements for twelve  $\Lambda^+ c$  decay modes, the branching fraction for  $\Lambda^+ c \rightarrow pK^+ \pi^-$  is determined to be  $(5.84 \pm 0.27 \pm 0.23)\%$ , where the first uncertainty is statistical and the second is systematic. In addition, the measurements of the branching fractions of the other eleven Cabibbo-favored hadronic decay modes are significantly improved.

**Web URL:** <https://arxiv.org/pdf/1511.08380.pdf>

**20. BESIII Collaboration. (2016). Measurement of the branching fraction for  $\psi(3770) \rightarrow \gamma \chi_{c0}$ . *Physics Letters B*, 753, 103-109.**

**ABSTRACT:**

By analyzing a data set of  $2.92 \text{ fb}^{-1}$  of  $e^+e^-$  collision data taken at  $\sqrt{s} = 3.773 \text{ GeV}$  and  $106.41 \times 106 \psi(3686)$  decays taken at  $\sqrt{s} = 3.686 \text{ GeV}$  with the BESIII detector at the BEPCII collider, we measure the branching fraction and the partial decay width for  $\psi(3770) \rightarrow \gamma \chi_{c0}$  to be  $B(\psi(3770) \rightarrow \gamma \chi_{c0}) = (6.88 \pm 0.28 \pm 0.67) \times 10^{-3}$  and  $[\psi(3770) \rightarrow \gamma \chi_{c0}] = (187 \pm 8 \pm 19) \text{ keV}$ , respectively. These are the most precise measurements to date

**Web URL:** [http://ac.els-cdn.com/S0370269315009302/1-s2.0-S0370269315009302-main.pdf?\\_tid=fcb78e44-6d18-11e7-8a50-00000aab0f6b&acdnat=1500534154\\_41f33326de7ed0bebf688aa6fe23b0bf](http://ac.els-cdn.com/S0370269315009302/1-s2.0-S0370269315009302-main.pdf?_tid=fcb78e44-6d18-11e7-8a50-00000aab0f6b&acdnat=1500534154_41f33326de7ed0bebf688aa6fe23b0bf)

**21. BESIII collaboration. (2016). Measurement of the  $e^+ e^- \rightarrow \pi^+ \pi^-$  cross section between 600 and 900 MeV using initial state radiation. *Physics Letters B*, 753, 629-638.**

**ABSTRACT:**

We extract the  $e^+e^- \rightarrow \pi^+\pi^-$  cross section in the energy range between 600 and 900 MeV, exploiting the method of initial state radiation. A data set with an integrated luminosity of  $2.93 \text{ fb}^{-1}$  taken at a center-of-mass energy of  $3.773 \text{ GeV}$  with the BESIII detector at the BEPCII collider is used. The cross section is measured with a systematic uncertainty of 0.9%. We extract the pion form factor  $|F_\pi|^2$  as well as the contribution of the measured cross section to the leading-order hadronic vacuum polarization contribution to  $(g-2)_\mu$ . We find this value to be  $a_{\pi\pi, \text{LO } \mu} (600-900 \text{ MeV}) = (368.2 \pm 2.5_{\text{stat}} \pm 3.3_{\text{sys}}) \cdot 10^{-10}$ , which is between the corresponding values using the BaBar or KLOE data.

**Web URL:** [http://ac.els-cdn.com/S0370269315008990/1-s2.0-S0370269315008990-main.pdf?\\_tid=bbd1b124-6d19-11e7-9340-00000aacb360&acdnat=1500534475\\_1d096bccb3b15558d1ef67094fe2cc49](http://ac.els-cdn.com/S0370269315008990/1-s2.0-S0370269315008990-main.pdf?_tid=bbd1b124-6d19-11e7-9340-00000aacb360&acdnat=1500534475_1d096bccb3b15558d1ef67094fe2cc49)

**22. Ablikim, M., Achasov, M. N., Ai, X. C., Albayrak, O., Albrecht, M., Ambrose, D. J., ...& Ferroli, R. B. (2016). Measurement of Azimuthal Asymmetries in Inclusive Charged Dipion Production in  $e^+ e^-$  Annihilations at  $s = 3.65$  GeV. *Physical review letters*, 116(4), 042001.**

**ABSTRACT:**

We present a measurement of the azimuthal asymmetries of two charged pions in the inclusive process  $e^+ e^- \rightarrow \pi\pi X$ , based on a data set of 62 pb<sup>-1</sup> at the center-of-mass energy of 3.65 GeV collected with the BESIII detector. These asymmetries can be attributed to the Collins fragmentation function. We observe a nonzero asymmetry, which increases with increasing pion momentum. As our energy scale is close to that of the existing semi-inclusive deep inelastic scattering experimental data, the measured asymmetries are important inputs for the global analysis of extracting the quark transversity distribution inside the nucleon and are valuable to explore the energy evolution of the 3 spin-dependent fragmentation function.

**Web URL:** <https://arxiv.org/pdf/1507.06824.pdf>

**23. Ablikim, M., Achasov, M. N., Ai, X. C., Albayrak, O., Albrecht, M., Ambrose, D. J., ...& Ferroli, R. B. (2015). Amplitude analysis of the  $\pi^0 \pi^0$  system produced in radiative  $J/\psi$  decays. *Physical Review D*, 92(5), 052003.**

**ABSTRACT:**

An amplitude analysis of the  $\pi^0 \pi^0$  system produced in radiative  $J/\psi$  decays is presented. In particular, a piecewise function that describes the dynamics of the  $\pi^0 \pi^0$  system is determined as a function of  $M_{\pi^0 \pi^0}$  from an analysis of the  $(1.311 \pm 0.011) \times 10^9$   $J/\psi$  decays collected by the BESIII detector. The goal of this analysis is to provide a description of the scalar and tensor components of the  $\pi^0 \pi^0$  system while making minimal assumptions about the properties or number of poles in the 3 amplitude. Such a model-independent description allows one to integrate these results with other related results from complementary reactions in the development of phenomenological models, which can then be used to directly fit experimental data to obtain parameters of interest. The branching fraction of  $J/\psi \rightarrow \gamma \pi^0 \pi^0$  is determined to be  $(1.15 \pm 0.05) \times 10^{-3}$ , where the uncertainty is systematic only and the statistical uncertainty is negligible.

**Web URL:** <https://arxiv.org/pdf/1506.00546.pdf>

**24. Alia, A., Ahmada, M., Akhtara, M. N., Shaukata, S. F., Mustafab, G., Atifc, M., & Farooqc, W. A. (2016). Magnetic Nanoparticles (Fe<sub>3</sub>O<sub>4</sub> & Co<sub>3</sub>O<sub>4</sub>) and Their Applications in Urea Biosensing<sup>1</sup>. *RUSSIAN JOURNAL OF APPLIED CHEMISTRY*, 89(4).**

**ABSTRACT:**

Nanobiotechnology has opened a new and exciting opportunities for exploring urea biosensor based on magnetic nanoparticles (NPs) mainly Fe<sub>3</sub>O<sub>4</sub> and Co<sub>3</sub>O<sub>4</sub>. These NPs have been extensively exploited to develop biosensors with stability, selectivity, reproducibility and fast response time. This review gives an overview of the development of urea biosensor based on Fe<sub>3</sub>O<sub>4</sub> and Co<sub>3</sub>O<sub>4</sub> for in vitro diagnostic applications along with significant improvements over the last few decades. Additionally, effort has been made to elaborate properties of magnetic nanoparticles (MNPs) in biosensing aspects. It also gives details of recent developments in hybrid nanobiocomposite based urea biosensor.

**Web URL:** <https://link.springer.com/article/10.1134/S1070427216040017>

**25. Smolyakov, A. I., Bashir, M. F., Elfimov, A. G., Yagi, M., & Miyato, N. (2016). On the dispersion of geodesic acoustic modes. *Plasma Physics Reports*, 42(5), 407-417.**

**ABSTRACT:**

The problem of dispersion of geodesic acoustic modes is revisited with two different methods for the solution of the kinetic equation. The dispersive corrections to the mode frequency are calculated by including the  $m = 2$  poloidal harmonics. Our obtained results agree with some earlier results but differ in various ways with other previous works. Limitations and advantages of different approaches are discussed.

**Web URL:** <https://link.springer.com/article/10.1134/S1063780X16050172>

**26. Atif, M., Idrees, M., Nadeem, M., Siddique, M., & Ashraf, M. W. (2016). Investigation on the structural, dielectric and impedance analysis of manganese substituted cobalt ferrite ie, Co<sub>1-x</sub>Mn<sub>x</sub>Fe<sub>2</sub>O<sub>4</sub> (0.0 ≤ x ≤ 0.4). *RSC Advances*, 6(25), 20876-20885.**

**ABSTRACT:**

Manganese substituted cobalt ferrites, i.e.,  $\text{Co}_{1-x}\text{Mn}_x\text{Fe}_2\text{O}_4$  ( $0.0 \leq x \leq 0.4$ ) were prepared by a solid state reaction method. XRD analysis confirmed the formation of a single-phase cubic spinel structure for all of the synthesized compositions, whereas an SEM study revealed that Mn substitution changes the microstructure.  $^{57}\text{Fe}$  Mossbauer spectroscopy measurements suggested that  $\text{Fe}^{3+}$  cations progressively migrate with Mn addition from tetrahedral (A) sites to octahedral (B) sites which have a relatively smaller covalency. Therefore, the distribution of cations between the A- and B-sites changed with increasing  $x$ . Moreover, interestingly, the  $\text{Fe}^{2+}/\text{Fe}^{3+}$  cation ratio remains zero and high spin  $\text{Fe}^{3+}$  is the only oxidation state observed at both sites for all of the synthesized compositions. In order to explore the effects of observed variations in the microstructure and cation distribution on the dielectric and resistive properties, the prepared samples were subjected to impedance spectroscopic experiments in a wide frequency range at room temperature. Mn substitution is found to improve the resistive properties by about two orders of magnitude. This increase in the resistive properties is explained in terms of the variations in the microstructure and decrease in the mobility of the charge carriers associated with the cations redistribution. Similarly, the variation in the dielectric permittivity is also conferred in terms of the change in microstructure and cation redistribution.

**Web URL:**

[https://www.researchgate.net/profile/Muhammad\\_Atif7/publication/294725641\\_Investigation\\_on\\_the\\_structural\\_dielectric\\_and\\_impedance\\_analysis\\_of\\_manganese\\_substituted\\_cobalt\\_ferrite\\_ie\\_Co1-xMnxFe2O4\\_00x04/links/56d662e508aeb4638ac7330.pdf](https://www.researchgate.net/profile/Muhammad_Atif7/publication/294725641_Investigation_on_the_structural_dielectric_and_impedance_analysis_of_manganese_substituted_cobalt_ferrite_ie_Co1-xMnxFe2O4_00x04/links/56d662e508aeb4638ac7330.pdf)

**27. Ahmad, I., Murtaza, G., Masood, S., Kanwal, M., Mustafa, G., Akhtar, M. N., ...& Ahmad, M. (2016). Effects of Pr-contents on the structural, magnetic and high frequency parameters of M-type hexagonal ferrites synthesized by sol–gel method. *Journal of Materials Science: Materials in Electronics*, 27(6), 6193-6201.**

**ABSTRACT:**

A series of M-type hexagonal ferrite having chemical formula  $\text{Ba}_{0.75}\text{Ca}_{0.25}\text{Pr}_x\text{Fe}_{12-2x}\text{O}_{19}$  ( $x = 0.00, 0.50, 1.00, 1.50, 2.00$ ) were prepared by using sol–gel auto combustion technique. These samples were firstly calcined at  $900\text{ }^\circ\text{C}$  for 3 h and finally sintered at  $1150\text{ }^\circ\text{C}$  for 5 h. The

effects of Pr-contents on the structural, magnetic, and electrical properties of M-type hexaferrite have been studied. The structure and morphology of the samples were studied by X-ray diffraction (XRD) and scanning electron microscopy respectively. Vibrating sample magnetometer was also used in order to study the magnetic properties of these ferrites. XRD patterns show that the samples have single phase M type Ba-hexagonal structure for  $x = 0.0, 0.5, 1.0$  whereas at higher Pr concentrations ( $x = 1.5, 2.0$ ) some peaks of  $\text{Fe}_2\text{O}_3$  appear as second phase. The large value of coercivity ( $>1$  kOe) for all the samples shows that these ferrites are permanent magnets and exhibit the hard magnetic behavior. The variation of AC conductivity and resistivity as a function of frequency could be explained on the basis of Koop's Phenomenological theory and Maxwell–Wagner model. The observed variation in dielectric constant can be described on the basis of space charge polarization and hopping conduction between  $\text{Fe}^{+3}$  and  $\text{Fe}^{+2}$ . The dispersion observed in the dielectric loss was due to Maxwell–Wagner interfacial type polarization and Koop's phenomenological theory.

**Web URL:** <https://link.springer.com/article/10.1007/s10854-016-4549-7>

**28. Elahi, A., Irfan, M., Munawar, M., Qasim, M., Mahmood, K., Saeed, M., ...& Ali, A. (2016). Study on conductivity and dielectric behavior of chemically synthesized polypyrrol dodecylbenzene sulfonic acid blended with poly (methyl methacrylate). *Polymer Science Series A*, 3(58), 429-437.**

**ABSTRACT:**

Polypyrrole (PPy) doped with dodecylbenzene sulfonic acid was synthesized and was blended with compatible polymer PMMA in chloroform. Flexible and free-standing films with compositions PPy : PMMA = 10 : 90, 20 : 80, 30 : 70 and 50 : 50 were obtained. The percentage of crystallinity and particle size of synthesized polymers were estimated from X-rays diffraction studies. Scanning Electron Micrographs showed that phase separation was observed and compatibility of the mixture decreased with increase of PMMA content. The dielectric measurements were performed in the frequency range 0.1 kHz-1 MHz in temperature range 303–473 K. The frequency dependent conductivity ( $\sigma_{ac}$ ) obeyed a power law of frequency with an exponent  $s < 1$ . Electric modulus formalism exhibits a peak in frequency. The peak of

conductivity relaxation shifted towards higher frequencies and the magnitude of relaxation decreased with the increase of PMMA content in the composites.

**Web URL:**

[https://www.researchgate.net/profile/Muhammad\\_Irfan70/publication/298357499\\_Study\\_on\\_Conductivity\\_and\\_Dielectric\\_Behavior\\_of\\_Chemically\\_Synthesized\\_Polypyrrol\\_Dodecylbenzene\\_Sulfonic\\_Acid\\_Blended\\_with\\_Polymethyl\\_Methacrylate/links/56f3691008ae95e8b6cb5577.pdf](https://www.researchgate.net/profile/Muhammad_Irfan70/publication/298357499_Study_on_Conductivity_and_Dielectric_Behavior_of_Chemically_Synthesized_Polypyrrol_Dodecylbenzene_Sulfonic_Acid_Blended_with_Polymethyl_Methacrylate/links/56f3691008ae95e8b6cb5577.pdf)

**29. Asif, M. (2016). Effects of internal inductance on the energy confinement time by using the solution of equilibrium problem. *Modern Physics Letters B*, 30(17), 1650211.**

**ABSTRACT:**

In this work, dependence of energy confinement time on plasma internal inductance has been studied by using the solution of Grad–Shafranov equation (GSE) for circular cross-section HT-7 tokamak. For this, the Shafranov parameter (asymmetry factor) and poloidal beta were obtained from solution of GSE. Then we can find the dependence of energy confinement time, on plasma internal inductance. It is observed that the maximum energy confinement time is related to the low values of internal inductance ( $0.7 < l_i < 0.9$ ).

**Web URL:** <http://www.worldscientific.com/doi/pdf/10.1142/S0217984916502110>

**30. Hakeem, A., Murtaza, G., Ahmad, I., MAOc, P., Guohua, X., Farid, M. T., ... & Ahmad, M. (2016). EFFECT OF MULTIWALLED CARBON NANOTUBES ON Co-Mn FERRITE PREPARED BY CO-PRECIPIATION TECHNIQUE. *DIGEST JOURNAL OF NANOMATERIALS AND BIOSTRUCTURES*, 11(1), 149-157.**

**ABSTRACT:**

Multiwalled carbon nanotubes (MWCNTs) are substituted in the soft ferrite  $\text{Co}_{0.5}\text{Mn}_{0.5}\text{Fe}_2\text{O}_4$ , with weight percent ratio of 1%, 5% and 9%. The effect of MWCNTs on the Structural, Thermal and Magnetic properties of Co-Mn ferrites is reported. The X-ray diffraction analysis reveals the ferrite possesses spinel cubic structure. Structural, Thermal analysis of the MWCNTs and Co-Mn ferrite composite are characterized by XRD, SEM and TGA/DSC techniques. The sintered powder at  $1000^\circ\text{C}$  under atmospheric environment shows spinel cubic structure. Particle size is

observed by SEM ranging from 20 nm to 35nm. The magnetic properties are measured by using the Physical property measurements (PPMS) technique. The Fourier transform infrared spectroscopy detects the presence of the metallic compounds in the ferrite sample.

**Web URL:** [http://www.chalcogen.ro/149\\_AHakeem.pdf](http://www.chalcogen.ro/149_AHakeem.pdf)

**31. Liao, Q. H., Nie, W. J., Xu, J., Liu, Y., Zhou, N. R., Yan, Q. R., ... & Ahmad, M. A. (2016). Properties of linear entropy of the atom in a tripartite cavity-optomechanical system. *Laser Physics*, 26(5), 055201.**

**ABSTRACT:**

We investigate the dynamics of linear entropy of an atom in a tripartite cavity-optomechanical system consisting of a two-level atom in a high-finesse optical cavity with a vibrating mirror at one end. The influence of atomic coherence on the time evolution of linear entropy is examined. It is shown that a Greenberger–Horne–Zeilinger like state can be generated. Moreover, it is found that the entanglement between the atom and the subsystem of field and mirror can be controlled by atomic coherence and the parameters of optomechanical coupling coefficient and atom-field coupling strength.

**Web URL:** <http://iopscience.iop.org/article/10.1088/1054-660X/26/5/055201/meta>

**32. Javed, M. S., Chen, J., Chen, L., Xi, Y., Zhang, C., Wan, B., & Hu, C. (2016). Flexible full-solid state supercapacitors based on zinc sulfide spheres growing on carbon textile with superior charge storage. *Journal of Materials Chemistry A*, 4(2), 667-674.**

**ABSTRACT:**

Nowadays, it is essential for us to design and fabricate efficient and cost-effective electrode materials for energy conversion and storage systems. Nanostructures are remarkable electrode materials due to their high surface area and large number of active sites. Herein zinc sulfide (ZnS) nanospheres with large surface area are hydrothermally grown on a flexible carbon textile (CT). The specific area and porosity are analyzed in detail under different pressures. The electrode based on the ZnS assembled CT (ZnS-CT) exhibits a high capacitance of 747 F g<sup>-1</sup> at a scan rate of 5 mV s<sup>-1</sup> in the LiCl aqueous electrolyte. The ZnS-CT is directly used as the binder free electrode for the fabrication of the symmetric flexible full solid state supercapacitor. The ZnS-CT supercapacitor shows excellent electrochemical performance along with light weight,

thinness and good flexibility. The ZnS-CT supercapacitor demonstrates good capacitive behavior with a high specific capacitance of 540 F g<sup>-1</sup> (areal capacitance of 56.25 F cm<sup>2</sup>) at a scan rate of 5 mV s<sup>-1</sup> with good rate capability and excellent cycling stability (94.6% retention of initial capacitance after 5000 cycles) at a constant current density of 0.8 mA cm<sup>-2</sup>. A high energy density of 51 W h kg<sup>-1</sup> at a power density of 205 W kg<sup>-1</sup> is achieved, indicating excellent ion accessibility and charge storage ability. Furthermore, three charged supercapacitors connected in series can light 4 red color light emitting diodes (2.0 V, 15 mA) for 2 min. ZnS nanospheres with large specific surface area combined with flexible carbon textile substrate offer to be a promising material in energy storage devices with high energy.

**Web URL:**

[https://www.researchgate.net/profile/Muhammad\\_Sufyan\\_Javed/publication/284880797\\_Flexible\\_full-solid\\_state\\_supercapacitor\\_based\\_on\\_zinc\\_sulfide\\_spheres\\_growing\\_on\\_carbon\\_textile\\_with\\_superior\\_charge\\_storage/links/567286f608ae54b5e462b0ae.pdf](https://www.researchgate.net/profile/Muhammad_Sufyan_Javed/publication/284880797_Flexible_full-solid_state_supercapacitor_based_on_zinc_sulfide_spheres_growing_on_carbon_textile_with_superior_charge_storage/links/567286f608ae54b5e462b0ae.pdf)

**33. Ullah, M., Rana, A. M., Ahmad, E., Raza, R., Hussain, F., Hussain, A., & Iqbal, M. (2016). Phenomenological effects of tantalum incorporation into diamond films: Experimental and first principle studies. *Applied Surface Science*, 380, 83-90.**

**ABSTRACT:**

Tantalum (Ta) incorporated diamond films are synthesized on silicon substrate by chemical vapor deposition under gas mixture of CH<sub>4</sub> + H<sub>2</sub>. Characterizations of the resulting films indicate that morphology and resistivity of as-grown diamond films are significantly influenced by the process parameters and the amount of tantalum incorporated in the diamond films. XRD plots reveal that diamond films are composed of TaC along with diamond for higher concentration of tantalum and Ta<sub>2</sub>C phases for lower concentration of tantalum. EDS spectra confirms the existence of tantalum in the diamond films. Resistivity measurements illustrate a sudden fall of about two orders of magnitude by the addition of tantalum in the diamond films. Band structure of Ta-incorporated diamond has been investigated based on density functional theory (DFT) using VASP code. Band structure calculations lead to the semiconducting

behavior of Ta-incorporated diamond films because of the creation of defects states inside the band gap extending towards conduction band minimum. Present DFT results support experimental trend of resistivity that with the incorporation of tantalum into diamond lattice causes a decrease in the resistivity of diamond films so that tantalum-incorporated diamond films behave like a good semiconductor

**Web URL:**

[https://www.researchgate.net/profile/Mahtab\\_Ullah/publication/293801295\\_Phenomenological\\_Effects\\_of\\_Tantalum\\_Incorporation\\_into\\_Diamond\\_Films\\_Experimental\\_and\\_First\\_Principle\\_Studies/links/576cc01408aedb18f3eb30d0.pdf](https://www.researchgate.net/profile/Mahtab_Ullah/publication/293801295_Phenomenological_Effects_of_Tantalum_Incorporation_into_Diamond_Films_Experimental_and_First_Principle_Studies/links/576cc01408aedb18f3eb30d0.pdf)

**34. Irshad, M., Siraj, K., Raza, R., Javed, F., Ahsan, M., Shakir, I., & Rafique, M. S. (2016). High performance of SDC and GDC core shell type composite electrolytes using methane as a fuel for low temperature SOFC. *AIP Advances*, 6(2), 025202.**

**ABSTRACT:**

Nanocomposites Samarium doped Ceria (SDC), Gadolinium doped Ceria (GDC), core shell SDC amorphous Na<sub>2</sub>CO<sub>3</sub> (SDCC) and GDC amorphous Na<sub>2</sub>CO<sub>3</sub> (GDCC) were synthesized using coprecipitation method and then compared to obtain better solid oxide electrolytes materials for low temperature Solid Oxide Fuel Cell (SOFCs). The comparison is done in terms of structure, crystallinity, thermal stability, conductivity and cell performance. In present work, XRD analysis confirmed proper doping of Sm and Gd in both single phase (SDC, GDC) and dual phase core shell (SDCC, GDCC) electrolyte materials. EDX analysis validated the presence of Sm and Gd in both single and dual phase electrolyte materials; also confirming the presence of amorphous Na<sub>2</sub>CO<sub>3</sub> in SDCC and GDCC. From TGA analysis a steep weight loss is observed in case of SDCC and GDCC when temperature rises above 725 °C while SDC and GDC do not show any loss. The ionic conductivity and cell performance of single phase SDC and GDC nanocomposite were compared with core shell GDC/amorphous Na<sub>2</sub>CO<sub>3</sub> and SDC/ amorphous Na<sub>2</sub>CO<sub>3</sub> nanocomposites using methane fuel. It is observed that dual phase core shell electrolytes materials (SDCC, GDCC) show better performance in low temperature range than their corresponding single phase electrolyte materials (SDC, GDC) with methane fuel.

**Web URL:** <http://aip.scitation.org/doi/full/10.1063/1.4941676>

35. Ahmed, A., Raza, R., Khalid, M. S., Saleem, M., Alvi, F., Javed, M. S., ...& Rafique, A. (2016). Highly efficient composite electrolyte for natural gas fed fuel cell. *International Journal of Hydrogen Energy*, 41(16), 6972-6979.

**ABSTRACT:**

Solid oxide fuel cells (SOFCs) have the ability to operate with different variants of hydro carbon fuel such as biogas, natural gas, methane, ethane, syngas, methanol, ethanol, hydrogen and any other hydrogen rich gas. Utilization of these fuels in SOFC, especially the natural gas, would significantly reduce operating cost and would enhance the viability for commercialization of FC technology. In this paper, the performance of two indigenously manufactured nanocomposite electrolytes; barium and samarium doped ceria (BSDCcarbonate); and lanthanum and samarium doped ceria (co-precipitation method LSDCcarbonate) using natural gas as fuel is discussed. The nanocomposite electrolytes were synthesized using co-precipitation and wet chemical methods (here after referred to as nano electrolytes). The structure and morphology of the nano electrolytes were examined by X-ray diffraction (XRD) and scanning electron microscopy (SEM). The fuel cell performance (OCV) was tested at temperature (300e600 C). The ionic conductivity of the nano electrolytes were measured by two probe DC method. The detailed composition analysis of nano electrolytes was performed with the help of Raman Spectroscopy. Electrochemical study has shown an ionic conductivity of 0.16 Scm<sup>-1</sup> at 600 C for BSDC-carbonate in hydrogen atmosphere, which is higher than conventional electrolytes SDC and GDC under

**Web URL:** [http://ac.els-cdn.com/S0360319916003736/1-s2.0-S0360319916003736-main.pdf?\\_tid=ede5acde-6d22-11e7-8a28-0000aacb362&acdnat=1500538424\\_93de2c8d02b4287d05a50dbf2b47ba15](http://ac.els-cdn.com/S0360319916003736/1-s2.0-S0360319916003736-main.pdf?_tid=ede5acde-6d22-11e7-8a28-0000aacb362&acdnat=1500538424_93de2c8d02b4287d05a50dbf2b47ba15)

36. Javed, M. S., Zhang, C., Chen, L., Xi, Y., & Hu, C. (2016). Hierarchical mesoporous NiFe<sub>2</sub>O<sub>4</sub> nanocone forest directly growing on carbon textile for high performance flexible supercapacitors. *Journal of Materials Chemistry A*, 4(22), 8851-8859.

**ABSTRACT:**

Binary metal oxides have been considered as promising electrode materials for high performance pseudocapacitors, because they offer higher electrochemical activity than mono metal oxides. The rational design of binder free electrode architecture is an efficient solution to the further enhancement of the performance of electrochemical supercapacitors. Herein, we report the synthesis of hierarchical mesoporous NiFe<sub>2</sub>O<sub>4</sub> (NFO) nanocone forest directly growing on carbon textile with ultra-high surface area by the hydrothermal method. The NiFe<sub>2</sub>O<sub>4</sub> nanocone forest on carbon textile (NFO-CT) is used as a binder free electrode which exhibits the high capacitance of 697 F g<sup>-1</sup> at scan rate of 5 mV s<sup>-1</sup> and further used for the fabrication of symmetric solid state supercapacitor. The open space between hierarchical nanocones allows easy diffusion for electrolyte ions and the carbon textile ensures fast electron transfer which leads to remarkable electrochemical performance. The NFO-CT solid state supercapacitor exhibits the high capacitance of 584 F g<sup>-1</sup> at scan rate of 5 mV s<sup>-1</sup> and 93.57 % capacitance retention after 10,000 cycles with advantage of light weight, thinness and good flexibility. A high energy density of 54.9 Wh kg<sup>-1</sup> at power density of 300 W kg<sup>-1</sup> is achieved, indicating the excellent energy storage features. Furthermore, three charged supercapacitors in series can light 4 red color LED's (2 V, 15 mA) for 2 min.

**Web URL:**

<http://pubs.rsc.org//content/articlelanding/2016/ta/c6ta01893a/unauth#!divAbstract>

**37.Khan, M. A., Raza, R., Chaudhry, M. A., Abbas, G., Rafique, A., Ullah, M. K., ...& Mushtaq, M. N. (2016). CERIA BASED NANO-COMPOSITE ELECTRODES FOR INTERMEDIATE TEMPERATURESOLID OXIDE FUEL CELLS (IT-SOFCs). *DIGEST JOURNAL OF NANOMATERIALS AND BIOSTRUCTURES*, 11(2), 465-475.**

**ABSTRACT:**

The world is presently focusing the innovation and development of energy technology at the nano levels for solid oxide fuel cell (SOFC) in terms of its application, devices and materials. The composite electrodes which would be showed the excellent performance have high demands for precise issues in SOFC for research point of view. Ceria based composite electrodes LiNiCuZn-YDC (1-5) were prepared by using the NANOCOFC (nanocomposite for advanced fuel

cell technology) approach. XRD analyses were shown that these electrodes have cubic structure. Its thermal and morphology studies were done by TGA and SEM techniques. Both analysis (XRD and SEM) were predicted that average crystallite size having the range of 30-80 nm. EIS technique was used to explore the polarization processes under H<sub>2</sub> atmosphere within the temperature range of (300-680 °C). The polarization resistance decreases from 0.19 to 0.05 Ωcm<sup>2</sup>. The activation energy was measured under air and hydrogen atmospheres. The maximum power density (769.54 mWcm<sup>-1</sup>) and open circuit voltage (1.02 V) were achieved at 680 °C by using the LiNiCuZnYDC(3) oxide as anode, NSDC as electrolyte and BSCF as cathode.

**Web URL:** [http://www.chalcogen.ro/465\\_KhanM.pdf](http://www.chalcogen.ro/465_KhanM.pdf)

**38. Asif, M., Mohamed, M., & Kim, E. J. (2016). Study of improved confinement by a stepwise increase of the input heating power for tokamak plasmas. *Modern Physics Letters B*, 30(24), 1650316.**

**ABSTRACT:**

This paper is an extension of the brief study by Sarah Douglas et al. [Phys. Plasmas 20 (2013) 114504] where in the study a sinusoidal perturbation of the heating power has been studied. In this paper a stepwise increase of the heating power and its influence on the L–H transition are studied. Using a function,  $A \tanh(t/T)$  for the transition of input heating power for tokamak plasmas, i.e. the addition of the perturbation,  $A \tanh(t/T)$ , to constant power  $q_0$  is shown to promote the confinement, leading to the L–H transition at a lower value of  $q_0$ , as compared to the case of constant  $q_0$  without the  $A \tanh(t/T)$  perturbation. It is seen that the input heating power  $Q$  that consists of constant part  $q_0$  in addition to a function  $A \tanh(t/T)$  provides the L–H transition for relatively small  $A$  and much wider range values of  $1/T$  as compared to Sarah Douglas et al. [Phys. Plasmas 20 (2013) 114504].

**Web**

**URL:** <http://www.worldscientific.com/doi/abs/10.1142/S0217984916503164?journalCode=mp1b>

**39. Amjed, N., Hussain, M., Aslam, M. N., Tárkányi, F., & Qaim, S. M. (2016). Evaluation of nuclear reaction cross sections for optimization of production of the emerging diagnostic radionuclide  $^{55}\text{Co}$ . *Applied Radiation and Isotopes*, 108, 38-48.**

**ABSTRACT:**

The excitation functions of the  $^{54}\text{Fe}(d,n)^{55}\text{Co}$ ,  $^{56}\text{Fe}(p,2n)^{55}\text{Co}$  and  $^{58}\text{Ni}(p,\alpha)^{55}\text{Co}$  reactions were analyzed with relevance to the production of the  $\beta$ -emitter  $^{55}\text{Co}$  ( $T_{1/2} = 17.53$  h), a promising cobalt radionuclide for PET imaging. The nuclear model codes ALICE-IPPE, EMPIRE and TALYS were used to check the consistency of the experimental data. The statistically fitted excitation function was employed to calculate the integral yield of the product. The amounts of the radioactive impurities  $^{56}\text{Co}$  and  $^{57}\text{Co}$  were assessed. A comparison of the three investigated production routes is given

**Web URL:**

[https://www.researchgate.net/profile/Mazhar\\_Hussain2/publication/284562864\\_Evaluation\\_of\\_nuclear\\_reaction\\_cross\\_sections\\_for\\_optimization\\_of\\_production\\_of\\_the\\_emerging\\_diagnostic\\_radionuclide\\_55Co/links/567276a408aeb8b21c70bff7/Evaluation-of-nuclear-reaction-cross-sections-for-optimization-of-production-of-the-emerging-diagnostic-radionuclide-55Co.pdf](https://www.researchgate.net/profile/Mazhar_Hussain2/publication/284562864_Evaluation_of_nuclear_reaction_cross_sections_for_optimization_of_production_of_the_emerging_diagnostic_radionuclide_55Co/links/567276a408aeb8b21c70bff7/Evaluation-of-nuclear-reaction-cross-sections-for-optimization-of-production-of-the-emerging-diagnostic-radionuclide-55Co.pdf)

**40. Javid, M. A., Khan, M. A., Amin, N., & Nabi, A. (2016). Calcification in Globus Pallidus and Putamen of Multiple Sclerosis Patients Versus Healthy Subjects Using Quantitative Susceptibility Mapping. *Iranian Journal of Radiology*, 13(4).**

**ABSTRACT:**

**Background**

Calcification has been well reported in basal ganglia and it grows rapidly in globus pallidus (GP) followed by putamen (PUT) and caudate nucleus because of their high metabolic rate and displays high susceptibility effects. Therefore, the current study focused on magnetic susceptibility effect of calcium content in normal and diseased tissue due to metabolic changes.

**Objectives**

To evaluate calcium content in GP and PUT structures of multiple sclerosis (MS) patients versus healthy subjects using quantitative susceptibility mapping.

### Patients and Methods

We compared 10 MS patients with mean age of 48.3 years (standard deviation [SD]=11.89) with 10 healthy subjects with mean age of 39.6 years (SD=11.52). Scanning of subjects was performed with high resolution (0.5×0.5×2 mm<sup>3</sup>) using susceptibility weighted imaging sequence on 3 Tesla (Trio-Siemens, Erlangen, Germany). Data was processed in homemade SPIN software to produce susceptibility mapping. Threshold was set in healthy subjects to detect calcium content in PUT and GP structures.

### Results

Magnetic susceptibility( $\chi$ ) of calcium content was assessed by number of pixels induced by GP and PUT in MS patients as well as healthy subjects. Two sample t-test was used to assess the difference between susceptibilities of GP and PUT of MS patients ( $P = 0.06$ ,  $P > 0.05$ ). Susceptibilities of GP and PUT also showed  $P = 0.3$  in healthy subjects. One way analysis of variance was used to assess the difference of susceptibilities in four variables of both populations. Insignificant results ( $P = 0.7$ ,  $P > 0.05$ ) were found among four variables. There was no statistically significant difference between magnetic susceptibilities of both populations.

### Conclusion

Statistical analysis of susceptibilities of MS patients versus healthy subjects found no excess deposition of calcium content in deep gray matter of MS patients. Calcification may not be considered as a biomarker of prognosis in MS.

**Web URL:** <https://www.ncbi.nlm.nih.gov/pmc/articles/PMC5116209/>

**41.** Khan, A. A., Razaq, A., Ali, J., Arshad, F., Mumtaz, M., & Khan, S. (2016). Antenna miniaturization using pulp fibres as a substrate for dual band operation. *Microwave and Optical Technology Letters*, 58(9), 2146-2148.

**ABSTRACT:**

Reduced size dual band patch antenna is designed on pulp fibers-based substrate, obtained from a self-growing plant, *Typha angustifolia*. The proposed design is low cost and has <10 dB return loss at 2.4 and 5.7 GHz, with 6.9 dBi antenna gain and also has potential for conformal designs.

**Web URL:** <http://onlinelibrary.wiley.com/doi/10.1002/mop.30002/full>

**42. Javed, M. S., Raza, R., Hassan, I., Saeed, R., Shaheen, N., Iqbal, J., & Shaukat, S. F. (2016). The energy crisis in Pakistan: A possible solution via biomass-based waste. *Journal of Renewable and Sustainable Energy*, 8(4), 043102.**

**ABSTRACT:**

Developing countries like Pakistan need a continuous supply of clean and cheap energy. It is a very common fear in today's world that the fossil fuels will be depleted soon and the cost of energy is increasing day-by-day. Renewable energy sources and technologies have the potential to provide solutions to longstanding energy problems faced by developing countries. Currently, Pakistan is experiencing a critical energy crisis and renewable energy resources can be the best alternatives for quickly terminating the need for fossil fuels. The renewable energy sources such as solar energy, wind energy, and biomass energy combined with fuel cell technology can be used to overcome the energy shortage in Pakistan. Biomass is a promising renewable energy source and is gaining more interest because it produces a similar type of fuel like crude oil and natural gas. Energy from biomass only depends upon the availability of raw materials; therefore, biomass can play an important role to fulfill the energy requirements of the modern age. The use of energy has increased greatly since the last century and almost all human activities have become more dependent on energy. Biomass, being a potential and indigenous candidate, could be a good solution to meet the energy needs of Pakistan. In this review paper, the detailed current energy requirements and solutions from available energy resources and the scope, potential, and implementation of biomass conversion to energy in Pakistan are explored with a special focus on the major province of Punjab and the advantages of biomass for energy purposes.

**Web URL:**

[https://www.researchgate.net/profile/Muhammad\\_Sufyan\\_Javed/publication/305893820\\_The\\_energy\\_crisis\\_in\\_Pakistan\\_A\\_possible\\_solution\\_via\\_biomass-based\\_waste/links/57ae1d0208aeb2cf17bdb312.pdf](https://www.researchgate.net/profile/Muhammad_Sufyan_Javed/publication/305893820_The_energy_crisis_in_Pakistan_A_possible_solution_via_biomass-based_waste/links/57ae1d0208aeb2cf17bdb312.pdf)

**43. G.Abbas, & Rizwan Raza (2016). Natural gas fueled electrodes for low-temperature solid oxide fuel cell, . Int. Journal of Modern Physics B**

**Not Found**

**44. Wang, B., Wang, Y., Fan, L., Cai, Y., Xia, C., Liu, Y., ...& Wang, H. (2016). Preparation and characterization of Sm and Ca co-doped ceria–La<sub>0.6</sub>Sr<sub>0.4</sub>Co<sub>0.2</sub>Fe<sub>0.8</sub>O<sub>3-δ</sub> semiconductor–ionic composites for electrolyte-layer-free fuel cells. *Journal of Materials Chemistry A*, 4(40), 15426-15436.**

**ABSTRACT:**

A series of Sm and Ca co-doped ceria, i.e. Ca<sub>0.04</sub>Ce<sub>0.96x</sub>Sm<sub>x</sub>O<sub>2d</sub> (x = 0, 0.09, 0.16, and 0.24) (SCDC), were synthesized by a co-precipitation method. Detailed morphology, composition, crystal structure and electrochemical properties of the prepared materials were characterized. The results revealed that Sm and Ca co-doping could enhance the ionic conductivity in comparison with that of single Ca-doped samples. The composition as Ca<sub>0.04</sub>Ce<sub>0.80</sub>Sm<sub>0.16</sub>O<sub>2d</sub> exhibited a highest ionic conductivity of 0.039 S cm<sup>-1</sup> at 600 C in comparison with the rest of the series, and the optimal ionic conductivity can be interpreted by the coupling effect of oxygen vacancies and mismatch between the dopant ionic radius and critical radius. Composite formation between the semiconductor La<sub>0.6</sub>Sr<sub>0.4</sub>Co<sub>0.2</sub>Fe<sub>0.8</sub>O<sub>3d</sub> (LSCF) and the as-prepared SCDC contributed to a remarkable improvement in the ionic conductivity, an unexpectedly high ionic conductivity of 0.188 S cm<sup>-1</sup> was obtained for LSCF–SCDC composites at 600 C, which was four times higher than that of pure SCDC. Using transmission electron microscopy and spectroscopy approaches, we detected an enrichment of oxygen in the LSCF–SCDC interface region and a depletion of oxygen vacancies in LSCF–SCDC and LSCF–LSCF grain boundaries was significantly mitigated, which resulted in the enhancement of ionic conductivity of semiconductor–ionic LSCF–SCDC composites. The electrolyte-layer-free fuel cell (EFFC)

fabricated from the LSCF–SCDC semiconductor–ionic membrane demonstrated excellent performances, e.g. 814 mW cm<sup>2</sup> at 550 C for using the LSCF–Ca<sub>0.04</sub>Ce<sub>0.80</sub>Sm<sub>0.16</sub>O<sub>2d</sub> (SCDC2).

**Web URL:**

[https://www.researchgate.net/profile/Chen\\_Xia9/publication/309232314\\_Preparation\\_and\\_characterization\\_of\\_Sm\\_and\\_Ca\\_co-doped\\_ceria-La06Sr04Co02Fe08O3-d\\_semiconductor-ionic\\_composites\\_for\\_electrolyte-layer-free\\_fuel\\_cells/links/580645c908ae0075d82c58b8.pdf](https://www.researchgate.net/profile/Chen_Xia9/publication/309232314_Preparation_and_characterization_of_Sm_and_Ca_co-doped_ceria-La06Sr04Co02Fe08O3-d_semiconductor-ionic_composites_for_electrolyte-layer-free_fuel_cells/links/580645c908ae0075d82c58b8.pdf)

**45. Bashir, M. F., & Chen, L. (2016). Asymmetric drift instability of magnetosonic waves in anisotropic plasmas. *Physics of Plasmas*, 23(10), 102107.**

**ABSTRACT:**

The general dispersion relation of obliquely propagating magneto-sonic (MS) waves for the inhomogeneous and anisotropic plasmas is analyzed including the effect of wave-particle interaction. The numerical analysis is performed without expanding both the plasma dispersion and the modified Bessel functions to highlight the effects of density inhomogeneity and the temperature anisotropy. The obtained results are compared with the recent work [Naim et al., *Phys. Plasmas* 22, 062117 (2015)], where only drift mode near the magnetosonic frequency is investigated. In our paper, we additionally analyzed two related modes depicting that the drift effect leads to an asymmetric behavior in the dispersion properties of drift MS waves. The possible application to the solar coronal heating problem has also been discussed. Published by AIP Publishing.

**Web URL:** <http://aip.scitation.org/doi/pdf/10.1063/1.4964361>

**46. Atif, M., Ahmed, S., Nadeem, M., Ali, M. K., Idrees, M., Grössinger, R., & Turtelli, R. S. (2016). Role of competing phases in the structural, magnetic and dielectric relaxation for (1–x) CoFe<sub>2</sub>O<sub>4</sub>+(x) BaTiO<sub>3</sub> composites. *Ceramics International*, 42(13), 14618-14626.**

**ABSTRACT:**

Magnetoelectric composites of (1-x)CoFe<sub>2</sub>O<sub>4</sub>+(x)BaTiO<sub>3</sub> (0.0<x<1.0) were prepared by ball milling method. X-ray diffraction analysis revealed the presence of cubic spinel (CoFe<sub>2</sub>O<sub>4</sub>) and tetragonal perovskite (BaTiO<sub>3</sub>) phases in the prepared composites. Scanning electron micrographs confirmed the homogeneous phase distribution in the obtained composites. The

magnitude of saturation magnetization and linear magnetostriction decreased with increasing BaTiO<sub>3</sub> content in the composite. Significant reduction in the magnetostrictive behavior is attributed to different elastic constants of the constituents which affect the mechanical coupling. In order to identify the different electro-active regions in the prepared composites, the experimental impedance spectroscopic data have been analyzed using different equivalent circuit models. The analysis of the impedance data is carried out by calculating the impedance of conductive (CoFe<sub>2</sub>O<sub>4</sub>) phase, resistive (BaTiO<sub>3</sub>) phase and interconnectivity between the two constituent phases. With increasing BaTiO<sub>3</sub> content 'x' in the system, the dielectric permittivity decreased at low frequencies and increased at high frequencies. The observed behavior is mainly ascribed to the polarization in the CoFe<sub>2</sub>O<sub>4</sub> and BaTiO<sub>3</sub> phases at low and high frequencies, respectively. Moreover, the AC conductivity analysis suggested the mixed polaron hopping type of conduction mechanism in the prepared composites.

**Web URL:**

[https://www.researchgate.net/profile/Muhammad\\_Atif7/publication/304059057\\_Role\\_of\\_competing\\_phases\\_in\\_the\\_structural\\_magnetic\\_and\\_dielectric\\_relaxation\\_for\\_1-xCoFe2O4xBaTiO3\\_composites/links/5770e31408ae0b3a3b7cb09d.pdf](https://www.researchgate.net/profile/Muhammad_Atif7/publication/304059057_Role_of_competing_phases_in_the_structural_magnetic_and_dielectric_relaxation_for_1-xCoFe2O4xBaTiO3_composites/links/5770e31408ae0b3a3b7cb09d.pdf)

**47. Sultana, I., Razaq, A., Idrees, M., Asif, M. H., Ali, H., Arshad, A., ...& Hussain, S. Q. (2016). Electrodeposition of Gold on Lignocelluloses and Graphite-Based Composite Paper Electrodes for Superior Electrical Properties. *Journal of Electronic Materials*, 45(10), 5140-5145.**

**ABSTRACT:**

Graphite-based composites are commonly used as an anode and current collector for energy storage devices; however, they have inherently limited potential for large scale rechargeable systems due to a brittle structure. In this study, flexible and light-weight graphite-based electrodes are prepared by incorporation of lignocelluloses fibers directly collected from a self-growing plant, *Typha Angistifolia*. Electrical properties of graphite and lignocelluloses composite sheets are enhanced by electrodeposition of gold in a three-electrode setup. Electrochemical deposition of gold on a lignocelluloses/graphite paper electrode was obtained in potentiostatic mode by the application of reduction potential 0.95 V for 2000 s, 600 s, and 100 s. The gold-deposited paper electrodes showed efficient kinetics by shifting redox peaks

towards lower potentials in cyclic voltammetry measurements, whereas impedance measurements revealed seven orders of magnitude reduction in the resistive properties. Incorporated flexibility and superior electrical/electrochemical performance within presented graphite-based composites will provide cuttingedge characteristics for high-tech application of energy storage devices by keeping a focus on modern disposable technology.

**Web URL:**

[https://www.researchgate.net/profile/Shahid\\_Iqbal46/publication/304365730\\_Electrodeposition\\_of\\_Gold\\_on\\_Lignocelluloses\\_and\\_Graphite-Based\\_Composite\\_Paper\\_Electrodes\\_for\\_Superior\\_Electrical\\_Properties/links/5772112c08ae10de639df4c8.pdf](https://www.researchgate.net/profile/Shahid_Iqbal46/publication/304365730_Electrodeposition_of_Gold_on_Lignocelluloses_and_Graphite-Based_Composite_Paper_Electrodes_for_Superior_Electrical_Properties/links/5772112c08ae10de639df4c8.pdf)

**48. Hong, W. P., Jamil, M., Rasheed, A., & Jung, Y. D. (2016). Shukla-Spatschek diffusion effects on the spatial damping of space-charge waves in a turbulent plasma waveguide. *The European Physical Journal Plus*, 131(11), 399.**

**ABSTRACT:**

The physical characteristics of the spatial damping of the space-charge plasma wave are investigated in a turbulent plasma waveguide. The dispersion relation for the space-charge plasma wave is derived including the propagation wave number as well as the spatial damping rate including the Shukla-Spatschek diffusion effect. The results show that the propagation wave number and the spatial damping rate increase with increasing the wave frequency. It is found that the influence of plasma turbulence enhances the spatial damping rate of the space-charge wave. It is also found that the propagation wave number and spatial damping rate with a higher-order root of the Bessel solution are greater than those with a lower-order root. In addition, it is found that the spatial damping rate decreases with an increase of the thermal energy. Moreover, it is found that the propagation wave number and the spatial damping rate decrease with increasing the radius of the waveguide. The variation of the spatial damping due to the turbulent diffusion, thermal, and geometric effects is also discussed.

**Web URL:** <https://link.springer.com/article/10.1140/epjp/i2016-16399-4>

**49. Khan, A. A., Rozina, C., & Jamil, M. (2016). Potential surface waves at the vacuum-radiative collisional plasma interface. *Physics of Plasmas*, 23(11), 112111.**

**ABSTRACT:**

The stability of potential surface waves at the interface of collisional radiative electron-ion plasma and a vacuum is investigated. It is shown that the dynamics of electrons are affected by electromagnetic thermal radiation pressure significantly. The fluid model along with full set of Maxwell's equations is used to develop dispersion relation of electrostatic surface waves on hot homogeneous radiative collisional plasma. It is found that electrostatic surface waves become unstable in the presence of electromagnetic thermal radiation and self collision of plasma particles; however, thermal radiations stabilize the surface waves in the absence of collisions. The analytical results are verified numerically for both the laboratory and ionosphere plasma environment. The study of surface waves may seek its applications at the nano as well as the astroscales. Published by AIP Publishing.

**Web URL:** <http://aip.scitation.org/doi/abs/10.1063/1.4967464>

**50. Anjum, S., Saleem, H., Rasheed, K., Zia, R., Riaz, S., & Usman, A. (2017). Role of Ni<sup>2+</sup> Ions in Magnetite Nano-particles Synthesized by Co-precipitation Method. *Journal of Superconductivity and Novel Magnetism*, 30(5), 1177-1186.**

**ABSTRACT:**

In the present work, nickel-doped iron oxide (Ni<sub>x</sub>Fe<sub>3-x</sub>O<sub>4</sub>) nanoparticles with different concentration of nickel ( $x = 0, 0.05, 0.1, \text{ and } 0.15$ ) have been prepared by co-precipitation method. These prepared nanoparticles have been characterized by using x-ray diffractometer, thermo gravimetric analysis and differential scanning calorimetry, Fourier transform infrared spectroscopy, scanning electron microscopy, vibrating sample magnetometer, and UV-Visible spectroscopy to study their structural, thermal, morphological, magnetic, and optical properties, respectively. The x-ray diffraction confirms the formation of single-phase inverse spinel cubic structure of NiFe<sub>3</sub>O<sub>4</sub> nanoparticles. Crystallite size has been estimated by the full width at half maximum of the most intense x-ray diffraction peak where vibrational and stretching modes of metal-oxygen bonds in 872 cm are shown in Fourier transform infrared

spectra which confirms the formation of nanoparticles. The thermal analysis revealed that the transition temperature and stability increases with increasing Ni concentration. The surface morphology indicated that the particles are spherical in shape with some agglomeration. The magnetic measurement revealed that the coercivity and anisotropy increases with nickel doping in magnetite nanoparticles. The optical analysis revealed that direct and indirect both types of band gap increases when the particle size decreases because the absorption spectra shift toward smaller wavelength. The blue shift confirms the formation of nanoparticles.

**Web URL:** <https://link.springer.com/article/10.1007/s10948-016-3832-4>

**51. Usman, A., Rafique, M. S., Shaukat, S. F., Siraj, K., Ashfaq, A., Anjum, S., ...& Sattar, A. (2016). Impact of Argon gas on optical and electrical properties of Carbon thin films. *Physica B: Condensed Matter*, 503, 157-161.**

**ABSTRACT:**

Nanostructured thin films of carbon were synthesized and investigated for their electrical, optical, structural and surface properties. Pulsed Laser Deposition (PLD) technique was used for the preparation of these films under Argon gas environment. A KrF Laser ( $\lambda=248$  nm) was used as source of ablation and plasma formation. It was observed that the carbon ions and the background gas environment has deep impact on the morphology as well as on the microstructure of the films. Time of Flight (TOF) method was used to determine the energies of the ablated carbon ions. The morphology of film surfaces deposited at various argon pressure was analysed using an atomic force microscope. The Raman spectroscopic measurement reveal that there is shift in phase from  $sp^3$  to  $sp^2$  and a decrease in FWHM of G band, which is a clear indication of enhanced graphitic clusters. The electrical resistivity was also reduced from  $85.3 \times 10^{-1}$  to  $2.57 \times 10^{-1}$   $\Omega$ -cm. There is an exponential decrease in band gap  $E_g$  of the deposited films from 1.99 to 1.37 eV as a function of argon gas pressure.

**Web URL:** <http://www.sciencedirect.com/science/article/pii/S0921452616304367>

**52. Majeed, A., Khan, M. A., ur Raheem, F., Ahmad, I., Akhtar, M. N., & Warsi, M. F. (2016). Morphological, Raman, electrical and dielectric properties of rare earth doped X-type hexagonal ferrites. *Physica B: Condensed Matter*, 503, 38-43.**

**ABSTRACT:**

The influence of rare-earth metals (La, Nd, Gd, Tb, Dy) on morphology, Raman, electrical and dielectric properties of Ba<sub>2</sub>NiCoRExFe<sub>28x</sub>O<sub>46</sub> ferrites were studied. The scanning electron microscopy (SEM) exhibited the platelet like structure of these hexagonal ferrites. The surface morphology indicated the formation of ferrite grains in the nano-regime scale. The bands obtained at lower wave number may be attributed to the metal-oxygen vibration at octahedral site which confirm the development of hexagonal phase of these ferrites. The resonance peaks were observed in dielectric constant, dielectric loss factor and quality factor versus frequency graphs. These dielectric parameters indicate that these ferrites nanomaterials are potential candidates in the high frequency applications. The enhancement in DC electric resistivity from 2.48 10<sup>8</sup> to 1.20 10<sup>9</sup> Ω cm indicates that the prepared materials are beneficial for decreasing the eddy current losses at high frequencies and for the fabrication of multilayer chip inductor (MLCI) devices.

**Web URL:** [http://ac.els-cdn.com/S0921452616303830/1-s2.0-S0921452616303830-main.pdf?\\_tid=b622ae26-6d33-11e7-8294-0000aab0f6c&acdnat=1500545632\\_b36915ca61f5846a4b2208233fea5e33](http://ac.els-cdn.com/S0921452616303830/1-s2.0-S0921452616303830-main.pdf?_tid=b622ae26-6d33-11e7-8294-0000aab0f6c&acdnat=1500545632_b36915ca61f5846a4b2208233fea5e33)

**53. Dousti, M. R., & Amjad, R. J. (2016). Enhanced 1.06 μm emission in Nd<sup>3+</sup>-doped lead-tellurite glasses doped with silver nanoparticles. *Journal of Nanophotonics*, 10(4), 046010-046010.**

**ABSTRACT:**

Increasing the emission cross section of rare earth (RE) ions-doped transparent oxide glasses is a challenging issue. The incorporation of the metal nanoparticles (NPs) has been proposed as a promising approach to improve the emission properties, though the mechanism behind such a phenomenon is a controversial topic. Tellurite glass doped with Nd<sup>3+</sup>+Nd<sup>3+</sup> ions and silver NPs is prepared and the optical absorption and emission properties are studied. The surface plasmon band of the silver NPs is observed at around 522 nm. Absorption and excitation bands of the Nd<sup>3+</sup>+Nd<sup>3+</sup> ions are detected in the visible spectral region and associated to the transitions from ground state to various excited states. Threefold enhancement in the 1.06 μm<sup>1.06 μm</sup> luminescence of Nd<sup>3+</sup>+Nd<sup>3+</sup> ions is observed under 800-nm laser

excitation by incorporation of AgNO<sub>3</sub> up to 1 mol. %. Probable energy transfer and local field enhancements are discussed to explain the possible interactions between metal and RE ions.

**Web URL:** <http://nanophotonics.spiedigitallibrary.org/article.aspx?articleid=2580282>

**54. Rajesh, D., Dousti, M. R., Amjad, R. J., & De Camargo, A. S. S. (2016). Quantum cutting and up-conversion investigations in Pr<sup>3+</sup>/Yb<sup>3+</sup> co-doped oxyfluoro-tellurite glasses. *Journal of Non-Crystalline Solids*, 450, 149-155.**

**ABSTRACT:**

In this work we have investigated quantum cutting, up-conversion and downconversion processes in new Pr<sup>3+</sup>/Yb<sup>3+</sup> co-doped transparent oxyfluoro-tellurite glasses with chemical composition TeO<sub>2</sub>-ZnO-YF<sub>3</sub>-NaF-0.5Pr<sub>2</sub>O<sub>3</sub>-xYb<sub>2</sub>O<sub>3</sub> (x= 0.25, 0.5, 0.75 and 1.0 mol%). In the down-conversion process, Pr<sup>3+</sup>-Yb<sup>3+</sup> co-doped samples present emission in the visible (Pr<sup>3+</sup>: 3 P<sub>0</sub> → 3 F<sub>2</sub> transition, 640 nm) and in the infrared (Yb<sup>3+</sup>: 2 F<sub>5/2</sub> → 2 F<sub>7/2</sub>, 980 nm) spectral regions upon excitation at 440 nm. The luminescence decay time of the emitting levels were obtained in codoped samples as a function of Yb<sup>3+</sup> concentration and the results confirmed the occurrence of energy transfer from Pr<sup>3+</sup> to Yb<sup>3+</sup> via a combination of two different cross relaxation processes: (1) Pr<sup>3+</sup>: 3 P<sub>0</sub> → 1 G<sub>4</sub> to Yb<sup>3+</sup>: 2 F<sub>7/2</sub> → 2 F<sub>5/2</sub> and (2) Pr<sup>3+</sup>: 1 D<sub>2</sub> → 3 F<sub>4</sub> to Yb<sup>3+</sup>: 2 F<sub>7/2</sub> → 2 F<sub>5/2</sub>. Furthermore due to the reverse-energy transfer mechanism from Yb<sup>3+</sup> 2F<sub>5/2</sub> level to Pr<sup>3+</sup> 1G<sub>4</sub> level, luminescence intensity quenching was observed for the 2 F<sub>5/2</sub> → 2 F<sub>7/2</sub> transition at 980 nm, for Yb<sup>3+</sup> concentrations higher than 0.5 mol%. The energy transfer efficiency was estimated from the intensity ratios and decay times associated to the 3 P<sub>0</sub> → 3 F<sub>2</sub> transition, and it reached 66% for a glass co-doped with 0.5Pr<sup>3+</sup> and 1.0Yb<sup>3+</sup> (mol%). The results indicate that these glasses are potential candidates for manipulation of the solar spectrum, via up-conversion and downconversion processes, in order to increase the absorption efficiency of currently used c-Si photovoltaic solar cells.

**Web URL:**

[https://www.researchgate.net/profile/Dr\\_Dagupati\\_Rajesh/publication/306066818\\_Quantum\\_cutting\\_and\\_up-conversion\\_investigations\\_in\\_Pr\\_3\\_Yb\\_3\\_co-doped\\_oxyfluoro-tellurite\\_glasses/links/57adbe3008ae42ba52b46916.pdf](https://www.researchgate.net/profile/Dr_Dagupati_Rajesh/publication/306066818_Quantum_cutting_and_up-conversion_investigations_in_Pr_3_Yb_3_co-doped_oxyfluoro-tellurite_glasses/links/57adbe3008ae42ba52b46916.pdf)

55. Dousti, M. R., Poirier, G. Y., Amjad, R. J., & de Camargo, A. S. (2016). Luminescence quenching versus enhancement in WO<sub>3</sub>-NaPO<sub>3</sub> glasses doped with trivalent rare earth ions and containing silver nanoparticles. *Optical Materials*, 60, 331-340.

**ABSTRACT:**

We report on the influence of silver nanoparticles (NPs) on the luminescence behavior of trivalent rare earth (RE) ion doped tungsten-phosphate glasses. In order to induce the growth of NPs, the as-prepared glass samples containing silver atoms, are exposed to heat-treatment above the glass transition temperature. The surface plasmon resonance band of the Ag NPs is observed in the visible range around 420 and 537 nm in the glasses with low and high tungsten content, respectively. Such difference in spectral shift of the plasmon band is attributed to the difference in the refractive index of the two studied glass compositions. Heat-treatment results in the general increase in number of NPs, while in the case of glasses with low tungsten content, it also imposes a shift to the Ag plasmon band. The NPs size distribution (4e10 nm) was determined in good agreement with the values obtained by using Mie theory and by transmission electron microscopy. The observed quenching in the visible luminescence of glasses doped with Eu<sup>3+</sup>, Tb<sup>3+</sup> or Er<sup>3+</sup> is attributed to energy transfer from the RE ions to Ag species, while an enhanced near-infrared emission in Er<sup>3+</sup> doped glasses is discussed in terms of the chemical contribution of silver, rather than the most commonly claimed enhancement of localized field or energy transfer from silver species to Er<sup>3+</sup>. The results are supported by the lifetime measurements. We believe that this study gives further insight and in-depth exploration of the somewhat controversial discussions on the influence of metallic NPs plasmonic effects in RE-doped glasses.

**Web URL:**

[https://www.researchgate.net/profile/M\\_Reza\\_Dousti/publication/307873984\\_Luminescence\\_quenching\\_versus\\_enhancement\\_in\\_WO3-NaPO3\\_glasses\\_doped\\_with\\_trivalent\\_rare\\_earth\\_ions\\_and\\_containing\\_silver\\_nanoparticles/links/57d6a12608ae5f03b494a29d.pdf](https://www.researchgate.net/profile/M_Reza_Dousti/publication/307873984_Luminescence_quenching_versus_enhancement_in_WO3-NaPO3_glasses_doped_with_trivalent_rare_earth_ions_and_containing_silver_nanoparticles/links/57d6a12608ae5f03b494a29d.pdf)

56. Ablikim, M., Achasov, M. N., Ahmed, S., Ai, X. C., Albayrak, O., Albrecht, M., ...& Bai, J. Z. (2016). Observation of  $J/\psi \rightarrow \gamma \eta \pi^0$ . *Physical Review D*, 94(7), 072005.

**ABSTRACT:**

We present the first study of the process  $J/\psi \rightarrow \gamma \eta \pi^0$  using  $(223.7 \pm 1.4) \times 10^6$   $J/\psi$  events accumulated with the BESIII detector at the BEPCII facility. The branching fraction for  $J/\psi \rightarrow \gamma \eta \pi^0$  is measured to be  $B(J/\psi \rightarrow \gamma \eta \pi^0) = (2.14 \pm 0.18(\text{stat}) \pm 0.25(\text{syst})) \times 10^{-5}$ . With a Bayesian approach, the upper limits of the branching fractions  $B(J/\psi \rightarrow \gamma a_0(980), a_0(980) \rightarrow \eta \pi^0)$  and  $B(J/\psi \rightarrow \gamma a_2(1320), a_2(1320) \rightarrow \eta \pi^0)$  are determined to be  $2.5 \times 10^{-6}$  and  $6.6 \times 10^{-6}$  at the 95% confidence level, respectively. All of these measurements are given for the first time.

**Web URL:** <https://journals.aps.org/prd/abstract/10.1103/PhysRevD.94.072005>

57. Ablikim, M., Achasov, M. N., Ai, X. C., Albayrak, O., Albrecht, M., Ambrose, D. J., ...& Bakina, O. (2016). Measurement of the  $D^+ \rightarrow \ell^+ \nu \ell$  branching fractions and the decay constant  $f_{D^+}$ . *Physical Review D*, 94(7), 072004.

**ABSTRACT:**

Using 482 pb<sup>-1</sup> of epe- collision data collected at a center-of-mass energy of  $\sqrt{s} \approx 4.009$  GeV with the BESIII detector, we measure the branching fractions of the decays  $D^+ \rightarrow \mu^+ \nu \mu$  and  $D^+ \rightarrow \tau^+ \nu \tau$ . By constraining the ratio of decay rates of  $D^+ \rightarrow \tau^+ \nu \tau$  and  $D^+ \rightarrow \mu^+ \nu \mu$  to the Standard Model prediction, the branching fractions are determined to be  $B(D^+ \rightarrow \mu^+ \nu \mu) = 0.495 \pm 0.067 \pm 0.026\%$  and  $B(D^+ \rightarrow \tau^+ \nu \tau) = 4.83 \pm 0.65 \pm 0.26\%$ . Using these branching fractions, we obtain a value for the decay constant  $f_{D^+}$  of  $241.0 \pm 16.3 \pm 6.5$  MeV, where the first error is statistical and the second systematic.

**Web URL:** <https://journals.aps.org/prd/pdf/10.1103/PhysRevD.94.072004>

58. Ablikim, M., Achasov, M. N., Ahmed, S., Ai, X. C., Albayrak, O., Albrecht, M., ...& Bai, J. Z. (2016). Measurements of the absolute branching fractions for  $D^+ \rightarrow \eta e^+ \nu e$  and  $D^+ \rightarrow \eta' e^+ \nu e$ . *Physical Review D*, 94(11), 112003.

**ABSTRACT:**

By analyzing 482 pb<sup>-1</sup> of e<sup>+</sup>e<sup>-</sup> collision data collected at  $\sqrt{s} \approx 4.009$  GeV with the BESIII detector at the BEPCII collider, we measure the absolute branching fractions for the semileptonic decays  $D^*_s \rightarrow \eta e^+ \nu_e$  and  $D^*_s \rightarrow \eta^0 e^+ \nu_e$  to be  $\mathcal{B}(D^*_s \rightarrow \eta e^+ \nu_e) = 2.30 \pm 0.31 \pm 0.08\%$  and  $\mathcal{B}(D^*_s \rightarrow \eta^0 e^+ \nu_e) = 0.93 \pm 0.30 \pm 0.05\%$ , respectively, and their ratio  $\mathcal{B}(D^*_s \rightarrow \eta^0 e^+ \nu_e) / \mathcal{B}(D^*_s \rightarrow \eta e^+ \nu_e) = 0.40 \pm 0.14 \pm 0.02$ , where the first uncertainties are statistical and the second ones are systematic. The results are in good agreement with previous measurements within uncertainties; they can be used to determine the  $\eta - \eta^0$  mixing angle and improve upon the  $D^*_s$  semileptonic branching ratio precision.

**Web URL:** <https://journals.aps.org/prd/abstract/10.1103/PhysRevD.94.112003>

**59. Nisar, S. (2016). Measurement of Singly Cabibbo Suppressed Decays  $\Lambda^+ c \rightarrow p \pi^+ \pi^-$ ,  $\Lambda^+ c \rightarrow p \pi^+ \pi^-$  and  $\Lambda^+ c \rightarrow p K^+ K^-$ . *Phys.Rev.Lett.* 117 (23).**

**ABSTRACT:**

Using 567 pb<sup>-1</sup> of data collected with the BESIII detector at a center-of-mass energy of  $\sqrt{s} = 4.599$  GeV, near the  $\Lambda^+ c \Lambda^+ c$  threshold, we study the singly Cabibbo-suppressed decays  $\Lambda^+ c \rightarrow p \pi^+ \pi^-$  and  $\Lambda^+ c \rightarrow p K^+ K^-$ . By normalizing with respect to the Cabibbo-favored decay  $\Lambda^+ c \rightarrow p K^+ \pi^+$ , we obtain ratios of branching fractions:  $[\mathcal{B}(\Lambda^+ c \rightarrow p \pi^+ \pi^-) / \mathcal{B}(\Lambda^+ c \rightarrow p K^+ \pi^+)] = (6.70 \pm 0.48 \pm 0.25)\%$ ,  $[\mathcal{B}(\Lambda^+ c \rightarrow p \phi) / \mathcal{B}(\Lambda^+ c \rightarrow p K^+ \pi^+)] = (1.81 \pm 0.33 \pm 0.13)\%$ , and  $[\mathcal{B}(\Lambda^+ c \rightarrow p K^+ K_{\text{non-}\phi}^-) / \mathcal{B}(\Lambda^+ c \rightarrow p K^+ \pi^+)] = (9.36 \pm 2.22 \pm 0.71) \times 10^{-3}$ , where the uncertainties are statistical and systematic, respectively. The absolute branching fractions are also presented. Among these measurements, the decay  $\Lambda^+ c \rightarrow p \pi^+ \pi^-$  is observed for the first time, and the precision of the branching fraction for  $\Lambda^+ c \rightarrow p K^+ K_{\text{non-}\phi}^-$  and  $\Lambda^+ c \rightarrow p \phi$  is significantly improved.

*Measurement of Singly Cabibbo Suppressed Decays  $\Lambda^+ c \rightarrow p \pi^+ \pi^-$  and  $\Lambda^+ c \rightarrow p K^+ K^-$ .*

Available from:

**Web URL:** <http://inspirehep.net/record/1478790>

**60. Feroze, A., Idrees, M., Nadeem, M., Siddiqi, S. A., Saleem, M., Atif, M., ...& Shaukat, S. F. (2016). Origin of magnetic and dielectric response in single phase nano crystalline BiFeO<sub>3</sub>. *Materials Research Express*, 3(12), 125015.**

**ABSTRACT:**

Stoichiometric and single phase synthesis of BiFeO<sub>3</sub> is critical both in its particle industrial applications as well as in understanding the origin of its attractive dielectric and magnetic properties. In this study, BiFeO<sub>3</sub> has been obtained at temperatures as low as 400 °C. Zero Fe<sup>+2</sup>/Fe<sup>+3</sup> ratio, and absence of bismuth and oxygen non-stoichiometry have been probed by <sup>57</sup>Fe Mössbauer spectroscopy. The appearance of different magnetic phases in <sup>57</sup>Fe Mössbauer spectrum, MH hysteresis curve and exchange bias effect have been conferred on the basis of magneto-crystalline anisotropy and particle size distribution. Dependence of the dielectric response on the applied electric field reveals that the colossal dielectric response in BiFeO<sub>3</sub> is dominated by extrinsic effects at grain-grain interface.

**Web URL:**

[https://www.researchgate.net/profile/Asad\\_Feroze2/publication/311619540-Origin-of-magnetic-and-dielectric-response-in-single-phase-nano-crystalline-BiFeO3/links/5856567c08ae81995eb69a29.pdf](https://www.researchgate.net/profile/Asad_Feroze2/publication/311619540-Origin-of-magnetic-and-dielectric-response-in-single-phase-nano-crystalline-BiFeO3/links/5856567c08ae81995eb69a29.pdf)

**61.Amin, N., Afzal, M., Yousaf, M., & Javid, M. A. (2015). Choice of the pulse sequence and parameters for improved signal-to-noise ratio in T1-weighted study of MRI. *JPMA. The Journal of the Pakistan Medical Association*, 65(5), 512-518.**

**ABSTRACT:**

Objective: To investigate the practical impact of alteration of imaging parameters on signal-to-noise ratio for the most commonly used T1-weighted magnetic resonance sequences. Methods: The study was conducted in the Department of Medical Physics, Ninewells Hospital and Medical School, Dundee, UK, in 2007. Magnetic resonance images of a tissue-equivalent material were generated with a set of T1 and T2 values. Experimental variations in the imaging parameters were performed in echo time and repetition time. Quantitative analysis consisted of signal-to-noise ratio. Results: Percentage inaccuracy in signal-to-noise ratio was the result of inappropriate choice of parameters. We have investigated conventional spin echo, fast spin echo and fast fluid attenuated inversion recovery with one of corresponding percentage errors 28.68%, -36.65% and -40.34%, respectively. Conventional spin echo presented moderately low percentage error with the choice of repetition time and echo time. Factual error in fast spin echo was slightly higher than conventional spin echo. Fast fluid attenuated inversion recovery

could create outstanding signal-to-noise ratio of high T1/T2 value phantoms in T1-weighted images. Conclusion: The role of repetition time and echo time in T1-weighted images was crucial to sustain the image quality.

**Web URL:** <http://www.jpma.org.pk/PdfDownload/7348.pdf>

**62. Nisar, S. (2016).** Observation of  $e^+e^- \rightarrow \eta' J\psi$  at center-of-mass energies between 4.190 and 4.600 GeV. *Phys. Rev. D*

**ABSTRACT: Not Found**

**Web URL**

**63. Ablikim, M., Achasov, M. N., Ai, X. C., Albayrak, O., Albrecht, M., Ambrose, D. J., ...& Ferroli, R. B. (2016).** Improved measurement of the absolute branching fraction of  $D^+ \rightarrow \bar{K}^0 \mu^+ \nu_{\mu}$ . *The European Physical Journal C*, 76(7), 1-10.

**ABSTRACT:**

By analyzing 2.93 fb<sup>-1</sup> of data collected at  $\sqrt{s}=3.773$  GeV with the BESIII detector, we measure the absolute branching fraction  $B(D^+ \rightarrow \bar{K}^0 \mu^+ \nu_{\mu}) = (8.72 \pm 0.07_{\text{stat}} \pm 0.18_{\text{sys}})\%$ , which is consistent with previous measurements within uncertainties but with significantly improved precision. Combining the Particle Data Group values of  $B(D^0 \rightarrow \bar{K}^0 \mu^+ \nu_{\mu})$ ,  $B(D^+ \rightarrow \bar{K}^0 e^+ \nu_e)$ , and the lifetimes of the  $D^0$  and  $D^+$  mesons with the value of  $B(D^+ \rightarrow \bar{K}^0 \mu^+ \nu_{\mu})$  measured in this work, we determine the following ratios of partial widths:  $\Gamma(D^0 \rightarrow \bar{K}^0 \mu^+ \nu_{\mu})/\Gamma(D^+ \rightarrow \bar{K}^0 \mu^+ \nu_{\mu}) = 0.963 \pm 0.044$  and  $\Gamma(D^+ \rightarrow \bar{K}^0 \mu^+ \nu_{\mu})/\Gamma(D^+ \rightarrow \bar{K}^0 e^+ \nu_e) = 0.988 \pm 0.033$ .

**Web URL** <https://link.springer.com/article/10.1140/epjc/s10052-016-4198-2/fulltext.html>

**64. BESIII Collaboration. (2016). Measurement of the leptonic decay width of  $J/\psi$  using initial state radiation. *Physics Letters B*, 761, 98-103.**

**ABSTRACT:**

Using a data set of  $2.93 \text{ fb}^{-1}$  taken at a center-of-mass energy of  $\sqrt{s} = 3.773 \text{ GeV}$  with the BESIII detector at the BEPCII collider, we measure the process  $e^+e^- \rightarrow J/\psi\gamma \rightarrow \mu^+\mu^-\gamma$  and determine the product of the branching fraction and the electronic width  $B_{\mu\mu} \cdot \Gamma_{ee} = (333.4 \pm 2.5_{\text{stat}} \pm 4.4_{\text{sys}}) \text{ eV}$ . Using the earlier-published BESIII result for  $B_{\mu\mu} = (5.973 \pm 0.007_{\text{stat}} \pm 0.037_{\text{sys}})\%$ , we derive the  $J/\psi$  electronic width

$\Gamma_{ee} = (5.58 \pm 0.05_{\text{stat}} \pm 0.08_{\text{sys}}) \text{ keV}$ . © 2016 The Author(s). Published by Elsevier B.V. This is an open access article under the CC BY license.

**Web URL:** [http://ac.els-cdn.com/S0370269316304312/1-s2.0-S0370269316304312-main.pdf?\\_tid=f4968bec-6d37-11e7-8f8a-0000aacb35e&acdnat=1500547462\\_f5944bdbf833572c03cf194bbbc1ed0e](http://ac.els-cdn.com/S0370269316304312/1-s2.0-S0370269316304312-main.pdf?_tid=f4968bec-6d37-11e7-8f8a-0000aacb35e&acdnat=1500547462_f5944bdbf833572c03cf194bbbc1ed0e)

**65. Ablikim, M., Achasov, M. N., Ahmed, S., Ai, X. C., Albayrak, O., Albrecht, M., ...& Bai, J. Z. (2016). Observation of an Anomalous Line Shape of the  $\eta' \pi^+ \pi^-$  Mass Spectrum near the  $p \bar{p}$  Mass Threshold in  $J/\psi \rightarrow \gamma \eta' \pi^+ \pi^-$ . *Physical review letters*, 117(4), 042002.**

**ABSTRACT:** Using  $1.09 \times 10^9$   $J/\psi$  events collected by the BESIII experiment in 2012, we study the  $J/\psi \rightarrow \gamma \eta' \pi^+ \pi^-$  process and observe a significant abrupt change in the slope of the  $\eta' \pi^+ \pi^-$  invariant mass distribution at the proton-antiproton ( $p \bar{p}$ ) mass threshold. We use two models to characterize the  $\eta' \pi^+ \pi^-$  line shape around  $1.85 \text{ GeV}/c^2$ : one which explicitly incorporates the opening of a decay threshold in the mass spectrum (Flatté formula), and another which is the coherent sum of two resonant amplitudes. Both fits show almost equally good agreement with data, and suggest the existence of either a broad state around  $1.85 \text{ GeV}/c^2$  with strong couplings to  $p \bar{p}$  final states or a narrow state just below the  $p \bar{p}$  mass threshold. Although we cannot distinguish between the fits, either one supports the existence of a  $p \bar{p}$  molecule-like state or bound state with greater than  $7\sigma$  significance.

**Web URL:** <https://arxiv.org/pdf/1603.09653.pdf>

66. Ablikim, M., Achasov, M. N., Ai, X. C., Albayrak, O., Albrecht, M., Ambrose, D. J., ...& Ferroli, R. B. (2016). Observation of  $h c$  Radiative Decay  $h c \rightarrow \gamma \eta'$  and Evidence for  $h c \rightarrow \gamma \eta$ . *Physical review letters*, 116(25), 251802.

**ABSTRACT:**

A search for radiative decays of the P-wave spin singlet charmonium resonance  $h c$  is performed based on  $4.48 \times 10^8 \psi'$  events collected with the BESIII detector operating at the BEPCII storage ring. Events of the reaction channels  $h c \rightarrow \gamma \eta'$  and  $\gamma \eta$  are observed with a statistical significance of  $8.4\sigma$  and  $4.0\sigma$ , respectively, for the first time. The branching fractions of  $h c \rightarrow \gamma \eta'$  and  $h c \rightarrow \gamma \eta$  are measured to be  $B(h c \rightarrow \gamma \eta') = (1.52 \pm 0.27 \pm 0.29) \times 10^{-3}$  and  $B(h c \rightarrow \gamma \eta) = (4.7 \pm 1.5 \pm 1.4) \times 10^{-4}$ , respectively, where the first errors are statistical and the second are systematic uncertainties.

**Web URL:** <https://arxiv.org/pdf/1603.04936.pdf>

67. Nisar, S. (2016). Study of  $D \rightarrow k \pi e \nu$ . *Phy. Rev. D*

**ABSTRACT: Not Found**

**Web URL:**

68. Aziz, M. H., Fakhar-e-Alam, M., Fatima, M., Shaheen, F., Iqbal, S., Atif, M., ...& Harbi, T. S. A. (2016). Photodynamic Effect of Ni Nanotubes on an HeLa Cell Line. *PloS one*, 11(3), e0150295.

**ABSTRACT:**

Nickel nanomaterials are promising in the biomedical field, especially in cancer diagnostics and targeted therapy, due to their distinctive chemical and physical properties. In this experiment, the toxicity of nickel nanotubes (Ni NTs) were tested in an *in vitro* cervical cancer model (HeLa cell line) to optimize the parameters of photodynamic therapy (PDT) for their greatest effectiveness. Ni NTs were synthesized by electrodeposition. Morphological analysis and magnetic behavior were examined using a Scanning electron microscope (SEM), an energy dispersive X-ray analysis (EDAX) and a vibrating sample magnetometer (VSM) analysis. Phototoxic and cytotoxic effects of nanomaterials were studied using the Ni NTs alone as well

as in conjugation with aminolevulinic acid (5-ALA); this was performed both in the dark and under laser exposure. Toxic effects on the HeLa cell model were evaluated by a neutral red assay (NRA) and by detection of intracellular reactive oxygen species (ROS) production. Furthermore, 10–200 nM of Ni NTs was prepared in solution form and applied to HeLa cells in 96-well plates. Maximum toxicity of Ni NTs complexed with 5-ALA was observed at 100 J/cm<sup>2</sup> and 200 nM. Up to 65–68% loss in cell viability was observed. Statistical analysis was performed on the experimental results to confirm the worth and clarity of results, with p-values = 0.003 and 0.000, respectively. Current results pave the way for a more rational strategy to overcome the problem of drug bioavailability in nanoparticulate targeted cancer therapy, which plays a dynamic role in clinical practice.

**Web URL:** <http://journals.plos.org/plosone/article?id=10.1371/journal.pone.0150295>

**69. Majeed, A., Khan, M. A., ur Raheem, F., Hussain, A., Iqbal, F., Murtaza, G., ...& Warsi, M. F. (2016). Structural elucidation and magnetic behavior evaluation of rare earth (La, Nd, Gd, Tb, Dy) doped BaCoNi-X hexagonal nano-sized ferrites. *Journal of Magnetism and Magnetic Materials*, 408, 147-151.**

**ABSTRACT:**

Rare-earth (RE<sub>¼</sub>La<sub>3p</sub>, Nd<sub>3p</sub>, Gd<sub>3p</sub>, Tb<sub>3p</sub>, Dy<sub>3p</sub>) doped Ba<sub>2</sub>NiCoRE<sub>x</sub>Fe<sub>28x</sub>O<sub>46</sub> (x<sub>¼</sub>0.25) hexagonal ferrites were synthesized for the first time via micro-emulsion route, which is a fast chemistry route for obtaining nano-sized ferrite powders. These nanomaterials were investigated by X-ray diffraction (XRD), Fourier transform infrared spectroscopy (FTIR), as well as vibrating sample magnetometer (VSM). The XRD analysis exhibited that all the samples crystallized into single X-type hexagonal phase. The crystalline size calculated by Scherrer's formula was found in the range 7–19 nm. The variations in lattice parameters elucidated the incorporation of rare-earth cations in these nanomaterials. FTIR absorption spectra of these X-type ferrites were investigated in the wave number range 500–2400 cm<sup>-1</sup>. Each spectrum exhibited absorption bands in the low wave number range, thereby confirming the X-type hexagonal structure. The enhancement in the coercivity was observed with the doping of rare-earth cations. The saturation magnetization was lowered owing to the redistribution of rare-

earth cations on the octahedral site (3bVI). The higher values of coercivity (664–926 Oe) of these nanomaterials suggest their use in longitudinal recording media.

**Web URL:**

[https://www.researchgate.net/profile/Majid\\_Akhtar/publication/295540151\\_Structural\\_elucidation\\_and\\_magnetic\\_behavior\\_evaluation\\_of\\_rare\\_earth\\_La\\_Nd\\_Gd\\_Tb\\_Dy\\_doped\\_BaCoNi-X\\_hexagonal\\_nano-sized\\_ferrites/links/56ced1b108ae4d8d649baae2/Structural-elucidation-and-magnetic-behavior-evaluation-of-rare-earth-La-Nd-Gd-Tb-Dy-doped-BaCoNi-X-hexagonal-nano-sized-ferrites.pdf](https://www.researchgate.net/profile/Majid_Akhtar/publication/295540151_Structural_elucidation_and_magnetic_behavior_evaluation_of_rare_earth_La_Nd_Gd_Tb_Dy_doped_BaCoNi-X_hexagonal_nano-sized_ferrites/links/56ced1b108ae4d8d649baae2/Structural-elucidation-and-magnetic-behavior-evaluation-of-rare-earth-La-Nd-Gd-Tb-Dy-doped-BaCoNi-X-hexagonal-nano-sized-ferrites.pdf)

**70. Rehman, J., Khan, M. A., Hussain, A., Iqbal, F., Shakir, I., Murtaza, G., ...& Warsi, M. F. (2016). Structural, magnetic and dielectric properties of terbium doped NiCoX strontium hexagonal nano-ferrites synthesized via micro-emulsion route. *Ceramics International*, 42(7), 9079-9085.**

**ABSTRACT:**

Terbium (Tb) doped X-type hexagonal nano-ferrites  $Sr_2NiCoTb_xFe_{28-x}O_{46}$  ( $x=0.00, 0.05, 0.1, 0.15, 0.2$ ) were synthesized via micro-emulsion route. Single phase X-type hexagonal structure was confirmed by X-ray diffraction (XRD) analysis. The crystallite size of the samples was found in the range of 15–25 nm. The bulk density and X-ray density were enhanced while porosity was reduced with the increased  $Tb^{3+}$  contents. The development of hexagonal phase was investigated by thermogravimetric analysis. The fourier-transform infrared (FTIR) spectra revealed the formation of spectral bands (metal-oxygen stretching vibration) which confirmed the hexagonal ferrites. The dielectric constant has high value at low frequency and decreased with increased frequency. The dielectric loss is appreciably decreased by the  $Tb^{3+}$  incorporation and resonance phenomenon occurred beyond  $1.7 \times 10^9$  Hz. The saturation magnetization (76–54 emu/g) and remanance (27–21 emu/g) decreased while coercivity increased (610–747 Oe) by  $Tb^{3+}$ -incorporation in  $Sr_2NiCoTb_xFe_{28-x}O_{46}$  ferrite. The values of squareness ratio (0.35–0.39) indicated that Tb-doped samples are single domain while un-doped material is multi domains. These synthesized nano-sized hexagonal ferrites have potential applications in high frequency and recording media devices.

**Web URL:** <http://www.sciencedirect.com/science/article/pii/S0272884216301146>

**71. Sharif, M. K., Khan, M. A., Hussain, A., Iqbal, F., Shakir, I., Murtaza, G., ...& Warsi, M. F. (2016). Synthesis and characterization of Zr and Mg doped BiFeO<sub>3</sub> nanocrystalline multiferroics via micro emulsion route. *Journal of Alloys and Compounds*, 667, 329-340.**

**ABSTRACT:**

BiFe<sub>1-x</sub>Zr<sub>x</sub>Mg<sub>y</sub>O<sub>3</sub> (x = 0.00, 0.05, 0.1, 0.15, 0.2 and 0.25) nano-sized multiferroics were synthesized by micro emulsion technique. The structure analysis, thermogravimetric analysis (TGA), fourier transform infrared spectroscopy (FTIR), magnetic measurements and dielectric properties were studied for prepared samples. Differential scanning calorimetry (DSC) and differential thermogravimetric analysis (DTA) confirm multiferroic characteristics of the samples. DTA curve indicates the presence of ferroelectric transition temperature at 806.79 C. XRD results indicated that crystallite size is found in the range of (22.5-18.00) nm and other parameters like bulk density, X-ray density and porosity were also measured from the XRD data and were greatly influenced by increasing the dopants concentration. FTIR spectra revealed that the characteristics bonds of BiFeO<sub>3</sub> are appreciably influenced by ZrMg contents. Magnetic analysis reveals that saturation magnetization (M<sub>s</sub>) and remanent (M<sub>r</sub>) increase with ZrMg doping because magnetic moment of Zr<sup>4+</sup> is zero and doping of Zr<sup>4+</sup> at Fe<sup>3+</sup> site increase align spin but Mg<sup>2+</sup> doping in BiFeO<sub>3</sub> increases saturation magnetization not too much as compared to other alkaline earth metal ions because Mg<sup>2+</sup> contain smallest ionic radius among alkaline earth metals. M<sub>s</sub> reaches maximum value of 0.979 emu/g for composition x = 0.25. Multiferroics BiFe<sub>1-x</sub>Zr<sub>x</sub>Mg<sub>y</sub>O<sub>3</sub> are useful for ferroelectric random access memories (FeRAM) where data can be written electrically and read magnetically. It is found that all dielectric parameters strongly dependent on ZrMg contents. At higher concentrations, complicated dielectric behavior is observed. Dielectric results exhibited that dielectric parameters decrease with increase in frequency in the range of 1 MHz-3 GHz suggest that these multiferroics are useful for high resonant circuits.

**Web URL:** [http://ac.els-cdn.com/S0925838816301827/1-s2.0-S0925838816301827-main.pdf?\\_tid=3130e112-6dcc-11e7-b60d-0000aab0f27&acdnat=1500611122\\_b156f9e9b3b2b95c6cc3f38683807986](http://ac.els-cdn.com/S0925838816301827/1-s2.0-S0925838816301827-main.pdf?_tid=3130e112-6dcc-11e7-b60d-0000aab0f27&acdnat=1500611122_b156f9e9b3b2b95c6cc3f38683807986)

**72. Junaid, M., Khan, M. A., Iqbal, F., Murtaza, G., Akhtar, M. N., Ahmad, M., ...& Warsi, M. F. (2016). Structural, spectral, dielectric and magnetic properties of Tb–Dy doped Li–Ni nano-ferrites synthesized via micro-emulsion route. *Journal of Magnetism and Magnetic Materials*, 419, 338-344.**

**ABSTRACT:**

Terbium (Tb) and dysprosium (Dy) doped lithium-nickel nano-sized ferrites ( $\text{Li}_{0.2}\text{Ni}_{0.8}\text{Tb}_{0.5x}\text{Dy}_{0.5x}\text{Fe}_{2-x}\text{O}_4$  where  $x=0.00-0.08$ ) were prepared by micro-emulsion technique. The X-ray diffraction (XRD) patterns confirmed the single phase cubic spinel structure. The lattice constant was increased due to larger ionic radii of  $\text{Tb}^{3+}$  and  $\text{Dy}^{3+}$  cations. The crystallite size was found in the range 30–42 nm. The FTIR (Fourier transform infrared spectroscopy) spectra revealed two significant absorption bands ( $\sim 400-600\text{ cm}^{-1}$ ) which indicate the formation of cubic spinel structure. The peaking behavior of dielectric parameters was observed beyond 1.5 GHz. The dielectric constant and dielectric loss were found to decrease by the increase of Tb–Dy contents and frequency. The doping of Tb and Dy in Li–Ni ferrites led to increase the coercive field (120–156 Oe). The smaller magnetic and dielectric parameters suggested the possible utility of these nano-materials in switching and microwave devices applications

**Web URL:** <http://www.sciencedirect.com/science/article/pii/S0304885316311428>

**73. Bashir, M. F., & Chen, L. (2016). Asymmetric drift instability of magnetosonic waves in anisotropic plasmas. *Physics of Plasmas*, 23(10), 102107.**

**ABSTRACT:**

The general dispersion relation of obliquely propagating magneto-sonic (MS) waves for the inhomogeneous and anisotropic plasmas is analyzed including the effect of wave-particle interaction. The numerical analysis is performed without expanding both the plasma dispersion and the modified Bessel functions to highlight the effects of density inhomogeneity and the temperature anisotropy. The obtained results are compared with the recent work [Naim et al., *Phys. Plasmas* 22, 062117 (2015)], where only drift mode near the magnetosonic frequency is

investigated. In our paper, we additionally analyzed two related modes depicting that the drift effect leads to an asymmetric behavior in the dispersion properties of drift MS waves. The possible application to the solar coronal heating problem has also been discussed. Published by AIP Publishing.

**Web URL:** <http://aip.scitation.org/doi/pdf/10.1063/1.4964361>

**74. Islam, S., Bidin, N., Riaz, S., Naseem, S., Sanagi, M. M., & Imran, M. (2016). Multilayer crack-free hybrid coatings for functional devices. *Journal of Nanophotonics*, 10(2), 026026-026026.**

**ABSTRACT:**

Porous acid catalyzed TiO<sub>2</sub> single, SiO<sub>2</sub>-TiO<sub>2</sub> hybrid, and TiO<sub>2</sub>/SiO<sub>2</sub>-TiO<sub>2</sub>/SiO<sub>2</sub> multilayer coatings are synthesized and characterized for optical and electro-optical applications. The reflection value is reasonably reduced from the surface of the glass by integrating sol-gel based spin-coated single and multilayer thin films. Structurally, the films show uniform, crackfree, and porous nanofilms with good surface roughness of below 10 nm, which has potential for optical applications. Wide range tunability of refractive index (2.83 to 1.59) with more than 78% optical transparency is observed. The multilayered reflection profile is observed around 0.18%, so these coatings are desirable for optochemical functional devices.

**Web URL:**

[https://www.researchgate.net/profile/S\\_Islam7/publication/303946244\\_Multilayer\\_crack-free\\_hybrid\\_coatings\\_for\\_functional\\_devices/links/57620edb08ae2b8d20ed6306.pdf](https://www.researchgate.net/profile/S_Islam7/publication/303946244_Multilayer_crack-free_hybrid_coatings_for_functional_devices/links/57620edb08ae2b8d20ed6306.pdf)

**75. Javed, M. S., Han, X., Hu, C., Zhou, M., Huang, Z., Tang, X., & Gu, X. (2016). Tracking Pseudocapacitive Contribution to Superior Energy Storage of MnS Nanoparticles Grown on Carbon Textile. *ACS applied materials & interfaces*, 8(37), 24621-24628**

**ABSTRACT:**

Transition metal chalcogenides have emerged as a new class of electrode materials for energy storage devices with superior electrochemical performance. We have directly synthesized manganese sulfide nanoparticles on carbon textile substrate and used them as electrodes to fabricate flexible all-solid-state supercapacitors. By voltammetry analysis, we have studied the

electrochemical properties of MnS-CT composites, which reveal that the Faradaic diffusion-controlled process dominates at low scan rates (82.85% at  $5 \text{ mV s}^{-1}$ ) and even at high scan rates (39% at  $20 \text{ mV s}^{-1}$ ). The MnS-CT electrode shows high capacitance of  $710.6 \text{ F g}^{-1}$  in LiCl aqueous electrolyte, and the surface redox reactions on MnS nanoparticles are found to be responsible for the high pseudocapacity, which is further analyzed by XRD and HRTEM. Furthermore, MnS-CT supercapacitor exhibits excellent pseudocapacitive performance ( $465 \text{ F g}^{-1}$  at  $5 \text{ mV s}^{-1}$ ), excellent stability, light weight (0.83 g as a whole device), and high flexibility. The device has also achieved high energy density and high power density ( $52 \text{ Wh kg}^{-1}$  at  $308 \text{ W kg}^{-1}$  and  $1233 \text{ W kg}^{-1}$  with  $28 \text{ Wh kg}^{-1}$ , respectively). In practice, three charged supercapacitors in series can power four red light-emitting diodes (LEDs) (2.0 V, 15 mA) for 2 min. All of the evidence shows that MnS nanoparticles combined with carbon textile is a promising electrode material for pseudocapacitors.

**Web URL:** <http://pubs.acs.org/doi/abs/10.1021/acsami.6b07924?journalCode=aamick>

**76. Javed, M. S., Jiang, Z., Zhang, C., Chen, L., Hu, C., & Gu, X. (2016). A high-performance flexible solid-state supercapacitor based on Li-ion intercalation into tunnel-structure iron sulfide. *Electrochimica Acta*, 219, 742-750.**

**ABSTRACT:**

A flexible solid-state supercapacitor based on iron sulfide ( $\text{FeS}_2$ ) nanospheres supported on carbon-paper is fabricated, which exhibits excellent electrochemical performance such as, high capacitance of  $484 \text{ F g}^{-1}$  at a scan rate of  $5 \text{ mV s}^{-1}$ , good rate capability, and excellent cycling stability (95.7% after 5000 cycles). The supercapacitor achieves high energy density of  $44 \text{ Wh kg}^{-1}$  at power density of  $175 \text{ W kg}^{-1}$  with high coulombic efficiency (97%). Three charged supercapacitors connected in series can power 12 green-color light-emitting-diodes (LED, 3.0 V, 20 mA) for 5.5 minutes. To understand the detailed electrochemistry, we have carried out both experimental and theoretical investigations. The pseudocapacitive characteristics of the  $\text{FeS}_2$  nanospheres are systematically investigated by a single electrode in aqueous electrolyte. According to our structural analysis, the  $\text{FeS}_2$  nanospheres have orthorhombic structure, where Fe atoms are surrounded by 6 S atoms to form a  $\text{FeS}_6$  octahedron. These octahedrons are

connected to form a network structure, which provide tunnels (2.55–4.77 Å). With all the evidence, we believe that the FeS<sub>2</sub> nanospheres could be a promising material for supercapacitor electrodes.

**Web URL:** [http://ac.els-cdn.com/S001346861632148X/1-s2.0-S001346861632148X-main.pdf?\\_tid=d8276800-6dcd-11e7-852a-0000aacb35e&acdnat=1500611832\\_eef3b0ff22b13dc5e5a1a07dd6d43289](http://ac.els-cdn.com/S001346861632148X/1-s2.0-S001346861632148X-main.pdf?_tid=d8276800-6dcd-11e7-852a-0000aacb35e&acdnat=1500611832_eef3b0ff22b13dc5e5a1a07dd6d43289)

**77. Hussain, S., Liu, T., Javed, M. S., Aslam, N., Shaheen, N., Zhao, S., ...& Wang, J. (2016). Amaryllis-like NiCo<sub>2</sub>S<sub>4</sub> nanoflowers for high-performance flexible carbon-fiber-based solid-state supercapacitor. *Ceramics international*, 42(10), 11851-11857.**

**ABSTRACT:**

Low-cost dynamic materials for Faradaic redox reactions are needed for high-energy storage supercapacitors. A simple and cost-effective hydrothermal process was employed to synthesize amaryllis-like NiCo<sub>2</sub>S<sub>4</sub> nanoflowers. The sample was characterized by X-ray powder diffraction, Brunauer–Emmett–Teller method, scanning electron microscopy, and transmission electron microscopy. NiCo<sub>2</sub>S<sub>4</sub> nanoflowers were coated onto carbon fiber fabric and used as a binder-free electrode to fabricate a solid-state supercapacitor compact device. The solid-state supercapacitor exhibited excellent electrochemical performance, including high specific capacitance of 360 F g<sup>-1</sup> at scan rate of 5 mV s<sup>-1</sup> and high energy density of 25 W h kg<sup>-1</sup> at power density of 168 W kg<sup>-1</sup>. In addition, the supercapacitor possessed high flexibility and good stability by retaining 90% capacitance after 5000 cycles. The high conductivity and Faradic-redox activity of NiCo<sub>2</sub>S<sub>4</sub> nanoflowers resulted in high specific energy and power. Thus, NiCo<sub>2</sub>S<sub>4</sub> nanoflowers are promising pseudocapacitive materials for low-cost and lightweight solid-state supercapacitors.

**Web URL:**

[https://www.researchgate.net/profile/Muhammad\\_Sufyan\\_Javed/publication/301545275\\_Amaryllis-like\\_NiCo2S4\\_nanoflowers\\_for\\_high-performance\\_flexible\\_carbon-fiber-based\\_solid-state\\_supercapacitor/links/5720da3108aeaced78907061/Amaryllis-like-NiCo2S4-nanoflowers-for-high-performance-flexible-carbon-fiber-based-solid-state-supercapacitor.pdf](https://www.researchgate.net/profile/Muhammad_Sufyan_Javed/publication/301545275_Amaryllis-like_NiCo2S4_nanoflowers_for_high-performance_flexible_carbon-fiber-based_solid-state_supercapacitor/links/5720da3108aeaced78907061/Amaryllis-like-NiCo2S4-nanoflowers-for-high-performance-flexible-carbon-fiber-based-solid-state-supercapacitor.pdf)

**78. Rozina, C., Tsintsadze, N. L., & Jamil, M. (2016). Propagation of ultra-intense electromagnetic waves through electron-positron-ion plasma. *Physics of Plasmas*, 23(7), 072303.**

**ABSTRACT:**

A kinetic approach is used to study the propagation of ultrarelativistic (amplitude) electromagnetic waves through electron-positron-ion plasma. For our purposes, we formulate a new plasma particle distribution function in the presence of ultrarelativistically intense circularly polarized electromagnetic (EM) waves. An effective dispersion relation of constant amplitude ultrarelativistic EM wave is derived, skin depth is calculated in particular, frequency regimes and has shown numerically that the penetration depth increases with the amplitude of ultra-intense electromagnetic waves,  $k \propto \omega^2$ , i.e., plasma will be heated more in the region of skin depth. Next, we have found that the nonlinear interaction of ultrarelativistically intense EM waves of time and space varying amplitude leads to construct kinetic nonlinear Schrödinger equation (KNSE), containing both local and non-local nonlinear terms, where nonlocal nonlinear term appears due to density perturbations of plasma species. Taking the effects of the latter into consideration, nonlinear Landau damping is discussed for KNSE, damping rate is computed, and numerically ultrarelativistic EM waves are shown to decay exponentially. The present results should be helpful to understand the specific properties of the ultrarelativistic EM waves in astrophysical plasmas, e.g., pulsars, black holes, and neutron stars. Published by AIP Publishing.

**Web URL:** <http://aip.scitation.org/doi/pdf/10.1063/1.4955215>

**79. Rehman, S., Rahmouni, A., Shaukat, S. F., Nesterenko, D. V., & Sekkat, Z. (2016). Optical characteristics of ultra-thin metallic films excited at visible range. *Thin Solid Films*, 615, 38-43.**

**ABSTRACT:**

An extensive research has been carried out in synthesizing and characterizing single layer Ag films and double layer Ag/Au films of different thicknesses including ultrathin films. AFM measurements confirmed the thickness and smoothness of the prepared films. Moreover, the refractive indices of the metal films and surface plasmon resonance (SPR) parameters like

height, full width at half maximum (FWHM) of SPR dip, average inclinations of the slopes have been determined successfully. SPR field enhancement of the film samples has been calculated as well. It has been revealed that the refractive index of Ag single layer decreases with increasing film thickness at different exciting wavelengths. While in case of double layer, the refractive index of Au ultra-thin layer (metal clusters) increases with increasing thickness (5–9 nm). The optical measurements divulged that the light of wavelength 633 nm is the best for measuring SPR thickness below 10 nm metal thin films.

**Web URL:** <http://www.sciencedirect.com/science/article/pii/S0040609016302917>

**80. Imran, M., Rahman, R. A., Ahmad, M., Akhtar, M. N., Usman, A., & Sattar, A. (2016). Fabrication of microchannels on PMMA using a low power CO2 laser. *Laser Physics*, 26(9), 096101.**

**ABSTRACT:**

This study presents a cheap and quick method for the formation of microchannels on poly methyl methacrylate (PMMA). A continuous wave CO2 laser with a wavelength of 10.6  $\mu\text{m}$  was used to inscribe periodic ripple structures on a PMMA substrate. A direct writing technique was employed for micromachining. As PMMA is very sensitive to such laser irradiations, a slightly low power CO2 laser was effective in inscribing such periodic structures. The results show that smooth and fine ripple structures can be fabricated by controlling the input laser parameters and interaction time of the laser beam. This direct laser writing technique is promising enough to prevent us from using complex optical arrangements. Laser power was tested starting from the ablation threshold and was gradually increased, together with the variation in scanning speed of the xy-translational stage, to observe the effects on the target surface in terms of depth and width of trenches. It was observed that the depth of the trenches increases on increasing the laser power, and the bulge formation on the outer sides of the trenches was also studied. It was evident that the formation of bulges across the trenches is dependent on the scanning speed and input laser power. The results depict that a focused laser beam with optimized parameters, such as controlling the scanning speed and laser power, results in fine, regular and tidy periodic structures.

**Web URL:**

[https://www.researchgate.net/profile/Majid\\_Akhtar/publication/304992635\\_Fabrication\\_of\\_microchannels\\_on\\_PMMA\\_using\\_a\\_low\\_power\\_CO\\_2\\_laser/links/57aab09308ae3765c3b5016d.pdf](https://www.researchgate.net/profile/Majid_Akhtar/publication/304992635_Fabrication_of_microchannels_on_PMMA_using_a_low_power_CO_2_laser/links/57aab09308ae3765c3b5016d.pdf)

**81. Ellahi, M., & Rafique, M. Y. (2016). Electro-optical properties of PDLC films using diethylenetriamine (DETA) hardener. *Molecular Crystals and Liquid Crystals*, 638(1), 103-110.**

**ABSTRACT:**

The author's results obtained today and in previous works are summarized. The present work has been performed to investigate the effects of the structure and electro-optical (E-O) properties of epoxy resin based polymer dispersed liquid crystal (PDLC) films smart glass using Diethylenetriamine (DETA) as hardener with 4-cyano-4 - pentylbiphenyl (5CB) liquid crystal. In this study we have been prepared PDLC films by the thermal polymerization-induced phase separation (PIPS) method, with a thickness of  $10.0 \pm 1.0 \mu\text{m}$  controlled by a polyethylene terephthalate (PET) spacer and optimal preparation condition were 25% and 30% 5CB LC, respectively, with a curing time 7 hours at  $70^\circ\text{C}$  temperature. In addition, PDLC films were prepared with different amounts of DETA to investigate the best ratio of the hardener. Results showed that when the weight ratio of LC 5CB was 30% in PDLC and mol 3% of DETA hardener, then dispersed state of LC were well proportioned, and the variation of transmittance reached the highest value. The optical characterization of the PDLC film indicates an improvement of the angular transmission of visible light. Meanwhile, it is examined that by adjusting the mol% of hardener and LC 5CB content possesses good E-O properties with a low energy efficient method for preparing PDLC smart glass display technology.

**Web URL:**

[https://www.researchgate.net/profile/Mujtaba\\_Ellahi/publication/310388001\\_Electro-optical\\_properties\\_of\\_PDLC\\_films\\_using\\_diethylenetriamine\\_DETA\\_hardener/links/587479bd08ae329d621d3dac/Electro-optical-properties-of-PDLC-films-using-diethylenetriamine-DETA-hardener.pdf](https://www.researchgate.net/profile/Mujtaba_Ellahi/publication/310388001_Electro-optical_properties_of_PDLC_films_using_diethylenetriamine_DETA_hardener/links/587479bd08ae329d621d3dac/Electro-optical-properties-of-PDLC-films-using-diethylenetriamine-DETA-hardener.pdf)

**82. Khattak, M. N., Mushtaq, A., & Ehsan, Z. (2016). Electrostatic baryonic solitary waves in ambiplasma with nonextensive leptons. *Chinese Journal of Physics*, 54(4), 503-514.**

**ABSTRACT:**

The nonlinear wave structures of baryon acoustic waves in ambiplasma consisting of baryons (positive and negative ions), and nonextensive leptons (electrons and positrons) are theoretically investigated by employing a pseudo-potential approach, which is valid for arbitrary amplitude structures. The propagation of small but finite amplitude solitary structures is also examined by using the reductive perturbation method. The presence of nonextensive  $q$ -distributed electrons and positrons has shown to influence the soliton structure quite significantly. From the analysis of our results it is shown that the present plasma model supports the coexistence of both the compressive and rarefactive solitons. Our present analysis should be useful for understanding the collective interactions in astronomical, space and laboratory plasmas such as capsule implosion, shock tube, star formation and supernova explosion.

**Web URL:** [http://ac.els-cdn.com/S0577907316302052/1-s2.0-S0577907316302052-main.pdf?\\_tid=4e037b7e-6dd1-11e7-9ca7-0000aacb35d&acdnat=1500613318\\_d37e3331d533e71ee8a1ef37e464536d](http://ac.els-cdn.com/S0577907316302052/1-s2.0-S0577907316302052-main.pdf?_tid=4e037b7e-6dd1-11e7-9ca7-0000aacb35d&acdnat=1500613318_d37e3331d533e71ee8a1ef37e464536d)

**83. Ehsan, Z., Tsintsadze, N. L., Shah, H. A., Trines, R. M. G. M., & Imran, M. (2016). New longitudinal mode and compression of pair ions in plasma. *Physics of Plasmas*, 23(6), 062125.**

**ABSTRACT:**

Positive and negative ions forming so-called pair plasma differing in sign of their charge but asymmetric in mass and temperature support a new acoustic-like mode. The condition for the excitation of ion sound wave through electron beam induced Cherenkov instability is also investigated. This beam can generate a perturbation in the pair ion plasmas in the presence of electrons when there is number density, temperature and mass difference in the two species of ions. Basic emphasis is on the focusing of ion sound waves and we show how, in the area of localization of wave energy, the density of pair particles increases while electrons are pushed away from that region. Further, this localization of wave is dependent on the shape of the pulse. Considering the example of pancake and bullet shaped pulses, we find that only the

former leads to compression of pair ions in the supersonic regime of the focusing region. Here possible existence of regions where pure pair particles can exist may also be speculated which is not only useful from academic point of view but also to mimic the situation of plasma (electron positron asymmetric and symmetric) observed in astrophysical environment.

**Web URL:** <https://arxiv.org/pdf/1603.05210.pdf>

**84. Sattar, A., Amjad, R. J., Yasmeen, S., Javed, H., Latif, H., Mahmood, H., ...& Dousti, M. R. (2016). The effect of semi-infinite crystalline electrodes on transmission of gold atomic wires using DFT. *Physica E: Low-dimensional Systems and Nanostructures*, 79, 8-12.**

**ABSTRACT:**

First principle calculations of the conductance of gold wires containing 3-8 atoms each with 2.39 Å bond length were performed using density functional theory. Three different configuration of wire/electrodes were used. For zigzag wire with semi-infinite crystalline electrodes, even-odd oscillation is observed which is consistent with the previously reported results. A lower conductance was observed for the chain in semi-infinite crystalline electrodes compared to the chains suspended in wire-like electrode. The calculated transmission spectrum for the straight and zig-zag wires suspended between semi-infinite crystalline electrodes showed suppression of transmission channels due to electron scattering occurring at the electrode-wire interface.

**Web URL:** <https://arxiv.org/ftp/arxiv/papers/1507/1507.08078.pdf>

**85. Imran, M., Rahman, R. A., Ahmad, M., Akhtar, M. N., Usman, A., & Sattar, A. (2016). Fabrication of microchannels on PMMA using a low power CO<sub>2</sub> laser. *Laser Physics*, 26(9), 096101.**

**ABSTRACT:**

This study presents a cheap and quick method for the formation of microchannels on poly methyl methacrylate (PMMA). A continuous wave CO<sub>2</sub> laser with a wavelength of 10.6 μm was used to inscribe periodic ripple structures on a PMMA substrate. A direct writing technique was employed for micromachining. As PMMA is very sensitive to such laser irradiations, a slightly low power CO<sub>2</sub> laser was effective in inscribing such periodic structures. The results show that

smooth and fine ripple structures can be fabricated by controlling the input laser parameters and interaction time of the laser beam. This direct laser writing technique is promising enough to prevent us from using complex optical arrangements. Laser power was tested starting from the ablation threshold and was gradually increased, together with the variation in scanning speed of the xy-translational stage, to observe the effects on the target surface in terms of depth and width of trenches. It was observed that the depth of the trenches increases on increasing the laser power, and the bulge formation on the outer sides of the trenches was also studied. It was evident that the formation of bulges across the trenches is dependent on the scanning speed and input laser power. The results depict that a focused laser beam with optimized parameters, such as controlling the scanning speed and laser power, results in fine, regular and tidy periodic structures.

**Web URL:**

[https://www.researchgate.net/profile/Majid\\_Akhtar/publication/304992635\\_Fabrication\\_of\\_microchannels\\_on\\_PMMA\\_using\\_a\\_low\\_power\\_CO\\_2\\_laser/links/57aab09308ae3765c3b5016d.pdf](https://www.researchgate.net/profile/Majid_Akhtar/publication/304992635_Fabrication_of_microchannels_on_PMMA_using_a_low_power_CO_2_laser/links/57aab09308ae3765c3b5016d.pdf)

**86. Anjum, S., Hameed, S., Awan, M. S., Amed, E., & Sattar, A. (2017). Effect of strontium doped M-Type barium hexa-ferrites on structural, magnetic and optical properties. *Optik-International Journal for Light and Electron Optics*, 131, 977-985.**

**ABSTRACT:**

The series of M-type  $Ba_{1-x}Sr_xFe_{12}O_{19}$  ( $x = 0.0, 0.2, 0.4, 0.6, 0.8, 1$ ) have been fabricated using powder metallurgy route. The effects of strontium ions have been systematically investigated. The samples are sintered at 1200 °C for 2 h. The structural properties and surface morphology is determined using X-ray diffraction technique, Fourier Infrared Spectroscopy and Field Emission Scanning Electron Microscope respectively. The magnetic and optical properties are carried out using vibrating sample magnetometer and UV–vis spectroscopy. The XRD analysis revealed that these samples have hexagonal structure. FTIR analysis confirmed that bands in the range 430–590  $cm^{-1}$  are due to the stretching vibration of oxygen atom and metal ions (M-O) that is Fe-O confirming the formation of hexa-ferrite. The average grain size is determined using FSEM i.e about 0.37–1.5  $\mu m$ . The VSM analysis showed that saturation magnetization

decreased with increasing concentration of Sr<sup>2+</sup> ions and this decrease is due to the different site occupation of Sr<sup>2+</sup> and Fe<sup>3+</sup> ions. The band gap energy decreased with the increasing concentration of strontium ions. This is due to the vacancies of electrons in the valence band of Ba and Sr. The decrease in the distance between conduction and valence band causes the increase in conductivity due to which band gap energy decreases. The widest applications of these hard ferrites permanent magnets are in motors, speakers sensors and MRI systems.

**Web URL:** [http://ac.els-cdn.com/S0030402616315467/1-s2.0-S0030402616315467-main.pdf?\\_tid=b1632c44-6dd3-11e7-8feb-00000aab0f6c&acdnat=1500614344\\_6472e8f2c5b09eb5a49cabda3ac60237](http://ac.els-cdn.com/S0030402616315467/1-s2.0-S0030402616315467-main.pdf?_tid=b1632c44-6dd3-11e7-8feb-00000aab0f6c&acdnat=1500614344_6472e8f2c5b09eb5a49cabda3ac60237)

**87. Akhtar, M. N., Sulong, A. B., Radzi, M. F., Ismail, N. F., Raza, M. R., Muhamad, N., & Khan, M. A. (2016). Influence of alkaline treatment and fiber loading on the physical and mechanical properties of kenaf/polypropylene composites for variety of applications. *Progress in Natural Science: Materials International*, 26(6), 657-664.**

**ABSTRACT:**

Due to current trend and increasing interest towards natural based fiber products, Kenaf (*Hibiscus cannabinus*) fibers have been used for the developments of many products. Therefore, Kenaf fiber-reinforced composites have been widely used in engineering and industrial applications. The present work deals with the fabricating and characterization of untreated and treated kenaf/polypropylene (PP)-reinforced composites. Composites of PP reinforced with treated and untreated kenaf fibers were fabricated using the injection molding technique. Different fiber loadings of 10, 20, 30, 40, 50 wt% treated and untreated kenaf composites were also prepared. X-ray diffraction (XRD), scanning electron microscopy (SEM), Fourier transform infrared (FTIR) spectroscopy and thermo gravimetric analysis (TGA) were performed on the treated, untreated kenaf fibers and kenaf/PP composites. Moreover, the alkaline-treated kenaf composites exhibit better physical, morphological, and mechanical properties because of the compatibility of kenaf with PP. However, variations in tensile and flexural properties depend on treatment and kenaf fiber contents. The percentage increase in the mechanical properties of the treated kenaf/PP composites relative to that of PP was also

measured. In addition, 40 wt% kenaf fiber loading resulted in higher mechanical properties. By contrast, kenaf/PP composite with 50% fiber loading was not successfully prepared because of improper mixing and the burning of kenaf fibers in the PP matrix. To conclude, 40% kenaf/PP composites with superior physical and mechanical properties may be used in variety of applications such as automotive, sports, construction, animal bedding, and mass production industries.

**Web URL:** [http://ac.els-cdn.com/S1002007116302283/1-s2.0-S1002007116302283-main.pdf?\\_tid=fb1ef6ec-6dd3-11e7-b859-0000aacb35d&acdnat=1500614468\\_80bbfcc43d83ad5f6234349768b74b5](http://ac.els-cdn.com/S1002007116302283/1-s2.0-S1002007116302283-main.pdf?_tid=fb1ef6ec-6dd3-11e7-b859-0000aacb35d&acdnat=1500614468_80bbfcc43d83ad5f6234349768b74b5)

**88. Amin, N., Arshad, M. I., Islam, M. U., Ali, A., Mahmood, K., Murtaza, G., ...& Mustafa, G. (2016). ROLE OF Y<sup>3+</sup> IONS ON THE STRUCTURAL AND DIELECTRIC PROPERTIES OF Ni-Zn-Cr FERRITES SYNTHESIZED BY CO-PRECIPIATION METHOD. *Digest Journal of Nanomaterials and Biostructures*, 11(2), 579-590.**

**ABSTRACT:**

In this study spinel ferrites Ni<sub>0.5</sub>Zn<sub>0.5</sub>Cr<sub>0.04</sub>Y<sub>x</sub>Fe<sub>1.96-x</sub>O<sub>4</sub> (x = 0.0, 0.02, 0.04 and 0.06) were synthesized using the co-precipitation method by varying the concentration of Yttrium. X-ray diffraction (XRD) and Fourier transform infrared (FTIR) analysis confirm the formation of spinel ferrites structure. The average particle size estimated by Scherrer formula found to be in the range 30.3-106 nm with cubic shape. Energy Dispersive Spectroscopy (EDS) measurement was in close agreement with the stoichiometry of the reactant solutions. UV-Vis-NIR spectroscopy evidenced intermediate energy levels within the band gap of the prepared ferrites system. Dielectric measurements showed that the inverse relation of permittivity of these ferrites with frequency that follows the Maxwell Wagner Model. The substituted samples exhibited very low dielectric constant and low loss tangent in the frequency range 1 MHz to 3GHz. AC conductivity increased with the increase in frequency and decreased with the increase of yttrium concentration. Such characteristics of these materials may be suitable for potential applications such as switching and microwave devices.

**Web URL:**

[https://www.researchgate.net/publication/305322019\\_Role\\_of\\_Y3\\_ions\\_on\\_the\\_structural\\_and\\_dielectric\\_properties\\_of\\_Ni-Zn-Cr\\_ferrites\\_synthesized\\_by\\_co-precipitation\\_method](https://www.researchgate.net/publication/305322019_Role_of_Y3_ions_on_the_structural_and_dielectric_properties_of_Ni-Zn-Cr_ferrites_synthesized_by_co-precipitation_method)

**89. Elahi, A., Irfan, M., Munawar, M., Qasim, M., Mahmood, K., Saeed, M., ...& Ali, A. (2016). Study on conductivity and dielectric behavior of chemically synthesized polypyrrol dodecylbenzene sulfonic acid blended with poly (methyl methacrylate). *Polymer Science Series A*, 3(58), 429-437.**

**ABSTRACT:**

Polypyrrole (PPy) doped with dodecylbenzene sulfonic acid was synthesized and was blended with compatible polymer PMMA in chloroform. Flexible and free-standing films with compositions PPy : PMMA = 10 : 90, 20 : 80, 30 : 70 and 50 : 50 were obtained. The percentage of crystallinity and particle size of synthesized polymers were estimated from X-rays diffraction studies. Scanning Electron Micrographs showed that phase separation was observed and compatibility of the mixture decreased with increase of PMMA content. The dielectric measurements were performed in the frequency range 0.1 kHz-1 MHz in temperature range 303–473 K. The frequency dependent conductivity ( $\sigma_{ac}$ ) obeyed a power law of frequency with an exponent  $s < 1$ . Electric modulus formalism exhibits a peak in frequency. The peak of conductivity relaxation shifted towards higher frequencies and the magnitude of relaxation decreased with the increase of PMMA content in the composites.

**Web URL:**

[https://www.researchgate.net/profile/Muhammad\\_Irfan70/publication/298357499\\_Study\\_on\\_Conductivity\\_and\\_Dielectric\\_Behavior\\_of\\_Chemically\\_Synthesized\\_Polypyrrol\\_Dodecylbenzene\\_Sulfonic\\_Acid\\_Blended\\_with\\_Polymethyl\\_Methacrylate/links/56f3691008ae95e8b6cb5577.pdf](https://www.researchgate.net/profile/Muhammad_Irfan70/publication/298357499_Study_on_Conductivity_and_Dielectric_Behavior_of_Chemically_Synthesized_Polypyrrol_Dodecylbenzene_Sulfonic_Acid_Blended_with_Polymethyl_Methacrylate/links/56f3691008ae95e8b6cb5577.pdf)

**90. Azim, M., Chaudhry, M. A., Amin, N., Arshad, M. I., Islam, M. U., Nosheen, S., ...& Mustafa, G. (2016). STRUCTURAL AND OPTICAL PROPERTIES OF Cr-SUBSTITUTED Co-FERRITE SYNTHESIS BY COPRECIPITATION METHOD. *DIGEST JOURNAL OF NANOMATERIALS AND BIOSTRUCTURES*, 11(3), 953-962.**

**ABSTRACT:**

A series of nanocrystalline Cr-substituted  $\text{CoCr}_x\text{Fe}_{2-x}\text{O}_4$  ferrite powder ( $x = 0.0 \leq x \leq 0.10$  with an interval of 0.02) has been synthesized by co-precipitation technique, the powder sintered at 9000C for 6h. X-ray diffraction (XRD) and Fourier Transform Infrared Techniques (FTIR) were employed for the confirmation of the formation of spinel cubic structure. The X-ray diffraction pattern revealed that secondary phase with increasing Cr<sup>+3</sup> contents  $x > 0.04$ . Moreover, the average crystallite size of the synthesized samples was found to be ranging from 70.4- 31.5 nm while lattice parameters decrease with increasing chromium contents. Fourier transform infrared techniques data shows the formation of two frequency bands tetrahedral and octahedral bands which are the basic characteristics of cubic spinel ferrites that corresponds to the metal oxide. Morphology of the spinel ferrites powder was analyzed by scanning electron microscope (SEM) and atomic force microscopy (AFM) technique. The observed results are explained on the basis of crystal size and elemental composition which were verified by energy dispersive X-ray spectroscopy (EDX). Furthermore, the effect of Cr<sup>+3</sup> on the structural and optical properties was studied by UV-visible spectra. The band gap energy for the sample having  $x = 0.10$  lies from 2.5 to 4.5 eV, while the Photoluminescence (PL) spectra have the maximum peak at about 3500 nm with an energy of 0.356 eV

**Web URL:**

[https://www.researchgate.net/profile/Ghulam\\_Mustafa38/publication/307994153\\_Structural\\_and\\_optical\\_properties\\_of\\_Cr-substituted\\_Co-ferrite\\_synthesis\\_by\\_co-precipitation\\_method/links/57e2883008ae9e25307f3ac2/Structural-and-optical-properties-of-Cr-substituted-Co-ferrite-synthesis-by-co-precipitation-method.pdf](https://www.researchgate.net/profile/Ghulam_Mustafa38/publication/307994153_Structural_and_optical_properties_of_Cr-substituted_Co-ferrite_synthesis_by_co-precipitation_method/links/57e2883008ae9e25307f3ac2/Structural-and-optical-properties-of-Cr-substituted-Co-ferrite-synthesis-by-co-precipitation-method.pdf)

**91. Hakeem, A., Ahmad, I., Murtaza, G., Mustafa, G., Kanwal, M., Farid, M. T., ...& Ahmad, M. (2016). EFFECT OF VARIATION OF Mn/Zn CONTENT ON THE STRUCTURAL, ELECTRICAL AND MAGNETIC PROPERTIES OF Mn-Zn FERRITE. *Digest Journal of Nanomaterials & Biostructures (DJNB)*, 11(3).**

**ABSTRACT:**

Nano sized Mn-Zn ferrite particles were synthesized by co-precipitation method. The Xray C reveals the ferrite possesses spinel<sup>o</sup>diffraction analysis of sintered powder at 1000 face

centered cubic structure. Particle size is observed by SEM ranging from 50nm to 85nm. The magnetic properties are measured by using the Physical property measurements (PPMS) technique. The Fourier transform infrared spectroscopy is used to detect the presence of the metallic compounds in the ferrite sample. Lattice constant is proportional to the Mn contents and it decreases with the increase of Zn contents. The actual density of the ferrites was found to be increasing, where as X-ray density depend on the molecular weight. Lattice constant of the material tends to decrease with an increase of Mn contents.

**Web URL:**

[https://www.researchgate.net/profile/Ghulam\\_Mustafa38/publication/305766816\\_EFFECT\\_OF\\_VARIATION\\_OF\\_MnZn\\_CONTENT\\_ON\\_THE\\_STRUCTUREALELECTRICAL\\_AND\\_MAGNETIC\\_PROPERTIES\\_OF\\_Mn-Zn\\_FERRITE/links/579fa7d708ae94f454e7c03c/EFFECT-OF-VARIATION-OF-Mn-Zn-CONTENT-ON-THE-STRUCTURAL-ELECTRICAL-AND-MAGNETIC-PROPERTIES-OF-Mn-Zn-FERRITE.pdf](https://www.researchgate.net/profile/Ghulam_Mustafa38/publication/305766816_EFFECT_OF_VARIATION_OF_MnZn_CONTENT_ON_THE_STRUCTUREALELECTRICAL_AND_MAGNETIC_PROPERTIES_OF_Mn-Zn_FERRITE/links/579fa7d708ae94f454e7c03c/EFFECT-OF-VARIATION-OF-Mn-Zn-CONTENT-ON-THE-STRUCTURAL-ELECTRICAL-AND-MAGNETIC-PROPERTIES-OF-Mn-Zn-FERRITE.pdf)

**92. Imran, S., Amin, N., Arshad, M. I., Islam, M. U., Anwar, H., Azam, A., ...& Mustafa, G. (2016). STRUCTURAL AND OPTICAL PROPERTIES OF Cr-SUBSTITUTED Mg-FERRITE SYNTHESIS BY CO-PRECIPIATION METHOD. *Digest Journal of Nanomaterials and Biostructures*, 11(4), 1197-1204.**

**ABSTRACT:**

A series of Cr substituted Mg-ferrites were synthesized by coprecipitation technique annealed at 900 oC for 6h. XRD analysis technique was used to confirm the formation of synthesized ferrites structure and the particle size estimated by Scherrer formula was found to be lying in the range 42.4 to 84.8 nm. All the prepared samples exhibited inverse cubic spinel structure and lattice parameter found in the range (8.3814-8.3756 Å). The morphology and the formation of nanoparticles were observed by scanning electron microscopy (SEM). For the elemental analysis, the energy dispersive X-ray (EDX) confirmed the existence of Mg, Cr, Fe and O orbital state. Moreover, the representative sample UV/Vis spectra of the Cr-substituted Mg-ferrites revealed that the absorbance shifted from 373 to 386 nm for reference samples at x=0.2 and x=0.5 and the wavelength lies most prominently in UV region wavelength 200-380 nm

approximately. The electrical measurements were done by two probe method. It was observed that at room temperature the DC resistivity decreased with the increase in chromium content while synthesized material have semiconductor behavior with the rise of temperature.

**Web URL:** [http://www.chalcogen.ro/1197\\_ShahdS.pdf](http://www.chalcogen.ro/1197_ShahdS.pdf)

**93. Hussain, S. Q., Balaji, N., Kim, S., Ahn, S., Park, H., Le Anh, H. T., ...& Razaq, A. (2016). Plasma Textured Glass Surface Morphologies for Amorphous Silicon Thin Film Solar Cells-A review. *Transactions on Electrical and Electronic Materials*, 17(2), 98-103.**

**ABSTRACT:**

The surface morphology of the front transparent conductive oxide (TCO) films plays a vital role in amorphous silicon thin film solar cells (a-Si TFSCs) due to their high transparency, conductivity and excellent light scattering properties. Recently, plasma textured glass surface morphologies received much attention for light trapping in a-Si TFSCs. We report various plasma textured glass surface morphologies for the high efficiency of a-Si TFSCs. Plasma textured glass surface morphologies showed high rms roughness, haze ratio with micro- and nano size surface features and are proposed for future high efficiency of a-Si TFSCs

**Web URL:**

[http://central.oak.go.kr/journalist/journaldetail.do?article\\_seq=20769&tabname=abst&resource\\_seq=-1&keywords=null](http://central.oak.go.kr/journalist/journaldetail.do?article_seq=20769&tabname=abst&resource_seq=-1&keywords=null)

**94. Ablikim, M., Achasov, M. N., Ai, X. C., Albayrak, O., Albrecht, M., Ambrose, D. J., ...& Ferroli, R. B. (2016). Measurements of the center-of-mass energies at BESIII via the di-muon process. *Chinese physics C*, 40(6), 063001.**

**ABSTRACT:**

From 2011 to 2014, the BESIII experiment collected about 5 fb<sup>-1</sup> data at center-of-mass energies around 4 GeV for the studies of the charmonium-like and higher excited charmonium states. By analyzing the di-muon process  $e^+e^- \rightarrow \gamma \text{ISR/FSR} \mu^+ \mu^-$ , the center-of-mass energies of the data samples are measured with a precision of 0.8 MeV. The center-of-mass energy is found to be stable for most of the time during data taking.

**Web URL:** <http://iopscience.iop.org/article/10.1088/1674-1137/40/6/063001/meta>

**95. Farooq, R., Jabeen, G., Siddique, M., Shaukat, S. F., & Rehman, S. U. Bioelectrochemical Reduction of Carbon Dioxide to Organic Compounds 2.**

**ABSTRACT:**

The present study demonstrates bioelectrochemical reduction of inorganic carbon dioxide to organic compounds using 6 *SporomusaOvata* in a tube shaped bioelectrochemical cell (BEC). Among biosynthesized products acetate, ethanol, n-butyric acid and iso- 7 pentanoic acid, 142.9 mg/L of acetate produced in 72 hours. This increase in acetate yield is attributed to improved parameters adopted 8 during reactor design. Average bioelectrochemical acetate synthesis rate was found to be  $1.3 \pm 0.67 \text{ mgL}^{-1} \text{ h}^{-1}$ . Cyclic voltametric study 9 confirmed redox activity of *S.Ovata* on poised biocathode. The percentage electron recovery as total organic compounds is found to be in 10 the range of  $84 \pm 13\%$  to  $65 \pm 11\%$ . The second major product is ethanol, formed by the conversion of acetaldehyde into ethanol. The 11 presence of ethanol assumed to be due to electro activity and metabolic shift from acetate to ethanol in the biochemical-producing *S.Ovata* 12 in BEC. The current research opens up the prospects of improving processes for bioelectrosynthesis of electron dense organic compounds 13 from renewable energies and waste greenhouse gases instead of synthesizing them from non-renewable and energy rich compounds.

**Web URL:** <https://www.ijser.org/researchpaper/Bioelectrochemical-Reduction-of-Carbon-Dioxide-to-Organic-Compounds.pdf>

# DEPARTMENT OF HUMANITIES

## Journal Papers

1. Gulzar, S., Fatima, S., & Shahzad, S. (2016). Indigenous Parent Child Communication Gap Scale. *International Journal for Social Studies*, 2(4), 68-76.

**ABSTRACT:**

Our first human relations and interactions are extremely important for human beings. Infant attachment set profound effect on the later development of the child. Across the life span, relationship contributes to the development of the children but the most important one is the interaction with the parents (Brent, 2010). Parents and their children hold a special relationship with each other. The relationship between parents and their children have a great effect on the child's life. This is a special relationship that has a huge effect on the way that the child will turn out. This relationship is formed through love, disappointment, and discipline. Parenting requires a great deal of adaptation. The parents want to develop a strong bond with their child but they also want to maintain a healthy relationship among themselves along with their other friendships. Through life, the bond between a child and parent will grow and expand in many ways. Whether the child makes mistakes or not the parent can't help but love their child unconditionally (Meng Pei, 2011). The origin of the child-parent conflict is the development of parental neglect or parental dominance. The researches have declared that parental detachment often leads to juvenile delinquency. Neglect or dominance on the part of the individual parent may not necessarily be derived from the cultural ideals, but such behavior may be part of the social situation and the mores in which he finds the origin of the child-parent conflict is the development of parental neglect or parental dominance (Nebel- Schwalm, 2006). Noller (1994) found that family relationships remain important throughout adolescence. In families where relationships are seriously attenuated, however, peer influence surges and adolescents are at greater risk for adjustment problems. And all the risk is due to the communication gap between the child and parent. And this gap can just ruin the whole life and development of the child (Fulgini & Eccles, 1993; Sheppard, Wright, & Goodstadt, 1985). Sons

and daughters report more conflict with their mothers than their fathers, and daughters report more intense conflict than sons (Allison & Schultz, 2004). Topics of conflict between parents and adolescents tend to revolve around issues of daily living, such as chores, hygiene, and homework, rather than issues such as smoking, alcohol, and sex (Smetana, 1988; Collins, 1998; Noller, 1994). Parenting Styles are typically defined along three dimensions: behavioral control (e.g., monitoring), psychological control (e.g., intrusiveness, demandingness), and parental support (e.g., warmth, acceptance, responsiveness) (Baumrind, 1966).

**Web**

[https://www.researchgate.net/profile/Saleha\\_Fatima2/publication/302092547\\_Indeginous\\_Parent-Child\\_Communication\\_Gap\\_Scale/links/572e2f5f08ae7441518f40d3.pdf](https://www.researchgate.net/profile/Saleha_Fatima2/publication/302092547_Indeginous_Parent-Child_Communication_Gap_Scale/links/572e2f5f08ae7441518f40d3.pdf)

**2. Ejaz, H. (2016). Relationship between Language and Culture. *International Journal for Social Studies*, 2(6), 75-81.**

**ABSTRACT:**

The relationship between language and culture is as old as mankind. Through the centuries, people and their living practices have evolved, resulting in wide-reaching changes in societal culture. This in turn, has influenced language to be what it is today.

**Web URL:** <https://edupediapublications.org/journals/index.php/IJSS/article/view/4719/4555>

**3. Bari, S. Subversive Resurrection-Perpetuation of Exploitation exposed by the Motif of Knock in Shahid Nadeem's The Third Knock.**

**ABSTRACT:**

This paper intends to study the representation of exploitation of the weak in Shahid Nadeem's play "The Third Knock". Nadeem employs the theme of resurrection to present the plight of poor and weak. Nadeem shows that how the poor has to go through repetitive oppression at the hands of the powerful and are deprived of their rights. Nadeem's skillful use of the concept of resurrection and the use of the metaphor of 'knock' highlights the corruption and power play victimizing the weak in our society.

**Web URL:** [http://www.ijee.org/yahoo\\_site\\_admin/assets/docs/2\\_Shumaila\\_Bari.0232739.pdf](http://www.ijee.org/yahoo_site_admin/assets/docs/2_Shumaila_Bari.0232739.pdf)

**4. Fatima, S., & Sheikh, H. (2016). Adolescent aggression as predicted from parent–child relationships and executive functions. *American Journal of Psychology*, 129(3), 283-294.**

**ABSTRACT:**

Previous research has emphasized the role of parent–child relationships (PCRs) in child and adolescent development. The present study extends the previous findings by examining the direct and mediated relationship between PCRs, executive functioning (EF), and adolescent aggression. Five hundred twelve adolescents of South Asian ethnic background, enrolled at the secondary and higher secondary levels (aged 13–19 years; 50% boys), participated in the study. The Parent–Child Relationship Scale (Rao, 2000), Aggression Scale (Mathur & Bhatnagar, 2004), and four tests from the Delis–Kaplan Executive Function System (Delis, Kaplan, & Kramer, 2001) were administered to measure the perceived quality of PCR, level of aggression, and EF, respectively, in participants. Pearson correlation coefficients revealed that perceived PCRs were related to EF and adolescent aggression among South Asian youth. Furthermore, multiple regression analyses using Baron and Kenny's (1986) guidelines showed that the influence of PCRs on aggression was partially mediated by EF. The findings suggest that PCRs and EF can be important factors to focus on in interventions aimed at preventing adolescent aggression in society.

**Web URL:**

[http://www.jstor.org/stable/10.5406/amerjpsyc.129.3.0283?seq=1#page\\_scan\\_tab\\_contents](http://www.jstor.org/stable/10.5406/amerjpsyc.129.3.0283?seq=1#page_scan_tab_contents)

**5. Fatima, S., Mehfooz, M., & Sharif, S. (2016). Role of Islamic Religiosity in Predicting Academic Motivation of University Students.**

**ABSTRACT:**

Previous research in the last 2 decades describes the connection between religiosity and academic outcomes, particularly in Christian samples. The present study was designed to find out the role of Islamic religious beliefs, practices, and positive religious coping in predicting academic motivation above and beyond the effects of demographic and academic-related factors among Muslim university students. Participants were 299 university students (mean age

= 19.35 years,  $SD = 3.21$ , 68% males) registered under different undergraduate programs. They were assessed on the Islamic Beliefs, Islamic Religious Duty and Obligation, and Islamic Positive Religious Coping and Identification subscales as well as the Global Religiousness scale from the Psychological Measure of Islamic Religiosity. In addition, the Academic Motivation Scale was also administered to assess 3 intrinsic motivation outcomes, 3 extrinsic motivation outcomes, and amotivation. The results showed a significant incremental variance due to a differential contribution of religiosity factors over the demographic and academic factors in predicting type of academic motivation. Nevertheless, the number of siblings and current semester remained significant predictors of academic motivation even in the presence of other stronger predictors. However, moderation analysis showed an interaction effect of semester only in predicting intrinsic motivation to know and to accomplish things and extrinsic motivation of external regulation. It was worth noting that the religiosity level of students was more weakly correlated with extrinsic motivation of external regulation than it was with other motivation constructs of intrinsic and extrinsic motivation. (PsycINFO Database Record (c) 2016 APA, all rights reserved)

**Web URL:** <http://psycnet.apa.org/record/2016-37954-001>

**6. Zubair, M. (2016).** Legislative and No Legislative Verbal Sunnah: An Analytic Study. Sheikh Zayed Islamic Center, University of Karachi, Karachi

#### **Not Found**

**7. BAIG, M. M. Z., & AHMAD, M. M. Learning with a Style: The Role of Learning Styles and Models in Academic Success.**

#### **ABSTRACT:**

The researchers have carried out an extensive review of research on learning styles to develop understanding of the main learning styles with their associated models and theorists. The paper studies the primary learning personality types which offer insights for the educationists and theorists to transform the approach to pedagogy by contextualizing the taught. The learners show strengths for varying sensory modalities and adapt themselves to an individual or a mix of learning approaches with the passage of time. The researchers discuss the implications of these learning styles and models for the teaching and learning to suggest if the teaching community

frames into view the particular type of students with respect to their learning habits and preferences, learning can improve and a shift may take place in teaching practices to differentiated pedagogy vis-a-vis differentiated learners. The critical review of learning style and models is likely to benefit the classroom practitioners, policymakers and research community.

**Web**

**URL:**[https://www.researchgate.net/profile/Mirza\\_Zubair\\_Baig/publication/310844037\\_Learning\\_with\\_a\\_Style\\_The\\_Role\\_of\\_Learning\\_Styles\\_and\\_Models\\_in\\_Academic\\_Success/links/5839d77508aef00f3bfbbcbe.pdf](https://www.researchgate.net/profile/Mirza_Zubair_Baig/publication/310844037_Learning_with_a_Style_The_Role_of_Learning_Styles_and_Models_in_Academic_Success/links/5839d77508aef00f3bfbbcbe.pdf)

**8. BAIG, M. M. Z., & AHMAD, M. M. Learning with a Style: The Role of Learning Styles and Models in Academic Success.**

**ABSTRACT:**

The researchers have carried out an extensive review of research on learning styles to develop understanding of the main learning styles with their associated models and theorists. The paper studies the primary learning personality types which offer insights for the educationists and theorists to transform the approach to pedagogy by contextualizing the taught. The learners show strengths for varying sensory modalities and adapt themselves to an individual or a mix of learning approaches with the passage of time. The researchers discuss the implications of these learning styles and models for the teaching and learning to suggest if the teaching community frames into view the particular type of students with respect to their learning habits and preferences, learning can improve and a shift may take place in teaching practices to differentiated pedagogy vis-a-vis differentiated learners. The critical review of learning style and models is likely to benefit the classroom practitioners, policymakers and research community.

**Web URL:**

[https://www.researchgate.net/profile/Mirza\\_Zubair\\_Baig/publication/310844037\\_Learning\\_with\\_a\\_Style\\_The\\_Role\\_of\\_Learning\\_Styles\\_and\\_Models\\_in\\_Academic\\_Success/links/5839d77508aef00f3bfbbcbe.pdf](https://www.researchgate.net/profile/Mirza_Zubair_Baig/publication/310844037_Learning_with_a_Style_The_Role_of_Learning_Styles_and_Models_in_Academic_Success/links/5839d77508aef00f3bfbbcbe.pdf)

**9. Fatima, S., & Sharif, I. (2016). Executive functions, parental punishment, and aggression: Direct and moderated relations. *Social neuroscience*, 1-13.**

**ABSTRACT:**

The main focus of the current study was to assess whether executive functions (EFs) moderate the effect of parental punishment on adolescent aggression. The sample were 370 participants (53% girls, 47% boys) enrolled at secondary and higher secondary levels and ranged in age between 13–19 years ( $M = 15.5$ ,  $SD = 1.3$ ). Participants were assessed on a self-report measure of aggression and two punishment measures, in addition to a demographic sheet. Then, they were individually assessed on four tests taken from the Delis–Kaplan Executive Functions System (DKEFS) namely Trial Making Test (TMT), Design Fluency Test (DFT), Color Word Interference Test (CWIT), and Card Sorting Test (CST) to assess cognitive flexibility, nonverbal fluency, inhibition, and problem-solving ability, respectively. Correlation coefficients indicated that all four executive functioning measures and the two punishment measures were significantly correlated with aggression. Moderation analysis indicated that all EFs moderated the relationship between physical punishment and aggression, and only inhibition and problem-solving ability, but not cognitive flexibility and nonverbal fluency, moderated the relations between symbolic punishment and aggression. The findings support the hypothesis that EFs are protective personal factors that promote healthy adolescent adjustment in the presence of challenging environmental factors.

**Web URL:**

<http://www.tandfonline.com/doi/pdf/10.1080/17470919.2016.1240710?needAccess=true>

**10. Suyfan, S., & BAIG, M. M. Z (2016). An apology for the Misrepresentation of Muslim Women in Tariq Ali’s The Stone Woman.**

**ABSTRACT:**

The purpose of this paper is to explore the representation of Muslim women in Tariq Ali’s novel The Stone Woman in which the writer gives sexual freedom to Muslim women on purpose. The present paper questions if the writer is truly representing the Muslim society, role of a Muslim woman in it and her rights or appropriating the social transgressions as appropriation for

'modernized' Islam. The textual analysis of the novel shows that the writer is toeing the line of Eurocentric approach that furthers stereotypical images of Muslim women and misrepresents their sexual life and freedom as transgressive contrary to their religion and society.

**Web URL:**

[https://www.researchgate.net/profile/Mirza\\_Zubair\\_Baig/publication/306230623\\_An\\_apology\\_for\\_the\\_misrepresentation\\_of\\_Muslim\\_women\\_in\\_Tariq\\_Ali's\\_The\\_Stone\\_Woman/links/57b6f27c08ae9fdf82ef19c4.pdf](https://www.researchgate.net/profile/Mirza_Zubair_Baig/publication/306230623_An_apology_for_the_misrepresentation_of_Muslim_women_in_Tariq_Ali's_The_Stone_Woman/links/57b6f27c08ae9fdf82ef19c4.pdf)

**11. Khalid, M., & BAIG, M. M. Z (2016). Patriarchal Consumerism: Critical Discourse Analysis of Pakistani Gendered TVCs. *Language in India*, 16(8).**

**ABSTRACT:**

TV Commercials (TVCs), a popular part of invasive advertisement culture, where play an important role in the promotion of consumerist ideology embedded in the language and visuals, the advertisers use innovative techniques to promote popular gender-specific ideology to persuade the targeted consumers and maximize the sale and profit of the product. The present study selects sample of 6 Pakistani TVCs and applies Fairclough's three dimensional model of Critical Discourse Analysis (CDA) to analyze how the T.V ads encourage stereotypical images of men and women. At the end, it is suggested that TVCs should promote gender equality by deconstructing and revising the patriarchal assumptions about women

**Web URL:** <http://languageinindia.com/aug2016/maryapatriarchalconsumerism.pdf>

**12. BAIG, M. M. Z. (2016). Book Review of Through White Noise: Autonarrative Exploration of Racism, Discrimination and the Doorways to Academic Citizenship in Canada. *NUML Journal of Critical Inquiry***

**ABSTRACT:** Not Found

**Web URL:**

**13. BAIG, M. M. Z., & AHMAD, M. M.(2016). Learning with a Style: The Role of Learning Styles and Models in Academic Success. *EUROPEAN ACADEMIC RESEARCH*. 4(8).**

**ABSTRACT:**

The researchers have carried out an extensive review of research on learning styles to develop understanding of the main learning styles with their associated models and theorists. The paper studies the primary learning personality types which offer insights for the educationists and theorists to transform the approach to pedagogy by contextualizing the taught. The learners show strengths for varying sensory modalities and adapt themselves to an individual or a mix of learning approaches with the passage of time. The researchers discuss the implications of these learning styles and models for the teaching and learning to suggest if the teaching community frames into view the particular type of students with respect to their learning habits and preferences, learning can improve and a shift may take place in teaching practices to differentiated pedagogy vis-a-vis differentiated learners. The critical review of learning style and models is likely to benefit the classroom practitioners, policymakers and research community.

**Web URL:**

[https://www.researchgate.net/profile/Mirza\\_Zubair\\_Baig/publication/310844037\\_Learning\\_with\\_a\\_Style\\_The\\_Role\\_of\\_Learning\\_Styles\\_and\\_Models\\_in\\_Academic\\_Success/links/5839d77508aef00f3bfbbcbe.pdf](https://www.researchgate.net/profile/Mirza_Zubair_Baig/publication/310844037_Learning_with_a_Style_The_Role_of_Learning_Styles_and_Models_in_Academic_Success/links/5839d77508aef00f3bfbbcbe.pdf)

**14. Fatima, S., Sheikh, H., & Ardila, A. (2016). Association of parent–child relationships and executive functioning in South Asian adolescents. *Neuropsychology*, 30(1), 65.**

**ABSTRACT:**

It is known that some environmental variables can significantly affect the development of executive functions (EF). The primary aim of this study was to analyze whether some family conditions, such as the adolescent’s perception of the quality of parent–child relationships and the socioeconomic status (SES; assessed according to education, occupational status, and income) are significantly associated with EF test scores. Methods: There were 370 Pakistani participants ranging in age 13 to 19 years who were selected and then individually administered the following tests taken from the Delis–Kaplan Executive Function System (D–KEFS): Trail Making Test (TMT), Design Fluency Test (DFT), Color Word Interference Test (CWIT), and Card Sorting Test (CST). In addition, a Parent–Child Relationship Scale (PCRS) also was administered.

Results: Results showed that perceived “neglect” in the PCRS was negatively associated with the 4 EF test scores. Parents’ education and SES were positively associated with 3 EF measures: DFT, CWIT, and CST. Further correlational analyses revealed that inhibition (as measured with the CWIT) and problem-solving ability (as measured with the CST) were significantly associated with the perceived parent– child relationships. Some gender differences also were observed: males outperformed females on TMT, DFT, and CST, while females outperformed males in the CWIT. Conclusion: It was concluded that perceived parent– child relationships, SES, and parents’ education are significantly associated with executive function test performance during adolescents.

**Web URL:**

[https://www.researchgate.net/profile/Alfredo\\_Ardila/publication/277893581\\_Association\\_of\\_Parent-Child\\_Relationships\\_and\\_Executive\\_Functioning\\_in\\_South\\_Asian\\_Adolescents/links/5642f4b908aec448fa62bb52.pdf](https://www.researchgate.net/profile/Alfredo_Ardila/publication/277893581_Association_of_Parent-Child_Relationships_and_Executive_Functioning_in_South_Asian_Adolescents/links/5642f4b908aec448fa62bb52.pdf)

**15. AmmadulHaq, M. (2016).**

ماں ٹلاو طو ونگلوک کے سجا حرقی واد استنادی اقتصادات

**Not Found**

**ABSTRACT:**

**Web URL**

**16. Mehfooz, M. (2016). A Rhetorical Analysis of Figures of Speech of simile, analogy and metaphor in Asrār al-Balāghah, by ‘Abd al-Qāhir Al-Jurjānī. AL-Qalam Journal, Islamic Department University of Punjab,**

**ABSTRACT: Not Foud**

**Web URL:**

**17. Ashraf, R, Azia,S. (2016). Recurrence of Romantic Aesthetics in Classicist Writings: A Survey of British Classical Poetry. Elixir Literature 96 , 41786-41789.**

**ABSTRACT:** Traditionally, classicism and romanticism are conceived as peculiar and mutually exclusive literary movements with distinct literary styles and stylistic characteristics. This paper

aims to trace some prominent writing traits of the Romantic era like spontaneity, preoccupation with imagination and subjectivity and focus on highlighting emotions and feelings in poetry as evident in the works of poets writing before the Romantic era. A close examination and in-depth reading of selected works showed that romantic traits are not confined to the Romantic era only but also appear to be recurring in the writings of Chaucer, Spenser and other poets who were writing much before Wordsworth proposed the characteristics of romantic poetry in *The Prelude*. This study, therefore, traces romantic traits in the works that do not fall into romantic era chronologically.

**Web URL:**

[https://www.researchgate.net/publication/305789566\\_Recurrence\\_of\\_Romantic\\_Aesthetics\\_in\\_Classicist\\_Writings\\_A\\_Survey\\_of\\_British\\_Classical\\_Poetry](https://www.researchgate.net/publication/305789566_Recurrence_of_Romantic_Aesthetics_in_Classicist_Writings_A_Survey_of_British_Classical_Poetry)

**18. Aziz, S., Naveed, A., & Mahfooz, M. (2016). FAMILY LIFE IN THE LIGHT OF QUR'ANIC METAPHORS. *Gomal University Journal of Research*, 32(1).**

**ABSTRACT:**

The present study explores the delicate Qur'anic metaphors related to the teachings on family life. The Quran is said to be a code of life for man. This study sets out to explore the guidelines related to family life, the basic unit of a society and human civilization, provided through metaphors in the Qur'an. It attempts to analyze those metaphors in depth in order to inform humans in different roles in a family set up as this fulfilling the duties related to these roles is the foundation of a balanced household which in turn is a fundamental unit of society. Moreover, it tries to relate the thin lined difference between metaphor, simile, and analogy through examples.

**Web URL:**

[https://www.researchgate.net/profile/Amna\\_Naveed/publication/306065365\\_Family\\_life\\_in\\_the\\_light\\_of\\_Qur'anic\\_Metaphors/links/57b14e9308ae0101f1794bdd.pdf](https://www.researchgate.net/profile/Amna_Naveed/publication/306065365_Family_life_in_the_light_of_Qur'anic_Metaphors/links/57b14e9308ae0101f1794bdd.pdf)

**19. Sheikh, U., & Naveed, A. (2016). THE IMPACT OF HR PRACTICES ON THE PERFORMANCE OF MULTINATIONAL COMPANIES OPERATING IN PAKISTAN. *Gomal University Journal of Research*, 32(1).**

**ABSTRACT:**

Multinational companies have always been ready to offer Fast Moving Consumer Goods (FMCG) in developed and under developed countries. They always focus on rapid expansion through employee performance. The current study is quantitative in nature and examines the function of human resource management and implication of its practices (including: performance appraisal, career planning, employee participation, job definition, compensation, selection and performance as perceived by the respondents) and its effects on employee performance. For the current study a closed ended questioner was used to collect the data. Respondents from (Nestle & Unilever Pakistan) were given Likert scale based survey questioners. Data was analyzed by using descriptive statistics correlation & regression method to find relationship between independent and dependent variables i.e. performance appraisal, career planning, employee participation, job definition, compensation, selection and performance as perceived by the respondents.

**Web URL:**

<http://web.b.ebscohost.com/abstract?direct=true&profile=ehost&scope=site&authtype=crawler&jrnl=10198180&AN=117769162&h=emhIXuoTrHISAovsl%2f2iPVLiBxf6pnNzy%2fXwMnXour4eccgNhoXWFCCXEOH3WWcGqQedUOBCbv6VEc6y0sYDJw%3d%3d&crl=c&resultNs=AdminWebAuth&resultLocal=ErrCrlNotAuth&crlhashurl=login.aspx%3fdirect%3dtrue%26profile%3dehost%26scope%3dsite%26authtype%3dcrawler%26jrnl%3d10198180%26AN%3d117769162>

**20. Jahangir, M. (2016). Common grammatical mistakes in ESL essay writing: A Case study of COMSATS Lahore Undergraduates. EUROPEAN ACADEMIC RESEARCH. 4(4)**

**ABSTRACT:**

English language has a sound, complex grammar and ESL learners face difficulties in application of these grammatical rules while writing essays. This paper highlights the major errors that Pakistani students make during the process of learning English as a second language and some

reasons which hinder the process of learning and even hinder their academic and writing growth. The major focus is on undergraduate students at the beginning of writing creatively with less exposure to English language and grammar. It is observed that students try to learn grammatical rules and can learn them in isolation but when it comes to their own writing, they fail to apply these rules in their compositions. This study presents most common errors in undergraduate students' essay writing and discusses them in the context of L1 interference, more rote learning and less reading habit. The participants were 200 undergraduate students of first semester at COMSATS Lahore. A questionnaire was used to examine the perceptions of students. The result clearly shows that ESL learners make major errors related to subject-verb agreement, tenses and articles. This study gives implications for further research to find the reasons of these errors and students' inability of grammar application in their essay writing

**Web URL:** <http://euacademic.org/UploadArticle/2688.pdf>

**21. Ejaz, H.(2016). Examining internal structure of Discourse Completion Test (DCT) on Arabic Learners of English. Review of Arts and Humanities. 5(1).**

**ABSTRACT:**

This study aims at finding out whether Arabic learners of English (Emarati Females in particular) produce target-like compliment responses in English and whether pragmatic transfer can occur. Discourse completion tests (DCTs) and interviews were used to study the strategies employed when responding to compliments by native speakers (NSs) and Arabic non-native speakers (NNSs) of English. Findings suggest that Arabic (L1) expressions and strategies were sometimes transferred to English (L2). This study also indicates that Emarati female learners of English transfer some of their L1 pragmatic norms to L2 because they perceive these norms to be universal among languages rather than being language specific. It also indicates that Arabic NNSs of English have some misconceptions about NSs that affect the way they respond to their compliments. Some important cultural and pedagogical implications are discussed at the end of the paper.

**Web URL:** <http://rah-net.com/journals/rah/Vol 5 No 1 June 2016/7.pdf>

**22. Ejaz, H. (2016). Curriculum Design and Its Implications. *International J. Soc. Sci. & Education. 6(4).***

**ABSTRACT:**

One of the most important objectives of the education is the socialization of the individual. School is a social agency, which is entrusted with the task of transmitting the cultural and social values to the coming generations. Curriculum is such a tool used by the school to achieve this objective. Therefore, revision and improvement in curriculum is necessary for making provision for the challenges and demands of the society. In this study, the focus of attention is on curriculum design, as an integral part of the larger view of the educational planning. It also examines the present state of the secondary level curriculum of English language in Pakistan. The general principles of curriculum design and its implications on the language teaching methodology will be discussed in chapter one. It will also include a discussion on various curriculum design models and their implementation. It will also explore the notion of communicative competence, which is now considered as imperative for an English medium student of secondary student to develop and acquire.

**Web URL:** <http://ijsse.com/sites/default/files/issues/2016/v6i4/Paper-05.pdf>

**23. Shahzad, A. K., Shaheen, H. & Saleem Sumaira. (2016). Impact of English Monolingual Dictionaries on ESL Learners' Reading Comprehension and Vocabulary Building. EUROPEAN ACADEMIC RESEARCH. 4(5).**

**ABSTRACT:**

The study aimed to investigate the impact of English monolingual dictionary on learners' performances in reading comprehension and vocabulary learning. The subjects were advance learners from Govt. Girls College, Vehari whose average age was 18 years old. The subjects in the experiment were randomly divided into two groups: the group who solved the test with the help of dictionary named as Achievers, and the group who solved the comprehension test without using dictionary named as non-achievers. The instruments used for collecting data were a questionnaire and a reading comprehension test. The data were statistically analyzed in terms of mean and standard deviation. The findings of this research would let us know that

consulting dictionary during the test had a significantly positive effect on the subjects' performances in reading comprehension and vocabulary learning. Asma Kashif Shahzad, Hina Shaheen, Sumaira Saleem- Impact of English Monolingual Dictionaries on ESL Learners' Reading Comprehension and Vocabulary Building

**Web URL:** <http://euacademic.org/UploadArticle/2727.pdf>

**24. BAIG, M. M. Z.(2016). His/Her Man Friday: Re-righting/-writing of an inaccessible cannibal in J.M. Coetzee's Foe. Kashmir Journal of Language Research (KJLR)**

**ABSTRACT: Not found**

**Web URL:**

**25. Bari, S., Abbas, F. (2016). Online Harassment - A Study of its Sources, Intensity and Psychological Impact on Students. EUROPEAN ACADEMIC RESEARCH. 4(5).**

**ABSTRACT:**

Online harassment is an online or Internet-based illegal act of threatening or humiliating someone. The problem of adolescent Online harassment has increased with easy access of technology. Though bullying still occurs in the traditional form of face-to-face contact, Online harassment is becoming more common as youth have more access to the Internet, cameras, and text messaging via cell phones. Online harassment has many of the same effects on its victims such as lower academic achievement and depression

**Web URL:** <http://euacademic.org/UploadArticle/2717.pdf>

**26. Bari, S., Ajmal S. (2016). The First Flight; Acquisition of Urdu Consonants in Native Children. International Journal of English and Education. 5(4)**

**ABSTRACT:**

Urdu is a language which is spoken by more than 100 million people across the world. But, unfortunately, no substantial work has been done on the acquisition of Urdu language in children. For the first time, this paper focuses on children's acquisition of Urdu consonants. The children selected for the study were 6 to 30 months old. The paper also discusses the difference in acquisition of Urdu consonants in both the genders, male and female, of this age group. This

study establishes the idea that children (male and female) learn Urdu language differently as the girls were found having acquired more consonants as compared to boys.

**Web URL:** [http://www.ijee.org/yahoo\\_site\\_admin/assets/docs/4.28103625.pdf](http://www.ijee.org/yahoo_site_admin/assets/docs/4.28103625.pdf)

**27. Fatima, S., & Sheikh, H. (2017). Moderators of Association between Adolescent's reports of Parent-child Relationship and Adolescent Aggression. *FWU Journal of Social Sciences*, 11(1), 82.**

**ABSTRACT:**

The primary focus of the present study was to determine the impact of parent-child relationships (PCR) on adolescent aggression as moderated by adolescent and parent gender, and socioeconomic status of parental family. Five hundred and twelve participants (males = 257, females = 255) enrolled at secondary and higher secondary levels ranging in age between 13-19 years ( $M = 15.5$ ,  $SD = 1.3$ ) were selected as the test sample. Self reported measures of socioeconomic status scale, parent-child relationship scale (Rao, 2000), and aggression scale (Mathur & Bhatnagar, 2004) were administered respectively, to measure the quality of PCR, level of aggression, and socioeconomic status in participants. Multiple regression analysis showed that the influence of PCR on aggression was moderated by adolescent and parent gender but socioeconomic status did not moderate the link. More specifically, the PCR was more strongly related to adolescent aggression for boys than for girls

**Web URL:**

<https://search.proquest.com/openview/5c07a296fbb93fad2069c835374de0fc/1?pq-origsite=gscholar&cbl=55194>

# AUTHOR INDEX

---

**A**

- A., Ullah** · 159, 217, 237  
**Abbas, F** · 293  
**Abbas, G.** · 78, 79, 80, 85, 102, 237  
**Abbas, K.** · 29, 30  
**Abbas, M.** · 77  
**Abbas, N.,** · 59  
**Abbas, Q.** · 9, 15  
**Abbas, S.** · 143, 149  
**Abbasi, A. S.** · 26, 27, 28  
**Abdullah, M. A.** · 65, 66  
**Abdullah, M. I.** · 34, 35  
**Abid, A.** · 150  
**Abid, K.** · 150  
**Abid, M.** · 100, 106  
**Abid, S. A.** · 146  
**Ablikim, M** · 224, 225, 227, 251, 252, 255, 256, 257, 277  
**Abosedra, S.** · 18  
**Abro, R.** · 47  
**Achasov, M. N.** · 224, 225, 227, 251, 252, 255, 256, 257, 277  
**Adeel Umer, M.** · 44  
**Afaq, A.** · 214  
**Afza, T.** · 15, 25  
**Afzal, A.** · 177  
**Afzal, H.** · 146  
**Afzal, M.** · 220, 254  
**AGARWAL, R. P.** · 104  
**Ahad, M.** · 25  
**Ahmad, A.** · 29, 66, 108, 156  
**Ahmad, E.** · 234  
**Ahmad, F.** · 57, 58, 140, 145, 147, 150, 151, 222  
**Ahmad, I.** · 230, 232, 248, 275  
**Ahmad, J.** · 198  
**Ahmad, M.** · 46, 115, 201, 216, 220, 223, 230, 232, 261, 267, 270, 276  
**AHMAD, M. M** · 283, 284, 287  
**Ahmad, M. S.** · 46  
**Ahmad, P.** · 155, 161, 167, 179, 188  
**Ahmad, R.** · 51, 190  
**Ahmad, S.** · 5, 70, 71, 72, 112, 113, 140, 164  
**Ahmad, S.,** · 5, 70, 72, 112, 113, 164  
**Ahmad, U.** · 70, 113  
**Ahmad, Y.** · 79  
**Ahmad, Z.** · 41, 51, 61  
**Ahmada, M.** · 228  
**Ahmadinia, A.** · 120, 125  
**Ahmed, A.** · 235  
**Ahmed, E.** · 157  
**Ahmed, J.** · 134  
**Ahmed, K.** · 15, 17, 21, 136, 143, 186  
**Ahmed, M. A.** · 44, 67  
**Ahmed, R.** · 217  
**Ahmed, S.** · 243, 251, 252, 256  
**Ahn, S.** · 277  
**Ahsan, M.** · 219, 235  
**Ahsan, Z.** · 218  
**Ai, X. C.** · 224, 225, 227, 251, 252, 255, 256, 257, 277  
**Airoidi, C.** · 186, 187  
**Ajmal S.** · 294  
**Akhtar, M. A.** · 53  
**Akhtar, M. N.** · 220, 222, 223, 230, 248, 261, 267, 270, 272  
**Akhtar, S.** · 201

- Akhtara, M. N.** · 228  
**Akhter, P.** · 49  
**Akram, M.** · 82, 83  
**Akram, N.** · 217  
**Akram, W.** · 33  
**Al Kaisy, G. M.** · 204  
**Alam, M. S.** · 15, 36  
**Albayrak, O.** · 224, 225, 227, 251, 252, 255, 256, 257, 277  
**Albrecht, M.** · 224, 225, 227, 251, 252, 255, 256, 257, 277  
**Aleem, U.** · 206  
**Ali Hassan, S. M.** · 80  
**Ali, A.** · 38, 134, 144, 191, 202, 213, 217, 223, 231, 273, 274  
**Ali, F.** · 102  
**Ali, G.** · 83  
**Ali, H.** · 83, 244  
**Ali, J.** · 119, 240  
**Ali, K.** · 68, 69, 77  
**Ali, M.** · 62, 126, 243  
**Ali, N.** · 80  
**Ali, S. A.** · 11, 30  
**Ali, S. M.** · 127, 128  
**Ali, Z.** · 48, 49  
**Alia, A.** · 228  
**Alia, I.** · 76  
**Alonso, G. A.** · 189  
**Alvi, F.** · 235  
**Ambrose, D. J.** · 224, 225, 227, 252, 255, 257, 277  
**Amed, E.** · 271  
**Amin, G.** · 129  
**Amin, M. B.** · 91, 101  
**Amin, N.** · 239, 254, 273, 275, 276  
**Amin, Y. M.** · 161, 179, 188  
**Amir, H.** · 12  
**Amir-ud-Din, R.** · 10  
**Amjad, R. J.** · 249, 250, 270  
**Amjed, N.** · 238  
**AmmadulHaq, M.** · 288  
**Andreescu, S.** · 165, 168  
**Angelov, P.** · 142  
**Anjum, S.** · 212, 246, 247, 271  
**Ansari, E. A.** · 121  
**Ansari, M. M.** · 214  
**Anwar, H.** · 276  
**Anwar, M. S.** · 122, 131  
**Anwar, T.** · 201  
**Ardila, A.** · 287  
**Areeb, F.** · 216  
**Arjmandi, R.** · 52  
**Arshad, A.** · 244  
**Arshad, F.** · 119, 240  
**Arshad, M. I.** · 273, 275, 276  
**Arshad, S.** · 86  
**Arshad, Z.** · 139  
**Asghar, A.** · 209  
**Asghar, K.** · 139  
**Asghar, S.** · 30  
**Ashfaq Butt, T.** · 63  
**Ashfaq, A.** · 247  
**Ashfaq, M.** · 43  
**Ashfaq, T.** · 62  
**Ashraf, A.** · 74  
**Ashraf, F.** · 55, 181  
**Ashraf, M. W.** · 229  
**Ashraf, R.** · 289  
**Ashraf, S.** · 78  
**Asif, M.** · 116, 117, 231, 238  
**Asif, M. R.** · 116, 117  
**Asim, S.** · 207  
**Aslam, M.** · 51, 118, 222, 238  
**Aslam, N.** · 264  
**Aslam, S.** · 216  
**Athar, A.** · 143, 149

**Atif, M.** · 197, 229, 243, 253, 257

**Atifc, M.** · 228

**Atiq, S.** · 177

**Awais, M. N.** · 118, 130

**Awan, M. S.** · 271

**Azam, A.** · 276

**Azam, M.** · 9, 121

**Azam, S.** · 216

**AZEEM, F.** · 40

**Azhar, N.** · 90, 92

**Azia, S.** · 289

**Azim, M.** · 275

**Azim, Q. A.** · 74

**Aziz, H. S.** · 158, 160

**Aziz, M. H.** · 257

**Aziz, S.** · 289

**AZMAN, K.** · 40

---

**B**

**Babar, M. E.** · 140

**Baca, M.** · 108

**Badea, M.** · 185

**Badshah, S.** · 162, 202

**Bai, J. Z.** · 251, 252, 256

**BAIG, M. M. Z** · 283, 284, 285, 286, 287, 293

**Baig, S.** · 116

**Bajda, M.** · 159, 193

**Bajwa, U. I.** · 147

**Bakar, A. A.** · 50

**Bakhsh, K.** · 33

**Bakina, O.** · 252

**Balaji, N.** · 277

**Bao, Z. N.** · 41

**Bari, S.** · 281, 293, 294

**Basheer, M. F.** · 34

**Bashir, M. A.** · 207

**Bashir, M. F.** · 228, 243, 262

**Bashir, Y.** · 87

**Batool, M.** · 171, 204

**Bazmi, A. A.** · 46, 47, 57, 58

**Bég, E. T.** · 80

**Bég, O. A.** · 72, 80

**Belich, M.** · 73

**BESIII** · 224, 225, 226, 227, 228, 251, 252, 253, 255, 256, 257, 278

**BESIII collaboration** · 226

**Bhand, S.** · 175, 200

**Bhattacharya, M.** · 38

**Bhatti, A. A.** · 99

**Bhatti, I.** · 57, 58

**Bhatti, M. K.** · 118, 122

**Bhatti, N. U. A.** · 198

**Bhrawy, A.** · 68

**Bhutto, A. W.** · 46, 47, 57, 58

**Bibi, S.** · 19

**Bidin, N.** · 262

**Bilal, M.** · 62, 63

**Biswasf, A.** · 73

**Brorsson, M.** · 122

**Brown, A. K.** · 114

**Bueno, D.** · 170, 178

**Bukhari, N.** · 46

**Bukhari, S. H.** · 216

**Bülbül, G.** · 165, 168

**Bustam, M. A.** · 167, 191, 194, 195, 203, 204

**Butt, M. S.** · 24

**Butt, N. S.** · 211

**Butt, S.** · 84, 89, 94, 97, 103, 104

**Butt, S. I.** · 84, 89, 103, 104

**BUTT, S. I.** · 104

---

**C**

**Cai, Y.** · 242

**Catanante, G.** · 160, 166, 173, 174, 175,  
178, 180, 184, 188, 196, 200  
**Chang, I. S.** · 42, 56  
**Chattopadhyay, S.** · 95  
**Chaudary, M. H.** · 148  
**Chaudhry, A. A.** · 171, 178, 192  
**Chaudhry, M. A.** · 237, 275  
**Chaudhry, M. T.** · 134  
**Cheemaa, N.** · 73, 105  
**Chema, I. Z.** · 77  
**Chen, G.** · 135  
**Chen, L.** · 135, 233, 236, 243, 262, 264  
**Chen, Y.** · 154, 173  
**Chighoub, F.** · 76  
**Choa, Y. H.** · 59  
**Choi, K. H.** · 131  
**Chun, Q.** · 116, 117  
**Clough, P.** · 138

---

**D**

**D. K. R Babajee** · 106  
**Damalas, C. A.** · 33  
**Danish, M.** · 198  
**de Camargo, A. S.** · 250  
**De Camargo, A. S. S.** · 249  
**Debnath, U.** · 102  
**Dew, L.** · 153  
**Dominic, P. D. D.** · 151  
**Dong, W.** · 220  
**Dousti, M. R.** · 249, 250, 270  
**Dur-e-Jabeen** · 106

---

**E**

**Ehsan, Z.** · 268, 269  
**Ejaz, H.** · 281, 291, 292  
**Elahi, A.** · 231, 274

**Elfimov, A. G.** · 228  
**Ellahi, M.** · 214, 267  
**Ellahi, R.** · 111

---

**F**

**Fakhar-e-Alam, M.** · 257  
**Fan, L.** · 242  
**Farah, N.** · 70  
**Farahani, M. R.** · 112  
**Fareed, M. S.** · 116  
**Farid, A.** · 215  
**Farid, M. T.** · 232, 275  
**Farkhondehfal, M. A.** · 49  
**Farooq, A.** · 82, 83, 163, 193  
**Farooq, E.** · 201  
**Farooq, M. S.** · 150  
**Farooq, R.** · 60, 61, 62, 65, 278  
**Farooq, U.** · 65, 118, 122, 130, 150, 201  
**Farooqc, W. A.** · 228  
**Fatima, M.** · 30, 257  
**Fatima, S.** · 280, 282, 285, 287, 294  
**Fatima, U.** · 61  
**Feng, W.** · 53, 197  
**Feroze, A.** · 197, 253  
**Ferroli, R. B.** · 224, 225, 227, 255, 257, 278  
**Fu, X.** · 198

---

**G**

**G.Abbas** · 242  
**Gao, Y.** · 155  
**Gardazi, S. M. H.** · 62  
**Ge, R.** · 155  
**Gebhardt, A.** · 206  
**Gencil, C.** · 133  
**Geng, Y. Y.** · 41  
**Ghazali, Z.** · 30

- Ghous, I. · 123, 124, 125  
 Gigliobianco, G. · 153  
 Gilani, A. H. · 167  
 Gilani, M. A. · 55, 157, 181, 182  
 Gilani, S. A. · 148  
 Gillani, A. · 207  
 Glogauer, M. · 183  
 Glower, J. · 128  
 Gobi, K. V. · 174, 184  
 Gonfa, G. · 191, 203  
 Goud, K. Y. · 174, 184  
 Grössinger, R. · 243  
 Gu, X. · 198, 263, 264  
 Gul, M. T. · 144  
 Gul, S. · 169, 194  
 Gull, N. · 191  
 Gulshan, F. · 95  
 Gulzar, S. · 280  
 Guo, F. · 128  
 Gurban, A. M. · 174
- 
- H**
- Haafiz, M. M. · 52  
 Habib, A. · 158  
 Habib, Z. · 139, 141, 142, 143, 149  
 Haider, A. · 116  
 Haider, M. S. · 59  
 Hakeem, A. · 232, 275  
 Hamayun, M. T., · 114, 130  
 Hameed, S. · 271  
 Hammoudeh, S. · 35  
 Han, J. I. · 44, 67  
 Han, X. · 263  
 Hanif, M · 208, 209, 210, 211  
 Hanif, M. · 208, 209, 210  
 Harbi, T. S. A. · 257  
 Harijan, K. · 47
- Haroon, H. · 62  
 Hassan, A. · 50, 52  
 Hassan, I. · 241  
 Hassan, S. M. A. · 89  
 Hassan, S. S. · 27  
 Hayat Nawaz, M. A. · 185  
 Hayat, A. · 53, 160, 165, 166, 168, 170, 173,  
 174, 175, 178, 180, 184, 185, 186, 188,  
 189, 196, 200  
 Hayat, S. · 112  
 HAZIQ, M. · 40  
 Hernández, S. · 49  
 Hong, W. P. · 245  
 Houndjo, M. J. S. · 98  
 Hu, C. · 233, 236, 263, 264  
 Huang, S. · 124  
 Huang, Z. · 263  
 Humayun, A. · 207  
 Hurr, M. · 32  
 Hussain Gardazi, S. M. · 63  
 Hussain, A. · 234, 258, 259, 260  
 Hussain, F. · 234  
 Hussain, G · 5, 13, 14  
 Hussain, G. · 13  
 Hussain, H. · 49  
 Hussain, I. · 135  
 Hussain, J. · 167  
 Hussain, M. · 48, 49, 59, 99, 100, 136, 139,  
 238  
 Hussain, N. · 150  
 Hussain, R. · 157  
 Hussain, S. · 116, 117, 144, 145, 147, 169,  
 194, 244, 264, 277  
 Hussain, T. · 201  
 Hussan, S. G. · 34  
 Hussin, H. M. R. · 11  
 Hwang, H. J. · 59

**I**

**Ibrahim, A. N.** · 52  
**Idrees, F.** · 206  
**Idrees, M.** · 197, 229, 243, 244, 253  
**Idreesa, S.** · 72  
**Iftikhar, M. A.** · 134, 136, 137  
**Ijaz, S.** · 114  
**Ilyas, A.** · 45, 55, 96, 181  
**Ilyas, M.** · 64  
**Imran Din, M.** · 204  
**Imran, A.** · 39  
**Imran, M.** · 70, 112, 262, 267, 269, 270  
**Imran, S.** · 59, 276  
**Imran, S. M.** · 59  
**Imtinan, U.** · 144  
**Inuwa, I. M.** · 52  
**Iqbal, A.** · 103, 214  
**Iqbal, F.** · 155, 171, 258, 259, 260, 261  
**Iqbal, J.** · 48, 49, 241  
**Iqbal, M.** · 214, 234  
**Iqbal, M. Z.** · 214  
**Iqbal, R.** · 148  
**Iqbal, S.** · 257  
**Iqbal, W.** · 199  
**Irfan, M.** · 61, 231, 274  
**Irfan, R. N. L. S.** · 207  
**Irfan, S. M.** · 207  
**Irshad, M.** · 213, 219, 235  
**Islam, F.** · 24  
**Islam, M. U.** · 223, 273, 275, 276  
**Islam, S.** · 262  
**Ismail, M.** · 211  
**Ismail, N. F.** · 272  
**Ismail, W. K. B. W.** · 5  
**Istamboulie, G.** · 160, 175, 189

**J**

**Jabeen, D.** · 77  
**Jabeen, G.** · 60, 62, 278  
**Jabran, M. A.** · 17  
**JAFFERY, M.** · 40  
**Jahangir, M.** · 291  
**Jahanzeb, A.** · 33  
**Jalil, A.** · 134, 136  
**Jam, F. A.** · 19  
**Jamal, A.** · 178, 190, 192  
**Jamil, A.** · 216  
**Jamil, M.** · 102, 216, 245, 246, 265  
**Jamil, T.** · 191  
**Jang, N.** · 42, 56  
**Janjua, N. K.** · 220  
**Javaid, A.** · 171  
**Javaid, M.** · 12, 99  
**Javaid, M. F.** · 12  
**Javaid, A.** · 211  
**Javed, A.** · 125  
**Javed, F.** · 219, 235  
**Javed, H.** · 270  
**Javed, M.** · 14, 217, 218, 233, 235, 236, 241, 263, 264  
**Javed, S.** · 107  
**Javid, M. A.** · 239, 254  
**Jawad, A.** · 69, 70, 75, 81, 90, 91, 92, 93, 94, 95, 96, 97, 98, 101, 102, 103, 107  
**Jawad, M.** · 126, 127, 128  
**Jawaid, M.** · 50  
**Jeong, Y.** · 42  
**Jiang, Z.** · 264  
**Jończyk, J.** · 159  
**JOYO, M.** · 40  
**Junaid, M.** · 261  
**Jung, Y. D.** · 245  
**Just, M.** · 120

**K**

**Kadilar, C.** · 208  
**Kadilar, C.** · 210  
**Kait, C. F.** · 167, 194  
**Kalsoom, A.** · 67  
**Kamal, A.** · 122  
**Kamarudin, K. S. N.** · 57, 58  
**Kamil, A.** · 201  
**Kamran, M.** · 190  
**Kanwal, F.** · 191  
**Kanwal, M.** · 230, 275  
**Kanwal, S.** · 107, 206  
**Karimi, H. R.** · 125  
**Kashif, M.** · 164, 220, 221  
**Kathia, M. A.** · 115  
**Kazmi, N.** · 194  
**Kerre, E.** · 78  
**Kertik, A.** · 54  
**Khalid, M.** · 235, 286  
**Khalid, M. S.** · 235  
**Khaliq, I. H.** · 10  
**Khan, A.** · 45, 48, 51, 53, 54, 55, 61, 81, 100, 110, 114, 119, 141, 143, 149, 153, 154, 156, 158, 160, 162, 163, 167, 172, 173, 179, 181, 183, 192, 194, 195, 197, 201, 202, 240, 246  
**Khan, A. F.** · 53, 153, 192, 197  
**Khan, A. L.** · 45, 54, 55, 181  
**Khan, A. R.** · 158  
**Khan, A. U.** · 48, 51, 156  
**Khan, B.** · 127, 128  
**Khan, D. M.** · 140  
**Khan, F. U.** · 162, 167, 172, 202  
**Khan, G.** · 161, 173, 179  
**Khan, H.** · 172, 173  
**Khan, I. U.** · 159, 162, 167, 202  
**Khan, K. A.** · 89, 104

**Khan, K. N.** · 43  
**Khan, M.** · 33, 67, 105, 117, 126, 159, 164, 167, 198, 220, 221, 223, 237, 239, 248, 258, 259, 260, 261, 272  
**Khan, N.** · 39, 81, 110, 145, 147, 151, 214  
**Khan, N. A.** · 81, 110, 145, 147, 151  
**Khan, N. Z. A.** · 39  
**Khan, R. A.** · 158, 160  
**Khan, R. S.** · 207  
**Khan, S.** · 38, 119, 126, 127, 128, 156, 162, 169, 202, 216, 240  
**Khan, T. A.** · 206  
**Khan, W. A.** · 149  
**Khan, Z. U. H.** · 154, 156, 173  
**Khanc, A. U.** · 167  
**Khandaker, M. U.** · 161, 179, 188  
**Khattak, M. N.** · 268  
**Khattak, R.** · 194  
**Khosa, I.** · 119  
**Khraief, N.** · 38  
**Khurram, R.** · 212  
**Khurshid, Z.** · 163  
**Kim, C.** · 56  
**Kim, E. J.** · 238  
**Kim, G. Y.** · 44  
**Kim, H. T.** · 59  
**Kim, I.** · 44  
**Kim, J.** · 51, 134  
**Kim, S.** · 64, 277  
**Kim, S. C.** · 64  
**Kousar, F.** · 90, 108  
**Kumar, R.** · 20, 32  
**KVESI, L.** · 104  
**Kyophilavong, P.** · 9, 21, 22

**L**

**Larijani, H.** · 125

- Latif, H.** · 270  
**Latif, U.** · 186  
**Le Anh, H. T.** · 277  
**Le, H. H.** · 49  
**Lee, E. Y.** · 56  
**Lee, J.** · 56, 144  
**Lee, M.** · 57  
**Lei, J.** · 199  
**Leitão, N. C.** · 7  
**Leveque, J. M.** · 204  
**Li, B.** · 204  
**Li, H.** · 41  
**Li, X.** · 45  
**Li, Y.** · 112  
**Liao, Q. H.** · 232  
**Ling, C. H.** · 21  
**Ling, T. C.** · 134  
**Liu, S.** · 35  
**Liu, T.** · 264  
**Liu, X.** · 165  
**Liu, Y.** · 232, 242  
**Loganathan, N.** · 17, 19, 20, 21, 23, 38  
**Lohi, M.** · 143  
**Lu, S.** · 55, 198  
**Lu, S. C.** · 55  
**Lung, C. Y. K.** · 158  
**Luqman, M. K.** · 12
- 
- M**
- M., Asif,** · 129, 244  
**M., Naeem Awais** · 129  
**MacNeil, S.** · 153, 169, 179  
**Mahalik, M. K.** · 23, 136  
**Mahfooz, M.** · 289  
**Mahmood, A.** · 34, 161  
**Mahmood, H.** · 30, 270  
**Mahmood, H. Z.** · 30
- Mahmood, K.** · 231, 273, 274  
**Mahmood, N.** · 49, 163, 176  
**Mahmood, Q.** · 63  
**Mahmood, S. A.** · 105  
**Mahrukh, K.** · 207  
**Majeed, A.** · 248, 258  
**Majeed, K.** · 48, 50, 52  
**Majid, F. B.** · 73  
**Malik, A. A.** · 207  
**Malik, S.** · 10  
**Mallick, H.** · 23, 38  
**Man, Z.** · 167, 172, 194, 195  
**Manzoor, F.** · 157, 176, 182, 190  
**Manzoor, N.** · 111  
**Maqbool, K.** · 72, 86, 111  
**Maroof Shah, M.** · 63  
**Martí, J. M. N.** · 163  
**Marty, J. L.** · 160, 166, 170, 173, 174, 175, 178, 180, 184, 185, 186, 188, 189, 196, 200  
**Masood, B.** · 116  
**Masood, M. H.** · 115  
**Masood, S.** · 230  
**Mastoi, N. R.** · 41, 51  
**Matinlinna, J. P.** · 158  
**Mehfooz, M.** · 282, 288  
**Mehfooz, M.** · 282  
**Mehmood, A.** · 128  
**Mehmood, C. A.** · 127, 128  
**Mehmood, S. A.** · 73  
**Mehmood, W.** · 146  
**Mehmood, Z.** · 207  
**Memon, I.** · 135  
**Milovic, D.** · 73  
**Mirza, H. T.** · 135  
**Mishra, R. K.** · 160, 166, 170, 178, 188, 189, 200  
**Miyato, N.** · 228

- Mohamed, M.** · 238  
**Mohsaneen, S.** · 93, 94, 97  
**Mohsin, M.** · 206  
**Momeni, D.** · 70  
**Muhamad, N.** · 222, 272  
**Muhammad, N.** · 53, 155, 161, 162, 167, 169, 172, 179, 188, 191, 195, 202, 203, 204  
**Muhammad, Q. K.** · 131  
**Muhammad, W.** · 207  
**Mujahid, A.** · 164, 201  
**Mujahid, N.** · 17  
**Mumtaz, M.** · 114, 119, 240  
**Mumtaz, M. F.** · 114  
**Munawar, M.** · 231, 274  
**Munir, S.** · 25, 27  
**Muñoz, R.** · 170, 178  
**Murid, A. H.** · 74, 109  
**Murtaza, G.** · 220, 230, 232, 258, 259, 260, 261, 273, 275  
**Murtaza, G.,** · 221  
**Mushtaq, A.** · 55, 181, 268  
**Mushtaq, M. N.** · 237  
**Mushtaq, Nadia** · 210  
**Mustafa, F.** · 216  
**Mustafa, G.** · 43, 230, 273, 275, 276  
**Mustafa, M.** · 130  
**Mustafab, G.** · 228  
**Mutahir, S.** · 159  
**Mutalib, M. I. A.** · 204  
**Muzaffar, A. T.** · 17  
**Myrzakulov, R.** · 70
- 
- N**
- Nabi, A.** · 239  
**Nadeem, F.** · 87  
**Nadeem, I.** · 84, 109  
**Nadeem, M.** · 88, 108, 197, 229, 243, 253  
**Nadeem, M. F.** · 88, 108  
**Naeem Awais** · 129  
**Naeem, N.** · 211  
**Najeeb, S.** · 163  
**Naqvi, S. M.** · 5, 29  
**NAREJO, G.** · 40  
**Naseem, S.** · 177, 262  
**Naseer, M.** · 147  
**Nash, D. H.** · 100  
**Nasir, M.** · 53, 189, 198, 199  
**Nasreen, S.** · 16  
**Nasrullah, A.** · 162, 172, 194, 202  
**Naveed, A.** · 289, 290  
**Nawab, J.** · 64  
**Nawab, R. M. A.** · 138, 141  
**Nawaz, B.** · 149  
**Nawaz, K.** · 18  
**Nawaz, M. A. H.** · 180  
**Nawaz, M. H.** · 53, 180, 197  
**Nawaz, T.** · 92, 93  
**Naz, T.** · 146  
**Nazar, K.** · 74, 109  
**Nazar, M. F.** · 43  
**Nazeer, S.** · 27, 28  
**Nazir, M. S.** · 65, 66  
**Nazli, H.** · 212  
**Nesterenko, D. V.** · 266  
**Ni, Q.** · 121  
**Nie, W. J.** · 232  
**Nisar, F.** · 5, 13  
**Nisar, J.** · 158, 160  
**Nisar, Q. A.** · 5, 39  
**Nisar, Q. A.,** · 5  
**Nisar, S.** · 253, 254, 257  
**Nishan, U.** · 155, 201  
**Niu, J.** · 134  
**Noor-ul-Amin, M.** · 210, 211

Nor, S. M. · 35  
 Noreen, I. · 141, 143, 149  
 Nosheen, S. · 275  
 Noureen, I. · 85  
 Numan, M. · 89  
 Nunes, G. · 180, 186, 196

---

**O**

Omar, M. A. · 222  
 Oz, I. · 122  
 Ozturk, I. · 8, 16, 37

---

**P**

Pan, L. · 214, 215  
 Paramati, S. R. · 7, 36  
 Park, H. · 277  
 Park, S. · 42, 59  
 Pasero, E. · 119  
 Patel, F. · 41  
 PECARI C, J. · 104  
 Pecaric, J. · 89, 104  
 Pečarić, J. · 84  
 Pervez, A. · 63  
 Pilz, J. · 206  
 Pires, C. T. · 186  
 Poirier, G. Y. · 250  
 Popov, K. · 122  
 PRALJAK, M. · 103

---

**Q**

Qadri, S. · 140  
 Qadri, S. F. · 140  
 Qaim, S. M. · 238  
 Qaisar, S. · 89  
 Qasim, M. · 231, 274

Qayyum, M. · 78  
 Qian, D. · 146  
 Qu, L. L. · 41  
 Qureshi, K. · 47, 57, 58

---

**R**

R., Ivanov, S · 20  
 Radusch, H. · 49  
 Radzi, M. F. · 272  
 Rafiq, M. A. · 122, 131  
 Rafiq, M. N. · 122, 131  
 Rafique, A. · 235, 237  
 Rafique, M. S. · 218, 219, 235, 247  
 Rafique, M. Y. · 214, 215, 267  
 Rafiullah, M. · 77  
 Rafiullah, M., · 106  
 Rahaman, F., · 79  
 Rahim, A. · 53, 158, 160, 186, 187  
 Rahman, A. U. · 214  
 Rahman, R. A. · 267, 270  
 Rahman, Z. · 64  
 Rahmouni, A. · 266  
 Rajesh, D. · 249  
 Ramay, S. M. · 161, 177, 198  
 Rana, A. M. · 234  
 Rani, S. · 69, 70, 90, 91, 92, 93, 94, 95, 96, 97, 98, 101, 107  
 Rasheed, A. · 216, 245  
 Rasheed, K · 61, 246  
 Rasheed, S. · 134, 158, 160  
 Rashid, M. A · 5, 13, 14  
 Rashid, N. · 44, 62, 63, 64  
 Rashid, S. · 81, 110  
 Rashidi, M. M. · 81, 87, 110  
 Rasool, G. · 133, 136, 139  
 Rasool, S. · 43  
 Rathore, S. · 134, 136, 137

- Ratyal, N. I.** · 147  
**Rauf, A.** · 163, 176, 193  
**Rauf, S.** · 180, 185, 207  
**Rayson, P.** · 141  
**Raza, I.** · 144  
**Raza, M. R.** · 65, 220, 222, 272  
**Raza, M. T.** · 45  
**Raza, N.** · 31  
**Raza, R.** · 213, 217, 218, 219, 220, 221, 234, 235, 237, 241  
**Raza, S. A.** · 7, 15, 23  
**Razani, A.** · 77  
**Razaq, A.** · 119, 240, 244, 277  
**Rehman, F.** · 169, 182, 186, 187, 194  
**Rehman, I. U.** · 163, 169, 190  
**Rehman, J.** · 259  
**Rehman, M. S. U.** · 44, 67  
**Rehman, S.** · 60, 266, 278  
**Rehman, S. U.** · 60, 278  
**Rejeb, I. B.** · 175  
**Rhouati, A.** · 170, 173, 189, 196  
**Riasat, A.** · 107  
**Riaz, S.** · 41, 53, 197, 212, 246, 262  
**Riaz, T.** · 191  
**Rizvi, S. T.** · 68, 69, 73, 77, 105  
**Rizvi, S. T. R.** · 68, 69, 73, 77  
**Rizwan Raza** · 242  
**Rizwan, S.** · 152  
**Roohpour, N.** · 183  
**Rozina, C.** · 246, 265
- 
- S**
- S. Nisar** · 224  
**S., Chen** · 233  
**S., Rafique** · 217  
**Sabir, N.** · 150  
**Saddiqa, A.** · 41  
**Sadiq, A.** · 145  
**Sadiq, M. W.** · 26  
**Sadorsky, P.** · 23  
**Saeed, A.** · 120, 125  
**Saeed, J.** · 100  
**Saeed, M.** · 231, 274  
**Saeed, R.** · 241  
**Saeed, Y.** · 143, 149  
**Saif Ur Rehman, M.** · 44  
**Saif-Ur-Rehman, M.** · 43  
**Sajid, M.** · 44, 147  
**Salako, I. G.** · 75, 81, 92, 95, 98  
**Saleem Sumaira.** · 292  
**Saleem, H.** · 246  
**Saleem, M.** · 177, 197, 198, 235, 253  
**Salimullah, M.** · 216  
**Sanagi, M. M.** · 262  
**Sanaullah, A.** · 208, 209  
**Sangawi, A. W.** · 74, 109  
**Santos, A. L.** · 186  
**Sardar, A.** · 68, 73  
**Sardar, I. H.** · 79  
**Sarfraz, M.** · 34, 35  
**Sarfraz, Z.** · 158  
**Sargano, A. B.** · 142  
**Sattar, A.** · 247, 267, 270, 271  
**Satyanarayana, M.** · 184  
**Sbia, R.** · 37  
**Sekkat, Z.** · 266  
**Seo, Y. H.** · 67  
**Shabbir, A.** · 87  
**Shabbir, J.** · 211  
**Shabbir, M. S.** · 17  
**Shafiq, M. K.** · 83  
**Shah, A.** · 154, 164, 171, 173, 192, 201, 204  
**Shah, F. T.** · 206  
**Shah, H. A.** · 269  
**Shah, H. U.** · 154

- Shah, N.** · 146  
**Shah, S. M.** · 66, 160  
**Shah, S. M. U.** · 66  
**Shah, S. N.** · 195  
**Shahzadi, L.** · 193  
**Shahbaz, M.** · 6, 7, 8, 9, 15, 16, 17, 18, 19, 20, 21, 22, 23, 24, 25, 31, 35, 36, 37, 38, 136, 210  
**Shahbaz, S. H.** · 211  
**Shaheen, F.** · 257  
**Shaheen, H.** · 292  
**Shaheen, N.** · 241, 264  
**Shahid, M.** · 140  
**Shahid, S. A.** · 170, 200  
**Shahzad, A. K.** · 292  
**Shahzad, K.** · 151, 164  
**Shahzad, M. U.** · 75, 102  
**Shahzad, S.** · 31, 32, 35, 176, 193, 280  
**Shahzad, S. J. H.** · 31, 32, 35  
**Shahzadi, K.** · 46  
**Shahzadi, L.** · 153, 163, 176, 178  
**Shahzadi, S.** · 218  
**Shaker, H.** · 84, 109  
**Shakir, I.** · 219, 235, 259, 260  
**Shao, G. N.** · 59  
**Sharif, A.** · 157  
**Sharif, F.** · 169  
**Sharif, I.** · 285  
**Sharif, M. K.** · 260  
**Sharif, S.** · 282  
**Shariff, A. M.** · 191  
**Sharjeel, M.** · 141  
**Sharma, A.** · 174, 175, 200  
**Sharma, V.** · 178  
**Shaukat, S. F.** · 60, 65, 197, 218, 241, 247, 253, 266, 278  
**Shaukata, S. F.** · 228  
**Shehzad, K.** · 201  
**Shehzad, M. N.** · 130  
**Shehzad, N.** · 118  
**Sheikh, H.** · 282, 287, 294  
**Sheikh, N. H.** · 207  
**Sheikh, R.** · 48  
**Sheikh, U.** · 290  
**Sheikh, Z.** · 183  
**Sherazi, H. H. R.** · 148  
**Sherazi, T. A.** · 62  
**Shukor, M. Y.** · 66  
**Shum, K. P.** · 82  
**Siddiqi, S. A.** · 153, 157, 176, 177, 178, 190, 191, 197, 198, 253  
**Siddique, M.** · 60, 216, 229, 278  
**Siddiqui, A. M.** · 74  
**Siddiqui, H. M. A.** · 83, 112  
**Singh, D. K.** · 144  
**Siraj, K.** · 213, 219, 235, 247  
**Smolyakov, A. I.** · 228  
**Sohail, A.** · 72, 74, 76, 80, 81, 86, 87, 99, 110, 111, 151  
**Solarin, S. A.** · 8  
**Stevenson, M.** · 138  
**Sulong, A. B.** · 220, 222, 223, 272  
**Sultana, I.** · 244  
**Sung, B. H.** · 64  
**Suyfan, S.** · 285
- 
- T**  
**Tabassum, S.** · 55, 157, 164, 181, 182  
**Tahir, K.** · 156  
**Tahir, T.** · 133  
**Taj, I.** · 147  
**Tang, C. F.,** · 6  
**Tang, X.** · 263  
**Tanoli, A.** · 127  
**TARIQ, A.** · 40

Tariq, M. · 190  
 Tárkányi, F. · 238  
 Terán-Hilares, R. · 67  
 Thebo, K. H. · 191  
 Tiwari, A. K. · 6, 31  
 Tiwari, P. · 213  
 Trines, R. M. G. M. · 269  
 Tsintsadze, N. L. · 265, 269  
 Turtelli, R. S. · 243

---

**U**

U. S., Abbas · 126  
 U., Li · 126  
 Uddin, G. S. · 22  
 Uddin, M. J. · 87  
 Uddin, R. · 201  
 ul Amin, M. N. · 208  
 Ul Hassan, S. · 148  
 ullah Khan, A. · 154  
 Ullah, M. · 234  
 Ullah, N. · 159, 193  
 Ullah, S. · 191, 203  
 Ullah, Z · 155, 172, 194, 195  
 Ulrich, J. · 48  
 Umair, T. · 12  
 ur Raheem, F. · 248, 258  
 ur Rehman, I. · 163, 171, 182, 183, 192  
 Usman, A. · 212, 213, 246, 247, 267, 270  
 Usman, M. · 122, 131  
 Uzair, L. · 10

---

**V**

Vankelecom, I. F · 45, 54, 55  
 Vasilescu, A. · 186  
 Volpe, P. L. · 187  
 VUKELIC, A. · 104

Vukelić, A. · 84

---

**W**

Waheed, N. · 55, 181  
 Waheed, S. · 79  
 Wahjoedi, B. A. · 65  
 Wajid, H. A. · 99, 100, 111  
 Wan Ismail, W. K. · 13  
 Wan, B. · 233  
 Wan, P. · 154, 173  
 Wang, B. · 242  
 Wang, H. · 242  
 Wang, J. · 264  
 Wang, L. · 135  
 Wang, Y. · 242  
 Waqar, M. · 122, 131  
 Waqas, M. · 146  
 Warsi, M. F. · 248, 258, 259, 260, 261  
 Wei, Y. · 156  
 Welker, V. · 72  
 Wong, S. L. · 52

---

**X**

Xi, Y. · 233, 236  
 Xia, C. · 242  
 Xiang, Z. · 123, 124, 125  
 Xu, J. · 232  
 Xu, M. · 198

---

**Y**

Yadzir, Z. H. M. · 66  
 Yagi, M. · 228  
 Yahya, F. · 30  
 Yan, L. · 112, 114  
 Yan, Q. R. · 232

**Yaqoob, A.** · 65  
**Yaqub, A.** · 220  
**Yar, M.** · 153, 159, 163, 176, 178, 193  
**Yasin, M.** · 42, 56  
**Yasir, H.** · 207  
**Yasmeen, S.** · 270  
**Yasmeen, U.** · 210  
**Yong, C. C.** · 134  
**Younis, M.** · 68, 69, 73, 105  
**Yousaf, M.** · 254  
**Yousaf, R.** · 113  
**Yu, C. P.** · 43  
**Yu, G.** · 47  
**Yuan, Q.** · 156  
**Yussof, A. W.** · 65

---

**Z**

**Zafar, M.** · 129, 163  
**Zafar, R. Z.** · 115  
**Zafar, S.** · 88  
**Zahid, A. N.** · 115  
**Zahid, S.** · 171, 178, 182, 192  
**Zahid, Z.** · 88

**Zakaria, M.** · 32  
**Zaman, A.** · 80  
**Zaman, K.** · 23  
**Zameer, A.** · 10  
**Zarif, F.** · 182  
**Zeb, N.** · 127  
**Zeeshan, T.** · 212  
**Zerrad, E.** · 68  
**Zhang, C.** · 233, 236, 264  
**Zhang, J.** · 199  
**Zhang, X.** · 198  
**Zhao, S.** · 264  
**Zhao, X.** · 134  
**Zhao, Z.** · 47  
**Zhou, M.** · 263  
**Zhou, N. R.** · 232  
**Zhou, Q.** · 68  
**Zhu, B.** · 213, 218, 220  
**Zia, R.** · 246  
**Zohaib, S.** · 163  
**Zomaya, A. Y.** · 126  
**Zubair, M.** · 78, 79, 80, 85, 86, 89, 90, 108, 283